THE ASTROPHYSICAL JOURNAL

AN INTERNATIONAL REVIEW OF SPECTROSCOPY AND ASTRONOMICAL PHYSICS

VOLUME 92 SEPTEMBER 1940 NUMBER 2

# TRANSITION PROBABILITIES OF FORBIDDEN LINES

SIMON PASTERNACK

ABSTRACT

The calculation of transition probabilities of forbidden lines is discussed for atoms in the $p^2$, $p^3$, $p^4$, $d^2$, and $d^3$ configurations. The results of numerical computations are given for a large number of elements in the $p^k$ configurations, for the $d^2$ configuration of *Fe* VII, and for the $d^3$ configuration of *Cr* IV, *Mn* V, and *Fe* VI. Some implications of the results are mentioned.

The identification of the forbidden lines of a number of elements in the spectra of nebulae and novae[1] was followed by the calculation, by Condon[2] and others,[3] of the theoretical transition probabilities of these lines. Recent extensive investigations of nebular spectra[4] have made it desirable to re-examine these calculations and to extend them to many more elements. This has been done with a view to providing numerical results useful to the observational astrophysicist.

In a preliminary report[5] the author listed the transition probabilities of the forbidden lines of thirty atoms in the $p^2$, $p^3$, and $p^4$ configurations. These tables have now been revised and extended, and calculations have also been made for atoms in the $d^2$ and $d^3$ configurations.

[1] I. S. Bowen, *Ap. J.*, **67**, 1, 1928. [2] *Ap. J.*, **79**, 217, 1934.

[3] A. Rubinowicz, *Zs. f. Phys.*, **65**, 662, 1930; A. F. Stevenson, *Proc. R. Soc.*, A, **137**, 298, 1932.

[4] I. S. Bowen, *Rev. Mod. Phys.*, **8**, 55, 1936; I. S. Bowen and A. B. Wyse, *Pub. A.S.P.*, **50**, 348, 1938; *Lick Obs. Bull.*, **19**, 1, 1940.

[5] S. Pasternack, *Pub. A.S.P.*, **51**, 160, 1939.

The method used in the calculations is essentially that developed by Condon, in which the magnetic dipole and electric quadrupole contributions are evaluated separately. Since much of the theory is developed in *The Theory of Atomic Spectra*, by Condon and Shortley, the notation set up in that book is used throughout this article. The book will, for convenience, be referred to as "*CS*."

## I. THE TRANSITION PROBABILITIES

The magnetic dipole transition probability for the transition from a level $A$ to a level $B$ is given by the formula[6]

$$\mathbf{A}(A, B) = \left(\frac{8\pi^3 e^2 \hbar}{3\mu^2 c^2}\right) \frac{\sigma^3}{2J_A + 1} \mathbf{S}(A, B), \tag{1}$$

where

$$\mathbf{S}(A, B) = \sum_{a, b} |(a|\boldsymbol{L} + 2\boldsymbol{S}|b)|^2, \tag{2}$$

the summation being taken over all the states $a$, $b$ comprising the levels $A$ and $B$, respectively. The wave number $\sigma$ is measured in reciprocal centimeters, and $\boldsymbol{L}$ and $\boldsymbol{S}$ are measured in units of $\hbar$. The numerical factor turns out to be $2.696 \times 10^{-11}$. Formulae for the line strengths $\mathbf{S}(A, B)$ in pure Russell-Saunders or $LS$ coupling may be easily obtained from the results given in *CS*, § 9[3] and § 10[3], with the correlation

$$\boldsymbol{J}_1 = \boldsymbol{S}, \qquad \boldsymbol{J}_2 = \boldsymbol{L}, \qquad \boldsymbol{J} = \boldsymbol{J}.$$

They are[7]

$$\left.\begin{aligned} &\mathbf{S}(SLJ, SLJ) \\ &\qquad = \frac{(2J+1)\{S(S+1) - L(L+1) + 3J(J+1)\}^2}{4J(J+1)} \\ &\text{and} \\ &\mathbf{S}(SLJ, SLJ-1) = \mathbf{S}(SLJ-1, SLJ) \\ &\qquad = \frac{\{J^2 - (L-S)^2\}\{(S+L+1)^2 - J^2\}}{4J}. \end{aligned}\right\} \tag{3}$$

[6] Condon, *loc. cit.*

[7] These formulae are also given in a recent paper by G. H. Shortley, *Phys. Rev.*, **57**, 255, 1940. The second formula was first derived by H. Brinkman in *Zur Quantenmechanik der Multipolstrahlung*, p. 53.

A sum rule useful for checking purposes is obtained by summation, viz.,

$$\left.\begin{aligned}\sum_{J'} \mathbf{S}(SLJ, SLJ') \\ = (2J+1)\{2J(J+1) + 2S(S+1) - L(L+1)\}\,.\end{aligned}\right\} \quad (4)$$

The breakdown of $LS$ coupling due to the spin-orbit interaction is introduced in the usual manner. If the wave function for the perturbed state is represented by

$$\Psi'(S_iL_iJM) = \sum_{k=1}^{r} a_{ik}\Psi(S_kL_kJM)\,, \quad (5)$$

then it is readily seen that the line strengths in this intermediate coupling are given by the formulae

$$\mathbf{S}'(S_iL_iJ, S_jL_jJ') = \left| \sum_k a_{ik}a_{jk}\sqrt{\mathbf{S}(S_kL_kJ, S_kL_kJ')} \right|^2 . \quad (6)$$

This follows from the fact that the matrix element in $LS$ coupling can be written in the form

$$(SLJM\,|\,2\boldsymbol{S} + \boldsymbol{L}\,|\,S'L'J'M') = (SLJ \,\vdots\, 2S + L \,\vdots\, S'L'J')f(JM, J'M')\,.$$

The introduction of the breakdown of coupling involves only the first factor on the right, whereas the process of summing squares of absolute values over $M$ and $M'$ to get the line strengths involves only the second factor. That the positive square root is to be taken in all cases under consideration follows from the derivation of formulae (3), in which all the nonvanishing matrix quantities $(SLJ \,\vdots\, 2S + L \,\vdots\, S'L'J')$ are found to be positive. (This is true for all equivalent electron configurations up to $nf^5$).

The electric quadrupole transition probability is given by the formula[8]

$$\mathbf{A}(A, B) = \left(\frac{16\pi^5\hbar^7}{5\mu^2 e^6}\right) \frac{\sigma^5}{2J_A + 1} \mathbf{S}(A, B) , \tag{7}$$

where

$$\mathbf{S}(A, B) = \sum_{a, b} |(a|\mathfrak{R}'|b)|^2 , \tag{8}$$

with $\sigma$ being measured in reciprocal centimeters, as before. Here $\mathfrak{R}'$ is the electric quadrupole moment of the atom under consideration *minus* its spherically symmetrical component (*CS*, § 6[4]). It is measured in Hartree units $ea_0^2$, where $a_0$ is the Bohr radius. The numerical factor in equation (7) is $1.679 \times 10^{-22}$.

In this case, simple expressions for the line strengths in *LS* coupling are not available. Formulae have been developed by Rubinowicz[9] for the dependence on $M$ and $M'$ of the matrix elements

$$(SLJM|\mathfrak{R}'|S'L'J'M')$$

in *LS* coupling (*CS*, § 6[4], eqs. [6]). These matrices are expressed in terms of quantities $D$, $E$, and $F$, which are functions of $S$, $L$, $J$, $S'$, $L'$, and $J'$. The line strengths in *LS* coupling are readily expressed in terms of these quantities (*CS*, § 7[4], eqs. [7]).

The problem of evaluating the electric quadrupole line strengths may then be treated in the following steps. First are evaluated the matrix elements

$$(nslm_s m_l| \; -e\mathbf{rr}|nslm_s' m_l')$$

in the one-electron scheme of wave functions. Next the matrix elements of $\mathfrak{R} = -e\sum_i \mathbf{r}_i\mathbf{r}_i$ are evaluated in the zero-order scheme of

[8] Condon, *loc. cit.*

[9] *Zs. f. Phys.*, **65**, 662, 1930; *Ergeb. der exakten Naturwiss.*, **11**, 176, 1932.

wave functions formed by antisymmetrizing products of one-electron wave functions. This step is facilitated by the theorem established in *CS*, § 6[6]. From these matrix elements the matrix elements of $\mathfrak{R}'$ in the pure Russell-Saunders scheme may be obtained if the wave functions in the *LSJM* scheme are known in terms of the antisymmetrized product wave functions. It is necessary to evaluate these matrix elements

$$(SLJM|\mathfrak{R}'|S'L'J'M')$$

for all possible quantum numbers $S, L, J, S', L', J'$, but for only one convenient pair of values of $M$ and $M'$. The Rubinowicz formulae referred to above then yield values of the quantities $D$, $E$, and $F$, from which the line strengths are immediately obtained.[10]

The breakdown of *LS* coupling due to spin-orbit interaction is taken into account in the same manner as for the magnetic dipole case:

$$\mathbf{S}'(S_iL_iJ, S_jL_jJ') = \left| \sum_{k,l} a_{ik}a_{jl}(\pm\sqrt{\mathbf{S}(S_kL_kJ, S_lL_lJ')}) \right|^2 . \quad (9)$$

Here, however, it is necessary to be careful in selecting the signs for the square roots of the line strengths. The same sign should be given to

$$\pm\sqrt{\mathbf{S}(S_kL_kJ, S_lL_lJ')}$$

as that possessed by the quantity $D$, $E$, or $F$ which is present in the corresponding matrix element $(S_kL_kJM \mid \mathfrak{R}' \mid S_lL_lJ'M')$.

A further reduction of the problem of evaluating the electric quadrupole line strengths could be effected by means of Rubinowicz' formulae[11] for the dependence of the line strengths on $J$ and $J'$ (*CS*,

[10] In a very recent article (*loc. cit.*) G. H. Shortley has obtained expressions for the matrix elements of $\mathfrak{R}'$ in the $SLM_SM_L$ scheme. This would simplify the calculations to some extent, since the wave functions in the $SLM_SM_L$ scheme are simpler than those in the *SLJM* scheme.

[11] *Zs. f. Phys.*, **65**, 662, 1930; *Ergeb. der exakten Naturwiss.*, **11**, 176, 1932.

Table 4[9]).[12] Use of these formulae would make it necessary to evaluate only one matrix element $(SLJM \mid \mathfrak{R}' \mid S'L'J'M')$ between each pair of terms $SL$ and $S'L'$ (or between the levels of one term), instead of one matrix element for each pair of levels. However, it was decided not to use these formulae directly in the calculations but to retain them instead for checking purposes.

In obtaining the matrix elements of $\mathfrak{R}'$ in the pure Russell-Saunders scheme, it is necessary to obtain expressions for the wave functions in $LS$ coupling in terms of the zero-order scheme of wave functions formed by antisymmetrizing products of one-electron wave functions. The wave functions $\Psi(SLJM)$ were expressed in terms of the wave functions $\Phi(SLM_SM_L)$, by means of Tables 1–4 of *CS*, § 13[3]. The evaluation of $\Phi(SLM_SM_L)$ in terms of the antisymmetrized product wave functions could be done in several ways (*CS*, chap. viii). For the two-electron configurations the vector-coupling method of Bartlett (*CS*, § 6[8]) was found to be most convenient. This method yields wave functions possessing definite phase relationships with each other (*CS*, §§ 3[3] and 10[3]). For the three-electron configurations the angular-momentum-operator method of Gray and Wills (*CS*, § 5[8]) was used. This method gives wave functions which have a definite phase relationship (*CS*, § 3[3]) for states of the same term but not for states of different terms.

The wave functions for the states of the $p^2$ configuration are listed in Condon's paper. The wave functions for the states of the $p^3$ configuration were chosen so as to have the same relative phases as the set given in *CS*, § 4[8], eq. (6*m*). For the $d^3$ configuration the relative phases for different terms are indicated by the following set of wave functions. (The notation used here is that of Condon's paper.)

[12] There is an ambiguity in the procedure described in *CS*, § 5[9], for obtaining the matrix quantities $D$, $E$, and $F$ from the quantities $G$, $H$, and $I$ involved in the Rubinowicz formulae. The statement that one should attach the sign given in the table to the positive square root of a certain quotient should be understood to imply the taking of a "formally positive" square root. That is, the signs in the formulae for $D$, $E$, and $F$ in terms of $G$, $H$, and $I$ are to be chosen independently of the signs which may later be introduced in the values of $G$, $H$, and $I$, as well as in some of the bracketed expressions in the table.

$$
\left.\begin{aligned}
\Psi(^4F^{4\frac{1}{2}}_{4\frac{1}{2}}) &= \Phi(2^+, 1^+, 0^+) .\\
\Psi(^4P^{2\frac{1}{2}}_{2\frac{1}{2}}) &= \frac{1}{\sqrt{5}}\{\sqrt{3}\,\Phi(2^+, 1^+, -2^+) - \sqrt{2}\,\Phi(2^+, 0^+, -1^+)\} .\\
\Psi(^2H^{2\frac{1}{2}}_{2\frac{1}{2}}) &= \Phi(2^+, 1^+, 2^-) .\\
\Psi(^2G^{4\frac{1}{2}}_{4\frac{1}{2}}) &= \frac{1}{\sqrt{5}}\{\sqrt{2}\,\Phi(2^+, 0^+, 2^-) - \sqrt{3}\,\Phi(2^+, 1^+, 1^-)\} .\\
\Psi(^2F^{3\frac{1}{2}}_{3\frac{1}{2}}) &= \frac{1}{2\sqrt{3}}\{\sqrt{6}\,\Phi(2^+, -1^+, 2^-) - 2\Phi(1^+, 0^+, 2^-)\\
&\quad - \Phi(2^+, 0^+, 1^-) + \Phi(2^+, 1^+, 0^-)\} .\\
\Psi(a^2D^{2\frac{1}{2}}_{2\frac{1}{2}}) &= \tfrac{1}{2}\{\Phi(2^+, -2^+, 2^-) - \Phi(2^+, -1^+, 1^-)\\
&\quad + \Phi(2^+, 0^+, 0^-) - \Phi(2^+, 1^+, -1^-)\} .\\
\Psi(b^2D^{2\frac{1}{2}}_{2\frac{1}{2}}) &= \frac{1}{2\sqrt{21}}\{5\Phi(2^+, -2^+, 2^-) - 4\Phi(1^+, -1^+, 2^-)\\
&\quad - \Phi(2^+, -1^+, 1^-) + 2\sqrt{6}\,\Phi(1^+, 0^+, 1^-)\\
&\quad - 3\Phi(2^+, 0^+, 0^-) + 3\Phi(2^+, 1^+, -1^-)\} .\\
\Psi(^2P^{1\frac{1}{2}}_{1\frac{1}{2}}) &= \frac{1}{\sqrt{210}}\{-2\sqrt{3}\,\Phi(1^+, -2^+, 2^-)\\
&\quad + 5\sqrt{2}\,\Phi(0^+, -1^+, 2^-) + 2\sqrt{3}\,\Phi(2^+, -2^+, 1^-)\\
&\quad + 4\sqrt{3}\,\Phi(2^+, 1^+, -2^-) - 3\sqrt{3}\,\Phi(1^+, -1^+, 1^-)\\
&\quad + \sqrt{2}\,\Phi(2^+, -1^+, 0^-) + 3\sqrt{3}\,\Phi(1^+, 0^+, 0^-)\\
&\quad - 4\sqrt{2}\,\Phi(2^+, 0^+, -1^-)\} .
\end{aligned}\right\} \quad (10)
$$

The wave functions for the actual $^2$D terms are given by

$$
\left.\begin{aligned}
\Psi(y^2D^M_J) &= \alpha\Psi(a^2D^M_J) + \beta\Psi(b^2D^M_J) ,\\
\Psi(z^2D^M_J) &= -\beta\Psi(a^2D^M_J) + \alpha\Psi(b^2D^M_J) ,
\end{aligned}\right\} \quad (11)
$$

where $\alpha$ and $\beta$ are given by the formulae in *CS*, § 7[8]. We shall take $y^2D$ to be the upper $^2$D term and $z^2D$ to be the lower $^2$D term.

In order to determine the extent of breakdown of *LS* coupling, it is necessary to have the matrices of spin-orbit interaction. For the $p^2$, $p^3$, and $d^2$ configurations these matrices are given in *CS*, Table 1[11]. For the $d^3$ configuration the matrix is tabulated below. (This matrix depends, of course, on the choice of relative term phases.)

## TABLE 1

### MATRIX OF SPIN-ORBIT INTERACTION FOR THE $d^3$ CONFIGURATION*

| | $^2H_{5/2}$ |
|---|---|
| $^2H_{5/2}$ | $\frac{1}{2}$ |

| | $^2H_{4/2}$ | $^4F_{4/2}$ | $^2G_{4/2}$ |
|---|---|---|---|
| $^2H_{4/2}$ | $-6$ | $0$ | $-2\sqrt{66}$ |
| $^4F_{4/2}$ | $0$ | $15$ | $-5\sqrt{10}$ |
| $^2G_{4/2}$ | $-2\sqrt{66}$ | $-5\sqrt{10}$ | $6$ |

$\times \frac{1}{10}$

| | $^2G_{3/2}$ | $^4F_{3/2}$ | $^2F_{3/2}$ |
|---|---|---|---|
| $^2G_{3/2}$ | $-3$ | $-\sqrt{10}$ | $-\sqrt{15}$ |
| $^4F_{3/2}$ | $-\sqrt{10}$ | $0$ | $-\sqrt{6}$ |
| $^2F_{3/2}$ | $-\sqrt{15}$ | $-\sqrt{6}$ | $-1$ |

$\times \frac{1}{4}$

| | $^2F_{2/2}$ | $^4F_{2/2}$ | $^4P_{2/2}$ | $a^2D_{2/2}$ | $b^2D_{2/2}$ |
|---|---|---|---|---|---|
| $^2F_{2/2}$ | $10$ | $-5\sqrt{10}$ | $0$ | $-10\sqrt{21}$ | $-10$ |
| $^4F_{2/2}$ | $-5\sqrt{10}$ | $-35$ | $0$ | $2\sqrt{210}$ | $-10\sqrt{10}$ |
| $^4P_{2/2}$ | $0$ | $0$ | $15$ | $-12\sqrt{15}$ | $0$ |
| $a^2D_{2/2}$ | $-10\sqrt{21}$ | $2\sqrt{210}$ | $-12\sqrt{15}$ | $15$ | $-5\sqrt{21}$ |
| $b^2D_{2/2}$ | $-10$ | $-10\sqrt{10}$ | $0$ | $-5\sqrt{21}$ | $-5$ |

$\times \frac{1}{30}$

| | $a^2D_{1/2}$ | $b^2D_{1/2}$ | $^4F_{1/2}$ | $^4P_{1/2}$ | $^2P_{1/2}$ |
|---|---|---|---|---|---|
| $a^2D_{1/2}$ | $-45$ | $15\sqrt{21}$ | $6\sqrt{210}$ | $-12\sqrt{10}$ | $-15\sqrt{14}$ |
| $b^2D_{1/2}$ | $15\sqrt{21}$ | $15$ | $-30\sqrt{10}$ | $0$ | $45\sqrt{6}$ |
| $^4F_{1/2}$ | $6\sqrt{210}$ | $-30\sqrt{10}$ | $-120$ | $0$ | $0$ |
| $^4P_{1/2}$ | $-12\sqrt{10}$ | $0$ | $0$ | $-20$ | $-20\sqrt{35}$ |
| $^2P_{1/2}$ | $-15\sqrt{14}$ | $45\sqrt{6}$ | $0$ | $-20\sqrt{35}$ | $20$ |

$\times \frac{1}{60}$

| | $^2P_{3/2}$ | $^4P_{3/2}$ |
|---|---|---|
| $^2P_{3/2}$ | $-4$ | $-2\sqrt{14}$ |
| $^4P_{3/2}$ | $-2\sqrt{14}$ | $-5$ |

$\times \frac{1}{6}$

* All these matrix elements should be multiplied by $\zeta_{nd}$, as well as by the fractions outside of the various rectangles.

The matrix elements involving the actual $^2D$ terms are easily obtained from this matrix and the definitions (11).

For the $p^4$ configuration use was made of Shortley's result[13] that the formulae for an almost closed shell with, say, $\eta$ electrons missing, can be taken over almost unchanged from the formulae for the same shell when it contains only $\eta$ electrons. Thus, the line strengths in *LS* coupling for the $p^4$ configuration are the same as those for the $p^2$ configuration. The application of the spin-orbit interaction also leads to similar results, the only difference being that the sign of the parameter $\zeta_{np}$ is changed.

The magnetic dipole line strengths in pure Russell-Saunders coupling are readily obtained from formulae (3). The electric quadrupole line strengths for the $p^2$, $p^3$, $d^2$, and $d^3$ configurations are listed in Table 2. These differ in a few cases from Condon's results. Each of these line strengths involves the square of the integral

$$s_2(n, l) = -e\int_0^\infty \{R(n, l)\}^2 r^2 dr ,$$

where $r^{-1}R(n, l)$ is the radial part of the atomic wave function. The plus or minus sign placed after each term in Table 2 means that the quantity $D$, $E$, or $F$ corresponding to that element is positive or negative, respectively. Also, the terms to the left of the principal diagonals are omitted, since the matrices are symmetrical. To conserve space, the line strengths in intermediate couplings are not given, since they may be obtained directly from the strengths in *LS* coupling by use of formulae (6) and (9).

## II. THE NUMERICAL CALCULATIONS

The wave numbers of the forbidden lines were computed from the term levels given in various sources. Most of the sources used for the term levels of atoms in the $p^k$ configurations are listed in the bibliography of a paper by Robinson and Shortley.[14] The term levels for *Fe* VII (except for the $^1S_0$ term) were taken from the results of

[13] *Phys. Rev.*, **40**, 185, 1932.

[14] *Phys. Rev.*, **52**, 713, 1937. For *Cl* II the term values were obtained from C. C. Kiess and T. L. de Bruin, *Bur. of Standards, J. of Research*, **23**, 443, 1939.

## TABLE 2

### ELECTRIC QUADRUPOLE LINE STRENGTHS IN *LS* COUPLING

*a*) THE $p^2$ CONFIGURATION

| | $^1D_2$ | $^3P_2$ | $^3P_1$ | $^3P_0$ | $^1S_0$ |
|---|---|---|---|---|---|
| $^1D_2$ | 28(−) | 0 | 0 | 0 | 16(−) |
| $^3P_2$ | | 7(+) | 9(−) | 4(−) | 0 |
| $^3P_1$ | | | 3(−) | 0 | 0 |
| $^3P_0$ | | | | 0 | 0 |
| $^1S_0$ | | | | | 0 |

$\times \frac{s_2^2}{15}$

*b*) THE $p^3$ CONFIGURATION

| | $^2D_{2\frac{1}{2}}$ | $^2D_{1\frac{1}{2}}$ | $^4S_{1\frac{1}{2}}$ | $^2P_{1\frac{1}{2}}$ | $^2P_{\frac{1}{2}}$ |
|---|---|---|---|---|---|
| $^2D_{2\frac{1}{2}}$ | 0 | 0 | 0 | 56(+) | 16(−) |
| $^2D_{1\frac{1}{2}}$ | | 0 | 0 | 24(+) | 24(+) |
| $^4S_{1\frac{1}{2}}$ | | | 0 | 0 | 0 |
| $^2P_{1\frac{1}{2}}$ | | | | 0 | 0 |
| $^2P_{\frac{1}{2}}$ | | | | | 0 |

$\times \frac{s_2^2}{25}$

*c*) THE $d^2$ CONFIGURATION

| | $^1G_4$ | $^3F_4$ | $^3F_3$ | $^3F_2$ | $^1D_2$ | $^3P_2$ | $^3P_1$ | $^3P_0$ | $^1S_0$ |
|---|---|---|---|---|---|---|---|---|---|
| $^1G_4$ | 39,600(−) | 0 | 0 | 0 | 5,760(−) | 0 | 0 | 0 | 0 |
| $^3F_4$ | | 2,475(−) | 525(+) | 24(−) | 0 | 12,096(−) | 0 | 0 | 0 |
| $^3F_3$ | | | 9,261(−) | 504(+) | 0 | 3,136(−) | 6,272(−) | 0 | 0 |
| $^3F_2$ | | | | 1,152(−) | 0 | 448(−) | 3,136(−) | 3,136(−) | 0 |
| $^1D_2$ | | | | | 1,800(+) | 0 | 0 | 0 | 0 |
| $^3P_2$ | | | | | | 4,802(+) | 6,174(−) | 2,744(+) | 0 |
| $^3P_1$ | | | | | | | 2,058(−) | 0 | 0 |
| $^3P_0$ | | | | | | | | 0 | 0 |
| $^1S_0$ | | | | | | | | | 0 |

$\times \frac{s_2^2}{10,290}$

*d*) THE $d^3$ CONFIGURATION

| | $^4F_{4\frac{1}{2}}$ | $^4F_{3\frac{1}{2}}$ | $^4F_{2\frac{1}{2}}$ | $^4F_{1\frac{1}{2}}$ | $^4P_{2\frac{1}{2}}$ | $^4P_{1\frac{1}{2}}$ | $^4P_{\frac{1}{2}}$ |
|---|---|---|---|---|---|---|---|
| $^4F_{4\frac{1}{2}}$ | 96,250(+) | 27,500(−) | 2,250(+) | 0 | 504,000(−) | 0 | 0 |
| $^4F_{3\frac{1}{2}}$ | | 40,000(+) | 30,420(−) | 2,880(+) | 161,280(−) | 241,920(−) | 0 |
| $^4F_{2\frac{1}{2}}$ | | | 19,602(+) | 23,328(−) | 36,288(−) | 172,032(−) | 94,080(−) |
| $^4F_{1\frac{1}{2}}$ | | | | 24,192(+) | 4,032(+) | 56,448(−) | 141,120(−) |
| $^4P_{2\frac{1}{2}}$ | | | | | 172,872(−) | 259,308(+) | 185,220(−) |
| $^4P_{1\frac{1}{2}}$ | | | | | | 131,712(+) | 20,580(−) |
| $^4P_{\frac{1}{2}}$ | | | | | | | 0 |

$\times \frac{s_2^2}{385,875}$

TABLE 2—*Continued*

*d*) THE $d^3$ CONFIGURATION (*continued*)

| | $^2H_{5/2}$ | $^2H_{3/2}$ | $^2G_{9/2}$ | $^2G_{7/2}$ | $^2F_{7/2}$ | $^2F_{5/2}$ | $a^2D_{5/2}$ | $a^2D_{3/2}$ | $b^2D_{3/2}$ | $b^2D_{1/2}$ | $^2P_{1/2}$ | $^2P_{3/2}$ |
|---|---|---|---|---|---|---|---|---|---|---|---|---|
| $^2H_{5/2}$ | 412,776(−) | 19,656(+) | 64,064(−) | 2,464(+) | 332,640(−) | 0 | 0 | 0 | 0 | 0 | 0 | 0 |
| $^2H_{3/2}$ | | 340,704(−) | 3,696(−) | 51,744(−) | 15,840(−) | 261,360(−) | 0 | 0 | 0 | 0 | 0 | 0 |
| $^2G_{9/2}$ | | | 27,104(−) | 1,936(+) | 116,160(−) | 7,040(+) | 231,000(−) | 0 | 11,000(−) | 0 | 0 | 0 |
| $^2G_{7/2}$ | | | | 21,296(−) | 10,560(−) | 88,000(−) | 18,480(−) | 166,320(−) | 880(−) | 7,920(−) | 0 | 0 |
| $^2F_{7/2}$ | | | | | 39,600(−) | 4,752(+) | 99,792(−) | 11,088(+) | 384,912(−) | 42,768(+) | 50,688(−) | 0 |
| $^2F_{5/2}$ | | | | | | 28,512(−) | 16,632(−) | 66,528(−) | 64,152(−) | 256,608(−) | 8,448(−) | 29,568(−) |
| $a^2D_{5/2}$ | | | | | | | 38,808(−) | 9,702(+) | 149,688(−) | 37,422(+) | 135,828(+) | 38,808(−) |
| $a^2D_{3/2}$ | | | | | | | | 22,638(−) | 37,422(+) | 87,318(−) | 58,212(+) | 58,212(+) |
| $b^2D_{5/2}$ | | | | | | | | | 7,128(−) | 1,782(+) | 6,468(−) | 1,848(+) |
| $b^2D_{3/2}$ | | | | | | | | | | 4,158(−) | 2,772(−) | 2,772(−) |
| $^2P_{1/2}$ | | | | | | | | | | | 7,392(+) | 7,392(−) |
| $^2P_{3/2}$ | | | | | | | | | | | | 0 |

$\times \frac{s_2^2}{169,785}$

Bowen and Edlén,[15] the $^1S_0$ value (65,707 $cm^{-1}$) being taken from some unpublished work of Edlén. The term levels for *Cr* IV, *Mn* V, and *Fe* VI were obtained from I. S. Bowen.[16] The latter has recently made a more complete analysis of the spectra of these elements. With his permission, the new levels of the $d^3$ configuration are recorded here in Table 3. The other $^2D$ term, and the $^2F$ term, could not be determined for these elements. Approximate values for these terms were obtained by use of the Slater formulae (*CS*, §§ 5[7] and 7[8]).

The matrices of spin-orbit interaction involve the parameter $\zeta_{nl}$. For the $p^2$ configuration, the values of $\zeta_{np}$ were taken directly from

TABLE 3

NEW LEVELS OF THE $d^3$ CONFIGURATION

| Multiplet | *Cr* IV | *Mn* V | *Fe* VI |
|---|---|---|---|
| $^2P_{1/2}$ | ..... | 23,078 | 26,483 |
| $^2P_{1\frac{1}{2}}$ | 19,429 | 22,902 | 26,204 |
| $^2D_{1\frac{1}{2}}$ | 20,642 | 24,651 | 28,607 |
| $^2D_{2\frac{1}{2}}$ | 20,661 | 24,610 | 28,469 |

the paper of Robinson and Shortley, in which the parameters $F_2(np, np)$ and $\zeta_{np}$ were calculated by applying the intermediate coupling theory to the intervals $^3P_c - {}^1D_2$ and $^3P_0 - {}^3P_2$. The values of $F_2(2p, 2p)$ would be increased by a factor of 1.4 if the interval $^1D_2 - {}^1S_0$ were used instead of the interval $^3P_c - {}^1D_2$, since the ratio of these intervals is only 1.14 for the elements in the $2p^2$ configuration, instead of the theoretical value of 1.5. However, this change in $F_2$ would not change the value of $\zeta_{2p}$ greatly. Also, the $^3P_c - {}^1D_2$ interval is the more natural one to use, since it is not affected very much by configuration interaction. The $^1D_2 - {}^1S_0$ interval, on the other hand, is greatly altered in magnitude by the interaction of the $2p^2$ configuration with the $2pnp$ and $2p^4$ configurations.[17]

For the $p^4$ configuration Robinson and Shortley used the intervals $^1D_2 - {}^1S_0$ and $^3P_2 - {}^3P_1$. Since in this case also the $^1D_2 - {}^1S_0$

[15] *Nature*, **143**, 374, 1939. [16] *Phys. Rev.*, **47**, 924, 1935; **52**, 1153, 1937.

[17] D. R. Hartree and B. Swirles, *Proc. Cambridge Phil. Soc.*, **33**, 240, 1937; D. R. Hartree, W. Hartree, and B. Swirles, *Phil. Trans. R. Soc., London*, A, **238**, 229, 1939.

interval is greatly affected by configuration interaction, it was considered advisable to recalculate the values of $\zeta_{np}$ and $F_2$, using the intervals $^3P_c - {}^1D_2$ and $^3P_2 - {}^3P_1$. For the $3p^3$ configuration Robinson and Shortley calculated the parameters from the $^2D_c - {}^2P_c$ and $^2P_{3/2} - {}^2P_{1/2}$ intervals, and their values were used here. For several elements in the $2p^3$ configuration the doublets are inverted, and hence it was necessary to obtain the values of $\zeta_{2p}$ by interpolation between the $2p^2$ and $2p^4$ configurations.

For the $d^2$ and $d^3$ configurations, the parameters $\zeta_{nd}$ were chosen by a trial-and-error method to give as good a fit as possible to the observed intramultiplet separations. The displacements of the energy levels from the mean term positions, owing to the spin-orbit interaction, were calculated by means of the approximate formula

$$E_i = E_i^0 + H'_{ii} + \sum_j \frac{(H'_{ij})^2}{E_i - E_j},$$

or by a successive approximation method in cases where this formula was not sufficiently accurate. The calculated separations are compared with the observed separations in Tables 4 and 5. In the columns headed "Calculated Separation," for *Fe* VII and *Cr* IV, the first term gives the separations calculated if only the diagonal elements of the spin-orbit interaction are taken into account. The second term gives the corrections due to the nondiagonal elements, which are seen to be large in many cases. The effect for *Mn* V and *Fe* VI is similar to that for *Cr* IV.

In the calculations of the multiplet separations for the $d^3$ configuration it was necessary to have values of the coefficients $\alpha$ and $\beta$ of equation (11). These are given in *CS*, § 7[8], in terms of the Slater parameters $F_2$ and $F_4$. The latter parameters were evaluated by fitting the Slater formulae (*CS*, § 5[7]) to the mean term positions of the $^2H$, $^4P$, and $^4F$ terms, which, according to Ufford,[18] are not affected by interaction with the configurations $nd^2n'$s and $ndn'^2$s. (The positions of the other terms of the $d^3$ configuration, calculated from these values of $F_2$ and $F_4$, are higher than the observed positions, as

[18] *Phys. Rev.*, **44**, 732, 1933.

they should be, but the differences between the calculated and observed values do not agree very well with Ufford's formulae. How-

TABLE 4

MULTIPLET SEPARATIONS FOR THE $d^2$ CONFIGURATION OF *Fe* VII

| Multiplet | Calculated Separation ($\zeta_{3d}=645$) | Observed Separation |
|---|---|---|
| $^3F$ | $967+57=1024$ | 1047 |
| | $1290-16=1274$ | 1280 |
| $^3P$ | $645+245=890$ | 847 |
| | $322+55=377$ | 391 |

TABLE 5

MULTIPLET SEPARATIONS FOR THE $d^3$ CONFIGURATION

| Multiplet | *Cr* IV ($\zeta_{3d}=275$) | | *Mn* V ($\zeta_{3d}=415$) | | *Fe* VI ($\zeta_{3d}=585$) | |
|---|---|---|---|---|---|---|
| | Calc. | Obs. | Calc. | Obs. | Calc. | Obs. |
| $^2H$ | $303-36=267$ | 253 | 387 | 362 | 520 | 473 |
| $^2G$ | $371-23=348$ | 349 | 517 | 504 | 712 | 696 |
| $^2F$ | $-160+11=-149$ | ..... | $-220$ | ..... | $-301$ | ..... |
| $y^2D$ | $-152+10=-142$ | ..... | $-203$ | ..... | $-273$ | ..... |
| $z^2D$ | $381-370=11$ | 19 | $-59$ | $-41$ | $-152$ | $-138$ |
| $^2P$ | $275-337=-62$ | ..... | $-143$ | $-176$ | $-229$ | $-279$ |
| $^4F$ | $413-9=404$ | 396 | 605 | 579 | 847 | 809 |
| | $321+4=325$ | 316 | 491 | 478 | 694 | 675 |
| | $229+8=237$ | 237 | 361 | 349 | 514 | 510 |
| $^4P$ | $229+47=276$ | 299 | 434 | 456 | 639 | 664 |
| | $138-33=105$ | 119 | 143 | 160 | 181 | 203 |

ever, this choice of terms for the calculation of the parameters is apparently the best available.) It is interesting that the values of $\alpha$ and $\beta$ thus obtained are nearly the same for the three atoms treated. Thus, $\alpha$ turns out to be 0.9012, 0.9030, and 0.9041 for *Cr* IV, *Mn* V,

and *Fe* VI, respectively.[19] This may be compared with Ufford's value of 0.8905 for *Ti* II.

The coefficients $a_{ij}$ were determined in the usual way by solving the secular equations. The first-order energies, $E_i'$, were determined either by use of the approximate formula

$$E_i - E_i' = \sum_j \frac{(H_{ij}')^2}{E_i - E_j}$$

or by a successive-approximation method in cases where this formula was not sufficiently accurate. For the $p^k$ configurations, especially in the lower stages of ionization, there would be little loss in accuracy if one used the first-order approximation formula

$$a_{ij} = \frac{H_{ij}'}{E_i^0 - E_j^0},$$

except where $H_{ij}'$ vanished, in which case the second-order approximation would have to be used.[20] However, in the $d^2$ and $d^3$ configurations, some of the coefficients were too large to be determined in this way.

The expressions for the transition probabilities in the electric quadrupole case also involve the square of the integral

$$s_2(n, l) = -e\int_0^\infty \{R(n, l)\}^2 r^2 dr .$$

These integrals were evaluated numerically by Condon[21] for *O* I, *O* II, and *O* III, using Hartree self-consistent field wave functions

[19] In obtaining these values, allowance was made for the displacement of the mean term positions due to the spin-orbit interaction. This correction, however, made practically no difference to the values of $\alpha$ and $\beta$.

[20] In the calculations for the $p^k$ configurations which were published by the author in a preliminary report in the *Pub. A.S.P.*, **51**, 160, 1939, these approximate formulae were used for the $a_{ij}$. The denominators in these formulae were determined by use of the Slater formulae, the values of $F_2$ being taken from the paper of Robinson and Shortley, *loc. cit.* However, it was subsequently decided that it would be more logical to use the observed energy levels, since the spin-orbit interaction effects depend on the actual separations of the levels involved. Also, the secular equations were solved directly without the aid of the approximate formulae.

[21] *Loc. cit.*

calculated by Hartree and Black.[22] However, such wave functions were not available for all the atoms treated here, so that a cruder approximation was necessary. It was decided to compute $s_2$ by using hydrogen-like wave functions, together with appropriate screening constants. The integral is then given by the formula, in atomic units,

$$s_2(n, l) = \frac{n^2(5n^2 + 1 - 3l^2 - 3l)}{2(Z - \sigma_{nl})^2} .$$

For the $p^2$ and $p^3$ configurations, the screening constants were determined by applying the hydrogen-like formulae for $F_2$ to the values obtained by Robinson and Shortley. For the $p^4$ configuration, the values of $F_2$ calculated from the interval $^3P_c - {}^1D_2$ were used.[23] These hydrogen-like formulae for $F_2$ are:[24]

$$F_2(2p, 2p) = 771.6(Z - S_{2p}) ,$$
$$F_2(3p, 3p) = 315.9(Z - S_{3p}) ,$$
$$F_2(4p, 4p) = 174.9(Z - S_{4p}) .$$

The screening constants for $F_2$ were used, rather than those for $\zeta$, because $\zeta$ is essentially an average value of $r^{-3}$, whereas $F_2$ is essentially an average value of $r^{-1}$ and $-s_2/e$ is the mean value of $r^2$. Hence, the screening constant for $F_2$ should be closer to the true screening constant for $s_2$ than that of $\zeta$. For the $d^2$ and $d^3$ configurations, the screening constants were determined from the absolute term energies by the formula

$$\nu(n, l) = \frac{R}{n^2}(Z - \sigma'_{nl})^2 .$$

[22] *Proc. R. Soc.*, A, **139**, 311, 1933.

[23] In obtaining the preliminary results published in the *Pub. A.S.P.*, **51**, 160, 1939, Robinson and Shortley's values of $F_2$ were used for the $p^4$ configuration. Also, the screening constants were determined from the intercepts on the $Z$-axis of Robinson and Shortley's graphs of $F_2$. This change in method of computing $s_2$ is responsible for the greater part of the differences which occur between the formerly published results and those given in the present article.

[24] For the $2p^3$ configuration the numerical constant in the expression for $F_2$ was taken to be 625 instead of 771.6, since the latter did not fit the data well.

This method was not used for the $p^k$ configurations, since it is not likely to give satisfactory values of the screening constants for atoms in low stages of ionization.

In order to give an idea of the uncertainties involved in the calculation of the integral $s_2$, Table 6 lists the values of $s_2$ obtained for

TABLE 6

COMPARATIVE VALUES OF THE INTEGRALS $s_2(n, l)$
(In Atomic Units)

| Configuration | Atom | $s_2$ from Approximate Wave Functions | $s_2$ from Screening Constants of $F_2$, $F_4$ | $s_2$ from Screening Constants of Absolute Term Values |
|---|---|---|---|---|
| $2p^2$ | *C* I | 5.35 | 6.23 | 9.06 |
| | *N* II | 2.5 | 2.78 | 3.45 |
| | *O* III | 1.32 | 1.59 | 1.86 |
| | *Al* VIII | ..... | 0.337 | 0.357 |
| $3p^2$ | *Si* I | ..... | 17.3 | 33.4 |
| | *Cl* IV | ..... | 3.96 | 5.09 |
| $2p^3$ | *N* I | 3.45 | 4.58 | 7.01 |
| | *O* II | 1.75 | 2.25 | 2.90 |
| | *Si* VIII | ..... | 0.323 | 0.335 |
| $2p^4$ | *O* I | 2.44 | 2.58 | 7.49 |
| | *Si* VII | ..... | 0.352 | 0.415 |
| $3d^2$ | *Ti* III | ..... | 7.62 | 6.46 |
| | *Fe* VII | ..... | 1.38 | 1.52 |

several atoms, using both of the approximate methods described above. For *O* I, *O* II, and *O* III the values of $s_2$ obtained by numerical integration, using the Hartree-Black approximate wave functions,[25] are also tabulated; and for *C* I, *N* I, and *N* II the values obtained by Condon[26] from the Brown, Bartlett, and Dunn approximate wave functions are listed.[27]

[25] *Loc. cit.*

[26] *Loc. cit.*

[27] The results shown in Table 5 suggest that the transition probabilities for *C* I, *N* I, *N* II, *O* I, *O* II, and *O* III would probably be somewhat improved if the *quadrupole* probabilities of Tables 7*a*–7*f* were multiplied by the ratios of the values of $s_2^2$ obtained from the third and fourth columns of Table 6.

### III. THE NUMERICAL RESULTS

In Tables 7*a*–7*f* are listed the transition probabilities for about fifty atoms in the configurations $np^2$, $np^3$, and $np^4$ (where $n = 2$ or 3). The magnetic dipole and electric quadrupole probabilities are

TABLE 7*a*

TRANSITION PROBABILITIES FOR THE $2p^2$ CONFIGURATION*

| Transition | | *C* I | *N* II | *O* III | *F* IV | *Ne* V | *Na* VI | *Mg* VII | *Al* VIII |
|---|---|---|---|---|---|---|---|---|---|
| $^1D_2-{}^1S_0$ | *e* | 1.4 | 2.2 | 2.8 | 4.2 | 4.2 | 4.4 | ..... | ..... |
| | λ | 8727.4 | *5755.0* | *4363.2* | 3532.2 | 2972 | ..... | ..... | ..... |
| $^3P_2-{}^1S_0$ | *e* | $0.0^{4}32$† | $0.0^{3}23$ | $0.0^{3}96$ | 0.0038 | 0.0089 | 0.020 | ..... | ..... |
| | λ | 4627.3 | 3070.8 | ..... | ..... | ..... | ..... | ..... | ..... |
| $^3P_1-{}^1S_0$ | *m* | 0.0017 | 0.025 | 0.19 | 0.94 | 3.6 | 12 | ..... | ..... |
| | λ | 4621.4 | 3063.0 | ..... | ..... | ..... | ..... | ..... | ..... |
| $^3P_2-{}^1D_2$ | *m* | $0.0^{3}15$ | 0.0022 | 0.016 | 0.081 | 0.31 | 1.1 | 2.9 | 6.1 |
| | *e* | $0.0^{5}21$ | $0.0^{4}14$ | $0.0^{4}57$ | $0.0^{3}22$ | $0.0^{3}51$ | 0.0012 | 0.0026 | 0.0043 |
| | λ | 9849.5 | *6583.9* | *5007.6* | *4059.3* | *3425.8* | ..... | ..... | ..... |
| $^3P_1-{}^1D_2$ | *m* | $0.0^{4}50$ | $0.0^{3}75$ | 0.0056 | 0.028 | 0.11 | 0.39 | 1.1 | 2.4 |
| | *e* | $0.0^{6}30$ | $0.0^{5}20$ | $0.0^{5}86$ | $0.0^{4}34$ | $0.0^{4}82$ | $0.0^{3}20$ | $0.0^{3}47$ | $0.0^{3}84$ |
| | λ | 9822.9 | *6548.4* | *4959.5* | *3996.3* | *3345.8* | ..... | ..... | ..... |
| $^3P_0-{}^1D_2$ | *e* | $0.0^{6}11$ | $0.0^{6}67$ | $0.0^{5}28$ | $0.0^{4}11$ | $0.0^{4}26$ | $0.0^{4}68$ | $0.0^{3}16$ | $0.0^{3}29$ |
| | λ | 9808.6 | 6527.4 | *4931.8* | 3960.6 | ..... | ..... | ..... | ..... |
| $^3P_1-{}^3P_2$ | *m* | $0.0^{6}28$ | $0.0^{5}75$ | $0.0^{4}98$ | $0.0^{3}79$ | 0.0046 | 0.021 | 0.080 | 0.25 |
| | *e* | $0.0^{13}12$ | $0.0^{12}58$ | $0.0^{10}14$ | $0.0^{9}23$ | $0.0^{8}18$ | $0.0^{7}12$ | $0.0^{7}68$ | $0.0^{6}30$ |
| $^3P_0-{}^3P_2$ | *e* | $0.0^{13}47$ | $0.0^{11}27$ | $0.0^{10}61$ | $0.0^{8}10$ | $0.0^{8}80$ | $0.0^{7}55$ | $0.0^{6}34$ | $0.0^{5}11$ |
| $^3P_0-{}^3P_1$ | *m* | $0.0^{7}58$ | $0.0^{5}21$ | $0.0^{4}26$ | $0.0^{3}21$ | 0.0012 | 0.0061 | 0.026 | 0.046 |
| $\zeta_{2p}(cm^{-1})$ | ..... | 27.1 | 85.0 | 201 | 405 | 730 | 1230 | 1940 | 2650 |
| $s_2$ (atomic units) | ..... | 6.23 | 2.78 | 1.59 | 1.13 | 0.738 | 0.526 | 0.416 | 0.337 |

* Rows labeled *m* contain magnetic dipole transition probabilities. Rows labeled *e* contain electric quadrupole transition probabilities. Rows labeled λ contain wave lengths. The wave lengths of lines observed in nebular spectra are set in italics.

† $0.0^{4}32$ is used, for brevity, to denote 0.000032. In general, $0.0^{n}r$ denotes $r \times 10^{-n-1}$.

listed separately (in the rows labeled *m* and *e*, respectively) in order to indicate the relative contributions of the two types of radiation to the total transition probabilities. The total transition probabilities are immediately obtained by summing the two. Blank spaces in the tables indicate cases where the term analysis was not sufficiently

complete to provide the necessary data for the calculations. In these tables (in the rows labeled λ) there are also given for convenience the wave lengths of the astronomically observable lines (2900–10,000 A). Many of these wave lengths were taken from an article

TABLE 7*b*

TRANSITION PROBABILITIES FOR THE $3p^2$ CONFIGURATION*

| Transition | | *Si* I | *P* II | *S* III | *Cl* IV | *A* V | *K* VI | *Ca* VII |
|---|---|---|---|---|---|---|---|---|
| $^1D_2-{}^1S_0$ | *e* | 3.3 | 4.6 | 5.6 | 6.6 | 7.3 | ..... | ..... |
| | λ | ..... | 7869.5 | *6310.2* | *5322.2* | ..... | ..... | ..... |
| $^3P_2-{}^1S_0$ | *e* | 0.0046 | 0.015 | 0.038 | 0.081 | 0.16 | ..... | ..... |
| | λ | 6589.7 | 4736.6 | 3796.8 | 3203.3 | ..... | ..... | ..... |
| $^3P_1-{}^1S_0$ | *m* | 0.036 | 0.22 | 0.87 | 2.6 | 6.8 | ..... | ..... |
| | λ | 6526.9 | 4669.5 | *3721.1* | 3118.3 | ..... | ..... | ..... |
| $^3P_2-{}^1D_2$ | *m* | 0.0027 | 0.017 | 0.066 | 0.20 | 0.51 | 1.2 | 2.5 |
| | *e* | $0.0^3310$ | $0.0^332$ | $0.0^379$ | 0.0017 | 0.0031 | 0.0056 | 0.010 |
| | λ | ..... | ..... | 9532.5 | 8046.1 | *7003* | *6229* | 5616 |
| $^3P_1-{}^1D_2$ | *m* | $0.0^396$ | 0.0062 | 0.025 | 0.080 | 0.22 | 0.55 | 1.2 |
| | *e* | $0.0^417$ | $0.0^454$ | $0.0^315$ | $0.0^333$ | $0.0^369$ | 0.0014 | 0.0029 |
| | λ | ..... | ..... | 9069.6 | 7530.9 | *6432* | *5603* | 4939 |
| $^3P_0-{}^1D_2$ | *e* | $0.0^526$ | $0.0^583$ | $0.0^421$ | $0.0^449$ | $0.0^497$ | $0.0^320$ | $0.0^343$ |
| | λ | ..... | ..... | 8831.5 | 7262.3 | 6131 | 5269 | 4571 |
| $^3P_1-{}^3P_2$ | *m* | $0.0^442$ | $0.0^338$ | 0.0021 | 0.0083 | 0.027 | 0.077 | 0.19 |
| | *e* | $0.0^940$ | $0.0^840$ | $0.0^728$ | $0.0^614$ | $0.0^656$ | $0.0^519$ | $0.0^565$ |
| $^3P_0-{}^3P_2$ | *e* | $0.0^815$ | $0.0^716$ | $0.0^611$ | $0.0^661$ | $0.0^527$ | $0.0^410$ | $0.0^438$ |
| $^3P_0-{}^3P_1$ | *m* | $0.0^582$ | $0.0^483$ | $0.0^347$ | 0.0021 | 0.0080 | 0.026 | 0.077 |
| $\zeta_{3P}$ ($cm^{-1}$) | ..... | 148 | 314 | 555 | 885 | 1330 | 1920 | 2650 |
| $s_2$ (atomic units) | ..... | 17.3 | 8.79 | 5.61 | 3.96 | 2.94 | 2.29 | 1.85 |

* See notes below Table 7*a*.

by Bowen and Wyse,[28] and the rest were calculated from the term values given in the various sources mentioned in that article. The lines which Bowen and Wyse list as already observed are indicated by setting the corresponding wave lengths in italic type.

Tables 8 and 9 contain similar results for the $d^2$ configuration of *Fe* VII and for the $d^3$ configuration of *Cr* IV, *Mn* V, and *Fe* VI. In

[28] *Lick Obs. Bull.*, **19**, 1, 1940.

these tables also the labels *m*, *e*, and λ refer, respectively, to magnetic dipole transition probabilities, electric quadrupole transition probabilities, and wave lengths of observable lines. The observed lines are again indicated by setting the corresponding wave lengths in italic type.

TABLE 7*c*

TRANSITION PROBABILITIES FOR THE $2p^3$ CONFIGURATION*

| Transition | | *N* I | *O* II | *F* III | *Ne* IV | *Na* V | *Mg* VI | *Al* VII | *Si* VIII |
|---|---|---|---|---|---|---|---|---|---|
| $^2P_{\frac{1}{2}}-{}^2P_{1\frac{1}{2}}$ | *m* | ..... | $0.0^{10}61$ | ..... | $0.0^{8}90$ | $0.0^{6}53$ | $0.0^{4}16$ | $0.0^{3}15$ | $0.0^{3}22$ |
| | *e* | ..... | $0.0^{24}66$ | ..... | $0.0^{20}48$ | $0.0^{17}46$ | $0.0^{14}15$ | $0.0^{13}65$ | $0.0^{12}12$ |
| $^2D_{2\frac{1}{2}}-{}^2P_{1\frac{1}{2}}$ | *m* | 0.0010 | 0.0088 | 0.049 | 0.20 | 0.67 | 2.0 | 4.6 | 11 |
| | *e* | 0.16 | 0.23 | 0.29 | 0.37 | 0.42 | 0.49 | 0.56 | 0.65 |
| | λ | ..... | *7319.0* | 5721.2 | 4714.1 | 4015.3 | 3488.1 | 3074.0 | ..... |
| $^2D_{1\frac{1}{2}}-{}^2P_{1\frac{1}{2}}$ | *m* | 0.0018 | 0.016 | 0.086 | 0.38 | 1.2 | 3.5 | 8.3 | 20 |
| | *e* | 0.069 | 0.097 | 0.12 | 0.16 | 0.18 | 0.21 | 0.24 | 0.28 |
| | λ | ..... | *7330.3* | 5733.0 | 4719.7 | 4021.6 | 3503.0 | 3098.7 | ..... |
| $^4S_{1\frac{1}{2}}-{}^2P_{1\frac{1}{2}}$ | *m* | 0.0067 | 0.057 | 0.32 | ..... | 4.3 | 12 | 29 | 69 |
| | *e* | $0.0^{8}18$ | $0.0^{7}22$ | $0.0^{6}20$ | ..... | $0.0^{5}57$ | $0.0^{4}25$ | $0.0^{4}75$ | $0.0^{3}24$ |
| | λ | 3466.4 | ..... | ..... | ..... | ..... | ..... | ..... | ..... |
| $^2D_{2\frac{1}{2}}-{}^2P_{\frac{1}{2}}$ | *e* | 0.093 | 0.13 | 0.17 | 0.21 | 0.24 | 0.28 | 0.31 | 0.36 |
| | λ | ..... | *7319.0* | 5721.2 | 4714.1 | 4011.2 | 3485.5 | 3068.8 | ..... |
| $^2D_{1\frac{1}{2}}-{}^2P_{\frac{1}{2}}$ | *m* | 0.0011 | 0.0097 | 0.054 | 0.22 | 0.74 | 2.2 | 5.1 | 12 |
| | *e* | 0.14 | 0.19 | 0.25 | 0.31 | 0.36 | 0.41 | 0.47 | 0.56 |
| | λ | ..... | *7330.3* | 5733.0 | 4719.7 | 4017.5 | 3500.4 | 3093.4 | ..... |
| $^4S_{1\frac{1}{2}}-{}^2P_{\frac{1}{2}}$ | *m* | 0.0027 | 0.023 | 0.13 | ..... | 1.7 | 5.0 | 12 | 29 |
| | *e* | $0.0^{8}37$ | $0.0^{7}47$ | $0.0^{6}43$ | ..... | $0.0^{4}14$ | $0.0^{4}60$ | $0.0^{3}18$ | $0.0^{3}58$ |
| | λ | 3466.4 | ..... | ..... | ..... | ..... | ..... | ..... | ..... |
| $^2D_{1\frac{1}{2}}-{}^2D_{2\frac{1}{2}}$ | *m* | $0.0^{8}83$ | $0.0^{6}15$ | $0.0^{6}76$ | $0.0^{6}25$ | $0.0^{6}25$ | $0.0^{6}15$ | $0.0^{5}19$ | $0.0^{5}21$ |
| | *e* | $0.0^{20}45$ | $0.0^{18}42$ | $0.0^{17}62$ | $0.0^{17}11$ | $0.0^{17}12$ | $0.0^{18}54$ | $0.0^{16}48$ | $0.0^{12}13$ |
| $^4S_{1\frac{1}{2}}-{}^2D_{2\frac{1}{2}}$ | *m* | $0.0^{8}84$ | $0.0^{6}22$ | $0.0^{5}33$ | ..... | $0.0^{3}22$ | 0.0012 | 0.0046 | 0.019 |
| | *e* | $0.0^{4}21$ | $0.0^{4}85$ | $0.0^{3}29$ | ..... | 0.0018 | 0.0040 | 0.0074 | 0.014 |
| | λ | *5200.7* | *3729.1* | 2933.1 | ..... | ..... | ..... | ..... | ..... |
| $^4S_{1\frac{1}{2}}-{}^2D_{1\frac{1}{2}}$ | *m* | $0.0^{6}51$ | $0.0^{4}13$ | $0.0^{3}19$ | ..... | 0.012 | 0.069 | 0.26 | 1.1 |
| | *e* | $0.0^{4}14$ | $0.0^{4}55$ | $0.0^{3}18$ | ..... | 0.0011 | 0.0025 | 0.0047 | 0.0090 |
| | λ | *5198.5* | *3726.2* | 2930.0 | ..... | ..... | ..... | ..... | ..... |
| $\zeta_{2p}$ ($cm^{-1}$) | ..... | 72 | 178 | 371 | 684 | 1155 | 1835 | 2650 | 3860 |
| $s_2$ (atomic units) | ..... | 4.58 | 2.25 | 1.38 | 0.955 | 0.684 | 0.522 | 0.408 | 0.323 |

* See notes below Table 7*a*.

## IV. DISCUSSION OF THE RESULTS

*a) Accuracy of the calculations.*—A major uncertainty in the calculation of the transition probabilities lies in the central field ap-

TABLE 7*d*

TRANSITION PROBABILITIES FOR THE $3p^3$ CONFIGURATION*

| Transition | | *P* I | *S* II | *Cl* III | *A* IV | *K* V | *Ca* VI | *Sc* VII |
|---|---|---|---|---|---|---|---|---|
| $^2P_{1/2}-{}^2P_{1\frac{1}{2}}$ | *m* | 0.$0^6$15 | 0.$0^5$10 | 0.$0^5$77 | 0.$0^4$53 | 0.$0^3$29 | 0.0015 | 0.0065 |
| | *e* | 0.$0^{15}$18 | 0.$0^{14}$20 | 0.$0^{13}$43 | 0.$0^{12}$94 | 0.$0^{10}$15 | 0.$0^9$22 | 0.$0^8$26 |
| $^2D_{2\frac{1}{2}}-{}^2P_{1\frac{1}{2}}$ | *m* | 0.017 | 0.057 | 0.16 | 0.42 | 0.98 | 2.1 | 4.3 |
| | *e* | 0.30 | 0.38 | 0.48 | 0.57 | 0.67 | 0.78 | 0.91 |
| | λ | ..... | ..... | 8481.6 | 7236.0 | 6316.6 | 5587.2 | 4986.6 |
| $^2D_{1\frac{1}{2}}-{}^2P_{1\frac{1}{2}}$ | *m* | 0.031 | 0.10 | 0.29 | 0.76 | 1.8 | 3.9 | 9.1 |
| | *e* | 0.13 | 0.17 | 0.21 | 0.25 | 0.29 | 0.35 | 0.41 |
| | λ | ..... | ..... | 8433.7 | 7169.1 | 6223.4 | 5460.0 | 4823.5 |
| $^4S_{1\frac{1}{2}}-{}^2P_{1\frac{1}{2}}$ | *m* | 0.099 | 0.32 | 0.90 | 2.3 | 5.4 | 12 | ..... |
| | *e* | 0.$0^5$15 | 0.$0^5$39 | 0.$0^4$13 | 0.$0^4$39 | 0.$0^3$11 | 0.$0^3$29 | ..... |
| | λ | 5332.4 | *4068.5* | *3342.7* | ..... | ..... | ..... | ..... |
| $^2D_{2\frac{1}{2}}-{}^2P_{\frac{1}{2}}$ | *e* | 0.17 | 0.22 | 0.27 | 0.31 | 0.35 | 0.39 | 0.43 |
| | λ | ..... | ..... | 8550.5 | 7332.0 | 6446.5 | 5766.4 | 5223.8 |
| $^2D_{1\frac{1}{2}}-{}^2P_{\frac{1}{2}}$ | *m* | 0.019 | 0.062 | 0.18 | 0.46 | 1.1 | 2.3 | 4.8 |
| | *e* | 0.25 | 0.33 | 0.41 | 0.48 | 0.56 | 0.64 | 0.74 |
| | λ | ..... | ..... | 8501.8 | 7263.3 | 6349.5 | 5631.0 | 5045.0 |
| $^4S_{1\frac{1}{2}}-{}^2P_{\frac{1}{2}}$ | *m* | 0.040 | 0.13 | 0.37 | 0.95 | 2.2 | 4.8 | ..... |
| | *e* | 0.$0^4$10 | 0.$0^4$27 | 0.$0^4$86 | 0.$0^3$26 | 0.$0^3$76 | 0.0020 | ..... |
| | λ | 5339.7 | *4076.5* | 3353.4 | ..... | ..... | ..... | ..... |
| $^2D_{1\frac{1}{2}}-{}^2D_{2\frac{1}{2}}$ | *m* | 0.$0^7$35 | 0.$0^6$34 | 0.$0^5$32 | 0.$0^4$23 | 0.$0^3$14 | 0.$0^3$76 | 0.0032 |
| | *e* | 0.$0^{16}$17 | 0.$0^{15}$36 | 0.$0^{13}$12 | 0.$0^{12}$27 | 0.$0^{11}$52 | 0.$0^{10}$82 | 0.$0^9$96 |
| $^4S_{1\frac{1}{2}}-{}^2D_{2\frac{1}{2}}$ | *m* | 0.$0^5$61 | 0.$0^4$28 | 0.$0^3$13 | 0.$0^3$54 | 0.0020 | 0.0066 | ..... |
| | *e* | 0.$0^3$58 | 0.0011 | 0.0021 | 0.0041 | 0.0055 | 0.013 | ..... |
| | λ | 8787.6 | *6717.3* | *5517.2* | *4711.4* | *4120* | ..... | ..... |
| $^4S_{1\frac{1}{2}}-{}^2D_{1\frac{1}{2}}$ | *m* | 0.$0^3$28 | 0.0013 | 0.0058 | 0.024 | 0.088 | 0.28 | ..... |
| | *e* | 0.$0^3$37 | 0.$0^3$67 | 0.0014 | 0.0026 | 0.0046 | 0.0081 | ..... |
| | λ | 8799.1 | *6731.5* | *5537.7* | *4740.3* | *4160* | ..... | ..... |
| $\zeta_{3p}$ (cm$^{-1}$) | ..... | 343 | 538 | 825 | 1230 | 1760 | 2440 | 3340 |
| $s_2$ (atomic units) | ..... | 12.1 | 6.93 | 4.77 | 3.49 | 2.70 | 2.15 | 1.77 |

* See notes below Table 7*a*.

proximation and the neglect of configuration interaction. This is especially serious in the $2p^k$ and $3d^k$ configurations, where the observed Slater ratios are quite different from the theoretically pre-

dicted values. For the electric quadrupole transition probabilities, the evaluation of the integral $s_2$ introduces a large additional uncertainty, which is greatest in the lower stages of ionization.

For the $d^3$ configuration, the presence of two $^2D$ terms introduces some uncertainty into the calculations, since the wave functions for

TABLE 7*e*

TRANSITION PROBABILITIES FOR THE $2p^4$ CONFIGURATION*

| Transition | | *O* I | *F* II | *Ne* III | *Na* IV | *Mg* V | *Al* VI | *Si* VII |
|---|---|---|---|---|---|---|---|---|
| $^1D_2-{}^1S_0$ | *e* | 2.2 | 3.3 | 4.2 | 5.6 | 7.2 | 8.7 | ..... |
| | λ | *5577.3* | 4157.5 | *3342.8* | ..... | ..... | ..... | ..... |
| $^3P_1-{}^1S_0$ | *m* | 0.090 | 0.56 | 2.4 | 8.3 | 25 | 65 | ..... |
| | λ | 2972.3 | ..... | ..... | ..... | ..... | ..... | ..... |
| $^3P_2-{}^1S_0$ | *e* | $0.0^380$ | 0.0027 | 0.0080 | 0.022 | 0.053 | 0.11 | ..... |
| | λ | 2958.3 | ..... | ..... | ..... | ..... | ..... | ..... |
| $^3P_0-{}^1D_2$ | *e* | $0.0^522$ | $0.0^572$ | $0.0^420$ | $0.0^446$ | $0.0^496$ | $0.0^319$ | $0.0^331$ |
| | λ | 6391.7 | 4904.8 | 4011.9 | 3420 | ..... | ..... | ..... |
| $^3P_1-{}^1D_2$ | *m* | 0.0026 | 0.015 | 0.065 | 0.21 | 0.60 | 1.5 | 3.4 |
| | *e* | $0.0^563$ | $0.0^422$ | $0.0^461$ | $0.0^315$ | $0.0^331$ | $0.0^361$ | $0.0^311$ |
| | λ | *6363.9* | 4869.2 | *3967.5* | 3366 | ..... | ..... | ..... |
| $^3P_2-{}^1D_2$ | *m* | 0.0078 | 0.049 | 0.21 | 0.71 | 2.1 | 5.5 | 14 |
| | *e* | $0.0^445$ | $0.0^317$ | $0.0^348$ | 0.0012 | 0.0029 | 0.0061 | 0.012 |
| | λ | *6300.2* | 4789.5 | *3868.7* | 3245 | ..... | ..... | ..... |
| $^3P_1-{}^3P_0$ | *m* | $0.0^417$ | $0.0^318$ | 0.0012 | 0.0056 | 0.022 | 0.071 | 0.19 |
| $^3P_2-{}^3P_0$ | *e* | $0.0^818$ | $0.0^729$ | $0.0^629$ | $0.0^524$ | $0.0^415$ | $0.0^478$ | $0.0^330$ |
| $^3P_2-{}^3P_1$ | *m* | $0.0^489$ | $0.0^390$ | 0.0060 | 0.030 | 0.13 | 0.46 | 1.5 |
| | *e* | $0.0^{10}22$ | $0.0^935$ | $0.0^831$ | $0.0^730$ | $0.0^620$ | $0.0^511$ | $0.0^544$ |
| $-\zeta_{2p}$ (cm$^{-1}$) | ..... | 157 | 339 | 635 | 1085 | 1735 | 2645 | 3865 |
| $s_2$ (atomic units) | ..... | 2.58 | 1.50 | 0.989 | 0.737 | 0.575 | 0.458 | 0.352 |

* See notes below Table 7*a*.

them depend on the parameters $F_2$ and $F_4$. Also, for the atoms in this configuration there is some uncertainty in the wave numbers of lines involving the $^2F$ and upper $^2D$ terms, since the positions of these terms had to be calculated on the basis of the Slater formulae.

By comparing the numerical results tabulated here with some obtained by modifications in the method of calculation, and from a crude evaluation of the effect of configuration interaction for *O* III, using hydrogen-like wave functions, it is roughly estimated that the

## TABLE 7*f*

### TRANSITION PROBABILITIES FOR THE $3p^4$ CONFIGURATION*

| Transition | | *S* I | *Cl* II | *A* III | *K* IV | *Ca* V | *Sc* VI | *Ti* VII | *V* VIII | *Cr* IX | *Mn* X | *Fe* XI |
|---|---|---|---|---|---|---|---|---|---|---|---|---|
| $^1D_2-{}^1S_0$ | *e* | ..... | ..... | ..... | ..... | 7.9 | 8.8 | 9.7 | 11 | 12 | 12 | 13 |
| | λ | ..... | ..... | ..... | ..... | 3996.3 | 3590.8 | 3261.7 | 2975.3 | ..... | ..... | ..... |
| $^3P_1-{}^1S_0$ | *m* | ..... | ..... | ..... | ..... | 24 | 51 | 100 | 190 | 350 | 590 | 1000 |
| $^3P_2-{}^1S_0$ | *e* | ..... | ..... | ..... | ..... | 0.27 | 0.41 | 0.67 | 1.1 | 1.6 | 2.3 | 3.4 |
| $^3P_0-{}^1D_2$ | *e* | $0.0^411$ | $0.0^427$ | $0.0^358$ | $0.0^311$ | $0.0^320$ | $0.0^332$ | $0.0^253$ | $0.0^280$ | 0.0012 | 0.0019 | 0.0028 |
| | λ | ..... | 9381.8 | 8036.4 | 7109.4 | 6427.0 | 5908.2 | 5487.0 | 5116.3 | 4744.2 | 4433.3 | 4155.1 |
| $^3P_1-{}^1D_2$ | *m* | 0.0083 | 0.030 | 0.085 | 0.20 | 0.44 | 0.84 | 1.5 | 2.6 | 4.3 | 6.6 | 9.9 |
| | *e* | $0.0^361$ | $0.0^314$ | $0.0^227$ | $0.0^249$ | $0.0^280$ | 0.0012 | 0.0018 | 0.0025 | 0.0033 | 0.0042 | 0.0053 |
| | λ | ..... | 9125.7 | 7751.0 | 6794.8 | *6085.9* | 5539.6 | 5105.8 | 4733.5 | 4407.9 | 4122.6 | 3871.9 |
| $^3P_2-{}^1D_2$ | *m* | 0.028 | 0.11 | 0.32 | 0.84 | 2.0 | 4.2 | 8.5 | 16 | 31 | 54 | 95 |
| | *e* | $0.0^253$ | 0.0013 | 0.0029 | 0.0058 | 0.011 | 0.020 | 0.035 | 0.060 | 0.099 | 0.16 | 0.26 |
| | λ | ..... | 8579.9 | *7135.7* | *6101.1* | *5308.9* | 4672.2 | 4144.8 | 3686.3 | 3273.5 | 2918.9 | ..... |
| $^3P_1-{}^3P_0$ | *m* | $0.0^330$ | 0.0014 | 0.0052 | 0.015 | 0.036 | 0.076 | 0.13 | 0.21 | 0.28 | 0.25 | 0.28 |
| $^3P_2-{}^3P_0$ | *e* | $0.0^318$ | $0.0^411$ | $0.0^356$ | $0.0^223$ | $0.0^278$ | 0.0024 | 0.0067 | 0.017 | 0.039 | 0.077 | 0.17 |
| $^3P_2-{}^3P_1$ | *m* | 0.0014 | 0.0076 | 0.031 | 0.10 | 0.31 | 0.84 | 2.1 | 4.8 | 11 | 22 | 44 |
| | *e* | $0.0^321$ | $0.0^314$ | $0.0^274$ | $0.0^232$ | $0.0^212$ | $0.0^242$ | $0.0^213$ | $0.0^236$ | $0.0^299$ | 0.0024 | 0.0057 |
| $-\zeta_{3p}$ (cm$^{-1}$) | ..... | 389 | 677 | 1070 | 1595 | 2265 | 3120 | 4175 | 5480 | 7030 | 8825 | 11030 |
| $s_2$ (atomic units) | ..... | 7.93 | 5.09 | 3.61 | 2.72 | 2.13 | 1.72 | 1.43 | 1.19 | 1.01 | 0.856 | 0.734 |

* See notes below Table 7*a*.

## TABLE 8

### TRANSITION PROBABILITIES FOR THE $3d^2$ CONFIGURATION OF Fe VII*

($\zeta_{3d}=645$ cm$^{-1}$; $s_2=1.52$ atomic units)

| Transition | *m* | *e* | λ | Transition | *m* | *e* | λ |
|---|---|---|---|---|---|---|---|
| $^3P_2-{}^1S_0$ | ..... | 3.8 | ..... | $^3P_0-{}^3P_1$ | 0.0011 | ..... | ..... |
| $^3P_1-{}^1S_0$ | 5.9 | ..... | ..... | $^1D_2-{}^3P_1$ | .037 | $0.0^515$ | ..... |
| $^1D_2-{}^1S_0$ | ..... | 71 | ..... | $^3F_3-{}^3P_1$ | ..... | .21 | *5158.3* |
| $^3F_2-{}^1S_0$ | ..... | 0.43 | ..... | $^3F_2-{}^3P_1$ | .0012 | .14 | *4893.9* |
| $^3P_2-{}^1G_4$ | ..... | $0.0^352$ | ..... | $^1D_2-{}^3P_0$ | ..... | $.0^671$ | ..... |
| $^1D_2-{}^1G_4$ | ..... | 0.0043 | ..... | $^3F_2-{}^3P_0$ | ..... | .38 | *4989.4* |
| $^3F_4-{}^1G_4$ | 0.37 | $0.0^372$ | *3759.9* | | | | |
| $^3F_3-{}^1G_4$ | 0.26 | $0.0^422$ | 3587.2 | $^3F_4-{}^1D_2$ | ..... | .0054 | 6599.7 |
| $^3F_2-{}^1G_4$ | ..... | 0.0016 | 3457.3 | $^3F_3-{}^1D_2$ | .49 | .0015 | *6085.5* |
| | | | | $^3F_2-{}^1D_2$ | .30 | $.0^322$ | *5720.9* |
| $^3P_1-{}^3P_2$ | 0.0076 | $0.0^719$ | ..... | | | | |
| $^3P_0-{}^3P_2$ | ..... | $0.0^756$ | ..... | $^3F_3-{}^3F_4$ | .042 | $.0^875$ | ..... |
| $^1D_2-{}^3P_2$ | 0.13 | $0.0^626$ | ..... | $^3F_2-{}^3F_4$ | ..... | $.0^858$ | ..... |
| $^3F_4-{}^3P_2$ | ..... | 0.20 | *5276.1* | | | | |
| $^3F_3-{}^3P_2$ | 0.042 | 0.075 | *4942.3* | $^3F_2-{}^3F_3$ | 0.029 | $0.0^835$ | ..... |
| $^3F_2-{}^3P_2$ | 0.012 | $0.0^423$ | 4699.0 | | | | |

* See notes below Table 7*a*.

## TABLE 9

### TRANSITION PROBABILITIES FOR THE $3d^3$ CONFIGURATION*

(*Cr* IV: $\zeta_{3d}=275$ cm$^{-1}$; $s_2=3.80$ atomic units
*Mn* V: $\zeta_{3d}=415$ cm$^{-1}$; $s_2=2.56$ atomic units
*Fe* VI: $\zeta_{3d}=585$ cm$^{-1}$; $s_2=1.81$ atomic units)

| TRANSITION | *Cr* IV | | | *Mn* V | | | *Fe* VI | | |
|---|---|---|---|---|---|---|---|---|---|
| | $m$ | $e$ | $\lambda$ | $m$ | $e$ | $\lambda$ | $m$ | $e$ | $\lambda$ |
| $y^2D_{2\frac{1}{2}}-y^2D_{1\frac{1}{2}}$ | $0.^{4}47$ | $0.^{10}13$ | | $0.^{3}14$ | $0.^{10}35$ | | $0.^{3}33$ | $0.^{10}78$ | |
| $^2F_{2\frac{1}{2}}-y^2D_{1\frac{1}{2}}$ | .060 | 2.8 | | .16 | 2.8 | | $0.^{3}8$ | 2.7 | |
| $^2F_{3\frac{1}{2}}-y^2D_{1\frac{1}{2}}$ | | 0.52 | | | 0.55 | | | 0.55 | |
| $z^2D_{2\frac{1}{2}}-y^2D_{1\frac{1}{2}}$ | .14 | 2.0 | | .39 | 2.1 | | 0.96 | 2.1 | |
| $z^2D_{1\frac{1}{2}}-y^2D_{1\frac{1}{2}}$ | $0.^{4}53$ | 0.042 | | $0.^{3}35$ | 0.0014 | | 0.0012 | 0.0057 | |
| $^2P_{\frac{1}{2}}-y^2D_{1\frac{1}{2}}$ | $0.^{4}19$ | 8.4 | | $0.^{4}92$ | 8.5 | .. | $0.^{3}41$ | 8.3 | |
| $^2P_{1\frac{1}{2}}-y^2D_{1\frac{1}{2}}$ | $0.^{3}27$ | 13 | | .0011 | 14 | | 0.0047 | 13 | |
| $^2G_{3\frac{1}{2}}-y^2D_{1\frac{1}{2}}$ | | 65 | | | 66 | | | 63 | |
| $^4P_{2\frac{1}{2}}-y^2D_{1\frac{1}{2}}$ | .022 | 0.0017 | | .055 | 0.0027 | | 0.13 | 0.0038 | |
| $^4P_{1\frac{1}{2}}-y^2D_{1\frac{1}{2}}$ | .089 | 0.17 | | .24 | 0.28 | | 0.54 | 0.41 | |
| $^4P_{\frac{1}{2}}-y^2D_{1\frac{1}{2}}$ | .023 | 0.064 | | .062 | 0.090 | | 0.14 | 0.15 | |
| $^4F_{3\frac{1}{2}}-y^2D_{1\frac{1}{2}}$ | | 0.027 | | | 0.046 | | | 0.070 | |
| $^4F_{2\frac{1}{2}}-y^2D_{1\frac{1}{2}}$ | .048 | 0.080 | | .13 | $0.^{3}15$ | | 0.31 | $0.^{3}23$ | |
| $^4F_{1\frac{1}{2}}-y^2D_{1\frac{1}{2}}$ | .025 | 0.0093 | | .067 | 0.016 | | 0.15 | 0.025 | |
| $^4F_{2\frac{1}{2}}-y^2D_{2\frac{1}{2}}$ | .10 | 0.48 | | .27 | 0.49 | | 0.62 | 0.48 | |
| $^4F_{3\frac{1}{2}}-y^2D_{2\frac{1}{2}}$ | .057 | 2.8 | | .16 | 2.9 | | 0.35 | 2.8 | |
| $^2H_{4\frac{1}{2}}-y^2D_{2\frac{1}{2}}$ | | 0.28 | | | 0.47 | | | 0.70 | |
| $z^2D_{2\frac{1}{2}}-y^2D_{2\frac{1}{2}}$ | $0.^{3}19$ | 4.8 | | $0.^{3}82$ | 4.9 | | 0.0037 | 4.7 | |
| $z^2D_{1\frac{1}{2}}-y^2D_{2\frac{1}{2}}$ | .063 | 7.9 | | .15 | 8.5 | | 0.32 | 8.6 | |
| $^2P_{\frac{1}{2}}-y^2D_{2\frac{1}{2}}$ | | 3.6 | | | 3.6 | | | 3.4 | |
| $^2P_{1\frac{1}{2}}-y^2D_{2\frac{1}{2}}$ | .040 | 5.5 | | .13 | 4.8 | | 0.33 | 4.2 | |
| $^4G_{2\frac{1}{2}}-y^2D_{2\frac{1}{2}}$ | | 57 | | | 57 | | | 54 | |
| $^4G_{3\frac{1}{2}}-y^2D_{2\frac{1}{2}}$ | $0.^{3}11$ | 4.9 | | $0.^{3}51$ | 5.0 | | 0.0018 | 4.8 | |
| $^4P_{2\frac{1}{2}}-y^2D_{2\frac{1}{2}}$ | .23 | 0.0010 | | .62 | 0.0014 | | 1.3 | 0.0016 | |
| $^4P_{1\frac{1}{2}}-y^2D_{2\frac{1}{2}}$ | .041 | 0.18 | | .11 | 0.28 | | 0.24 | 0.39 | |
| $^4P_{\frac{1}{2}}-y^2D_{2\frac{1}{2}}$ | | 0.017 | | | 0.027 | | | 0.038 | |
| $^4F_{4\frac{1}{2}}-y^2D_{2\frac{1}{2}}$ | | 0.12 | | | 0.19 | | | 0.28 | |
| $^4F_{3\frac{1}{2}}-y^2D_{2\frac{1}{2}}$ | .043 | 0.0074 | | .12 | 0.013 | | 0.27 | 0.015 | |
| $^4F_{2\frac{1}{2}}-y^2D_{2\frac{1}{2}}$ | .0046 | 0.0060 | | .011 | 0.0098 | | 0.028 | 0.014 | |
| $^4F_{1\frac{1}{2}}-y^2D_{2\frac{1}{2}}$ | .0016 | 0.0022 | | .0043 | 0.0036 | | 0.0089 | 0.0051 | |
| $^2F_{3\frac{1}{2}}-{}^2F_{2\frac{1}{2}}$ | $0.^{4}51$ | $0.^{3}60$ | | $0.^{3}16$ | $0.^{10}18$ | | $0.^{4}42$ | $0.^{3}37$ | |
| $^2H_{4\frac{1}{2}}-{}^2F_{2\frac{1}{2}}$ | | 0.32 | | | 0.31 | | | 0.29 | |
| $z^2D_{2\frac{1}{2}}-{}^2F_{2\frac{1}{2}}$ | .0039 | 0.045 | | .010 | 0.043 | | 0.021 | 0.040 | |
| $z^2D_{1\frac{1}{2}}-{}^2F_{2\frac{1}{2}}$ | .0010 | 0.16 | | .0024 | 0.14 | | 0.0049 | 0.12 | |
| $^2P_{\frac{1}{2}}-{}^2F_{2\frac{1}{2}}$ | | 0.066 | | | 0.065 | | | 0.064 | |
| $^2P_{1\frac{1}{2}}-{}^2F_{2\frac{1}{2}}$ | $0.^{3}56$ | 0.028 | | .0017 | 0.039 | | 0.0042 | 0.046 | |
| $^2G_{3\frac{1}{2}}-{}^2F_{2\frac{1}{2}}$ | | 0.0081 | | | 0.0025 | | | $0.^{4}55$ | |
| $^4G_{3\frac{1}{2}}-{}^2F_{2\frac{1}{2}}$ | .022 | 0.68 | | .059 | 0.67 | | 0.13 | 0.65 | |
| $^4P_{2\frac{1}{2}}-{}^2F_{2\frac{1}{2}}$ | $0.^{3}12$ | $0.^{3}11$ | | $0.^{4}53$ | $0.^{3}16$ | | 0.0018 | $0.^{3}21$ | |
| $^4P_{1\frac{1}{2}}-{}^2F_{2\frac{1}{2}}$ | $0.^{4}21$ | $0.^{4}36$ | | $0.^{4}98$ | $0.^{4}20$ | | $0.^{3}36$ | $0.^{4}26$ | |
| $^4P_{\frac{1}{2}}-{}^2F_{2\frac{1}{2}}$ | | $0.^{3}99$ | | | 0.0016 | | | 0.0023 | |
| $^4F_{4\frac{1}{2}}-{}^2F_{2\frac{1}{2}}$ | | $0.^{3}41$ | | | $0.^{3}58$ | | | $0.^{3}70$ | |
| $^4F_{3\frac{1}{2}}-{}^2F_{2\frac{1}{2}}$ | .0060 | 0.0016 | | .015 | 0.0026 | | 0.042 | 0.0039 | |
| $^4F_{2\frac{1}{2}}-{}^2F_{2\frac{1}{2}}$ | .0046 | 0.0018 | | .013 | 0.0029 | | 0.027 | 0.0043 | |
| $^4F_{1\frac{1}{2}}-{}^2F_{2\frac{1}{2}}$ | .031 | 0.0073 | | .084 | 0.012 | | 0.19 | 0.018 | |
| $^2H_{5\frac{1}{2}}-{}^2F_{3\frac{1}{2}}$ | | 0.27 | | | 0.26 | | | 0.24 | |
| $^2H_{4\frac{1}{2}}-{}^2F_{3\frac{1}{2}}$ | $0.^{4}44$ | 0.0082 | | $0.^{3}19$ | 0.0064 | | $0.^{3}67$ | 0.0047 | |
| $z^2D_{2\frac{1}{2}}-{}^2F_{3\frac{1}{2}}$ | .0015 | 0.19 | | .0037 | 0.18 | | 0.0082 | 0.16 | |
| $z^2D_{1\frac{1}{2}}-{}^2F_{3\frac{1}{2}}$ | | $0.^{4}73$ | | | $0.^{4}48$ | | | $0.^{3}84$ | |
| $^2P_{1\frac{1}{2}}-{}^2F_{3\frac{1}{2}}$ | | 0.11 | | | 0.11 | | | 0.10 | |
| $^2G_{4\frac{1}{2}}-{}^2F_{3\frac{1}{2}}$ | .019 | 0.61 | | .049 | 0.60 | | 0.11 | 0.56 | |
| $^2G_{3\frac{1}{2}}-{}^2F_{3\frac{1}{2}}$ | .041 | 0.059 | | .10 | 0.058 | | 0.23 | 0.055 | |
| $^4P_{2\frac{1}{2}}-{}^2F_{3\frac{1}{2}}$ | $0.^{4}10$ | $0.^{3}49$ | | $0.^{4}43$ | $0.^{3}71$ | | $0.^{3}14$ | $0.^{4}95$ | |
| $^4P_{1\frac{1}{2}}-{}^2F_{3\frac{1}{2}}$ | | 0.0036 | | | 0.0058 | | | 0.0085 | |
| $^4F_{4\frac{1}{2}}-{}^2F_{3\frac{1}{2}}$ | .034 | 0.0078 | | .092 | 0.013 | | 0.21 | 0.018 | |
| $^4F_{3\frac{1}{2}}-{}^2F_{3\frac{1}{2}}$ | .0034 | $0.^{3}85$ | | .0085 | 0.0014 | | 0.065 | 0.0019 | |
| $^4F_{2\frac{1}{2}}-{}^2F_{3\frac{1}{2}}$ | 0.013 | 0.0030 | | 0.037 | 0.0050 | | 0.080 | 0.0072 | |
| $^4F_{1\frac{1}{2}}-{}^2F_{3\frac{1}{2}}$ | | 0.0010 | | | 0.0017 | | | 0.0025 | |

* See notes below Table 7*a*.

TABLE 9—*Continued*

| Transition | Cr IV | | | Mn V | | | Fe VI | | |
|---|---|---|---|---|---|---|---|---|---|
| | *m* | *e* | λ | *m* | *e* | λ | *m* | *e* | λ |
| $^2H_{1\frac{1}{2}} - {}^2H_{5\frac{1}{2}}$ | 0.0$^3$20 | 0.0$^{10}$31 | ..... | 0.0$^3$58 | 0.0$^{10}$92 | ..... | 0.0013 | 0.0$^9$19 | ..... |
| $^2G_{1\frac{1}{2}} - {}^2H_{5\frac{1}{2}}$ | .016 | 0$^3$50 | ..... | .043 | .0$^3$49 | ..... | .10 | .0$^3$45 | ..... |
| $^2G_{3\frac{1}{2}} - {}^2H_{5\frac{1}{2}}$ | ..... | 0$^4$20 | ..... | ..... | .0$^4$19 | ..... | ..... | .0$^4$18 | ..... |
| $^4F_{1\frac{1}{2}} - {}^2H_{5\frac{1}{2}}$ | .0$^4$46 | 0$^3$24 | 4907.6 | .0$^3$21 | 0$^3$39 | 4181.4 | .0$^3$71 | 0$^3$56 | 3675.2 |
| $^4F_{3\frac{1}{2}} - {}^2H_{5\frac{1}{2}}$ | ..... | 0$^4$21 | 4814.0 | ..... | 0$^4$38 | 4082.5 | ..... | 0$^4$46 | 3569.0 |
| $^2D_{2\frac{1}{2}} - {}^2H_{1\frac{1}{2}}$ | ..... | 0$^{12}$43 | ..... | ..... | 0$^{12}$13 | ..... | ..... | 0$^{13}$22 | ..... |
| $^2G_{1\frac{1}{2}} - {}^2H_{1\frac{1}{2}}$ | .030 | 0$^4$72 | ..... | .081 | 0$^4$83 | ..... | .18 | .0$^4$91 | ..... |
| $^2G_{3\frac{1}{2}} - {}^2H_{1\frac{1}{2}}$ | .016 | 0$^4$60 | ..... | .045 | 0$^4$62 | ..... | .11 | 0$^4$62 | ..... |
| $^4P_{1\frac{1}{2}} - {}^2H_{1\frac{1}{2}}$ | ..... | .0$^5$23 | ..... | ..... | 0$^5$82 | ..... | ..... | .0$^5$21 | ..... |
| $^4F_{1\frac{1}{2}} - {}^2H_{1\frac{1}{2}}$ | 0$^4$29 | .0$^5$98 | 4969.3 | .0015 | .0$^4$14 | 4245.6 | .0056 | .0$^4$15 | *3740.2* |
| $^4F_{3\frac{1}{2}} - {}^2H_{1\frac{1}{2}}$ | 0$^5$19 | 0$^4$90 | 4873.4 | 0$^5$90 | 0$^5$15 | 4143.7 | 0033 | 0$^5$23 | 3630.3 |
| $^4F_{2\frac{1}{2}} - {}^2H_{1\frac{1}{2}}$ | ..... | 0$^4$30 | 4799.4 | ..... | 0$^4$53 | 4063.2 | ..... | 0$^4$82 | 3543.5 |
| $^2D_{1\frac{1}{2}} - {}^2D_{2\frac{1}{2}}$ | 0$^5$51 | .0$^{15}$26 | ..... | 0$^6$72 | .0$^{14}$84 | ..... | .0$^4$26 | .0$^{11}$19 | ..... |
| $^2P_{\frac{1}{2}} - {}^2D_{2\frac{1}{2}}$ | ..... | 0$^6$78 | ..... | ..... | 0$^6$14 | ..... | ..... | .0$^6$25 | ..... |
| $^2P_{1\frac{1}{2}} - {}^2D_{2\frac{1}{2}}$ | 0.0$^3$62 | 0$^6$13 | ..... | .019 | 0$^6$26 | ..... | .049 | 0$^6$46 | ..... |
| $^4G_{1\frac{1}{2}} - {}^2D_{2\frac{1}{2}}$ | ..... | 0$^5$12 | ..... | ..... | 0$^5$12 | ..... | ..... | 0$^5$11 | ..... |
| $^4G_{3\frac{1}{2}} - {}^2D_{2\frac{1}{2}}$ | 0$^6$53 | 0$^4$10 | ..... | .0$^5$25 | 0$^4$10 | ..... | 0$^5$90 | 0$^5$96 | ..... |
| $^4P_{1\frac{1}{2}} - {}^2D_{2\frac{1}{2}}$ | 0077 | 0$^5$14 | ..... | 021 | 0$^5$25 | ..... | 048 | 0$^5$39 | ..... |
| $^4P_{3\frac{1}{2}} - {}^2D_{2\frac{1}{2}}$ | 0$^5$60 | 0$^4$79 | ..... | .0011 | 0$^5$14 | ..... | .0016 | 0$^5$22 | ..... |
| $^4P_{\frac{1}{2}} - {}^2D_{2\frac{1}{2}}$ | ..... | 0$^6$30 | ..... | ..... | 0$^6$68 | ..... | ..... | .0$^5$13 | ..... |
| $^4F_{1\frac{1}{2}} - {}^2D_{2\frac{1}{2}}$ | ..... | 0$^5$88 | 5071.6 | ..... | 0013 | 4308.4 | ..... | .0018 | 3776.1 |
| $^4F_{3\frac{1}{2}} - {}^2D_{2\frac{1}{2}}$ | .16 | 0$^4$42 | 4971.8 | .42 | 0$^5$67 | 4203.5 | .95 | 0$^4$91 | 3664.1 |
| $^4F_{2\frac{1}{2}} - {}^2D_{2\frac{1}{2}}$ | 020 | 0$^4$38 | 4894.8 | 053 | 0$^4$59 | 4120.7 | 12 | 0$^4$83 | 3575.6 |
| $^4F_{1\frac{1}{2}} - {}^2D_{2\frac{1}{2}}$ | .0073 | 0$^6$76 | 4838.7 | .019 | 0$^5$14 | 4062.2 | 045 | 0$^5$28 | 3511.6 |
| $^2P_{\frac{1}{2}} - {}^2D_{1\frac{1}{2}}$ | .0041 | .0$^6$21 | ..... | 012 | .0$^6$48 | ..... | .034 | .0$^5$11 | ..... |
| $^2P_{1\frac{1}{2}} - {}^2D_{1\frac{1}{2}}$ | 011 | 0$^5$75 | ..... | 036 | 0$^6$15 | ..... | .098 | 0$^6$27 | ..... |
| $^4G_{1\frac{1}{2}} - {}^2D_{1\frac{1}{2}}$ | ..... | 0$^5$13 | ..... | ..... | 0$^5$15 | ..... | ..... | 0$^5$16 | ..... |
| $^4P_{1\frac{1}{2}} - {}^2D_{1\frac{1}{2}}$ | 018 | 0$^6$77 | ..... | 057 | 0$^5$22 | ..... | 14 | 0$^5$41 | ..... |
| $^4P_{2\frac{1}{2}} - {}^2D_{1\frac{1}{2}}$ | 0$^6$64 | 0$^5$74 | ..... | 0028 | 0$^5$15 | ..... | .0058 | 0$^5$25 | ..... |
| $^4P_{3\frac{1}{2}} - {}^2D_{1\frac{1}{2}}$ | 0$^5$69 | 0$^6$17 | ..... | 0049 | 0$^6$25 | ..... | 013 | 0$^6$42 | ..... |
| $^4P_{\frac{1}{2}} - {}^2D_{1\frac{1}{2}}$ | ..... | .0018 | 4976.5 | ..... | 0034 | 4196.3 | ..... | .0053 | 3645.7 |
| $^4F_{3\frac{1}{2}} - {}^2D_{1\frac{1}{2}}$ | 13 | 0$^5$55 | 4899.4 | 32 | 0011 | 4113.7 | 68 | 0018 | 3558.1 |
| $^4F_{2\frac{1}{2}} - {}^2D_{1\frac{1}{2}}$ | 071 | 0$^5$29 | 4843.1 | 17 | 0$^5$54 | 4055.5 | 37 | 0$^5$85 | 3494.7 |
| $^4P_{1\frac{1}{2}} - {}^4P_{\frac{1}{2}}$ | 0$^5$30 | 0$^{14}$14 | ..... | .0$^6$64 | 0$^{12}$26 | ..... | .0$^5$24 | 0$^{11}$21 | ..... |
| $^4P_{2\frac{1}{2}} - {}^4P_{\frac{1}{2}}$ | ..... | 0$^5$38 | ..... | ..... | 0$^6$66 | ..... | ..... | 0$^5$93 | ..... |
| $^4P_{1\frac{1}{2}} - {}^4P_{\frac{1}{2}}$ | 0$^6$91 | 0$^6$73 | ..... | 0$^5$25 | 0$^6$21 | ..... | 0$^5$10 | 0$^6$43 | ..... |
| $^4P_{\frac{1}{2}} - {}^4P_{\frac{1}{2}}$ | 052 | ..... | ..... | 14 | ..... | ..... | 33 | ..... | ..... |
| $^4F_{3\frac{1}{2}} - {}^4P_{\frac{1}{2}}$ | ..... | 0018 | ..... | ..... | 0029 | 4398.4 | ..... | .0042 | 3849.1 |
| $^4F_{1\frac{1}{2}} - {}^4P_{\frac{1}{2}}$ | .0$^4$83 | .0024 | ..... | 0$^5$35 | 0038 | 4331.9 | .0012 | .0055 | 3774.9 |
| $^4G_{1\frac{1}{2}} - {}^4P_{1\frac{1}{2}}$ | ..... | 0$^4$20 | ..... | ..... | 0$^4$21 | ..... | ..... | .0$^4$20 | ..... |
| $^4P_{1\frac{1}{2}} - {}^4P_{1\frac{1}{2}}$ | 020 | 0$^5$69 | ..... | 047 | 0$^4$11 | ..... | 097 | 0$^4$15 | ..... |
| $^4P_{2\frac{1}{2}} - {}^4P_{1\frac{1}{2}}$ | 028 | 0$^6$12 | ..... | 080 | 0$^6$12 | ..... | 18 | 0$^6$78 | ..... |
| $^4P_{3\frac{1}{2}} - {}^4P_{1\frac{1}{2}}$ | 013 | 0$^6$54 | ..... | 036 | 0$^6$98 | ..... | 081 | 0$^5$15 | ..... |
| $^4P_{\frac{1}{2}} - {}^4P_{1\frac{1}{2}}$ | ..... | 0074 | 5296.3 | ..... | 011 | 4528.7 | ..... | 015 | 3995.8 |
| $^4F_{3\frac{1}{2}} - {}^4P_{1\frac{1}{2}}$ | 055 | 0045 | 5209.1 | 17 | 0069 | 4432.8 | 42 | 0091 | 3890.9 |
| $^4F_{2\frac{1}{2}} - {}^4P_{1\frac{1}{2}}$ | 034 | 0$^4$96 | 5145.5 | 11 | .0015 | 4365.2 | 27 | 0020 | 815.1 |
| $^4F_{1\frac{1}{2}} - {}^4P_{1\frac{1}{2}}$ | ..... | ..... | ..... | ..... | ..... | ..... | ..... | ..... | ..... |
| $^4G_{1\frac{1}{2}} - {}^4G_{1\frac{1}{2}}$ | 0$^5$51 | 0$^{11}$33 | ..... | 0015 | 0$^{11}$42 | ..... | .0040 | 0$^{11}$23 | ..... |
| $^4P_{1\frac{1}{2}} - {}^4G_{1\frac{1}{2}}$ | ..... | 0$^{10}$42 | ..... | ..... | 0$^9$21 | ..... | ..... | 0$^9$54 | ..... |
| $^4F_{1\frac{1}{2}} - {}^4G_{1\frac{1}{2}}$ | 093 | 0$^5$12 | 6915.6 | 24 | 0$^6$20 | 5889.0 | 56 | 0$^5$29 | *5177.0* |
| $^4F_{3\frac{1}{2}} - {}^4G_{1\frac{1}{2}}$ | 036 | 0$^5$39 | 6731.2 | 096 | 0$^5$59 | 5694.8 | 22 | 0$^5$90 | *4968.8* |
| $^4F_{2\frac{1}{2}} - {}^4G_{1\frac{1}{2}}$ | ..... | 0$^5$58 | 6591.0 | ..... | 0$^5$92 | 5543.9 | ..... | 0$^4$13 | 4807.5 |
| $^4P_{2\frac{1}{2}} - {}^4G_{3\frac{1}{2}}$ | 0$^{12}$94 | 0$^{12}$39 | ..... | 0$^{10}$12 | 0$^{11}$21 | ..... | 0$^{10}$67 | 0$^{11}$41 | ..... |
| $^4P_{1\frac{1}{2}} - {}^4G_{3\frac{1}{2}}$ | ..... | 0$^{12}$73 | ..... | ..... | 0$^{11}$26 | ..... | ..... | 0$^{11}$32 | ..... |
| $^4F_{1\frac{1}{2}} - {}^4G_{3\frac{1}{2}}$ | 0023 | 0$^5$72 | 7087 | .0059 | 0$^4$11 | 6069.2 | 012 | 0$^4$15 | 5370.5 |
| $^4F_{3\frac{1}{2}} - {}^4G_{3\frac{1}{2}}$ | 035 | 0$^4$26 | 6893.2 | 096 | 0$^4$44 | 5863.1 | 22 | 0$^4$64 | *5146.8* |
| $^4F_{2\frac{1}{2}} - {}^4G_{3\frac{1}{2}}$ | 032 | 0$^5$22 | 6746.2 | 088 | 0$^5$46 | 5703.3 | 20 | 0$^5$52 | *4074.0* |
| $^4F_{1\frac{1}{2}} - {}^4G_{3\frac{1}{2}}$ | ..... | 0$^4$17 | 6640.0 | ..... | 0$^4$30 | 5591.9 | ..... | 0$^4$45 | *4850.9* |
| $^4P_{1\frac{1}{2}} - {}^4P_{2\frac{1}{2}}$ | 0$^5$43 | 0$^6$64 | ..... | 0015 | 0$^5$24 | ..... | 0046 | 0$^5$78 | ..... |
| $^4P_{\frac{1}{2}} - {}^4P_{2\frac{1}{2}}$ | ..... | 0$^5$25 | ..... | ..... | 0$^5$78 | ..... | ..... | 0$^5$21 | ..... |
| $^4F_{3\frac{1}{2}} - {}^4P_{2\frac{1}{2}}$ | ..... | 24 | 7391 | ..... | 22 | 6396.2 | ..... | 20 | *5678.0* |
| $^4F_{1\frac{1}{2}} - {}^4P_{2\frac{1}{2}}$ | 0$^5$11 | 088 | 7180 | 0$^5$44 | 086 | 6167.7 | 0020 | 081 | *5428.6* |
| $^4F_{2\frac{1}{2}} - {}^4P_{2\frac{1}{2}}$ | 0$^5$47 | 022 | 7021 | 0$^5$19 | 022 | 5991.0 | 0$^5$64 | 022 | *5236.6* |
| $^4F_{1\frac{1}{2}} - {}^4P_{2\frac{1}{2}}$ | 0.0$^4$11 | 0.0027 | 6906 | 0.0$^4$44 | 0.0027 | 5868.3 | 0.0$^5$14 | 0.0027 | 5100.4 |

TABLE 9—*Continued*

| Transition | Cr IV | | | Mn V | | | Fe VI | | |
|---|---|---|---|---|---|---|---|---|---|
| | *m* | *e* | λ | *m* | *e* | λ | *m* | *e* | λ |
| $^4P_{5/2}-{}^4P_{3/2}$ | $0.0^438$ | $0.0^{12}77$ | | $0.0^491$ | $0.0^{11}15$ | | $0.0^322$ | $0.0^{11}25$ | |
| $^4F_{3/2}-{}^4P_{3/2}$ | | .18 | 7338 | | .17 | 6346.2 | | .15 | 5631.6 |
| $^4F_{5/2}-{}^4P_{3/2}$ | $.0^449$ | .14 | 7172 | $.0^325$ | .14 | 6159.3 | .0010 | .13 | *5425.3* |
| $^4F_{7/2}-{}^4P_{3/2}$ | $.0^311$ | .051 | 7052 | $.0^351$ | .050 | 6029.7 | .0020 | .048 | 5279.2 |
| $^4F_{5/2}-{}^4P_{5/2}$ | | .15 | 7233 | | .14 | 6220.7 | | .13 | *5485.7* |
| $^4F_{7/2}-{}^4P_{5/2}$ | $.0^575$ | .24 | 7111 | $.0^436$ | .24 | 6088.5 | $.0^314$ | .23 | *5336.4* |
| $^4F_{3/2}-{}^4F_{9/2}$ | .0017 | $.0^917$ | | .0052 | $.0^951$ | | .014 | $.0^814$ | |
| $^4F_{5/2}-{}^4F_{9/2}$ | | $.0^926$ | | | $.0^987$ | | | $.0^824$ | |
| $^4F_{5/2}-{}^4F_{7/2}$ | .0014 | $.0^{10}75$ | | .0047 | $.0^927$ | | .013 | $.0^975$ | |
| $^4F_{7/2}-{}^4F_{7/2}$ | | $.0^912$ | | | $.0^940$ | | | $.0^812$ | |
| $^4F_{7/2}-{}^4F_{5/2}$ | $0.0^357$ | $0.0^{10}18$ | | 0.0018 | $0.0^{10}57$ | | 0.0057 | $0.0^919$ | |

magnetic dipole transition probabilities are good in absolute value to within a factor of about 1.25 for the $3p^k$ configurations and about 1.5 for the $2p^k$ and $3d^k$ configurations. The presence of the integral $s_2$ introduces an additional uncertainty of a factor of 2 in the electric quadrupole transition probabilities, in the lower stages of ionization. The relative values for purely dipole transitions, or for purely quadrupole transitions, should be considerably more accurate.

*b) Agreement with observation.*—From the results given in the article of Bowen and Wyse[29] it is seen that, in general, the observed lines are those of relatively high transition probability. It is also found that, in general, considering the difficulties of observation, the calculated transition probabilities agree fairly well with the observed relative intensities, wherever the latter have been determined.

*c) General features of the results.*—As Condon pointed out from his calculations,[30] it is of interest to note that in many cases the magnetic dipole transition probabilities in a multiplet are much larger than the electric quadrupole probabilities for the same multiplet. In particular, this is true for all the atoms in the $p^2$ and $p^4$ configurations. It is also of some interest to note that, in all of the cases that were treated, the probabilities of transitions between levels of the same term are negligibly small in comparison with the probabilities of other transitions from the same upper level. If this were not the case, the intensities of the lines corresponding to the latter transitions would be greatly reduced.[31]

[29] *Lick Obs. Bull.*, **19**, 1, 1940.

[30] *Loc. cit.*

[31] I. S. Bowen, *Rev. Mod. Phys.*, **8**, 55, 1936.

*d*) *Some special results for O* III.—

1. *The line* ($^3P_0 - {}^1D_2$): From Table 7*a* we find that the transition probability for the ($^3P_0 - {}^1D_2$) transition has a small, but nonzero, value, whereas Condon's work indicated a zero value for this transition. The nonzero value agrees with some calculations by Stevenson.[32] This line was recently observed in *O* III by Bowen and Wyse.[33]

2. *The permitted lines of O* III: Bowen has pointed out a result of considerable interest which can be deduced from the calculation of transition probabilities. His interpretation of the mechanism of excitation of the permitted lines of *O* III observed in nebular spectra[34] requires the existence of a substantial fraction of the atoms of *O* III in the $^3P_2$ level instead of in the ground level $^3P_0$. This would be impossible if the probability of removal from the $^3P_2$ level by spontaneous emission were much larger than the collision probability.

From Table 7*a* we see that the probability of transition downward from the $^3P_2$ level is approximately $1 \times 10^{-4}$ sec$^{-1}$. That this is smaller than the probability *C* of removal from the $^3P_2$ level by collison can be seen from the following consideration. In comparing the intensities of the forbidden lines of *O* I, *O* II, and *O* III in the nebulae it is found[35] that the transition ($^4S_{1½} - {}^2D_{2½}$) of *O* II is of the order of magnitude of one-tenth as strong as it should be if the collision probability were not taken into consideration in the intensity formulae. This implies that the collision probability is about ten times larger than the probability of this transition. But, from Table 7*c*, the value of $\mathbf{A}(^4S_{1½} - {}^2D_{2½})$ of *O* II is about $8 \times 10^{-5}$ sec$^{-1}$. Hence, the probability *C* of removal from the $^3P_2$ level by collision is, roughly, ten times larger than $\mathbf{A}(^3P_1 - {}^3P_2)$, and the condition for existence of the absorption mechanism of excitation of *O* III is fulfilled.

In conclusion, I should like to express my appreciation to Professor W. V. Houston, under whose supervision this research was done, for his assistance and advice. I wish also to thank Professor I. S. Bowen for suggesting the problem and for many helpful discussions.

California Institute of Technology
February 1940

[32] *Proc. R. Soc.*, A, **137**, 298, 1932.

[33] *Pub. A.S.P.*, **50**, 348, 1938.

[34] *Ap. J.*, **81**, 1, 1935.

[35] I. S. Bowen and A. B. Wyse, *Lick Obs. Bull.*, **19**, 1, Table 3, 1940.

# ACCIDENTAL AND SYSTEMATIC ERRORS IN SPECTROSCOPIC ABSOLUTE MAGNITUDES FOR DWARF Go–K2 STARS*

GUSTAF STRÖMBERG

ABSTRACT

The errors in the spectroscopic absolute magnitude ($M_s$) for dwarf stars of spectral types Go–K2 have been studied to determine the regression lines and the mean errors in the individual values of $M_s$. The stars were grouped according to the reduced proper motion $H = m + 5 \log \mu$, which is correlated with the true absolute magnitude ($M$). Trigonometric parallaxes were used to determine values for the mean and the dispersion in $M$. The two regression lines were determined, and the proper corrections to $M_s$ were derived for two cases: first, the stars are selected or grouped on a basis directly connected with $M$ itself and, second, on a basis directly connected with the special spectral features which define $M_s$ for a given spectral interval. The mean errors of $M_s$ as published have been found to be 0.51 for the Go–G7 stars and 0.75 for the G8–K2 stars. After the corrections have been applied, the mean errors for the two spectral groups are 0.41 and 0.49, respectively, when the stars are grouped according to $M_s$, and 0.60 and 0.65, respectively, when the stars are grouped according to $M$ itself.

In *Mount Wilson Contribution* No. 603[1] the writer has studied the relation between absolute magnitude and reduced proper motion for the stars of spectral types G and K. This investigation showed the advantages of grouping the stars on a basis correlated with $M$ but independent of the errors in the spectroscopic absolute magnitudes and the trigonometric parallaxes. The investigation was prompted by a comparison of spectroscopic and trigonometric parallaxes made by Russell and Miss Moore,[2] who had found some interesting results regarding the probable errors in the spectroscopic absolute magnitudes.

## CORRELATION THEORY

Let us assume that we have two correlated variates, $x$ and $y$, with the dispersions $\sigma_1$ and $\sigma_2$, respectively, connected by the coefficient of correlation $r$. The correlation is assumed to be linear, and the origin

* *Contributions from the Mount Wilson Observatory, Carnegie Institution of Washington*, No. 628.

[1] *Ap. J.*, **89**, 10, 1939.

[2] *Mt. W. Contr.*, No. 589; *Ap. J.*, **87**, 389, 1938.

is shifted so as to make the algebraic sums of $x$ and $y$ equal to zero. We have then

$$\bar{x} = \bar{y} = 0\,, \qquad \overline{x^2} = \sigma_1^2\,, \qquad \overline{y^2} = \sigma_1^2\,, \qquad \overline{xy} = r\sigma_1\sigma_2\,. \tag{1}$$

For another origin the last equation takes the form

$$\overline{x_1 y_1} = \overline{(x_1 - \bar{x}_1)(y_1 - \bar{y}_1)} + \bar{x}_1\bar{y}_1 = r\sigma_1\sigma_2 + \bar{x}_1\bar{y}_1\,. \tag{1a}$$

A "statistical equality" will in the following be denoted by the symbol $\equiv$, and for such an equality the means and the dispersion must be identical. We thus write

$$y \equiv ax\,, \tag{2}$$

where $a$ is a factor of proportionality.

Hence

$$\overline{y^2} = a^2\overline{x^2}\,,$$

or

$$a = \frac{\sigma_2}{\sigma_1}\,. \tag{3}$$

Denoting the basis of grouping by subscripts, we have the following equations for the two regression lines:

$$\left.\begin{aligned} \bar{y}_x &= \frac{\sigma_2}{\sigma_1} rx = arx\,, \\ \bar{x}_y &= \frac{\sigma_1}{\sigma_2} ry = \frac{ry}{a}\,. \end{aligned}\right\} \tag{4}$$

We denote the slopes of the two regression lines by $a_1$ and $a_2$ and thus have

$$a_1 = ar\,, \qquad a_2 = \frac{a}{r}\,, \qquad \sqrt{a_1 a_2} = a\,. \tag{5}$$

For a "neutral" or "impartial" basis of grouping, that is, one correlated in equal measure with both $x$ and $y$, we have for any subgroup

$$\bar{y}_n \equiv a\bar{x}_n\,. \tag{6}$$

The line which best represents this set of values of $x_n$ and $y_n$ we shall call the "impartial relation line," or simply the "impartial line." This line is defined by the equation $y = ax$.

From equations (5) it follows that the slope of the impartial relation line is equal to the geometrical mean of the slopes of the two regression lines.

It should be noted that the impartial relation line is not in general identical with the axis of the "correlation ellipse," which also lies between the two regression lines. The correlation ellipse is defined by the equation

$$\frac{x^2}{\sigma_1^2} + \frac{y^2}{\sigma_2^2} - \frac{2rxy}{\sigma_1\sigma_2} = 1 .$$

The inclination $\alpha$ of the major axis of the correlation ellipse to the $x$-axis is defined by the equation

$$\tan 2\alpha = \frac{2r\sigma_1\sigma_2}{\sigma_1^2 - \sigma_2^2} = \frac{2ra}{1 - a^2} .$$

The slope of this axis is thus

$$a' = \tan \alpha = \frac{1}{2ra}\left(\sqrt{1 + a^4 - 2a^2(1 - 2r^2)} + a^2 - 1\right) . \qquad (7)$$

By changing the units in which $x$ and $y$ are expressed, we can always make $a = 1$.

We have then

$$a_1 = r ,$$

$$a_2 = \frac{1}{r} ,$$

$$a' = 1 = \frac{\sigma_2}{\sigma_1} .$$

In this case the impartial line and the axis of the correlation ellipse coincide and form an angle of 45° with the $x$-axis.

In the present application $x$ is identified with the measured absolute magnitude $M_s$, and $y$ with a measured absolute magnitude $M_\pi$. The latter often cannot be given for individual stars, but mean val-

ues of $M_\pi$ can be determined with a certain degree of accuracy for stars grouped either on the basis of $M_s$ itself or on some other basis correlated with the true absolute magnitude $M$.

When the line intensities were converted into absolute magnitudes, the stars were first grouped according to line intensities, and the mean absolute magnitudes were determined for each group from trigonometric parallaxes or from proper-motion data. The different values of the mean absolute magnitudes for the different lines used were combined into means, and a provisional system of spectroscopic absolute magnitudes then derived. New stars were added, and the provisional system was corrected by grouping the stars according to the provisional $M_s$. This method obviously gave the first regression line $\overline{y_x} = r\sigma_2 x/\sigma_1$, and the scale was so adjusted as to make the slope equal to unity. The published absolute magnitudes were supposed to be used for statistical investigations in which the stars were grouped according to $M_s$, and for this case the calibration was the proper one.

But in most cases we want the most probable absolute magnitude for an individual star or for groups of stars selected on a basis other than $M_s$ itself. In the simple case of linear correlation, we should then use another slope in the calibration. The scale factor to be used depends upon the way the star or stars whose absolute magnitudes are to be determined are selected or grouped. If the stars are selected or grouped on the basis of any quality directly connected with $M_s$, the first regression line gives the proper calibration. If the stars are selected or grouped on the basis of any quality directly connected with $M$ itself, the second regression line should be used.

The variables which Russell and Miss Moore use are not $M_s$ and $M_\pi$ but are proportional to $\pi_s 10^{0.2m}$ and $\pi_t 10^{0.2m}$, where $\pi_s$ is the spectroscopic, $\pi_t$ the trigonometric parallax, and $m$ the apparent magnitude. The former is proportional to $10^{0.2M_s}$, and the latter to $10^{0.2M} + \epsilon'$, where $\epsilon'$ is the error in $\pi_t$ reduced to a fixed apparent magnitude. These variables have the advantage that both can be plotted in a scatter diagram, and both regression lines can be directly derived from the individual observations. In the present study I have used $M_s$ and $M_\pi$ as the two correlated variables in order better to visualize the physical meaning of the results.

## METHOD

In the present study the reduced proper motion $H = m + 5 \log \mu$ (where $\mu$ is the annual proper motion) has been used as a basis for grouping. $H$ is a simple function of the true absolute magnitude and the linear tangential motion, and it is obviously independent of the errors in $M_s$ and $\pi_t$ and gives us a method of finding the second regression line. Only the dwarfs of spectral type Go–K2 have been studied, and the stars have been divided into two groups, types Go–G7 and G8–K2. The former are referred to as "G stars," and the latter as "Ko stars." The "dwarfs" have been defined by the condition that $M_s \geq 3.3$ for the G stars and $M_s \geq 4.0$ for the Ko stars, $M_s$ being given in *Mt. W. Contr.* No. 511.[3] The values of $M_s$ show a gap between 2.9 and 3.2 for the G stars and between 2.6 and 3.9 for the Ko stars. The stars thus selected have all been reduced by the same curves, and the limits in $M_s$ are the same as those used by Russell and Miss Moore.

The stars were first grouped on the basis of the reduced proper motion $H$, which is correlated with the true absolute magnitude $M$. In computing the mean absolute magnitudes for the group from the trigonometric parallaxes, the method outlined in *Mt. W. Contr.* No. 603[1] was used. Some refinements in the method were adopted, however. The weighting system used in the previous study was based entirely on the probable errors in $\pi_t 10^{0.2m}$. A few apparently bright stars with well-determined parallaxes would have an overwhelming weight, and the errors of measurements in the line intensities would not be properly eliminated in the formation of means. The following weighting system was therefore introduced.

The equations of condition for determining $M$, as given in *Mt. W. Contr.* No. 603, are

$$0.1I - \pi_0 = \epsilon_0 ,$$

where

$$\left.\begin{aligned} I &= 10^{0.2M} , \\ \pi_0 &= \pi_t 10^{0.2m} , \\ \epsilon_0 &= \epsilon 10^{0.2m} , \\ \pi &= \pi_t + \epsilon . \end{aligned}\right\} \qquad (8)$$

[3] *Ap. J.*, **81**, 187, 1935.

We write

$$I = \bar{I} + s\,,$$
$$\bar{s} = 0$$
$$\overline{s^2} = \sigma_1^2\,.$$

Hence,

$$0.1\bar{I} - \pi_0 = \epsilon_0 - 0.1s\,.$$

Denoting the weight of this equation by $g$, we have

$$\left.\begin{aligned} \frac{1}{g} &= \epsilon_0^2 + 0.01\sigma_1^2\,, \\ \bar{I} &= \frac{10\Sigma g\pi_0}{\Sigma g}\,, \end{aligned}\right\} \tag{9}$$

in which $\epsilon_0$ can be identified with the mean error in $\pi_l 10^{0.2m}$. A provisional value of $\sigma_1$, the dispersion in $I$, must be adopted, but no high accuracy is required. An improved value of $\sigma_1$ is then found from the equation

$$\sigma_1^2 = \frac{100\Sigma g(\pi_0 - A)^2}{\Sigma g} - 100\left(\frac{\bar{I}}{10} - A\right)^2 - \frac{\Sigma g\epsilon_0^2}{\Sigma g}\,, \tag{10}$$

where $A$ has an arbitrary value, which, for convenience, should have the order of magnitude of $\bar{I}/10$.

The formulae for computing the mean absolute magnitude $\bar{M}$ and the dispersion $q$ in $M$ are, as shown in *Mt. W. Contr.* No. 603,

$$\left.\begin{aligned} \bar{M} &= 5\log\bar{I} - 5\log C\,, \\ q^2 &= 50\,\mathrm{Mod}\log C = 21.71\log C\,, \\ C^2 &= 1 + \frac{\sigma_1^2}{\bar{I}^2}\,. \end{aligned}\right\} \tag{11}$$

In the determination of the mean values $\bar{M}_s$ and the dispersion $q_s$ in $M_s$, the same weights ($g$) were applied as in the computation of $M$ and $q$.

The new method of deriving $\bar{M}$ still gives higher weights to the apparently brighter stars, and the resultant means and dispersions are hence not quite representative for the stars in the groups, but are, instead, computed quantities which can be compared with well-determined measured quantities. The new weighting system, how-

ever, brings the mean and the dispersion much closer to their unweighted values.

Since the calibration to be used in practice depends upon the method of selection and grouping of the stars whose absolute magnitudes are to be determined from their spectral characteristics, the value of the mean errors $\theta$ of an individual determination of $M$ depends upon the nature of the grouping used. We shall denote by $M_s'$ the absolute magnitudes calibrated in such a way that they represent the first regression line. By $M_s''$ we denote the corrected values of $M_s$ which represent the second regression line. The corresponding values of $\theta$ are denoted by $\theta'$ and $\theta''$, respectively, and the corresponding values of the dispersion by $q_s'$ and $q_s''$, respectively. For the simple case of linear correlation we have then

$$\left.\begin{aligned} \theta^2 &= \overline{(M - M_s)^2} = q^2 + q_s^2 - 2rqq_s + (\overline{\overline{M}} - \overline{\overline{M}}_s)^2 , \\ \theta'^2 &= \overline{(M - M_s')^2} = q^2 + q_s'^2 - 2rqq_s' + (\overline{\overline{M}} - \overline{\overline{M}}_s')^2 , \\ \theta''^2 &= \overline{(M - M_s'')^2} = q^2 + q_s''^2 - 2rqq_s'' + (\overline{\overline{M}} - \overline{\overline{M}}_s'')^2 . \end{aligned}\right\} \quad (12)$$

In these equations $r$ is the coefficient of correlation between $M$ and $M_s$, a coefficient not affected by any linear change in scale. The double bars above $M$ and $M_s$ indicate the general means for all the stars in the spectral interval. According to our definition and according to equations (3) and (4), we have

$$M_s' - \overline{\overline{M}}_s' = a_1(M_s - \overline{\overline{M}}_s) ,$$

$$M_s'' - \overline{\overline{M}}_s'' = a_2(M_s - \overline{\overline{M}}_s) ,$$

$$a_1a_2 = q^2/q_s^2 , \qquad a_1/a_2 = r^2 , \qquad \overline{\overline{M}}_s' = \overline{\overline{M}}_s'' .$$

Hence,

$$\left.\begin{aligned} q_s' &= a_1q_s = rq , \\ q_s'' &= a_2q_s = \frac{q}{r} , \\ \theta''^2 - \theta'^2 &= \frac{q^2(1 - r^2)^2}{r^2} , \end{aligned}\right\} \quad (13)$$

where $\theta''$ is always greater than $\theta'$.

If the correlation between $M$ and $M_s$ is not linear, the change in scale of $M_s$ involved in the calibration always makes that line straight on which the calibration has been based. In the following I have used the second regression line as the main calibration line; the first calibration line may then be either straight or curved. If both regression lines are straight, $r$ is a constant for the whole group, otherwise we must use different values of $r$ for the different subgroups.

TABLE 1

GROUPING ACCORDING TO $H$

| $H$ | No. | $\overline{\Pi}$ | $\overline{M}$ | Mean Error | $q$ | $\overline{M}_s$ | $q_s$ | $\overline{M}-\overline{M}_s$ | Mean Error | $q/q_s$ |
|---|---|---|---|---|---|---|---|---|---|---|
| | Dwarfs Go–G7 | | | | | | | | | |
| 0.0– 2.9 | 28 | 2.1 | 3.92 | ±0.24 | 1.02 | 4.39 | 0.46 | −0.47 | ±0.26 | 2.20 |
| 3.0– 3.9 | 28 | 3.4 | 3.98 | .23 | 0.98 | 4.39 | .45 | − .41 | .25 | 2.20 |
| 4.0– 4.9 | 64 | 4.5 | 4.32 | .11 | 0.47 | 4.39 | .36 | − .07 | .13 | 1.31 |
| 5.0– 5.9 | 54 | 5.5 | 4.78 | .12 | 0.54 | 4.55 | .35 | + .23 | .14 | 1.55 |
| 6.0– 6.9 | 55 | 6.5 | 5.02 | .12 | 0.39 | 4.63 | .31 | + .39 | .14 | 1.26 |
| 7.0– 7.9 | 18 | 7.2 | 5.64 | .22 | 0.50 | 4.92 | .36 | + .72 | .26 | 1.40 |
| 8.0–12.2 | 12 | 9.4 | 5.8 | .43 | 1.10 | 4.88 | 0.50 | + .9 | .46 | 2.2 |
| ζ Herc. | 1 | 1.9 | 3.2 | .15 | ..... | 3.7 | ..... | − .5 | .55 | ..... |
| α Cent. | 1 | 3.1 | 4.7 | .10 | ..... | 4.8 | ..... | − .1 | .54 | ..... |
| μ Cass. | 1 | 8.2 | 5.9 | .20 | ..... | 5.4 | ..... | + .5 | .57 | ..... |
| τ Ceti | 1 | 5.0 | 6.0 | .10 | ..... | 5.6 | ..... | + .4 | .54 | ..... |
| Gr. 1830 | 1 | 10.7 | 6.7 | ±0.15 | ..... | 6.3 | ..... | +0.4 | ±0.55 | ..... |
| All | 264 | 5.2 | 4.66 | ±0.06 | 0.87 | 4.55 | 0.43 | +0.11 | ±0.07 | 2.02 |
| | Dwarfs G8–K2 | | | | | | | | | |
| 2.3– 4.7 | 25 | 4.0 | 5.20 | ±0.20 | 0.82 | 5.38 | 0.41 | −0.18 | ±0.22 | 2.01 |
| 4.8– 6.0 | 32 | 5.3 | 5.17 | .19 | .83 | 5.48 | .54 | − .31 | .21 | 1.53 |
| 6.1– 6.9 | 32 | 6.5 | 5.76 | .13 | .46 | 5.54 | .25 | + .22 | .15 | 1.86 |
| 7.0–12.7 | 21 | 7.8 | 5.62 | .25 | 0.81 | 5.63 | 0.28 | − .01 | .27 | 2.88 |
| β Aquil. | 1 | 2.3 | 3.3 | .20 | ..... | 4.0 | ..... | − .7 | .47 | ..... |
| δ Erid. | 1 | 3.1 | 4.0 | .20 | ..... | 4.6 | ..... | − .6 | .47 | ..... |
| 40 Erid. | 1 | 7.6 | 6.0 | ±0.10 | ..... | 6.0 | ..... | 0.0 | ±0.44 | ..... |
| All | 113 | 5.8 | 5.41 | ±0.10 | 0.81 | 5.44 | 0.42 | −0.03 | ±0.11 | 1.91 |

The results from the grouping according to $H$ are given in Table 1 and those from the grouping according to $M_s$ in Table 2, and are

shown graphically in Figures 1 and 2, respectively. There are five G stars and three Ko stars which are either apparently very bright or, in addition, have extreme values of $M$. In spite of the relatively large mean errors in $M - M_s$ for these stars, they are of a certain interest, in particular since they offer a means of extending the curves in Figures 1 and 2 beyond the range defined by the means for the larger groups.

TABLE 2

GROUPING ACCORDING TO $M_s$

| $M_s$ | No. | $\bar{M}$ | Mean Error | $q$ | $\bar{M}_s$ | $\bar{M} - \bar{M}_s$ |
|---|---|---|---|---|---|---|
| | Dwarfs Go–G7 | | | | | |
| 3.4–3.9 | 23 | 3.28 | ±0.26 | 0.88 | 3.76 | −0.48 |
| 4.0–4.5 | 112 | 4.24 | .10 | .72 | 4.29 | − .05 |
| 4.6–4.9 | 86 | 4.73 | .10 | .52 | 4.75 | − .02 |
| 5.0–5.3 | 32 | 5.22 | .14 | .48 | 5.14 | + .08 |
| 5.4–6.3 | 11 | 6.08 | ±0.12 | 0.17 | 5.65 | +0.43 |
| 3.4–6.3 | 264 | 4.51 | ±0.06 | 0.87 | 4.55 | −0.04 |
| | Dwarfs G8–K2 | | | | | |
| 4.0–5.2 | 26 | 4.32 | ±0.27 | 1.06 | 4.81 | −0.49 |
| 5.3–5.5 | 31 | 5.43 | .15 | 0.61 | 5.40 | + .03 |
| 5.6–5.9 | 31 | 5.65 | .17 | 0.77 | 5.68 | − .03 |
| 5.9–6.5 | 25 | 5.84 | ±0.12 | 0.48 | 5.99 | −0.15 |
| 4.0–6.5 | 113 | 5.33 | ±0.10 | 0.81 | 5.47 | −0.14 |

The second regression line defined by the grouping according to $H$ is drawn as a continuous curve passing as nearly as possible through the dots. The first regression line is represented by a dashed line drawn through the crosses. For the Ko stars the extension of the first regression line for the brighter stars cannot be obtained from the means. It has been assumed that the very brightest stars form a separate group; a special first regression line has been drawn for these stars, and as a consequence this regression line is not straight but has an S-shaped form. The individual stars are selected on the basis of apparent magnitude and should hence be regarded as falling

on the second regression line. The ratio of the dispersions $q$ and $q_s$ is indicated by the slopes of the straight lines through the dots. This

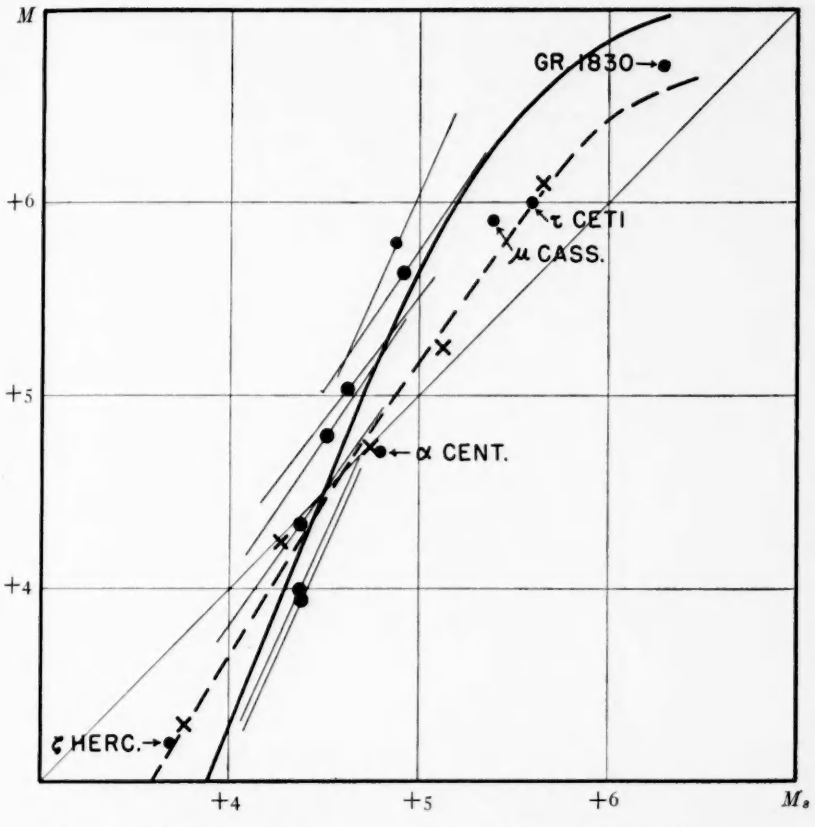


FIG. 1.—Relation between spectroscopic absolute magnitudes $M_s$ (abscissae) and true absolute magnitudes $M$ (ordinates) derived from trigonometric parallaxes, for Go–G7 stars. Dots represent means of $M$ and $M_s$ when stars are grouped according to $H=m+5 \log \mu$; crosses, means for a grouping according to $M_s$. A few apparently bright stars are individually marked. The slope of the lines through the dots equals the ratio of the dispersion in $M$ to that in $M_s$. The full-drawn curve is the second regression line; it represents the dots and has a local slope somewhat larger than that of the "slope lines." The dashed curve is the first regression line ($M$ on $M_s$) and represents the crosses. The straight line at 45° angle represents identity between $M$ and $M_s$.

slope should, in principle, represent the local slope of the impartial line and should hence be intermediate between that of the two regres-

sion lines. Little weight has, however, been given to these "slope lines."

The mean error $\theta$ in an individual value of $M_s$ as given in *Mt. W. Contr.* No. 511[3] is 0.51 for the G stars and 0.75 for the Ko stars. These values include effects of systematic corrections to the whole

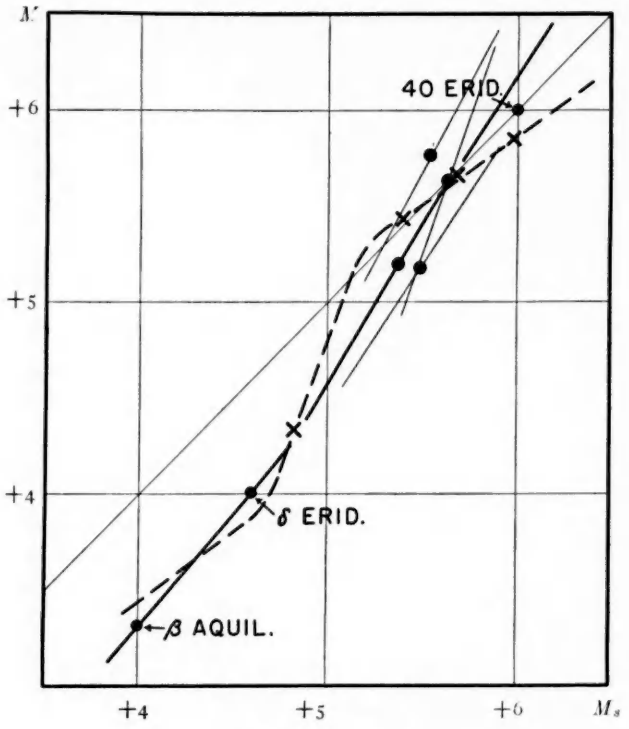


FIG. 2.—Same as Fig. 1, but for G8–K2 stars

system. They are computed by aid of the formulae given in equations (12).

In studying the curves in Figures 1 and 2 we find that neither of the regression lines coincides with the 45° line denoting identity between $\bar{M}$ and $\bar{M}_s$. The total dispersion is underestimated; as seen from Tables 1 and 2, the ratio $q/q_s$ for the dwarfs as a whole (derived by weighting according to the number of stars) is 2.02 for the G stars and 1.91 for the Ko stars. These large ratios are partly

due to systematic errors in the calibration-curves used in determining the first regression line. It should be noted that Schlesinger's extended list of parallaxes was not available when the calibration-

TABLE 3

VALUES OF $M_s$ FOR IMPARTIAL AND BIASED GROUPINGS

| $M_s$ (*Contr.* No. 511) | Grouping According to $M$ | | Grouping According to $M_s$ | | Regression Effect | |
|---|---|---|---|---|---|---|
| | Go–G7 | G8–K2 | Go–G7 | G8–K2 | Go–G7 | G8–K2 |
| +3.4 | +2.4 | ..... | +2.7 | ..... | +0.3 | ..... |
| 3.5 | 2.6 | ..... | 2.9 | ..... | + .3 | ..... |
| 3.6 | 2.7 | ..... | 3.0 | ..... | + .3 | ..... |
| 3.7 | 2.9 | ..... | 3.1 | ..... | + .2 | ..... |
| 3.8 | 3.0 | ..... | 3.3 | ..... | + .3 | ..... |
| 3.9 | 3.1 | ..... | 3.5 | ..... | + .4 | ..... |
| 4.0 | 3.3 | +3.3 | 3.6 | +3.4 | + .3 | +0.1 |
| 4.1 | 3.5 | 3.4 | 3.8 | 3.5 | + .3 | + .1 |
| 4.2 | 3.7 | 3.5 | 4.0 | 3.6 | + .3 | + .1 |
| 4.3 | 3.9 | 3.6 | 4.1 | 3.6 | + .2 | .0 |
| 4.4 | 4.2 | 3.8 | 4.3 | 3.7 | + .1 | − .1 |
| 4.5 | 4.5 | 3.9 | 4.4 | 3.8 | − .1 | − .1 |
| 4.6 | 4.8 | 4.0 | 4.6 | 3.9 | − .2 | − .1 |
| 4.7 | 5.0 | 4.1 | 4.7 | 4.0 | − .3 | − .1 |
| 4.8 | 5.2 | 4.3 | 4.9 | 4.3 | − .3 | .0 |
| 4.9 | 5.4 | 4.5 | 5.0 | 4.5 | − .4 | .0 |
| 5.0 | 5.6 | 4.6 | 5.2 | 4.8 | − .4 | + .2 |
| 5.1 | 5.8 | 4.8 | 5.3 | 5.1 | − .5 | + .3 |
| 5.2 | 6.0 | 4.9 | 5.4 | 5.3 | − .6 | + .4 |
| 5.3 | 6.1 | 5.1 | 5.5 | 5.4 | − .6 | + .3 |
| 5.4 | 6.3 | 5.2 | 5.7 | 5.5 | − .6 | + .3 |
| 5.5 | 6.4 | 5.4 | 5.8 | 5.5 | − .6 | + .1 |
| 5.6 | 6.5 | 5.6 | 6.0 | 5.6 | − .5 | .0 |
| 5.7 | 6.6 | 5.7 | 6.1 | 5.6 | − .5 | − .1 |
| 5.8 | 6.7 | 5.8 | 6.2 | 5.7 | − .5 | − .1 |
| 5.9 | 6.8 | 6.0 | 6.3 | 5.8 | − .5 | − .2 |
| 6.0 | 6.8 | 6.1 | 6.4 | 5.8 | − .4 | − .3 |
| 6.1 | 6.9 | 6.3 | 6.4 | 5.9 | − .5 | − .4 |
| 6.2 | 6.9 | 6.5 | 6.5 | 6.0 | − .4 | − .5 |
| 6.3 | +6.9 | 6.6 | +6.6 | 6.1 | −0.3 | − .5 |
| 6.4 | ..... | 6.8 | ..... | 6.2 | ..... | − .6 |
| +6.5 | ..... | +6.9 | ..... | +6.2 | ..... | −0.7 |

curves were derived, and the calibration was based on only a part of the stars in *Mt. W. Contr.* No. 511.[3]

Since the second regression line is the one usually of greater importance in the application of the spectroscopic absolute magnitudes

to astrophysical problems, the corrections from the given $M_s$ to this line, in the figure represented by the deviations of the continuous curve from the 45° line, were applied to the initial values of $M_s$.

TABLE 4

GROUPING ACCORDING TO $H$
(Corrected Calibration of $M_s$)

| $H$ | No. | $\bar{M}$ | Mean Error | $q$ | $\bar{M}_s$ | $q_s$ | $\bar{M}-\bar{M}_s$ | Mean Error | $q/q_s$ |
|---|---|---|---|---|---|---|---|---|---|
| | Dwarfs Go–G7 | | | | | | | | |
| 0.0– 2.9 | 28 | +3.92 | ±0.24 | 1.02 | +4.24 | 0.99 | −0.32 | ±0.26 | 1.02 |
| 3.0– 3.9 | 28 | 3.98 | .23 | 0.98 | 4.24 | 0.97 | − .26 | .25 | 1.01 |
| 4.0– 4.9 | 64 | 4.32 | .11 | 0.47 | 4.22 | 0.83 | + .10 | .13 | 0.57 |
| 5.0– 5.9 | 54 | 4.78 | .12 | 0.54 | 4.74 | 0.94 | + .04 | .14 | 0.58 |
| 6.0– 6.9 | 55 | 5.02 | .12 | 0.39 | 4.79 | 0.91 | + .23 | .14 | 0.43 |
| 7.0– 7.9 | 18 | 5.64 | .22 | 0.50 | 5.39 | 0.76 | + .25 | .26 | 0.65 |
| 8.0–12.2 | 12 | 5.8 | .43 | 1.10 | 5.74 | 1.07 | + .06 | .46 | 1.03 |
| ζ Herc. | 1 | 3.2 | .15 | ..... | 2.9 | ..... | + .3 | .55 | ..... |
| α Cent. | 1 | 4.7 | .10 | ..... | 5.2 | ..... | − .5 | .54 | ..... |
| μ Cass. | 1 | 5.9 | .20 | ..... | 6.3 | ..... | − .4 | .57 | ..... |
| τ Ceti | 1 | 6.0 | .10 | ..... | 6.5 | ..... | − .5 | .54 | ..... |
| Gr. 1830 | 1 | +6.7 | ±0.15 | ..... | +6.9 | ..... | −0.2 | ±0.55 | ..... |
| All. | 264 | +4.66 | ±0.06 | 0.87 | +4.62 | 1.00 | +0.04 | ±0.07 | 0.87 |
| | Dwarfs G8–K2 | | | | | | | | |
| 2.3– 4.7 | 25 | +5.20 | ±0.20 | 0.82 | +5.20 | 0.52 | 0.00 | ±0.22 | 1.58 |
| 4.8– 6.0 | 32 | 5.17 | .19 | .83 | 5.37 | .77 | − .20 | .21 | 1.08 |
| 6.1– 6.9 | 32 | 5.76 | .13 | .46 | 5.44 | .41 | + .32 | .15 | 1.12 |
| 7.0–12.7 | 21 | 5.62 | .25 | 0.81 | 5.57 | 0.41 | + .05 | .27 | 1.95 |
| β Aquil. | 1 | 3.3 | .20 | ..... | 3.3 | ..... | 0 | .47 | ..... |
| δ Erid. | 1 | 4.0 | .20 | ..... | 4.0 | ..... | 0 | .47 | ..... |
| 40 Erid. | 1 | +6.0 | ±0.10 | ..... | +6.0 | ..... | 0.0 | ±0.44 | ..... |
| All. | 113 | +5.41 | ±0.10 | 0.81 | +5.36 | 0.61 | +0.05 | ±0.11 | 1.33 |

Table 3 gives the resultant values of $M$ which represent the new second regression line. The first regression line, which should be used when the grouping is made on the basis of $M_s$ itself, is also given. The difference between the two sets of values is the "regression effect," which appears in the table as a function of the values of $M_s$ given in *Mt. W. Contr.* No. 511.[3]

The corrected values of $M_s$ for a grouping according to $M$ were used to recompute values of $\overline{M}_s$ and $q_s$, which are shown in Table 4. The agreement between $\overline{M}$ and $\overline{M}_s$ is, of course, now better than before, and the values of $q/q_s$ are now equivalent to $q/q_s''$.

The recomputation of the mean errors of an individual $M_s$ calibrated to represent the two regression lines gives for the G stars $\theta' = 0.41$, $\theta'' = 0.60$, and for the Ko stars $\theta' = 0.49$, $\theta'' = 0.65$.

After this study was nearly finished, the work of van Rhijn[4] was received. He has made an extensive study of the spectroscopic absolute magnitudes for all spectral types and derived corrections to $M_s$ based on both trigonometric parallaxes and proper motions. In comparing his results with those derived here, we find them, when the data are actually comparable, in good agreement. He starts from a comparison between $\pi_s$ and $\pi_t$ for different limits of $m$ and $M_s$, and in deriving an "impartial calibration" he assumes implicitly a linear correlation between $M_s$ and $M$. His "impartial calibration" does not aim at statistical equality between $M$ and $M_s$ for a neutral grouping, since the dispersion in $M$ is, in principle, smaller than the dispersion in the "impartially reduced" $M_s$. As a matter of fact, his "impartially reduced" $M_s$ corresponds very nearly to the reduction corresponding to the second regression line. He finds that the mean error in $M_s$ is for the dwarfs of type G and K equal to 0.54, which agrees well with my determination.

The work here presented has been done in close co-operation with Professor Russell. Many subtle questions regarding the proper calibration to be used in practice, the nature of the grouping according to $H$, and the significance of the mean errors $\theta$ have been settled by our joint efforts.

CARNEGIE INSTITUTION OF WASHINGTON
MOUNT WILSON OBSERVATORY
February 1940

[4] *Kapteyn Astron. Lab. Pub.*, No. 49, 1939.

# GALACTIC ROTATION AND ABSORPTION*

RALPH E. WILSON

ABSTRACT

The observed radial velocities of O and B stars, Cepheid variables, non-Cepheid c stars, and interstellar gases, all located within 30° of the galactic plane, have been analyzed to determine values of the galactic rotation constant, $A$. The values derived from objects at different distances from the sun are brought into fair agreement by assuming a mean effective absorption $a = 0.65$ mag/kpc for both visual and photographic light. Since the distribution of the absorbing material is definitely not uniform, this assumption does not lead to a true value of $A$.

A linear relation between the observed values of $A$ and the photometric distances is found. This brings all the observed values into satisfactory accord and gives a mean value

$$A = 17.7 \pm 0.7 \text{ km/sec kpc} .$$

Applied to visual and photographic sequences for $\bar{r}A$, this value of $A$ gives values of the mean absorption consistent with values derived on the assumption of uniform distribution.

Comparison of results based upon the planetary rotation theory and upon Milne's more general formulae indicates that the values of $a$ and $A$ are nearly independent of the underlying theory.

According to the planetary theory of galactic rotation, the constant $A$, the value of the rotation at unit distance (1 kiloparsec), is connected with the mean radial velocities of stars in a given region of the sky, corrected for solar motion, by the relation

$$\overline{V} = \bar{r}A \, \overline{\sin 2\lambda} \, \overline{\cos^2 b} + K , \qquad (1)$$

where $V$ is the corrected radial velocity; $r$, stellar distance; $\lambda = l - l_0$, the angle in galactic longitude between the star and the center of rotation; $b$, the galactic latitude; and $K$, a constant introduced to reduce $\Sigma\overline{V}$, over $n$ areas, to zero. By means of this relation one may determine from radial velocities of stars distributed over the sky the parameters $l_0$, the longitude of the rotational center, and $\bar{r}A$, the rotation at the mean distance of the reference stars. Solutions based upon suitable data give quite accordant values for $l_0$, but the better determinations of $A$ differ considerably. It is de-

* *Contributions from the Mount Wilson Observatory, Carnegie Institution of Washington,* No. 631.

sirable that this value be fixed as accurately as possible, especially since, if $A$ is known, the factor $\bar{r}A$ affords an effective basis for estimating mean stellar distances.

In theory the determination of $A$ is simple. Given the radial velocities of any well-distributed set of stars, a value of $\bar{r}A$ results directly from solutions based upon equation (1). Choose a set for which the mean distance $\bar{r}$ can be accurately derived and $A$ becomes known. In practice, however, three sources of difficulty are immediately apparent. First, the peculiar motions and distributions of most types of objects with known radial velocities are such as to render determinations of $\bar{r}A$ uncertain. Second, the values of $\bar{r}A$ near the sun, where the data are plentiful and the values of $r$ fairly determinate, are small; and even if they are not completely masked by the effects of peculiar and group motions, the values of $A$ derived from the quotient $\bar{r}A/\bar{r}$, which is rapidly approaching indeterminacy, will still be unreliable. Third, for large distances the data are scarce, and for values of $r$ one is forced to rely mainly upon differences between apparent and mean absolute magnitudes. Thus, any phenomenon which affects the apparent magnitudes necessarily enters into what we may call the "photometric distances."

It may be recalled that Oort[1] originally attempted to determine $A$ from stars of all types, but he found such a wide variety of results that his final solution[2] was based mainly upon the B stars and a few Cepheids and other c stars. Even with this limitation, his mean value, 19 km/sec kpc, was the result of judicious weighting of values ranging from 4 to 39 km/sec kpc, and among them there appears no correlation between $A$ and $\bar{r}$. The uncertainty was apparently reduced when Plaskett and Pearce[3] found $A = 15.5 \pm 0.9$ km/sec kpc from the O and B stars and the interstellar calcium. The probable error attached to this result seems rather small in view of the fact that the mean was derived from values ranging from 5.7 to 24.4 km/sec kpc. Later, Merrill and Sanford,[4] from an analysis of extensive interstellar material, found $A = 14.8$ km/sec kpc, apparently confirming the Plaskett-Pearce value.

[1] *B.A.N.*, **3**, 275, 1927.

[2] *Ibid.*, **4**, 79, 1927.

[3] *M.N.*, **94**, 679, 1934.

[4] *Mt. W. Contr.*, No. 585; *Ap. J.*, **87**, 118, 1938.

Joy's recent investigation[5] of rotation based upon the Cepheid variables reopened the whole problem. The Cepheids cover a range in photometric distance several times that covered by the O and B stars and the interstellar data. The radial velocities give a beautiful determination of the rotation and the longitude of the center, in spite of the fact that the southern third of the Milky Way is not represented. The peculiar motions, after rotation has been taken into account, are small, and the photometric distances presumably are accurately determined from the period-luminosity relation and the median apparent magnitudes. The rough mean of Joy's group values of $A$ is 14.0 km/sec kpc, but he found a definite correlation between the group values of $A$ and $\bar{r}$, ranging from 19.9 at 0.5 kpc to 6.8 at 5.5 kpc. Merrill and Sanford recognized a similar correlation in their results, and it can also be detected in the group values of Plaskett and Pearce, although in neither of these cases is it so prominent, owing to the smaller range in distance covered.

The correlation between $A$ and $\bar{r}$ is readily explained as the effect of an absorbing medium upon the apparent magnitudes and through them upon the photometric distances. To bring the values of $A$ derived from the Cepheid data into some sort of agreement, Joy assumed what seemed to be a rather high value of the absorption, $a = 0.85$ mag/kpc; the resultant mean value of the rotational constant was $A = 20.9 \pm 0.8$ km/sec kpc. This high value of the absorption was apparently confirmed by Merrill and Sanford in their investigation of the interstellar data; its adoption would raise their value of $A$ from 14.8 to 19.8 km/sec kpc. Recognition of the fact that allowance for galactic absorption might change the value of $A$ from 14 to 21 km/sec kpc was rather startling, and it thus became clear that an attempt should be made to determine the effect of absorption upon all the usable data and to reconcile the various derived values of the rotation constant.

## DATA

The selection of the data to be used was influenced by four considerations. Owing to the indeterminacy in $\bar{r}A/\bar{r}$ for small values of $\bar{r}$ and the masking of small values of $\bar{r}A$ by peculiar and group mo-

[5] *Mt. W. Contr.*, No. 607; *Ap. J.*, **89**, 356, 1939.

tions, near-by stars should not be used. Since galactic absorption is effective only near the galactic plane, stars in low latitudes only should be used. The peculiar motions should not be large enough to mask the rotation effect, and the distances should be determinable. Four sets of stars satisfy the conditions fairly well: the Cepheids, the non-Cepheid c stars, the O and B stars, and those in the spectra of which interstellar lines appear. These stars are all strongly concentrated toward the galaxy, their peculiar motions are small, their photometric distances may be determined with reasonable accuracy, and, taken together, they cover a wide range in distance. A study of all these data should give a better picture of galactic rotation and absorption than any single set.

All stars within a distance of 250 parsecs, except those revealing interstellar material for which the peculiar motion must be very small, and all stars more than 30° from the galaxy were excluded. By far the larger proportion of those used lie between latitudes $\pm 10°$, and essentially all of them are within 200 parsecs of the galactic plane.

The radial velocities of the O–B7 and the c stars were taken from Moore's "Catalogue of Radial Velocities"[6] and later Mount Wilson lists. Those of the Cepheids are from Joy's list;[5] the interstellar data are taken from Table 7 of the discussion by Merrill and Sanford.[4] All the velocities were corrected for a solar motion of 20 km/sec in the direction $A_0 = 270°$, $D_0 = +30°$.

The uncertainty in the direction of the rotational center is small and can hardly influence the results for the rotation constant. The determinations based upon the four sets of data to be used are given in Table 1. The rounded value, $l_0 = 325°$, was adopted.

The photometric distances were determined from the relation

$$\log r = 1 - 0.2\,(\overline{M} - m)\,, \qquad (2)$$

where $m$ is the apparent, and $\overline{M}$ the mean absolute, magnitude. For the Cepheids Joy's median photographic magnitudes were used, and for $M$, values from Shapley's[7] photographic period-luminosity relation. The absolute magnitudes adopted for the O–B and c stars are

[6] *Pub. Lick Obs.*, **18**, 1932. [7] *Star Clusters*, p. 135, 1930.

shown in Table 2. The former are adjusted means of the values derived by Merrill and Sanford and by Plaskett and Pearce. The latter are preliminary values from an unpublished investigation by the writer which includes only stars whose c characteristics have been verified from observations with slit spectrographs.

The data were divided in such a manner as to give a reasonable representation in various distance shells. The numerous O–B stars

TABLE 1

DETERMINATIONS OF THE DIRECTION OF THE ROTATIONAL CENTER

| Data | $l_0$ | Authority |
|---|---|---|
| O–B stars | 324°.4 | Plaskett-Pearce |
| Interstellar | 329. | Merrill-Sanford |
| Cepheids | 325.3 | Joy |
| Cepheids | 326.9 | Wilson |
| c stars | 324.4 | Wilson (unpub.) |
| Mean | 326.0 | |

TABLE 2

MEAN ABSOLUTE MAGNITUDES OF O, B, AND c STARS

| Spec. | $M$ | Spec. | $M$ | Spec. | $M$ |
|---|---|---|---|---|---|
| O | −3.6 | $B_3$ | −2.2 | cBo–cB6 | −5.7 |
| Bo | 3.3 | $B_4$ | 1.8 | $cB_7$–$cA_4$ | 5.1 |
| B1 | 3.0 | $B_5$ | 1.5 | $cA_5$–$cF_6$ | 4.2 |
| B2 | −2.6 | $B_7$ | −1.2 | $cF_7$–$cG_6$ | 3.3 |
| | | | | $cG_7$–$cK_5$ | −3.0 |

have not been observed over as great a distance range as the Cepheids and other c stars. Moreover, Plaskett and Pearce found notable differences in the values of $A$ derived from O–B2 and $B_3$–$B_7$ stars. These stars were therefore divided into four groups, two each according to type and distance. The Cepheids and c stars were divided into four distance groups, the c stars being represented in the first three only. The interstellar material was divided by Merrill and Sanford into four groups. In order to make the mean distances of the groups comparable, their first two groups were combined to form

a single group with $\bar{r} = 0.50$. The distance limits of the various groups are shown in Table 3.

The radial velocities and distances were, in general, averaged over zones of 15° in longitude and then smoothed by taking means of overlapping 30° zones. In most of the data the representation of the southern half of the galaxy is poor. The radial velocities found there were in all cases averaged with the zone 180° distant to give a single, rather than the actual double sine-curve. This procedure destroys any evidence of systematic differences of motion in different longi-

TABLE 3

DISTANCE LIMITS OF GROUPS

| Interstellar | O–B | | c—Cepheids |
|---|---|---|---|
| kpc | | kpc | kpc |
| < 0.80 | O–B2 | 0.25–0.75 | 0.25– 0.99 |
| 0.80–1.40 | | >0.75 | 1.00– 2.49 |
| >1.40 | B3–B7 | 0.25–0.75 | 2.50– 4.99 |
| | | >0.75 | 5.00–10.00 |

tudes but should, for this reason, tend to smooth the normals and to give a reliable mean value of $\bar{r}A$ or of $A$. In the case of the O–B stars the correction for the radial motion of the Scorpio-Centaurus group, suggested and used by Plaskett and Pearce, was not applied, inasmuch as Smart[8] has shown that the procedure is incorrect.

The mean radial velocities were divided by the mean distances to give normals in terms of $A$. The number of normals in each group varies from 8 to 12. These were weighted according to the square root of the number of radial velocities entering into them. The observed normals in each distance group for each set of data are shown in the left half of Figure 1. The groups, in order of increasing distance, are indicated by crosses, open circles, dots, and triangles.

Three general conclusions may be drawn from an inspection of these figures. First, with the exception of the nearest Cepheid and c stars, for which the data are not numerous, and of the B3–B7 stars in longitudes 120°–150° and 300°–330°, the normals may be well represented by a series of simple sine-curves cutting the $x$-axis at ap-

[8] *M.N.*, **96**, 568, 1936.

proximately 325° and 55°. Second, with the same exceptions, there is a general decrease in the amplitudes of the curves with increasing distance. Third, the amplitudes of the O–B2-curves are large, and those of the B3–B7-curves are small, as compared with those of the other sets of data.

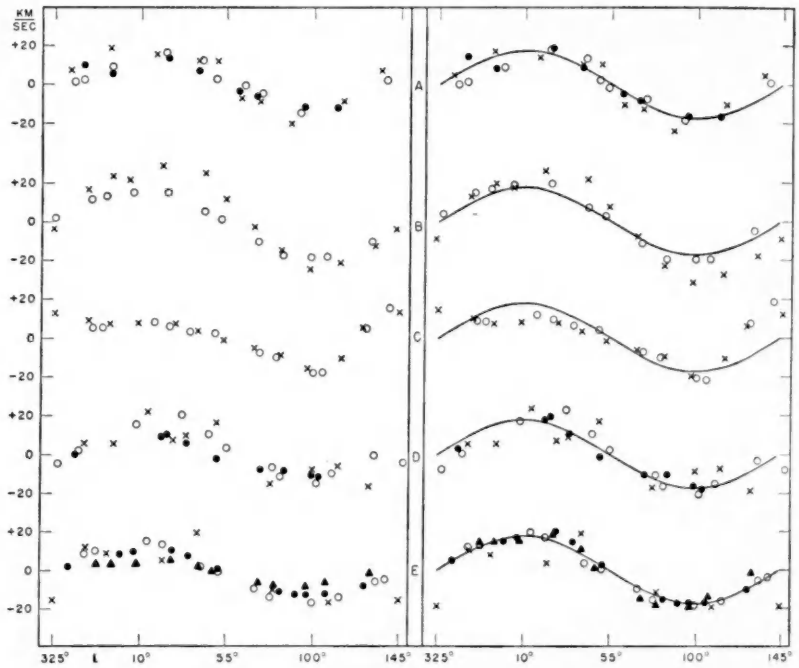


FIG. 1.—Distribution of normal radial velocities in galactic longitude. On the left are the observed normals; on the right, the normals corrected empirically for absorption and selection effects and reduced to the mean, and the mean curve of semiamplitude 17.7 km/sec, representing the combined data. The pairs of plots represent, respectively: *A*, interstellar gases; *B*, O−B2 stars; *C*, B3−B7 stars; *D*, c stars; and *E*, Cepheids. Groups in order of increasing distance are indicated by crosses, open circles, dots, and triangles.

## THE OBSERVED VALUES OF $\bar{r}A$ AND $A$

The weighted normals were analyzed by means of equation (1); and the resulting values of $\bar{r}A$ and $A_0$, where $A_0 = \bar{r}A/\bar{r}_0$, are given in Table 4. The table also gives the results from similar investigations of the O–B stars by Plaskett and Pearce and of the Cepheids by Joy, and the mean $A_0$ is derived from the interstellar data by Merrill

and Sanford. In the first two of these studies $\bar{r}A$ was derived from the solutions and $A_0$ from $\bar{r}A/\bar{r}_0$. In the latter study, as well as in the solutions for this paper, the normals were reduced to unit distance, and $A_0$ was determined directly, $\bar{r}A$ being the product $\bar{r}_0A_0 = \bar{r}A$. Owing to the manner in which the interstellar lines are formed, the

TABLE 4

OBSERVED VALUES OF $\bar{r}A$ AND $A_0$

| Date | No. | $\bar{r}_0$ | $\bar{r}A$ | $A_0$ | $2A_0$ | Authorities* |
|---|---|---|---|---|---|---|
| | | kpc | km/sec | km/sec | km/sec | |
| Interstellar | 272 | 0.50 | 4.40 | 8.8 | 17.6 | W |
| | 460 | 1.00 | 7.40 | 7.4 | 14.8 | MS |
| | 99 | 1.20 | 8.16 | 6.8 | 13.6 | W |
| | 89 | 2.40 | 14.8 | 6.2 | 12.4 | W |
| B3–B7, $m<5.5$ | 272 | 0.20 | 3.44 | 17.2 | ..... | PP |
| O, $m<5.0$; B0–B2, $m<6.0$ | 101 | 0.40 | 9.74 | 24.4 | ..... | PP |
| B3–B7 | 468 | 0.44 | 4.53 | 10.3 | ..... | W |
| B3–B7, $m>5.5$ | 317 | 0.48 | 3.33 | 7.0 | ..... | PP |
| O–B2 | 143 | 0.52 | 14.1 | 27.1 | ..... | W |
| B3–B7 | 48 | 1.02 | 13.0 | 12.7 | ..... | W |
| O–B2 | 128 | 1.26 | 22.0 | 17.5 | ..... | W |
| O, $m>5.0$; B0–B2, $m>6.0$ | 159 | 1.41 | 18.0 | 12.8 | ..... | PP |
| c stars | 83 | 0.54 | 7.51 | 13.9 | ..... | W |
| | 44 | 1.53 | 22.2 | 14.5 | ..... | W |
| | 24 | 3.40 | 34.7 | 10.2 | ..... | W |
| Cepheids | 35 | 0.52 | 10.35 | 19.9 | ..... | J |
| | 32 | 0.62 | 9.55 | 15.4 | ..... | W |
| | 33 | 1.56 | 22.7 | 14.5 | ..... | J |
| | 32 | 1.66 | 26.7 | 16.1 | ..... | W |
| | 34 | 3.20 | 38.9 | 12.2 | ..... | J |
| | 43 | 3.21 | 36.6 | 11.4 | ..... | W |
| | 26 | 5.56 | 37.7 | 6.8 | ..... | J |
| | 23 | 6.45 | 41.3 | 6.4 | ..... | W |

* J, Joy; MS, Merrill and Sanford; PP, Plaskett and Pearce; W, Wilson.

values of $A_0$ derived from normals based upon the distances of the stars in which these lines are found must be multiplied by a factor of 2 to give true values.

The scatter in the values of $A_0$ derived from the nearer stars, together with the scatter in the normals for the same stars shown in Figure 1, is evidence of the uncertainty inherent in any attempt to determine $A$ from them alone. At greater distances the results become more uniform, those from different sets of data and from differ-

ent groupings by different investigators agreeing reasonably well. The discordance between the values of $A_0$ given by the nearer O–B2 and B3–B7 stars is shown in the results of both Plaskett and Pearce and the writer. While the decrease in the values of $A_0$ with increase in photometric distance, found by Joy in the case of the Cepheids, is unmistakable, the scatter in the values, especially among the O–B stars, is large enough to render any estimate of the rate of that decrease quite uncertain. The best one can do, apparently, is to construct from the results in Table 4, for each set of data, a table of straight means taken for various distances. No system of weighting seems justifiable, since the greater part of the data naturally falls in the nearer groups, where the uncertainty of the quotient $\bar{r}A/\bar{r}$ is greatest. These mean results are shown in the second, third, and fourth columns of Table 5.

### CALCULATION OF ABSORPTION AND A MEAN VALUE OF THE ROTATION CONSTANT

The parameter $\bar{r}A$ is a result of observation, independent of any assumption other than that the radial velocities can be represented by a double-wave term, the amplitude of which varies with distance. According to the theory of planetary rotation, $A$ is a constant except for second-order terms in $\bar{r}/R$, where $R$ is the distance to the rotational center. At distances covered by the data under consideration the second-order terms, as Joy has shown,[5] can have little influence upon the determination of $A$. Hence, since the values of $A_0$ decrease with increasing distance, either the theory is wrong and $A$ is not constant or the photometric distances increase too rapidly. In the light of several lines of evidence, one can scarcely doubt that the latter alternative holds. Direct photographs of extragalactic nebulae showing obscuration, the zone of avoidance appearing in counts of these nebulae, interstellar lines in stellar spectra, and the calculated dimensions of galactic clusters constitute evidence of the existence of a shallow layer of absorbing matter in the galactic plane. The principal difference of opinion about this material is whether or not its distribution is uniform. The forms of diffuse nebulae, irregularities in star counts, observations of color excess, and the irregular limits of the zone of avoidance in the nebular counts show definitely that the distribution is not uniform. This conclusion offers a satisfactory

explanation of a wide variety of results found from investigations covering limited fields.

On the other hand, Trumpler's [9,10] studies of the dimensions of the galactic clusters seem to indicate that in its effect upon fairly extensive data the absorption may be quite uniform in the mean out to a distance of 2.0 kpc. In his study of the Cepheids Joy clearly reached out to distances where the effects of spotty distribution of the absorbing material were readily apparent. He was forced to reject the radial velocities of a number of the Cepheids because they are situated in regions in which direct photographs show abnormally large amounts of absorbing matter. And, even on the assumption of what seemed a rather large value of uniform absorption, he was unable to bring the value of $A$ from the most distant group into agreement with the others. It is doubtful, therefore, if we should expect to find a single-valued absorption which will bring all the values of $A_0$ in Table 5 into accord. Nor is there evidence that within a single set of data the mean absorption is the same at all distances; in fact, what evidence we have would indicate that it is not.

What we actually observe is a nonlinear correlation between $\bar{r}_0$ and $\bar{r}A$. The problem is to express this in terms of a linear correlation, $A$ being a constant. Recognizing that the distribution of the absorbing material is not uniform, but lacking means of estimating its effects in different galactic areas, we are faced with two alternatives. (I) We may assume, as was done by Trumpler and Joy, that in the data under consideration the effects of nonuniform absorption are largely washed out, and may attempt to find a mean value of $a$, the absorption per kiloparsec, which will bring the values of $A$ into agreement. Or (II), assuming that we know nothing about the distribution of the absorbing material in the galactic zone, we may attempt to determine how $A_0$ varies with distance and, if an empirical relation can be established, we may from it find a value of $A$.

I. On the first assumption, values of the rotation and absorption are derived from distance sequences of the form

$$\left.\begin{aligned} \bar{r}_{0i}A_{0i} &= \bar{r}_i A \ , \\ \log \bar{r}_{0i} &= \log \bar{r}_i + 0.2\, a\bar{r}_i \ , \end{aligned}\right\} \qquad (3)$$

where

[9] *Lick Obs. Bull.*, **14**, 154, 1930. [10] *Ap. J.*, **91**, 191, 1940.

and $\bar{r}_{oi}$ and $A_{oi}$ represent the observed sequences in $\bar{r}_o$ and $A_o$ given in the second and fourth columns of Table 5. If only two groups are available, $a$ and $A$ are determined uniquely. For example, for the O–B stars we find $a = 0.75$, $A_1 = 19.5 = A_2$. When more than two groups are available, the situation is complicated by the fact that the end-groups, which naturally play the principal part in the determination of $a$, are just those in which the determinations of $A_{oi}$ are weakest. For example, if from Table 4 one takes the extreme cases, $A_{01} = 27.1$ ($\bar{r}_o = 0.52$ kpc) or 7.0 ($\bar{r}_o = 0.48$), in combination with $A_{04} = 6.4$ ($\bar{r}_o = 6.45$), he gets in the first case a large absorption and in the second practically none, and neither calculated value of $a$ will satisfy the intermediate values of $A_{oi}$. Furthermore, relations (3) imply a direct correlation between $a$ and $A$; if $a$ is small, $A$ likewise is relatively small, and vice versa. The problem thus becomes one largely of personal judgment as to what constitutes reasonable agreement between values of $A$.

Trial of a number of values of $a$ showed surprisingly little variation in those which would bring the separate sets of data in Table 5 into fair accord. It appears that a mean value $a = 0.65$ mag/kpc satisfies all the values of $A_i$ save two, those derived from the nearer group of c stars and those from the most distant group of Cepheids. The scatter in the normals given by the nearer c stars (Fig. 1) indicates considerable uncertainty in the first case. In the second, an absorption of 1.10 mag/kpc will bring the value $A_4$ into agreement with the others. Since this absorption reduces $\bar{r}_4$ nearly to $\bar{r}_3$, the large value of $\bar{r}_{04}$ and the consequent low value of $A_{04}$ should be attributed to the effect of abnormal absorption upon the limited data involved, and the assumption of uniform distribution becomes invalid. The discordant values for these two groups are put in parentheses in Table 5, and they have been given half-weight in taking means. The mean value, $a = 0.65$ mag/kpc, is in harmony with recent values of photographic absorption: 0.72, derived by Berman[11] from studies of the planetary nebulae, and 0.70, by Trumpler[10] from the galactic clusters.

The distances $r_o$ in the first three sets of data are based upon visual magnitudes, $m_v$, and those of the Cepheids upon photographic, $m_{pg}$.

[11] *Lick Obs. Bull.*, **18**, 64, 1937.

The values of $\bar{r}_0$ and $A_0$ in the first three sets were combined to give a visual sequence (fourth division of Table 5) for comparison with the photographic defined by the Cepheids alone. It was surprising to find that the two sequences give the same value of $a$. If the absorption is caused by scattering, the consequent loss of light is greater for short wave lengths than for long, and the value of $a$ should be greater for photographic magnitudes than for visual. The probable error of $a$ is of the order of $\pm 0.05$ mag/kpc. A color excess as large

TABLE 5

MEAN VALUES OF $\bar{r}A$ AND $A$

| Data | $\bar{r}_0$ | $\bar{r}A$ | $A_0$ | $\bar{r}$ | $A_{\mathrm{I}}$ | $A_{\mathrm{II}}$ |
|---|---|---|---|---|---|---|
| | kpc | km/sec | km/sec | kpc | km/sec | km/sec |
| Interstellar ($m_v$) | 0.50 | 8.8 | 17.6 | 0.439 | 20.0 | 18.7 |
| | 1.10 | 15.6 | 14.2 | 0.852 | 18.3 | 16.6 |
| | 2.40 | 29.6 | 12.4 | 1.52 | 19.5 | 17.5 |
| O–B stars ($m_v$) | 0.41 | 7.05 | 17.2 | 0.367 | 19.2 | 18.1 |
| | 1.23 | 17.6 | 14.3 | 0.933 | 18.9 | 16.9 |
| c stars ($m_v$) | 0.54 | 7.51 | (13.9) | 0.469 | (16.0) | (15.1) |
| | 1.53 | 22.2 | 14.5 | 1.10 | 20.2 | 17.8 |
| | 3.40 | 34.7 | 10.2 | 1.91 | 18.2 | 17.5 |
| All ($m_v$) | 0.47 | 7.85 | 16.7 | 0.415 | 18.9 | 17.7 |
| | 1.25 | 17.9 | 14.3 | 0.943 | 19.0 | 17.0 |
| | 2.40 | 29.6 | 12.4 | 1.52 | 19.5 | 17.5 |
| | 3.40 | 34.7 | 10.2 | 1.92 | 18.1 | 17.5 |
| Cepheids ($m_{pg}$) | 0.57 | 10.0 | 17.6 | 0.492 | 20.4 | 18.8 |
| | 1.61 | 24.8 | 15.4 | 1.14 | 21.8 | 18.7 |
| | 3.20 | 37.8 | 11.8 | 1.84 | 20.5 | 18.3 |
| | 6.00 | 39.6 | 6.6 | (2.69) | (14.7) | 18.8 |

as that found by Trumpler,[9] 0.32 mag/kpc, should show up in the comparison of the $m_v$ and $m_{pg}$ sequences. On the other hand, a mean color excess of the order of 0.1 mag/kpc, indicated by the work of Stebbins, Huffer, and Whitford,[12,13] might not be readily apparent. We must conclude that, within the uncertainty inherent in the data and the method, the results from the two sequences show no difference between visual and photographic absorption if we assume that the distribution of the absorbing matter is uniform.

[12] *Mt. W. Contr.*, No. 617; *Ap. J.*, **90**, 209, 1939.

[13] *Mt. W. Contr.*, No. 621; *Ap. J.*, **91**, 20, 1940.

The mean value of the rotation correlated with the absorption $a = 0.65$ mag/kpc is

$$\overline{A}_I = 19.2 \text{ km/sec kpc},$$

the three visual sequences giving 19.0 and the single photographic, 20.0 km/sec kpc. The value of $A$ derived from the most distant group of Cepheids, however, is definitely discordant.

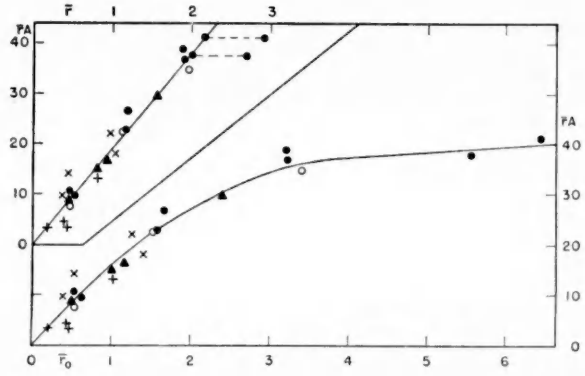


FIG. 2.—Rotation effect and distance (kpc). The lower figure shows the correlation between the rotation factors and photometric distances; the upper, the correlation with distances corrected for an absorption of 0.65 mag/kpc. The different sets of data are indicated as follows: interstellar, triangles; O–B2 stars, crosses; B3–B7 stars, plus signs; c stars, open circles; and Cepheids, dots. The two pairs of points representing values of $\bar{r}A$ derived from the most distant Cepheids are based upon two values of the absorption, 0.65 and 1.10 mag/kpc.

II. The assumption of uniform distribution of the absorbing material is only justifiable as a method of arriving at an estimate of its mean effect upon stellar distances. Nonuniform distribution is certainly a better postulate. In this case we may expect to find an apparent increase in absorption with distance, either actual or arising as a selection effect from the process of basing the distances $r_0$ on apparent magnitudes affected by nonuniform absorption.

Suppose that all the stars are of the same true magnitude, $m$, and situated at a true distance of 1 kpc, behind a veil of spotty absorption. Since they are at the same distance, the rotational factor determined from the radial velocities is constant no matter how the data may be divided, i.e., $\bar{r}A = \text{const}$. Owing to variations in ab-

sorption, however, the apparent magnitudes and the computed distances, $r_0$, based upon them will vary, and relations (3) will no longer give true values of $A_0$. In this case

$$\log \bar{r}_{0i} = \log \bar{r}_i + 0.2\, a_i \bar{r}_i , \tag{4}$$

which implies a correlation between $r_0$ and $a$ rather than between $r_0$ and $A_0$. Obviously, unless $a$ is a constant or $A$ can be determined independently, the problem becomes indeterminate. A simple numerical example will serve as an illustration.

Let $\bar{r}A = 18.0$ km/sec and $\bar{r} = 1.0$ kpc. Let $r_0$ vary, owing to absorption, as shown in Table 6. There results from the relation

TABLE 6

SELECTIVE EFFECTS OF NONUNIFORM ABSORPTION

| $r_0$ | $\bar{r}A$ | $A_0$ | $a_c$ | $r_c$ | $A_c$ |
|---|---|---|---|---|---|
| kpc | km/sec | km/sec | mag/kpc | kpc | km/sec |
| 1.0..... | 18.0 | 18.0 | 0.00 | 0.70 | 25.7 |
| 1.5..... | 18.0 | 12.0 | 0.88 | 0.93 | 19.4 |
| 2.0..... | 18.0 | 9.0 | 1.50 | 1.13 | 15.9 |
| 2.5..... | 18.0 | 7.2 | 2.00 | 1.30 | 13.8 |
| (Mean) 1.66.... | 18.0 | 10.8 | 1.10 | 1.00 | 18.0 |

$r_0 A_0 = \bar{r}A$ an apparent correlation between $r_0$ and $A_0$ due wholly to the correlation between $r_0$ and $a$. The mean absorption, 1.10 mag/kpc, in combination with the logarithmic mean distance, gives true values of $r$ and $A$ but leaves in the distance-sequence a correlation between $r_0$ and $A_c$ which is purely a selection effect. The equalization of the values of $A_c$ clearly involves the assumption of a much larger value of $\bar{a}$ and results in an absurdly high value of $\overline{A}_c$.

The true value of $A_0$ is obviously given by the unveiled stars, since in this case, if the errors in the values of $m$ and $\overline{M}$ are neglected, $\bar{r}_0 = \bar{r}$. This suggests that, in general, a close approximation to the true value of $A$ should be given by the stars near the sun, where the correction to the distance, owing to absorption, is small. Unfortunately, these values are just those which for other reasons are most uncertain. However, a plot (Fig. 3) of the values of $r_0$ and $A_0$ (Table 5) for the separate $m_v$ and $m_{pg}$ sequences shows that the

change in $A_0$ with distance is not only essentially linear but that the slopes of the correlations are approximately the same for both series. Least-squares solutions of the form

$$A = A_0 + \varphi r_0 , \tag{5}$$

give

$$A_v = 17.4 \pm 0.13 \text{ km/sec kpc} ,$$

$$A_{pg} = 18.6 \pm 0.07 \text{ km/sec kpc} ,$$

$$\varphi_v = 2.14 \pm 0.10 ,$$

$$\varphi_{pg} = 2.04 \pm 0.04 .$$

The difference $\varphi_v - \varphi_{pg}$ reduces to zero if either the mean absolute magnitudes of the visual sequence are brightened by 0.25 mag. or those of the Cepheids are made fainter by 0.2 mag. The former is a quite acceptable correction. The values of $A$ given by substituting the computed values of $\varphi$ in equation (5) are given under the heading $A_{II}$ in the last column of Table 5. The agreement is eminently satisfactory, and the most distant group of Cepheids no longer stands out from the others.

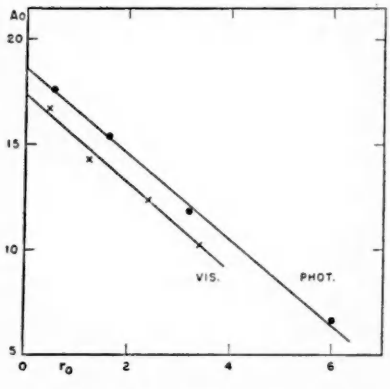


FIG. 3.—Correlation between $r_0$ and $A_0$. *Above*, the photographic sequence, represented by the Cepheids alone; *below*, the visual sequence.

In view of the large differences in the values of $A_0$ and $A$ given by the O–B2 and B3–B7 stars, as well as the nearer c stars, the difference $A_v - A_{pg}$ (1.2 km/sec, comparable to 1.0 derived on assumption I) must be laid to uncertainties innate in the determinations of rotation; i.e., to peculiar and group motions and poor representation of the southern third of the galaxy. The four sets of data in Table 5 give for $A$ the values in Table 7. The residuals from the mean are roughly proportional to the number of stars involved in the solutions

for rotation, and the agreement is as good as can be expected from the data. The mean is

$$\bar{A}_{II} = 17.7 \text{ km/sec kpc}.$$

The representation of the normals in the left half of Figure 1, after correction for the derived values of $K$ and by means of the linear

TABLE 7

MEAN VALUES OF $A$

| Data | $A$ | O−C | No. of Stars |
|---|---|---|---|
| | km/sec kpc | km/sec kpc | |
| Interstellar | 17.6 | −0.1 | 460 |
| O–B stars | 17.5 | −0.2 | 787 |
| c stars | 17.1 | −0.6 | 151 |
| Cepheids | 18.6 | +0.9 | 130 |
| Mean | 17.7 | 0.0 | 1528 |

TABLE 8

COMPUTED VALUES OF $\bar{a}$

| VISUAL | | | PHOTOGRAPHIC | | |
|---|---|---|---|---|---|
| $\bar{r}_o$ | $\bar{r}_c$ | $\bar{a}$ | $\bar{r}_o$ | $\bar{r}_c$ | $\bar{a}$ |
| kpc | kpc | mag/kpc | kpc | kpc | mag/kpc |
| 0.47 | 0.444 | 0.12 | 0.57 | 0.565 | 0.02 |
| 1.25 | 1.01 | 0.46 | 1.61 | 1.40 | 0.30 |
| 2.40 | 1.68 | 0.78 | 3.20 | 2.14 | 0.88 |
| 3.40 | 1.96 | 1.20 | 6.00 | 2.24 | 2.14 |
| Mean | 1.27 | 0.64 | Mean | 1.59 | 0.84 |

factor $\varphi r_o$, by the mean curve of semiamplitude $A$ is shown in the right half of the figure. In general, this representation is much closer than that secured by using a constant value of the absorption instead of $\varphi\bar{r}_o$.

Assuming that $\bar{A}_{II}$ represents the true value of the rotation constant, one may estimate the apparent change in mean absorption

with distance by computing the distances $r_c = \bar{r}A/\overline{A}_{II}$ and comparing them with $\bar{r}_o$. The results for the visual and photographic sequences are shown in Table 8. The mean values of $\bar{a}$ agree fairly well with the values derived on the assumption of uniform distribution above and with those by Berman, Trumpler, and Joy. While the difference $\bar{a}_{pg} - \bar{a}_v$ is of the sign to be expected, if the absorption is due to the scattering of light, this difference is entirely due to the large value derived in the last photographic group. The values of $\bar{a}$ are too uncertain to warrant any conclusions as to color excess.

Thus, without making any assumption as to the distribution of the absorbing material, we reach practically the same conclusion as to the mean effective absorption as is reached on the assumption of uniform distribution. The two postulates, however, result in quite different values of the rotation constant. If the evidence of nonuniform distribution of the absorbing material presented above is not completely convincing, additional evidence as to the probability of one or the other postulate may perhaps be derived statistically from the application of the two values of $A$ to the determination of mean stellar distances and mean absolute magnitudes.

### EFFECT UPON DETERMINATIONS OF MEAN ABSOLUTE MAGNITUDE

The foregoing investigation was suggested by the large difference in the corrections to the Cepheid period-luminosity relation derived[14] from comparisons of parallactic and peculiar motions and from the rotational factor with the aid of Joy's values of $A$ and $a$. This difference, between $-0^M.38$ and $+0^M.37$, seemed altogether too large in view of the accuracy of the determinations of $\bar{\pi}$ and $\bar{r}A$. In a later discussion of the mean absolute magnitudes of the N stars[15] it was found that large values of $A$ gave quite improbable results.

In the determination of mean absolute magnitudes two methods were used. The first involves the determination of mean parallax from comparisons of parallactic and peculiar motions, based upon proper motions and radial velocities separately. In the second, the mean distances are determined from the combination of the rotation

[14] *Mt. W. Contr.*, No. 604, pp. 21–22; *Ap. J.*, **89**, 238–39, 1939.

[15] *Mt. W. Contr.*, No. 615, p. 10; *Ap. J.*, **90**, 361, 1939.

constant with the rotational factors derived from the radial velocities alone. The relations applying are[15]

$$\left.\begin{aligned} \overline{M}_\pi &= \overline{m}_1 + 5 + 5 \log \bar{\pi} + 5C_1 - \frac{ac}{1000\bar{\pi}}, \\ \overline{M}_r &= \overline{m}_2 + 5 - 5 \log \bar{r} - 5C_2 - \frac{a\bar{r}}{1000}, \end{aligned}\right\} \tag{6}$$

in which $m_1$ and $m_2$ are the mean apparent magnitudes of the stars involved, $C_1 = \overline{\log \pi} - \log \bar{\pi}$, and $C_2 = \overline{\log r} - \log \bar{r}$, corrections for dispersion in distance; $a$ is the absorption and $c = \bar{\pi} \cdot \bar{r}$. If the distribution of $\log \pi$ is Gaussian and the same stars are used in each case, $m_1 = m_2$ and $C_1 = C_2$, and in the mean, $\overline{M} = \frac{1}{2}(\overline{M}_\pi + \overline{M}_r)$, the troublesome correction for dispersion disappears. If only a fairly large proportion of the stars are common to the two sets, as generally happens, the difference between the corrections for dispersion is small and has little effect upon $\overline{M}$. Though the difference, $\overline{M}_\pi - \overline{M}_r$, which equals $10C$, approximately, is more sensitive to differences in data, it enables one to obtain an estimate at least of the value of $c$, since $\log c = -2C$, approximately. The values of the mean distance $\bar{r}$, and hence of $\overline{M}_r$, naturally depend upon the value adopted for $A$. Since $c = \bar{\pi} \cdot \bar{r} > 1$, values of the rotation constant which satisfy this condition must a priori be considered more probable than those which do not.

The two values of $A$ derived above have been used in determinations of the mean absolute magnitudes and dispersions for the Cepheids and N stars, the results being given in Table 9. Since the two sets of Cepheids, i.e., those used in the determinations of $\overline{M}_\pi$ and of $\overline{M}_r$, respectively, have different mean periods, implying different mean absolute magnitudes, comparisons must be made of the corrections to the period-luminosity-curve, $\Delta M_\pi$ and $\Delta M_r$. With the estimated absorptions, which appear reasonable, it is clear that 17.7 km/sec kpc is the maximum value of $A$ which will give real dispersions in distance. To permit any appreciable increase in $A$ would involve considerable increases in the values of $a$, which are not reasonable. This value of $A$ brings the values of the corrections to the period-luminosity-curve of the Cepheids derived by the two

relations into exact agreement, in contrast to the difference of 0.8 $M$ found by using Joy's values of $a$ and $A$, though changing the mean correction by only $-0.03M$. It brings the two values for the N stars into agreement but changes the mean by but $-0.04M$ from that derived by using Plaskett's value of $A$. The exact agreement in the two cases is, of course, fortuitous. It implies no dispersion in distance. Smaller values of $A$ will give real dispersions; larger values produce imaginary dispersions. Granting a certain degree of tolerance, in

TABLE 9

COMPARISONS OF MEAN ABSOLUTE MAGNITUDES

| | $a$ | $\bar{M}_\pi$ | $\Delta\bar{M}_\pi$ | $A=19.2$ | | | $A=17.7$ | | |
|---|---|---|---|---|---|---|---|---|---|
| | | | | $\bar{M}_r$ | $\Delta\bar{M}_r$ | $c$ | $\bar{M}_r$ | $\Delta\bar{M}_r$ | $c$ |
| Cepheids | 0.65 | −1.87 | −0.17 | −1.86 | −0.02 | <1 | −2.11 | −0.17 | 1.0 |
| N stars | 0.50 | −1.88 | ..... | −1.68 | ..... | <1 | −1.88 | ..... | 1.0 |

view of the uncertainties involved in both data and method, the value $A_{II}$ is statistically satisfactory; $A_I$ is not.

## CONCLUSIONS

The evidence gathered from practically every line of significant research makes it clear that the distribution of the absorbing matter in the Milky Way zone is not uniform.

The mean effective absorption out to a true distance of 2 kpc is 0.65 ± 0.05 mag/kpc on visual magnitudes and probably not more than 0.1 mag/kpc greater on photographic. The method of determining distances from differences between mean absolute magnitudes and apparent magnitudes affected by nonuniform absorption, however, necessarily introduces into sequences of the form $\bar{r}_{0i}A_{0i} = \bar{r}_1 A$ based upon these distances a selection effect which produces an apparent correlation between $\bar{r}_0$ and $A_0$. Attempts to reduce nonlinear correlations between $\bar{r}_0$ and $\bar{r}A$ to linear ones by means of constant values of the absorption lead to values of $A$ which are too great.

The observed correlation between $\bar{r}_0$ and $A_0$, probably a composite of that due to selection and a real correlation between $r_0$ and $a$, ap-

pears to be linear. This leads to the value of the rotation constant

$$A = 17.7 \pm 0.7 \text{ km/sec kpc}.$$

The probable error is estimated from the dispersion in the values derived from the individual solutions, Table 4—not from the means in Table 5. In the two cases considered, this value of $A$ gives distances derived from the rotational factors $\bar{r}A$ which are statistically satisfactory. Larger values of $A$ do not give satisfactory results.

This value of $A$ may be used to calculate the period of revolution of the sun about the center of the Galaxy and its distance from that center. Both values are given by the relation between the rotation constants[16]

$$B = A - \frac{V}{R}, \tag{7}$$

in which $V$ is the speed of rotation at the sun and $R$ the distance of the sun from the galactic center. $V/R$ represents the total angular rotation, $\omega$, and equation (7) may be written

$$\omega = \frac{A}{4.74} - \frac{B}{4.74}. \tag{8}$$

With $A = +17.7$ km/sec kpc, $A/4.74 = +0''.0037$ per annum. From the mean of three modern determinations, $B/4.74 = -0''.0027$ per annum.[17] Hence $\omega = 0''.0064$ per annum, and the period of rotation of the Galaxy at the distance of the sun from the center is $2.02 \times 10^8$ years.

The distance of the sun from the galactic center depends largely upon what value of $V$ is used. The true value probably lies between 275 and 300 km/sec. With $A = +0.0177$ and $B = -0.0128$ in km/sec parsec,

$$9000 < R < 9800 \text{ parsecs}.$$

[16] Oort, *B.A.N.*, **4**, 80, 1927.

[17] $-0''.0025$, Plaskett-Pearce, 850 O–B stars
$-0''.0025$, Raymond-Wilson, 30,000 GC stars
$-0''.0030$, van de Kamp-Vyssotsky, 18,000 faint stars.

## ROTATION OR EXPANSION?

In the foregoing investigation it has been assumed that the theory of planetary galactic rotation holds. This theory offers such a reasonable explanation of the double-wave term in both radial velocities and proper motions, of the asymmetry in stellar motions, and of the shapes of the extragalactic systems that it has met with general acceptance as a working hypothesis. There are two main objections to it. First, in the few cases observed in extragalactic systems, the rotation is like that of a cart wheel, increasing linearly from the center outward. If the rotation is not as a solid, the differential effect is certainly much smaller than that apparent in our own system. Second, it is difficult to explain the present existence of clusters like the Hyades with a shearing effect as large as that observed, though possibly the fact that the solar zone has completed but a few rotations about the galactic center in its history may be a sufficient explanation.

Milne has shown[18] that

> any spatio-velocity stellar distribution-function whatever which possesses certain differential coefficients is accompanied by, in general, a K-term and a double wave in radial velocities, and a systematic drift and an associated double wave in the transverse motions, in any arbitrary plane.

In so far as the effect upon the radial velocities is concerned, the relation is of the form

$$\overline{V} = \bar{r}(K + A \sin 2\lambda + B \cos 2\lambda) \cos^2 b \,. \tag{9}$$

This equation may be applied to the particular cases of galactic rotation and expansion, since for pure rotation

$$K = B = 0 \,,$$

and for pure expansion

$$A = 0 \,.$$

Since the coefficients of $A$ and $B$ are respectively the sine and the cosine of the same angle, however, it is impossible to tell from relations of this form alone whether the terms in the radial velocities

[18] *M.N.*, **95**, 562, 1935.

represent galactic rotation or expansion or both, or rotation or expansion or both, of the local system. It thus appears that the double-wave term in the radial velocities is not in itself evidence of galactic rotation, though it is difficult to explain the asymmetry in stellar motions or the motions of the globular clusters and extragalactic systems on any other basis.

The data collected above afford an opportunity to compare quantitatively the results from 2-parameter solutions based on equation

TABLE 10

COMPARISON OF 2- AND 3-PARAMETER SOLUTIONS

| No. of Stars | $\bar{r}_0$ | $\bar{r}K$ | $\bar{r}A$ | $\bar{r}K$ | $\bar{r}A$ | $\bar{r}B$ |
|---|---|---|---|---|---|---|
| | kpc | km/sec | km/sec | km/sec | km/sec | km/sec |
| 551 | 0.53 | −0.3 | + 6.4 | −0.3 | + 6.4 | −0.1 |
| 143 | 1.48 | 3.2 | 22.0 | 3.0 | 21.9 | +2.4 |
| 71 | 3.35 | 6.3 | 35.9 | 6.7 | 35.9 | −3.8 |
| 23 | 6.19 | −8.0 | +40.4 | −7.9 | +40.0 | +5.0 |

| No. of Stars | $r$ | $K$ | $A$ | $K$ | $A$ | $B$ |
|---|---|---|---|---|---|---|
| 551 | 0.46 | −0.7 | +13.9 | −0.7 | +13.9 | −0.2 |
| 143 | 1.07 | 3.0 | 20.6 | 2.8 | 20.5 | +2.2 |
| 71 | 1.90 | 3.3 | 18.9 | 3.5 | 18.9 | −2.0 |
| 23 | 2.73 | −2.9 | +14.8 | −2.9 | +14.7 | +1.8 |

(1) and 3-parameter solutions based on equation (9). For this comparison the combined data for stars in latitudes $b \leqslant \pm 10°$ were divided into four distance-groups—0.25–0.99, 1.00–2.49, 2.50–4.99, and $> 5.00$ kpc—and normals formed for each 15° of longitude. The results for the first group will not be comparable with those obtained earlier, because the mean normals here used reflect the small values given by the numerous B3–B7 stars, but the two sets of solutions are *inter se* strictly comparable. The results of these two analyses are shown in Table 10. The value of the absorption $a = 0.65$ mag/kpc was used to determine the values of $\bar{r}$ in the second division of the table.

The introduction of the third parameter $\bar{r}B$ reduces but slightly the probable errors of the different parameters. The values of $B$ are

small in comparison with $A$ and alternate in sign, showing no correlation with $r$. One may safely conclude that in the mean $B = 0$. The increase in $\bar{r}K$ with $\bar{r}$ is interesting, but its significance is doubtful. It might be interpreted as a contraction of the local system. However, if a rotational velocity of 300 km/sec produces a differential effect of but 17.7 km/sec kpc, certainly a contraction of but 2.4 km/sec kpc in the local system is too small to produce the same effect. Rotation, therefore, rather than expansion or contraction, appears to be the factor producing the double-wave term in the radial velocities. It is significant also that the introduction of an extra parameter produces little or no change in the values of $\bar{r}A$, so that the earlier conclusions as to the value of $A$ hold for 3- as well as for 2-parameter solutions. As far as the data under consideration are concerned, therefore, the physical definition of $A$ is not essential to the determinations of its value.

CARNEGIE INSTITUTION OF WASHINGTON
MOUNT WILSON OBSERVATORY
April 1940

# THE MEAN COEFFICIENT OF SELECTIVE ABSORPTION IN THE GALAXY*

JOEL STEBBINS,[1] C. M. HUFFER, AND A. E. WHITFORD

ABSTRACT

From the colors of B stars near the plane of the Galaxy and out to 2000 parsecs from the sun it is concluded that the effect of the interstellar material is too irregular to be represented by a mean coefficient of selective or of total absorption.

In two recent papers[2, 3] on the colors of B stars we concluded that the interstellar material near the plane of the Galaxy is so irregular in distribution that a mean coefficient of selective or of total absorption can have little significance. Even when taken over a limited region, say 5° or 10° square, the dispersion in color excess of stars of the same spectrum and apparent magnitude is so great that we are forced to admit the existence of small clouds of obscuration. Moreover, the dark areas of the Milky Way, such as the Great Rift and the Coal Sack, visible to the naked eye, the small nebulae photographed by Barnard and others, and the less obvious obscurations of greater extent brought to light by star counts are all sufficient to cast doubt upon a general coefficient of absorption. It is not a question whether these irregularities exist, but rather whether they can be smoothed out over volumes of space extending, say, 1000 or 2000 parsecs from the sun. There are many problems of stellar distribution in the Galaxy which depend fundamentally upon an assumed mean absorption, and a number of investigations have been based upon such a mean. Therefore, it seems worth while to present in greater detail the evidence from our colors of B stars.

In the first study of 733 stars[4] we derived values of the coefficient

* *Contributions from the Mount Wilson Observatory, Carnegie Institution of Washington*, No. 632.

[1] Research associate of the Mount Wilson Observatory, Carnegie Institution of Washington.

[2] *Mt. W. Contr.*, No. 617; *Ap. J.*, **90**, 209, 1939.

[3] *Mt. W. Contr.*, No. 621; *Ap. J.*, **91**, 20, 1940.

[4] *Pub. Washburn Obs.*, **15**, Part 5, 1934.

of color excess per kiloparsec for the stars within 5° of the galactic equator in each section of 20° of longitude. We now give the same coefficient for 1332 stars, which include the stars of the earlier list. In Table 1 the first column gives the limits of longitude. The second column gives $c_1$, the color excess per kiloparsec, which was derived simply by adding up all the color excesses and dividing by the total distances of the stars. It is the same coefficient as $c_1$ in Table X,

$$c_1 = 1000 \frac{\Sigma E_1}{\Sigma r} . \qquad (1)$$

TABLE 1

COEFFICIENTS OF SELECTIVE ABSORPTION

($b < 5°$)

| $l$ | $c_1$ | $\bar{r}$ | No. | $c$ | $\bar{r}$ | No. |
|---|---|---|---|---|---|---|
| 300°–340° | +0.16 | 1030 | 93 | ..... | ..... | ..... |
| 340 –360 | .22 | 1060 | 98 | ..... | ..... | ..... |
| 0 – 20 | .23 | 690 | 13 | ..... | ..... | ..... |
| 20 – 40 | .16 | 670 | 34 | +0.10 | 630 | 30 |
| 40 – 60 | .19 | 780 | 81 | .13 | 780 | 65 |
| 60 – 80 | .22 | 750 | 44 | .16 | 760 | 28 |
| 80 –100 | .18 | 930 | 68 | .17 | 850 | 52 |
| 100 –120 | .19 | 1080 | 68 | .14 | 1130 | 45 |
| 120 –140 | .16 | 700 | 26 | .14 | 740 | 24 |
| 140 –160 | .16 | 790 | 36 | .14 | 900 | 30 |
| 160 –180 | .09 | 820 | 51 | .08 | 790 | 47 |
| 180 –200 | .09 | 950 | 30 | .07 | 910 | 23 |
| 200 –240 | +0.14 | 1050 | 17 | +0.05 | 1070 | 11 |
| Mean | +0.17 | 870 | (659) | +0.12 | 860 | (355) |

page 248, of the *Washburn Publication*.[4] The third and fourth columns give the mean distance and number of stars for each section. The last three columns are the same as the second, third, and fourth, respectively, with the omission of stars which seem to be too red for their distances. These may be unidentified supergiant c stars,[5] other stars with unusually bright absolute magnitudes, or stars in heavily obscured regions. In some longitudes these reddened stars stand out

[5] The spectra of many of these strongly reddened stars are being obtained at Yerkes Observatory, and a large proportion have the sharp lines characteristic of supergiants. See O'Keefe, *Pub. A.S.P.*, **52**, 144, 1940.

by themselves; but in the first three sections near the galactic center, $l = 300°$–$20°$, there are so many such stars that it becomes impossible even to guess which ones may be abnormal, and so the values of $c$ are omitted in the fifth column. In a sense, $c$ is a coefficient of selective absorption with much of the absorption left out.

The distances in Table 1 depend upon the assumed mean absolute magnitudes and were computed from the formula

$$5 \log r = m - 7E_1 - M + 5 , \qquad (2)$$

where $m$ is the apparent and $M$ the absolute visual magnitude and where $A_V = 7E_1$ is the total visual absorption. For the 733 stars the adopted absorption was $A_V = 2E_1$, but it is now generally agreed that this estimate was too small. The increased allowance for absorption brings the reddened stars nearer than before, but this effect is more than counterbalanced by the assumed absolute magnitudes being nearly a whole magnitude brighter in the new list. The reason why the mean $c_1$ in the second column comes out smaller than before, 0.17 instead of 0.28, is that the additional fainter stars in the new list are not redder in proportion to their distance.

The data of Table 1 are shown graphically in Figure 1, where for each section the color excess $E_1$ of each star is plotted against the distance $r$ computed from (2). The curved boundary to the upper right of each figure represents the approximate limit set by observational selection. If we substitute in (2) the values $m = 9.0$ and $M = -3.9$ for a Bo star, we get

$$5 \log r = 10.1 - 7E_1 , \qquad (3)$$

which is the equation of each curve in Figure 1. In order to appear above this line, a Bo star must be fainter than apparent magnitude 9.0; stars of later types would be still fainter, while the more luminous c and O stars could be brighter than $9^m.0$; but very few of the latter have been identified among stars fainter than $8^m.0$. With an observational limit of a certain apparent magnitude some such blank region must appear in the upper right portion of the figure, even if the adopted ratio of $A_V/E_1 = 7$ is too large. Therefore, in

discussing the colors of stars, say beyond 1000 parsecs, we must continually bear in mind the limit set by equation (3).

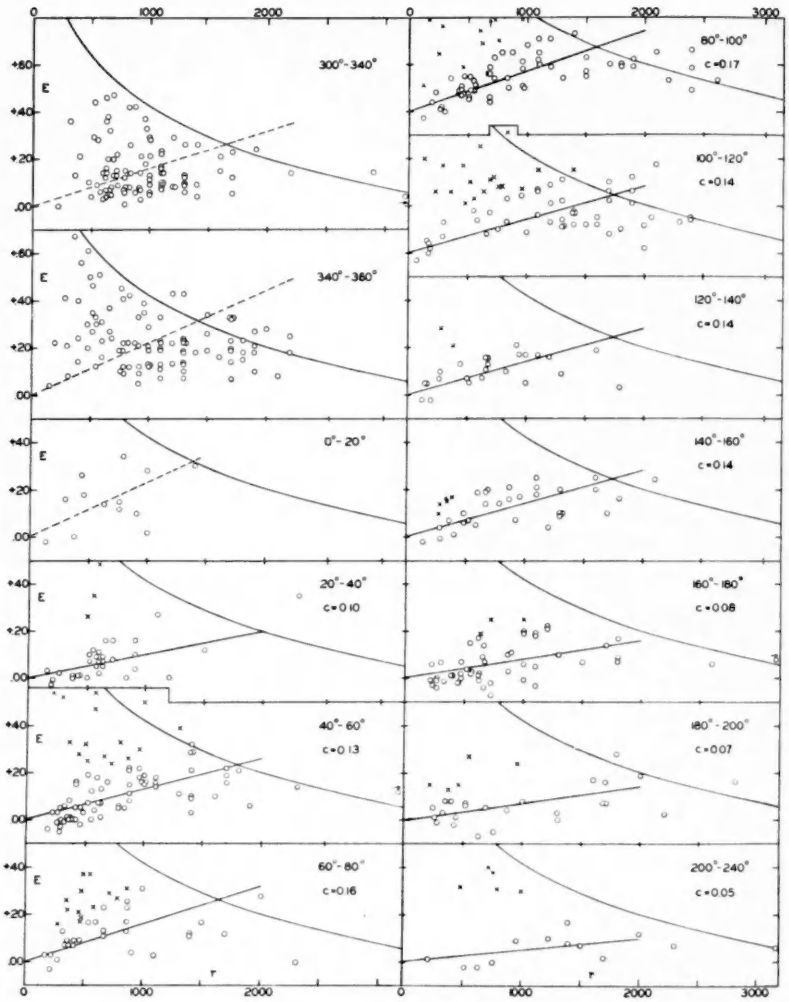


FIG. 1.—Colors of B stars at different galactic longitudes

The stars plotted as × in Figure 1 are those omitted in deriving the values of $c$ in the fifth column of Table 1, and they exhibit the arbitrary procedure of the rejection. The straight line in each section is

drawn to represent a linear absorption with a coefficient $c$, but in the first three sections the broken lines are drawn for the $c_1$ of Table 1.

It might be better to represent the selective absorption by the equation

$$E_1 = E_0 + cr/1000\,, \tag{4}$$

where $E_0$ gives the zero point of the color excess. Using this relation for the section 160°–180°, for instance, we get $E_0 = -0.01$ and $c = +0.10$, instead of $E_0 = 0$ and $c = +0.08$. On the other hand, in the section 340°–360° the value of $E_0$ would come out positive, as there is no star at any distance with a negative $E_1$. It has seemed like overdiscussion to attempt to improve the zero points for different longitudes. Many of the stars toward the galactic center were measured at Mount Wilson during the summer, and those toward the anticenter at Madison during the winter, giving favorable conditions for a systematic difference between the two regions; but we think we have enough cross-checks with the Polar Sequence and other standard stars to eliminate any such error. Moreover, the faint and distant stars are usually of spectra B0–B2, while the nearest stars of the list are likely to be of spectra B5 or later; so the possible errors in the zero points may change differentially between the subclasses of spectrum. For these reasons we let the zero points stand as they are.

At first sight it might seem better to use, instead of equation (1), the least-squares relation

$$c = 1000\,\frac{\Sigma E_1 r}{\Sigma r r}\,, \tag{5}$$

but this procedure gives undue weight to large values of $r$ which have probable errors nearly proportional to $r$. Moreover, $E_1$ and $r$ are not independent but are connected by equation (2). If we combine (2) and (4), we get

$$\log c = 1.4(E_1 - E_0) + \log\,(E_1 - E_0) - \frac{m - M + 5}{5} + 3\,. \tag{6}$$

When $E_0$ is found from stars in high latitude, $\log c$ can be determined from equation (6), weighting each observation with regard to the

probable errors of $E_1$ and $M$, the error in $m$ being negligible. All this is on the assumption that it would be worth while to attempt an accurate solution for $c$, which we doubt. We therefore adopt the simple relation (1) as being good enough for our purpose.

There are enough B stars within, say, 500 parsecs of the sun to get some sort of measure of the selective absorption in the local region, but these stars should be measured all at one time under conditions which would eliminate errors in the zero points. We have in hand a study of the more numerous A stars in low and high latitudes which are suited to this purpose. However, we have found that the Draper spectra are not accurate enough for detection of differences of mean color excess of 0.02 or 0.03 mag. between groups of a dozen stars each, and we are waiting for more accurate spectra of A stars of the eighth and ninth magnitude.

As for the graphs in Figure 1, the dispersion in absolute magnitude of the B stars would account for part of the scattering of the points, but no reasonable treatment of the data can make the points fall on the straight lines representing absorption proportional to the distance. In fact, after the first 500 parsecs there is little increase in absorption at any longitude. Toward the center, the observational limit cuts out distant stars with strong reddening; but toward the anticenter, or say from longitude 120° to 200°, there is practically as much reddening at 1000 as at 2000 parsecs. The values of the coefficient $c$ marked on the graphs represent something like the amount of color excess to be expected at 1000 parsecs rather than a measure of uniform absorption.

It is true, however, that if we take the mean value $c = 0.12$, and $A_{pg} = 9c = 1.1$ mag/kpc as the total photographic absorption, we get the same figure that van Rhijn[6] derived from Joy's radial velocities of Cepheid variable stars for distances up to 2500 parsecs. Allowance was made for the fact that the observed Cepheids are probably in regions less obscured than the average, but this difference is, of course, very uncertain. From a preliminary discussion of the photoelectric colors of several dozen Cepheids, we also have found that the Cepheids give less selective absorption than near-by B stars with the same apparent distance modulus $m - M$. The discrepancy

[6] *Groningen Pub.*, **47**, 9, 1936.

could also be due to errors in the assumed scales of absolute magnitude, but the whole question of color excess of faint Cepheids is being investigated further.

Also $A_{pg} = 1.1$ mag/kpc is near the median of the values which Bok[7] and his colleagues get from star counts in Selected Areas in low latitudes and for distances up to 2000 parsecs. Our new value of $c = 0.12$ does not get us into such difficulties with large absorption and with the density function increasing outward as was the case with $c = 0.28$ and $A_{pg} = 9c = 2.5$ mag/kpc.

However, despite all the figures that can be obtained for the selective and the total absorption, our conclusion from the colors of B stars is that in the first 2000 parsecs from the sun the effect of the interstellar material near the plane of the galaxy is too irregular to be represented by a mean coefficient of absorption.

CARNEGIE INSTITUTION OF WASHINGTON
MOUNT WILSON OBSERVATORY,
UNIVERSITY OF WISCONSIN
WASHBURN OBSERVATORY
April 1940

[7] *Ap. J.*, **90**, 249, 1939.

# ON THE CLUSTERING TENDENCIES AMONG THE NEBULAE*

ERIK HOLMBERG

ABSTRACT

Part I gives an investigation of double and multiple nebulae contained in the *General Catalogue*. An analysis of the distribution of angular distances between nebulae results in a statistical separation of physical and optical companions (Fig. 2); double and multiple systems are revealed as they actually exist in the sky. The average distances between physically connected nebulae (Tables 1 and 2) appear to be considerably larger than those previously assumed.

In Parts II–IV possible interpretations of the clustering tendencies are discussed. Double and multiple systems, as well as clusters, may be explained as a result of captures between nebulae, effected by tidal forces at close encounters. A summary of the main conclusions is given in Part V.

## I. DOUBLE AND MULTIPLE SYSTEMS AS DERIVED FROM A STUDY OF THE SMALL-SCALE DISTRIBUTION OF EXTRA-GALACTIC NEBULAE

1. Double and multiple objects represent an important structural feature of the extragalactic universe. It is well known that most of the brighter nebulae, including our Galaxy, are members of double or multiple systems. An analysis of the small-scale distribution of nebulae suggests an unbroken transition from single objects, through pairs and small groups, up to the occasional great clusters. The present paper represents a study of these clustering tendencies, in which attention is concentrated on double objects and small groups.

In previous discussions of the subject[1] double and multiple systems have been selected according to predetermined definitions, based generally on the apparent distances between the nebulae; all separations less than a certain limiting value dependent on the apparent dimensions, or apparent magnitudes, of the objects have been assumed to correspond to physical companions. In order to exclude, as far as possible, optical companions, the limiting separations have

* *Contributions from the Mount Wilson Observatory, Carnegie Institution of Washington*, No. 633.

[1] A bibliography compiled by the present writer is given in "A Study of Double and Multiple Galaxies," *Lund Ann.*, No. 6, 1937.

been given rather small values. This procedure necessarily introduced serious selection effects and furnished incomplete descriptions of the phenomena. The present investigation approaches the subject from the opposite direction. The apparent distances between nebulae are analyzed by a method which, in a statistical sense, separates optical from physical companions and, consequently, reveals the double and multiple systems as they actually exist in the sky. Part I of the paper describes the method of analysis and gives certain results which indicate the present structural order of the extragalactic universe. Possible interpretations of the observed structural order are discussed in Parts II–IV.

If complete lists of positions and magnitudes of nebulae were available to quite faint limits, it would be possible to derive a complete description of the clustering effects. As regards double objects and small groups, a solution of the problem could be approached by selecting all the nebulae belonging to a certain class of apparent magnitude and surveying the surrounding areas. By determining the distances of neighboring objects from each selected central nebula and noting their magnitudes, a collection of material consisting of physical companions, mingled with optical ones, would be obtained. An analysis of the frequency distribution of the distances, for different intervals of apparent magnitude, would then furnish a complete picture of the separations of physically connected nebulae.

Although such ideal data are not yet available, there are two catalogues which can be used to advantage now. One, the Shapley-Ames list,[2] furnishes reliable photographic magnitudes and is essentially complete down to $m_{pg} = 12.9$. A second, the *General Catalogue*,[3] is much more extensive than the Harvard list, but the lumi-

[2] "A Survey of the External Galaxies Brighter than the Thirteenth Magnitude," *Harvard Ann.*, **88**, No. 2, 1932.

[3] Sir John Herschel, "Catalogue of Nebulae and Star Clusters," *Phil. Trans.*, **154**, 1864, now known as the *General Catalogue* (GC) in order to distinguish it from Dreyer's *New General Catalogue* (NGC) of 1887. The NGC is more extensive than the GC but is not sufficiently homogeneous for the present purpose. The GC is based largely on visual surveys of the entire sky by one observer using one telescope, a speculum reflector of 18¼ inches aperture and 20 feet focal length. When the known star clusters and galactic nebulae are removed, the remainder forms a moderately homogeneous catalogue of extragalactic nebulae. In the higher galactic latitudes, the numbers of galactic objects are negligible, and no revision is necessary for statistical investigations.

nosities are not determined precisely, and there is a considerable dispersion in the limiting magnitude. For the sky north of declination $-20°$, the *General Catalogue* has been revised and corrected by Reinmuth;[4] and, because of the somewhat greater homogeneity, the revised list, rather than the original *General Catalogue*, has been used here.

The choice of catalogues restricts the area of the sky covered by the investigation. Another restriction is introduced by the exclusion of a galactic belt extending to latitude 30° (to avoid the gross effects of galactic obscuration). In order to increase the homogeneity of the material, it has seemed advisable to limit the investigation to the north galactic hemisphere. Finally, the Virgo cluster has been excluded (to avoid the dominating influence of a concentrated group of bright nebulae). The area covered by the investigation is thus reduced to about 23 per cent of the entire sky.

The Harvard list contains, within this area, 132 nebulae in the magnitude class $10^m1$–$12^m0$, and 301 in the class $12^m1$–$13^m0$. Circular survey areas with radii of 2°, centered on each of these nebulae, have been examined; the *General Catalogue* objects within the areas have been identified; and their distances from the central nebula determined. The numbers of objects per area (omitting the central nebula) range from 0 to about 30 and average about 6. The observed frequency distribution of numbers per area is shown in Figure 1, together with a theoretical curve[5] that represents a purely accidental distribution. The conspicuous difference between the two distributions reflects the pronounced clustering tendencies among the nebulae considered (together with some effects introduced by the dispersion in limiting magnitude in the *General Catalogue*).

It should be remarked that the survey areas sometimes overlap,

[4] *Heidelberg Veröff.*, **9**, 1926. Reinmuth verified on photographs most of the GC objects north of dec. $-20°$, revised the descriptions, and corrected the positions. The results are published in a form convenient for the present purpose.

[5] The curve represents Poisson's law

$$P_n = e^{-\bar{n}} \frac{(\bar{n})^n}{n!},$$

which gives the probability, $P_n$, of a certain number, $n$, of objects in a given area, provided that the objects are distributed at random. The average number of objects per area is denoted by $\bar{n}$.

and in some cases distances between nebulae are counted twice. From a statistical point of view this circumstance has no influence on the results derived below.

The objects within a survey area represent a combination of optical and physical companions of the central nebula. As already mentioned, an analysis of the frequency distribution of the distances of these objects from the central nebula will result in a statistical separation of the two kinds of companions. The first step is the formula-

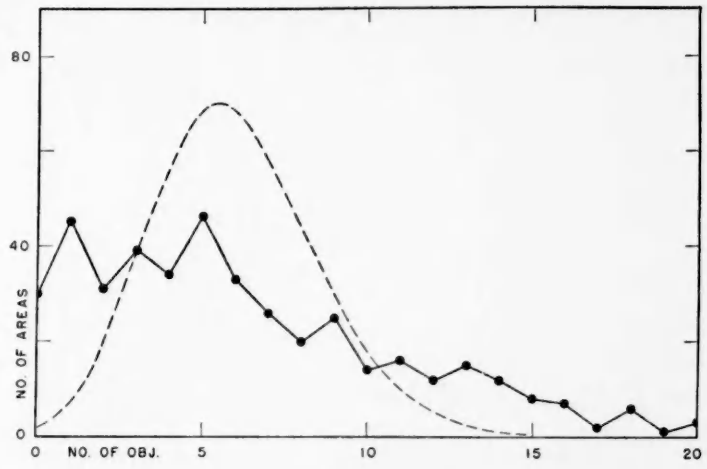


FIG. 1.—Distribution of numbers of objects in the survey areas. The dotted curve represents the accidental distribution corresponding to an average number of six objects.

tion of a representative distribution including all objects found in the survey areas. For this purpose, it has seemed advisable to exclude the exceptionally populous areas—those with more than 12 objects, or double the average number. The numbers of areas, and hence of central nebulae, in the two magnitude classes, are thus reduced to 114 and 267, respectively. The resulting distributions of apparent distances are shown in Figure 2.

On the plausible assumption that the optical companions are distributed at random within the survey areas, the frequency-curve for the distance of optical companions alone should be a straight line passing through the origin. The diagrams indicate that this condi-

tion is satisfied by objects at distances greater than about 80′ for the brighter, and about 50′ for the fainter, magnitude class. The data beyond these limits have accordingly been used to determine the in-

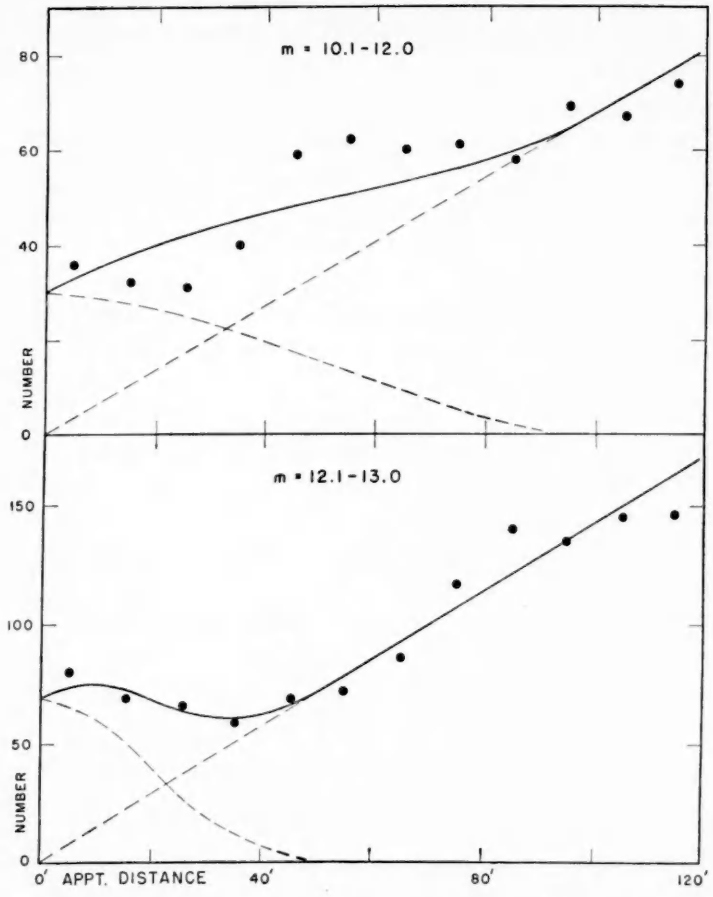


FIG. 2.—Distributions of apparent distance of physical and optical companions (from the *General Catalogue*) of nebulae of magnitude classes 10.1–12.0 and 12.1–13.0. The straight lines represent random distributions of optical companions.

clination of the straight lines representing the distribution of optical companions. When the optical companions are thus removed, the distribution of the remaining objects—the physical companions—corresponds more or less to normal error-curves. Some numerical

values derived from these curves are given in Table 1. The average apparent distances of the physical companions are 36′ and 15′, respectively.

**2.** These results may be used to formulate definitions (or descriptions) of double and multiple systems as actually found in the sky. As a preliminary step, a convenient quantity, called the "effective distance," will be introduced. The effective distance is the radius of a circle around a given nebula such that the average number of optical companions within the circle equals the average number of physical companions outside the circle. Evidently, the effective distance

TABLE 1

PHYSICAL COMPANIONS OF BRIGHT NEBULAE

| $m$ | Number of Nebulae | Number of Companions | Average Distance | Effective Distance |
|---|---|---|---|---|
| 10.1–12.0..... | 114 | 166 | 36′ | 40′ |
| 12.1–13.0..... | 267 | 167 | 15 | 23 |

will depend on the limiting magnitude of the material used. In Table 1 the values given refer, of course, to the material represented by the *General Catalogue*. For a general definition of the effective distance a certain limit of apparent magnitude must be adopted. Since, according to present observations, the spread in the absolute magnitudes of nebulae is about 5 mag., it may be assumed that standard limits of 2.5 mag. below and above the average magnitude of the components of a system will include practically all physical companions.

The definitions of double and multiple systems are given in Table 2, where the average separations of components and the effective distances are listed for successive values of the mean apparent magnitude of the components.[6] The zero points are furnished by the present investigation, and the other values are calculated on the as-

[6] An example of the selection effects inherent in the previous definitions of multiple nebulae is furnished by a list of about eight hundred double and multiple systems assembled by the present writer (*Lund Ann.*, No. 6, 1937). The systems were selected on the basis of angular separations measured in terms of angular diameters of the components. The average separation for the class $12^{m}1$–$13^{m}0$ was about 6′, as compared with 15′ found here.

sumption of constant density of nebulae in the space considered (i.e., no correlation between apparent and absolute magnitudes; an increment of one magnitude in the mean apparent magnitude of the components corresponds to a factor of 1.6 in the average separations). The average separation for $\bar{m} = 13^{m}.0$ has been given the value 15′, which is actually observed for the class $12^{m}.1-13^{m}.0$. This procedure is justified by the fact that, since the dispersion in absolute magnitudes of nebulae is about $0^{M}.85$,[7] the average distance of nebulae of the observed class $12^{m}.1-13^{m}.0$ (selected according to apparent magnitude and having a mean magnitude of about $12^{m}.6$) will be comparable with the average distance of a double system with $\bar{m} = 13^{m}.0$.

TABLE 2

DEFINITIONS OF DOUBLE AND MULTIPLE OBJECTS

| $\bar{m}$ | Average Distance | Effective Distance ($\Delta m \leqslant 2^{m}.5$) | $\bar{m}$ | Average Distance | Effective Distance ($\Delta m \leqslant 2^{m}.5$) |
|---|---|---|---|---|---|
| 10.0 | 60′ | 85′ | 14.0 | 9′ | 8′ |
| 11.0 | 38 | 45 | 15.0 | 6 | 5 |
| 12.0 | 24 | 27 | 16.0 | 4 | 3 |
| 13.0 | 15 | 14 | | | |

The values of the effective distance given in Table 2 were derived from the observed values in Table 1. Evidently, this transformation involves some knowledge of the limiting magnitude and the completeness of the *General Catalogue*. The Harvard list is known to be complete to $m = 12.9$, inclusive; and the *General Catalogue*, within the area considered, contains five times as many objects. Consequently, the effective limit of the *General Catalogue*, on the assumption of constant space density, is about $14^{m}.1$. A comparison of the two catalogues demonstrates that the *General Catalogue* is practically complete to $12^{m}.5$ and about 90 per cent complete at $13^{m}.0$. Furthermore, it may be assumed that the very faintest objects in the *General Catalogue* are somewhat fainter than the fifteenth magnitude. From these data, reasonable estimates of the completeness at different magnitudes may be derived, provided the frequency distribution of magnitudes can be represented by a smooth curve. The adopted

[7] Hubble, *Mt. W. Contr.*, No. 548; *Ap. J.*, **84**, 158, 1936.

values are given in Table 3. These values represent, of course, approximations sufficient for the immediate problem but not necessarily valid for other purposes. They show that the *General Catalogue* gives a fairly complete picture of physical companions belonging to nebulae of the class $10^{m}.1-12^{m}.0$ and that for the class $12^{m}.1-13^{m}.0$ about one-third of the probable number of companions is missing.

A study of the clustering effects will not be complete without giving the relative numbers of single, double, and multiple nebulae. The present material forms an adequate basis for an investigation of the distribution of nebulae in systems of different orders. If all companions within the effective distance are supposed to be physical ones, we arrive at the frequencies given in Table 4. In this case, all survey areas have been included. In the class $12^{m}.1-13^{m}.0$, corrections must be applied on account of the incompleteness of the *General Catalogue*. The transformation of the observed frequencies into the corrected ones presents a simple statistical problem and has been carried out by means of successive approximations. For the two magnitude classes together, it is found that about 47 per cent of all nebulae are single objects, while 24 per cent are components of doubles, and 15 per cent, of triplets, etc. For systems with more than five components, the numbers are so small that the listed frequencies may not be significant.

TABLE 3

ASSUMED MAGNITUDE DISTRIBUTION FOR *General Catalogue* OBJECTS

| $m$ | Completeness | $m$ | Completeness |
|---|---|---|---|
| $\leqslant 12.5$ | 100 per cent | 14.0 | 40 per cent |
| 13.0 | 90 | 14.5 | 15 |
| 13.5 | 70 | 15.0 | 5 |

**3.** In conclusion, a more detailed examination will be made of the distances of physical companions. The assumption of an accidental distribution for optical companions led (Fig. 2) to an approximately normal distribution of physical companions. A somewhat more complete picture may be obtained by combining the two classes, $10^{m}.1-12^{m}.0$ and $12^{m}.1-13^{m}.0$, the separations in the brighter group

being reduced to the scale of the fainter group. Since the mean magnitudes of the two groups are $11^m.5$ and $12^m.6$, respectively, the reduction factor to be applied is 0.6. The combined data on the density distribution of physical companions of nebulae for the class $12^m.1-13^m.0$ are shown graphically in Figure 3. The observed values, indicated by dots, define rather precisely a smooth curve, which represents the logarithm of the number of companions per square minute of arc as a function of angular distance from the central nebulae.

TABLE 4

FREQUENCIES OF NEBULAE WHICH ARE COMPONENTS OF SYSTEMS OF DIFFERENT ORDERS

| $n$ | $10^m.1-12^m.0$ | $12^m.1-13^m.0$ | | $10^m.1-13^m.0$ |
|---|---|---|---|---|
| | | Obs. | Corr. | |
| 1 | 45 | 187 | 157 | 202 = 47 per cent |
| 2 | 35 | 60 | 69 | 104 24 |
| 3 | 28 | 32 | 39 | 67 15 |
| 4 | 8 | 14 | 21 | 29 7 |
| 5 | 10 | 5 | 9 | 19 4 |
| 6 | 3 | 2 | 4 | 7 (2) |
| 7 | 3 | 1 | 2 | 5 (1) |

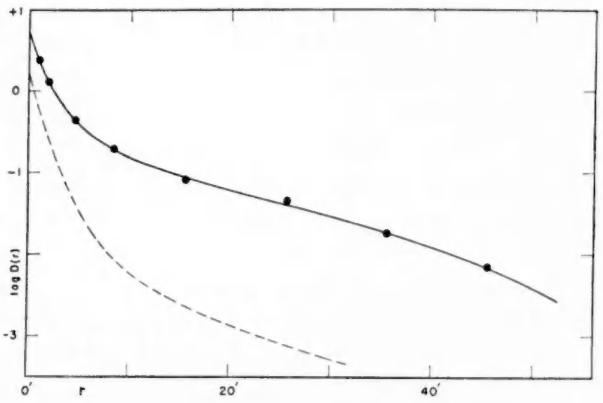


FIG. 3.—Distribution of apparent density (full-line curve) and of space density (dotted curve) of physical companions belonging to nebulae of magnitude class 12.1–13.0. The units are 1′ and the average linear distance corresponding to 1′, respectively.

This curve may be used to find the space arrangement of the physical companions. The problem of determining the space density corresponding to an observed apparent density has been the subject of several investigations, especially in connection with the study of globular star clusters.[8] In the present case, the curve is very steep near the density axis; and, by assuming spherical symmetry, the space density of physical companions can be derived by a graphical method based on successive approximations. The result is shown by the dotted curve in Figure 3. This curve is based on a unit of linear distance which corresponds to $1'$ at the average distance of the nebulae in the class $12^m.1-13^m.0$. The increase in density near the center is very pronounced. Using the value of the mean absolute magnitude of nebulae adopted in Part II of this paper, $\bar{M}_m = -15.2$, we find the maximum value of space density, as indicated by Figure 3, to be of the order $2 \cdot 10^{-12}$ nebulae per cubic parsec, as compared with the average density of $1 \cdot 10^{-17}$ in the general field.

## II. ON THE FORMATION OF DOUBLE AND MULTIPLE NEBULAE

**4.** The present clustering of nebulae in double and multiple systems may be assumed to represent a certain stage of structural evolution in the extragalactic universe. It seems possible to approach an interpretation of the clustering tendencies from two opposite directions. We may assume, a priori, that a more or less uniform space distribution is either an initial, or a final, stage—that the observed groups of nebulae are in a state of formation or of disintegration. Since the following discussion refers principally to a nonexpanding nebular universe, a natural starting-point is offered by the first alternative, namely, that the present structural order represents a gradual evolution from an originally random distribution. Although no conclusive evidence can be given for or against either of the alternatives, the results derived below seem to be thoroughly consistent with the present body of knowledge, and to this extent they support the validity of the assumption about structural evolution on which they are founded.

Starting from a random distribution, we may explain the forma-

[8] See *Handb. d. Ap.*, **5**, Part II, 720, 1933, where the problem is discussed and further references are given.

tion of double and multiple nebulae as a result of captures. The average space separation of extragalactic objects is rather small, compared with the dimensions of single objects. In a stationary universe we must expect a large number of encounters. Every close encounter between two objects will create large tidal disturbances, and the resulting loss of kinetic energy may be sufficient to effect a capture, i.e., to change the hyperbolic orbits of the objects into elliptical ones. Immediately after the capture the elliptical orbits may be assumed to have rather large eccentricities. Every subsequent passage of a component through the pericenter of the relative orbit will, however, create new tidal effects and thus tend to decrease the eccentricity. The general result will be a gradual contraction of the relative orbit, which may continue until the two components form practically one object; or the orbital contraction may be accompanied by a contraction in size of the components and a resulting decrease of tidal disturbances. The discussion of nebular types in Part IV indicates that the latter alternative is consistent with observed facts.

The formation of double and multiple systems according to the scheme thus outlined seems to be possible only in a stationary universe. In a universe expanding uniformly the number of encounters, and consequently the number of captures, will be very small. The present average distance of $10^6$ parsecs between nebulae corresponds to an expansion of about 500 km/sec. According to the available observations, the dispersion in the peculiar radial velocities of single nebulae is about 200 km/sec. If the latter value is assumed to be independent of the time, it is apparent that the probability of encounter between objects having a space separation larger than $10^6$ parsecs will be extremely small. The objects situated within a sphere having a radius of this size are too few to account for the formation of double and multiple systems by captures. Since it does not seem possible to explain a multiple system by divisions of a single nebula, the necessary conclusion is that the present clustering of nebulae in double and multiple systems is the result either of a corresponding nonuniformity of space distribution in the original universe (before the expansion) or of certain irregularities in the expansion.

Because of the incompleteness of our knowledge of the internal motions and of the distribution of mass within the nebulae, it is not

possible to prove, theoretically, that a close encounter between two objects will result in a capture. However, photographs of several double nebulae exhibit peculiar features which suggest strong disturbances effected by tidal forces. One of the most interesting cases is that of NGC 4038, 4039.[9] Although catalogued as a double nebula, the components cannot be distinguished on the photographs. Nevertheless, the internal structure appears to be highly disrupted, and two faint extensions suggest that luminous material has been thrown far out into the surrounding space.

As already remarked, the relative orbit of a double system, immediately after a capture, may have a large eccentricity and, consequently, a long major axis. On this account various pairs of widely separated nebulae, where physical connection seems to be highly probable on account of similarity of radial velocities, are noteworthy. Three well-known cases are listed in Table 5, and others have been noticed among the unpublished velocities assembled at the Mount Wilson Observatory. The separations amount to several degrees and are considerably larger than those derived in Part I of this paper.

**5.** Any attempt to interpret theoretically the clustering tendencies in the extragalactic universe must account for the observed distribution of nebulae in systems of different orders as summarized in Table 4, the frequencies decreasing as the number of components of a system increases. Let us now examine the possible explanation of these facts offered by the capture theory on the assumption of an originally random space distribution in a stationary universe.

In order to facilitate the discussion, a system of the order $n$ will be denoted by $S_n$, and the number of systems per unit of space by $N_n$. According to the capture theory, a system of the $n$th order can be formed in $n - 1$ different ways. For the special case of a formation of $S_n$ by captures between $S_l$ and $S_m$ systems, the process may be described by the equation

$$dN_{l+m} = P_{l,m} N_l N_m dt .$$

The increase in number is proportional to the numbers $N_l$ and $N_m$, to the time $dt$, and to a factor $P_{l,m}$ which expresses the probability of

[9] Reproductions are given in *Mt. W. Contr.*, No. 256; *Ap. J.*, **57**, 137, 1923, and in *Proc. Nat. Acad. Sci.*, **26**, 31, 1940.

capture between $S_l$ and $S_m$. The total increase in the number of $S_n$ systems will then be given by the equation

$$dN_n^t = dt\left[\sum_{l+m=n} P_{l,m}N_l^tN_m^t - \sum_{l=1}^{\infty} P_{l,n}N_l^tN_n^t - P_{n,n}N_n^tN_n^t\right]. \quad (1)$$

The term $N^t$ is used to express the dependence of $N$ on the time. The first term within the brackets gives the increase in the number of $S_n$ systems resulting from captures between systems of a lower order, whereas the second and third terms give the decrease corresponding

TABLE 5

DOUBLE NEBULAE OF WIDE SEPARATION

| Components | $m$ | Type | Radial Velocity* | Separation |
|---|---|---|---|---|
| | | | km/sec | |
| NGC 247 | 10.7 | Sc | − 15 (H) | 4'.6 |
| 253 | 7.0 | Sc | − 50 (H) | |
| NGC 2366 | 12.6 | Ir | +130 (M) | 3.5 |
| 2403 | 10.2 | Sc | +125 (H) | |
| NGC 5236 | 8.8 | Sc | +500 (S) | 1.9 |
| 5253 | 11.0 | Ir | +450 (H) | |

*H, Humason; M, Mayall; S, Slipher.

to captures of $S_n$ systems by other systems. An integration of this equation will give the number of $S_n$ systems as a function of time. A numerical value of the integration constant may be found if we suppose that the distribution of nebulae in systems of different orders is known for at least one instant of time.

In order to integrate equation (1), some assumption must be made concerning the probability $P_{l,m}$. As a first simplification, this probability may be expressed as a product of two independent factors $p_l$ and $p_m$, which may be defined as the "capturabilities" of systems of order $l$ and $m$. This approximation seems to be justified, at least for small values of $l$ and $m$. In order to obtain a theoretical picture of the clustering tendencies corresponding to the capture theory, the quantity $p_n$ must be expressed as a function of $p_1$, i.e., of the "capturability" of a single nebula. In the absence of any detailed knowl-

edge about capture processes the simplest assumption is probably represented by the relation $p_n = np_1$—in other words, by supposing that a system of $n$ components will, during a certain interval of time, capture $n$ times as many outside objects as will a single nebula. These assumptions may be summarized as follows:

$$P_{l,m} = p_l p_m = l p_1 m p_1 . \qquad (2)$$

With the help of relation (2), it is now possible to integrate equation (1) numerically. The time is divided into small intervals, and the successive values of $dN_n^t$ are determined. A random space distribution is used as a starting-point, and the process of integration is continued until the number of single nebulae is reduced to 47 per cent of the total number, in agreement with the observed value in Table 4. The resulting theoretical distribution of nebulae in systems of different orders is shown by the full-line curve in Figure 4, *a*. The observed numbers as given in Table 4 are represented by dots. For the sake of completeness, two more distribution-curves have been determined, corresponding to the assumptions $p_n = p_1$ and $p_n = n^{3/2}p_1$, which may be considered as limiting cases.

The full-line curve of Figure 4, *a*, is in good agreement with the observed frequencies, whereas the dotted curves exhibit large deviations. Since the former curve is founded on the most likely assumption that can be made at present about capturabilities of systems of different orders, it seems permissible to conclude that the capture theory gives a good representation of the present numbers of single, double, and multiple nebulae.

Figure 4, *b*, shows graphically the structural evolution of the extragalactic universe corresponding to equations (1) and (2). The different curves give, as a function of the time, the relative numbers of nebulae which are members of systems of different orders. For convenience, the point in time corresponding to a random space distribution is put equal to zero, and the time interval required to reduce the number of single nebulae from 100 to 47 per cent is chosen as the unit of time. The dots represent the observed frequencies. The good agreement between observed numbers and theoretical curves is clearly indicated by the figure. An interesting feature of the evolu-

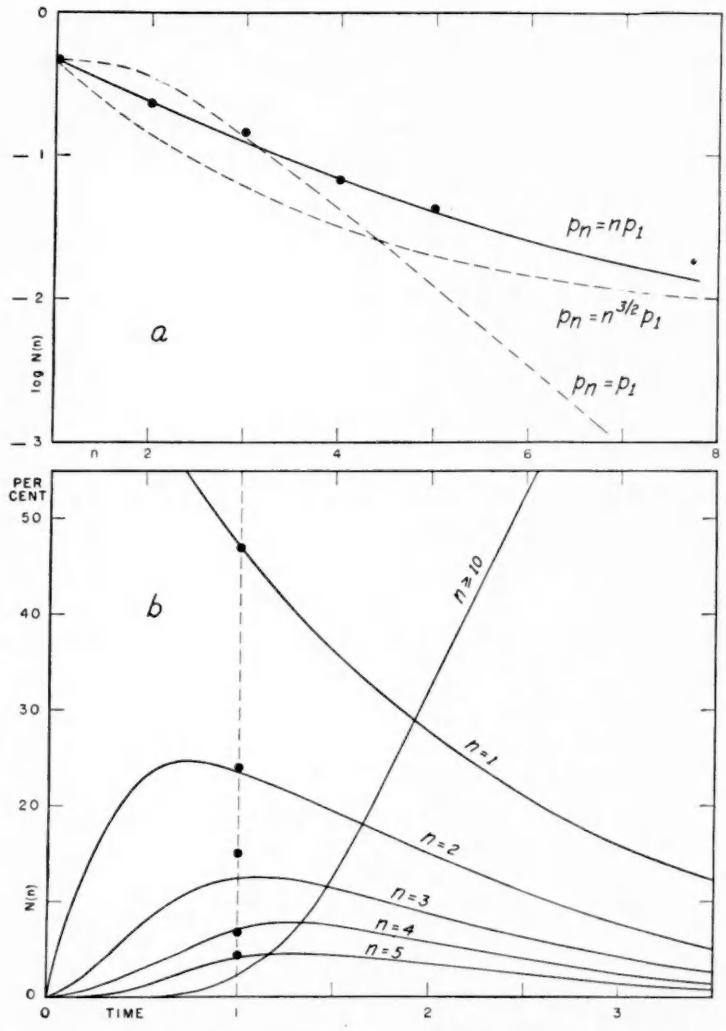


FIG. 4.—(*a*) Distribution of nebulae (relative number = $N(n)$) in systems of different order ($n$). The dots represent observed numbers, whereas the curves give theoretical distributions corresponding to different assumptions for the "captureability" ($p_n$) of systems of different order. (*b*) Relative numbers of nebulae in systems of different order as a function of time. The curves are based on the assumption $p_n = np_1$. The time interval corresponding to the formation of the present number of double and multiple nebulae is chosen as unit of time. The dots represent the observed numbers.

tion is the fact that the number of double systems, as well as the numbers of multiple systems of a small order, shows a maximum at a point in time corresponding approximately to the present epoch. An increase in time beyond this value leads to a gradual decrease in numbers. Evidently most of the nebulae will finally be accumulated in systems of high order.

**6.** A highly interesting problem is presented by the possibility of using the relative frequencies of single, double, and multiple nebulae as a basis for establishing a time scale for the extragalactic universe. According to the curves of evolution given in Figure 4, *b*, the present numbers of systems of different orders correspond approximately to the same interval of time. If the value of this interval in years could be determined, valuable information would be obtained concerning the time scale corresponding to a stationary universe. A comparison of this time scale with the time scale of about $10^9$ years for an expanding universe might help us to decide whether the foregoing scheme of structural evolution has a real meaning.

In order to evaluate the time interval under discussion, we may use a simple relation of statistical mechanics as a starting-point. The following simplification will be introduced. Assume that spherical bodies, having a diameter equal to $A$ and an average space velocity equal to $\overline{W}$, are uniformly distributed in a comparatively large volume of space. Let $D$ represent the average space density or the average number of bodies per unit of space. On the assumption that the directions of the motions of the bodies are distributed at random, the number of collisions per unit of space and time will be

$$\text{Number of Collisions} = \sqrt{2\pi} A^2 D^2 \overline{W} ,$$

a formula first given by Maxwell and later discussed by Charlier.[10] If the motions in space of the nebulae in a stationary universe are assumed to be distributed at random, the above relation may be used to find the number of encounters between single nebulae. Let us now assume that it is possible to define a certain "effective capture distance," corresponding to the largest distance of closest approach between two nebulae that results in a capture. More correctly, the

[10] *Lund Medd.*, Ser. 2, No. 16, 1917.

number of captures taking place outside this distance should, on an average, be equal to the number of encounters inside that do not result in captures. If the effective capture distance is denoted by $A$, the above relation will give the average number of captures taking place between nebulae per unit of space and time. Knowing the total number of captures, we may use the relation to find the corresponding interval of time. In the latter case, we have to assume that the effective capture distance, as well as the average space velocity of nebulae, does not change with time or, more correctly, that the product $A^2\overline{W}$ is independent of the time.

The average peculiar space velocity of nebulae can be determined from the observed radial motions. According to Hubble,[11] the dispersion in the radial velocities (corrected for red shift) of nebulae in the general field is about 200 km/sec. If the motions are assumed to have a random distribution, the corresponding average space velocity will be about 320 km/sec, or approximately $3 \cdot 10^{-4}$ parsecs/year, the value used below. As regards the space density of nebulae in the nearer extragalactic space, some information may be obtained from the Shapley-Ames catalogue. Until a large number of individual distances are available, a determination of space density must be founded on certain assumptions about the average absolute magnitude of nebulae. Following Hubble,[12] let us adopt

$$\overline{M} = -14.2\,, \qquad \overline{M}_m = -15.2\,.$$

Here $\overline{M}$ means average absolute magnitude in a given volume of space, whereas $\overline{M}_m$ is the average absolute magnitude corresponding to a certain class of apparent magnitude. Starting from these values, we find that the Shapley-Ames catalogue gives an average space density of about $1 \cdot 10^{-17}$ nebulae per cubic parsec. This value refers to the same area of the sky as was used in collecting the data on double and multiple objects. It may be remarked that within this area the distribution of apparent magnitudes indicates a fairly constant distribution of space density.

The most difficult step in establishing an extragalactic time scale

[11] *Mt. W. Contr.*, No. 549; *Ap. J.*, **84**, 270, 1936.

[12] *Mt. W. Contr.*, No. 548; *Ap. J.*, **84**, 158, 1936.

is the determination of an effective capture distance. It does not seem possible at present to derive theoretically any reliable numerical value of this distance. However, an analysis of the observed distances of the components of double (and multiple) systems may suggest the order of the corresponding capture distances. Let us denote the present orbital distance of the components of a double system by $r$, and the capture distance by $a$. The corresponding space densities may then be denoted by $D(r)$ and $D'(a)$, respectively. If all encounters within the effective capture distance ($A$) result in captures, the following relation ($a < A$) will be valid:

$$D'(a) = \text{const} \geqslant D(r) .$$

The orbits of double systems may be assumed to have large eccentricities, and consequently the distances $r$ will be distributed over a much larger volume of space than the distances $a$. Figure 3 shows graphically the density function $D(r)$, which increases very rapidly for decreasing values of $r$. As a first approximation, let us put the function $D'(a)$ equal to $D(0)$, i.e., to the maximum value of $D(r)$. This assumption implies that, if the capture distance is very small, the tidal effects will be so large that the resulting orbit will be more or less circular. For $\bar{M}_m = -15.2$, the above approximation indicates an effective capture distance of about 4000 parsecs. In view of the absolute dimensions of single nebulae, this distance does not seem unreasonable. Furthermore, in spite of the fact that a division of the capture distance by a factor 2 quadruples the time scale, a comparatively large uncertainty in the adopted value of the effective capture distance will not affect the general order of the time scale.

The final determination of the time scale will be founded on the present number of single nebulae. Let $N_1^t$ be the number of single nebulae in a unit of space at the time $t$, and $N$ the total number of nebulae. According to the above discussion of the formation of double and multiple systems, the following relation should be valid:

$$dN_1^t = -(\sqrt{2}\pi A^2 \bar{W})(N + N_1^t)N_1^t dt . \qquad (3)$$

This equation is to be integrated from the time $t_1$, corresponding to $N_1 = N$, to the time $t_2$, corresponding to $N_1 = 0.47N$. The resulting

interval $t_2 - t_1$ furnishes the time scale corresponding to the formation of the present numbers of double and multiple nebulae. For an effective capture distance of 4000 parsecs, the interval is

$$t_2 - t_1 = 2 \cdot 10^{12} \text{ years} .$$

This value represents a considerably longer interval of time than that corresponding to an expanding universe. It is true that the uncertainties of the numerical values adopted for the average space velocity, average space density, and effective capture distance introduce a corresponding uncertainty in the calculated interval; but it seems unlikely that the general order of the time interval is affected. It may be of interest in this connection to compare the time scale with the orbital periods of double nebulae. Starting from the data concerning separations of physical companions given in Part I and assuming a maximum value for the average nebular mass of about $10^{11}$ solar units, we find that the average period of a double system will be of the order of $10^9$ years or longer. An orbital period of this duration suggests a time scale considerably larger than that corresponding to an expanding universe.

## III. ON THE FORMATION OF CLUSTERS OF NEBULAE

**7.** We have found that in a stationary universe the capture theory leads to a good agreement with the observed relative frequencies of single, double, and multiple nebulae. The question now arises whether this theory will also account for the formation of the large clusters, containing hundreds or thousands of nebulae. On the assumption of an initially uniform space distribution in a stationary universe, is it possible for clusters to have been formed by captures during the time interval within which the existing numbers of double and multiple nebulae have been formed? If this question can be answered in the affirmative, the capture theory apparently will present no disagreement with any of the known structural features of the extragalactic universe. The following discussion is based on the assumption of a stationary universe; the modifications caused by a possible expansion of the universe will be considered at the end.

In trying to explain the formation of a cluster we must take into

consideration the fact that the cluster is surrounded by a strong gravitational field. The total mass of a cluster is of a higher order of magnitude than the mass of a single nebula or of a multiple system with few components. Consequently, the number of outside nebulae attracted by the cluster and passing through it will be much larger than the number of objects passing through an equal volume of space remote from the cluster. Let us designate by the term "temporary members" those nebulae which pass through the cluster in hyperbolic orbits. The real cluster members, moving in closed orbits,

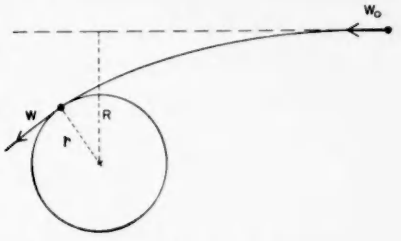


FIG. 5

will be called "permanent members." Any increase in the size of the cluster must occur through a transformation of temporary members into permanent members. The temporary members represent the building material of the cluster.

In Figure 5 the radius of a cluster (assumed to be spherical) is denoted by $r$, and the radius of the surrounding sphere from which the cluster collects its temporary members, by $R$. The linear space velocity of an outside nebula is denoted by $W_0$, and the hyperbolic velocity of a temporary member entering (or leaving) the cluster, by $W$. Simple mechanical interpretation gives the following relations:

$$\frac{R}{r} = \frac{W}{W_0} = \sqrt{1 + C^2 \frac{N\mathrm{M}}{r}} \simeq C\mathrm{M}^{\frac{1}{2}} \cdot \sqrt{\frac{N}{r}}, \qquad (4a)$$

in which

$$C = \frac{\sqrt{2\gamma}}{W_0}$$

and $N$ is the total number of cluster members, M the average mass of a single nebula in the cluster, and $\gamma$ the gravitational constant. The

number of temporary members contained in the cluster at a certain time is given approximately by the relation

$$\frac{N_{\text{temp}}}{N} \simeq \frac{1}{N} \cdot \tfrac{4}{3}\pi R^3 D \cdot \frac{2W_0}{W} \simeq C' \mathrm{M} r^2 , \qquad (4b)$$

in which

$$C' = \tfrac{8}{3}\pi D C^2 ,$$

and $D$ is the average space density in the general field outside the cluster. The coefficient 2 in the factor $W_0/W$ partly accounts for the fact that temporary members, in their hyperbolic orbits through the cluster, traverse paths which are longer than straight-line paths through the cluster. Using parsec, year, and solar mass as units and introducing the previously adopted values (sec. 6), $W_0 = 3 \cdot 10^{-4}$ parsecs per year, $D = 1 \cdot 10^{-17}$ nebulae per cubic parsec, we find for the constants in equations (4*a*) and (4*b*) the values $C = 3.3 \cdot 10^{-4}$ and $C' = 9 \cdot 10^{-24}$, respectively.

Let us now apply these relations to the Virgo cluster, for which we adopt a distance of $2.3 \cdot 10^6$ parsecs, an angular radius of 10°, and a population, in round numbers, of 500 members. For $\mathrm{M} = 10^{11}$ solar units,

$$\frac{W}{W_0} = 3.5 , \qquad \frac{N_{\text{temp}}}{N} = 0.2 .$$

About 20 per cent of the nebulae in the Virgo cluster should therefore be temporary members, with space velocities about three or four times larger than those in the general field.

It is well known that in the large clusters of nebulae the dispersion of radial velocities is larger than that in the general field. In the Virgo cluster the factor is about 3, while the Coma cluster gives a factor twice as large, or even larger. It does not seem possible to accept the high velocities as belonging to permanent cluster members, unless we suppose that a great amount of mass—the greater part of the total mass of the cluster—is contributed by dark material distributed among the cluster members—an unlikely assumption. The temporary members with their hyperbolic velocities seem to offer a more plausible solution of the difficulty.

It is interesting to use relations (4*a*) and (4*b*) for a comparison of the Virgo and Coma clusters. If the diameters of the two clusters are comparable, the relative numbers of temporary members should also be comparable. If the Coma cluster is assumed to have four times as many members as the Virgo cluster, the hyperbolic velocities of its temporary members should be twice as large. These results agree well with the observed facts.

The relations (4*a*) and (4*b*) are very dependent on the value assumed for the average mass of a single nebula. Hitherto we have used a value of $10^{11}$ solar units. The following data seem to justify this procedure as a first approximation. Thus an average mass value of about $2 \cdot 10^{11}$ solar units was found by Smith[13] from an analysis of radial velocities of members of the Virgo cluster. A preliminary investigation of double nebulae by the present writer[14] resulted in an average value of about $1 \cdot 10^{11}$ solar masses. Furthermore, current theories of galactic rotation correspond to a mass value of $2 \cdot 10^{11}$ units, and the rotation of the Andromeda spiral, as investigated by Horace Babcock,[15] gave a value of about $1 \cdot 10^{11}$ units. The galactic system and M 31, however, are known to be giant nebulae. The corresponding mass values should perhaps be considered as maximum, rather than as average, values.

**8.** After this digression on the temporary members and their velocities, we turn to the problem of the formation of a cluster. As already mentioned, the growth of a cluster represents a transformation of temporary members into permanent ones. In its passage through the cluster a temporary member may have one, or several, close encounters with other members, and the loss of kinetic energy due to tidal effects may be sufficient to change the orbit into an elliptical one. Thus the capture process in a cluster is not quite analogous to that which accounts for the formation of double nebulae. In a cluster the orbit of a captured nebula may be very large; and consequently the loss of energy, divided by the number of close encounters, may be comparatively small. On the other hand, the duration of any close encounter will be relatively short because of the high velocities of the temporary members.

[13] *Mt. W. Contr.*, No. 532; *Ap. J.*, **83**, 23, 1936.

[14] *Lund Ann.*, No. 6, 101, 1937.

[15] *Lick Obs. Bull.*, **19**, 41, 1939.

In order to simplify the mathematical treatment of the cluster problem, a parameter, $p$, will be introduced, defined in the following way: A temporary cluster member is, in general, transformed into a permanent one if it passes another nebula in the cluster within a distance $pA$, $A$ being the effective capture distance defined in section 6. The parameter $p$ is evidently a statistical quantity, and for decreasing values of $N$ (number of cluster members) it should approach unity. It seems likely that the present value of $p$ should not be much larger than unity. On the other hand, the higher velocity of temporary cluster members, together with the probability of more than one close encounter, seems to suggest a lower limit, not much smaller than $\frac{1}{2}$.

Assuming a time scale of $2 \cdot 10^{12}$ years and a space density in the general field of $1 \cdot 10^{-17}$ per cubic parsec, we find from the data given in Part I that there are, in a unit of space, about $4 \cdot 10^{-30}$ captures per year. Starting from this figure, we are now able to derive a relation giving the rate of increase of the number of cluster members. The increase per year will be equal to the above figure multiplied by a number of different factors, namely, (1) the volume of the cluster, (2) the square of the parameter $p$, (3) the ratio of the average space densities in the cluster and in the general field, respectively, (4) the ratio of the space density of temporary cluster members to the density in the general field, and (5) the average space velocity of temporary and permanent cluster members. For simplicity, the last factor may be put equal to the velocity $W$ defined in formula (4$a$). This velocity may seem to be somewhat high, but at the pericenter of the hyperbolic orbit the velocity of a temporary member will be still larger. On the other hand, the orbital velocities of the permanent cluster members are generally rather large.

In view of formulae (4$a$) and (4$b$) the desired relation takes the form

$$dN_{\text{perm}} = +1 \cdot 10^{-10} \rho^{1/2} M^{3/2} p^2 N^2 dt \,. \qquad (5)$$

In this equation the time scale derived in the preceding part of this paper is used as unit of time, while the parsec and the solar mass are kept as units of distance and mass. The average space density in the cluster is denoted by $\rho$. It may be mentioned that the relation is

founded on the assumption of an average space density and an average space velocity of nebulae in the general field of $1 \cdot 10^{-17}$ per cubic parsec and $3 \cdot 10^{-4}$ parsecs per year, respectively; and it should be emphasized that no other assumptions have been made.

Relation (5) gives the rate of increase in the number of permanent cluster members. The total increase will be expressed by

$$dN = dN_{\text{perm}} + dN_{\text{temp}} ,$$

the last term of which may be obtained by differentiating the expression (4*b*).

In order to integrate this differential equation, we must make some assumption regarding the relations between time and the parameters contained in equations (4*b*) and (5). The simplest assumption is that they are all independent of time. As regards the average space velocity of nebulae in the general field, this assumption agrees with that used in the derivation of a time scale from double and multiple nebulae. In the present case, however, the assumption must be extended to the average mass value of a single nebula, to the factor $p$, and to the average space density in a cluster. As regards the latter density, we do not know whether or not it is related to time. The relation may be different in different clusters. It appears from the above equations, however, that the rate of increase of cluster members is approximately proportional to only the square root of the density. As a first approximation, we will consider the cluster density as independent of the time and give it a numerical value of $1 \cdot 10^{-15}$ per cubic parsec, corresponding approximately to the present density of the Virgo cluster.

Performing the integration, we reach the following final equation:

$$N^{-1} - (2 \cdot 10^{-13}\text{M})N^{-1/3} = \text{const} - (4 \cdot 10^{-18}\text{M}^{3/2}p^2)t . \qquad (6)$$

The total number, $N$, of cluster members is expressed as a function of time by means of the two parameters $p$ and M. A graphical solution of the equation appears in Figure 6. In order to obtain a numerical value of the integration constant, we have assumed that the average population of clusters has now reached 500, or approximately

the present population of the Virgo cluster. In the figure, the time is expressed in terms of the time scale derived from double and multiple nebulae; and, for convenience, the present time has been assumed to correspond to $t = 1.0$. Four different curves have been computed, corresponding to average mass values (M) of $10^{10}$ and $10^{11}$ solar units, and to values of the parameter $p$ equal to $\frac{1}{2}$ and to 1.

It is apparent from Figure 6 that the time necessary for the formation of a cluster is, to a large extent, dependent on the average mass

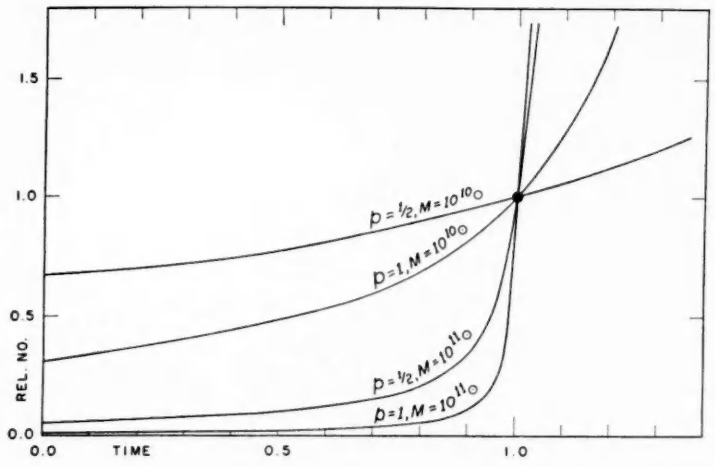


FIG. 6.—Evolution of a cluster of nebulae corresponding to different values of the parameters M (average mass) and $p$. The present number of cluster members is put equal to unity. The time interval corresponding to the formation of the present number of double and multiple nebulae is chosen as unit of time.

of a single nebula. If the mass is of the order of only $10^{10}$ solar units, the necessary time interval seems to be comparatively large. On the other hand, a mass value of $10^{11}$ solar units seems to give a good agreement with the time scale derived from double and multiple objects. Since the parameter $p$ should be approximately equal to unity for small values of the ordinate, it seems possible in the latter case for a multiple system of 10–20 nebulae to grow into a cluster, comparable to the Virgo cluster, during a time interval equal to only half the time scale. According to the investigations on double and multiple nebulae, it also seems quite possible that, in exceptional

cases, a multiple system of 10–20 members could be formed during a time interval equal to the first half of the time scale. If the parameter $p$ has a value considerably smaller than $\frac{1}{2}$, the time necessary for the formation of a cluster will be larger. On the other hand, an increase of the mass value by a factor 2 will speed up the formation process by a factor of about 3. Summing up, we may conclude that it seems not impossible for a cluster to be formed by capture processes during the time interval corresponding to the formation of double and multiple nebulae, provided that the average mass of nebulae is of the order of $10^{11}$ solar units. It is likely that some significance should be attributed to the fact that the same average value of about $10^{11}$ solar masses is necessary not only to explain the formation of a cluster but also, as mentioned above, to explain the high dispersion of radial velocities observed in clusters.

The following remarks should be made in connection with Figure 6. On account of the approximations used in equation (4*a*), relation (6) is not valid for small values of $N$. According to the preceding part of this paper, the relation should, if $N$ is small, have the approximate form

$$\log N = \text{const} \cdot t .$$

This relation gives a somewhat larger rate of increase in $N$ than equation (6). As regards the very rapid rate of increase corresponding to the time $t = 1$ and a mass of $10^{11}$ units, it may be asked if the process will not deplete the space surrounding the cluster. It appears, however, that this increase corresponds to a transformation of only 5 per cent (for $p = \frac{1}{2}$) of the temporary members into permanent ones. The great majority of the temporary members will leave the cluster without any appreciable loss of energy.

The foregoing discussion refers exclusively to a stationary universe. In conclusion the modification of the results required by the assumption of an expanding universe may be noted. As mentioned in Part II, if a uniform expansion is assumed, the number of close encounters will be too small to explain the formation of double and multiple nebulae as a result of captures. Apparently the same thing must be valid for a cluster. On account of the expansion, the number of temporary cluster members, moving in hyperbolic orbits, should

be very small. Consequently, it does not seem possible to explain the high velocities observed in the clusters as due to the temporary members. Furthermore, it seems impossible to explain the formation of a cluster as a result of capture processes. The conclusion is therefore the same as that regarding the formation of double and multiple systems, namely, the present clusters must be the result either of corresponding clustering effects in the original universe (before the expansion) or of certain irregularities in the expansion.

## IV. TYPES OF NEBULAE AND THEIR DEPENDENCE ON THE PRESENCE OF PHYSICAL COMPANIONS

**9.** It is known that the types of nebulae in the great clusters are systematically earlier[16] than those found in the general field. Elliptical and early spiral types seem to favor the clusters, whereas late spirals dominate the general field. Since the difference in average type is rather pronounced, it is of some importance to learn whether this difference presents any inconsistency with the theory of the formation of clusters outlined in Part III. The theory suggests that clusters are being gradually formed by captures of outside nebulae. It may be assumed, however, that, when they enter a cluster, the captured objects are of the same average type as those in the general field. If the theory is to give a complete and consistent picture of the observed conditions in the extragalactic universe, it must explain, in some way, the transformation of types.

In Part III cluster nebulae were divided into two classes, permanent and temporary members. For an average nebular mass of $10^{11}$ solar units we found that in the Virgo cluster the temporary members should number about 20 per cent. Since the temporary members were supposed to represent outside nebulae passing through the cluster, their types should agree, more or less, with those of the field nebulae. Thus it becomes of interest to compare the types of the two classes of cluster members.

Table 6 shows the radial velocities of 47 nebulae in the Virgo cluster, divided into two groups.[17] We may expect the group having

[16] The terms "earlier" and "later" have here, as usual, only a descriptive meaning and do not imply a dependence of the type on time.

[17] The writer wishes to express his gratitude to Mr. Milton Humason for a number of unpublished velocities placed at his disposal.

velocities $\geqslant$ 400 km/sec to include a considerable percentage of temporary members, while the other group, with velocities $<$ 400 km/sec, should be dominated by the permanent members. Table 6 does give some indication of a difference in type, spirals of types Sb and Sc belonging almost exclusively to the high-velocity group. The material is too limited, however, to establish any definite conclusion. It should be remarked that any division of the material according to radial velocity will always give mixtures of permanent and temporary cluster members.

TABLE 6

NEBULAR TYPES IN THE VIRGO CLUSTER

| Type | $\|V\| < 400$ km/sec | $\|V\| \geqslant 400$ km/sec |
|---|---|---|
| E | $N = 12$ | $N = 10$ |
| Sa, SBa | 7 | 6 |
| Sb, SBb | 2 | 6 |
| Sc, SBc | ..... | 4 |
| Total | 21 | 26 |

Some further information about the problem of nebular types may be derived from a comparison of single nebulae and components of double and multiple systems. It seems to be of great importance to try to decide whether or not the distribution of types among the latter objects shows any deviation from the distribution for single nebulae. Let us limit the investigation to nebulae brighter than the twelfth magnitude, for which reliable types may be obtained from the Shapley-Ames catalogue. In some few cases, where this catalogue does not give a detailed classification, the types, as classified on Mount Wilson plates, were kindly put at the writer's disposal by Dr. Hubble. In Part I it was found that, as far as *General Catalogue* objects are concerned, the magnitude class $10^{m}1-12^{m}0$ corresponds to an effective distance of about 40′ for physical companions. If there are no *General Catalogue* objects within this limit, we may provisionally assume that the nebula is single.

The resulting distributions of types are shown in Figure 7. Single nebulae seem to belong almost exclusively to the late spiral type. Among double and multiple objects, elliptical types and early spirals

seem to be the most frequent. In the latter case a correction has been applied for nonphysical companions. Within the circular area having a radius of 40′ we should expect a certain number (about 30 per

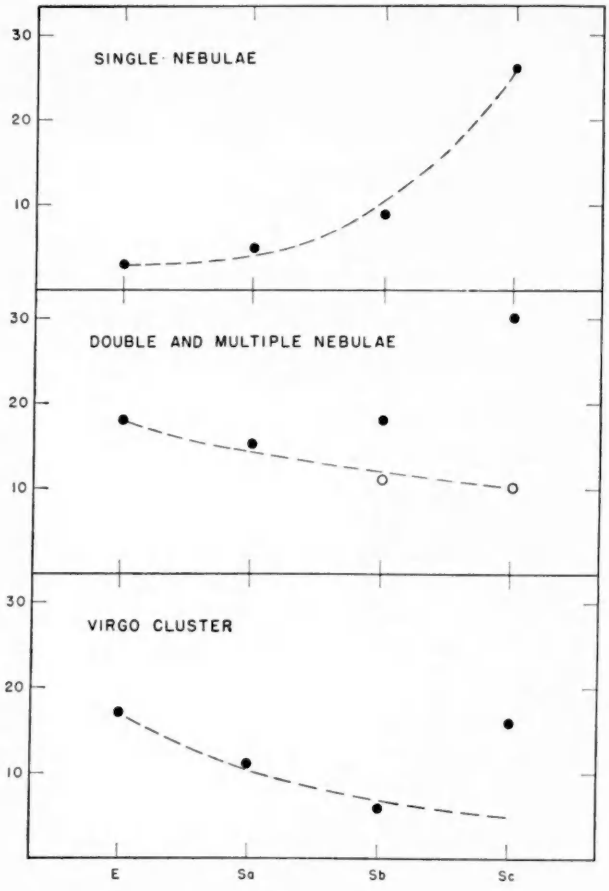


FIG. 7.—Distribution of types of nebulae of the magnitude class 10.1–12.0

cent) of optical companions. By assuming that the types of the optical companions have the same distribution as those of single objects, we arrive at the distribution-curve given in the figure. For comparison, we have included the distribution of types for nebulae (magnitudes $10^{m}.1$–$12^{m}.0$) in the Virgo cluster. For these it has been

assumed, as appears from the adopted curve, that some of the late-type spirals are temporary cluster members. A comparison of the three distribution-curves reveals a great similarity between those for double and multiple objects, on the one hand, and for the cluster nebulae, on the other. In both cases elliptical objects and early spirals seem to be the most frequent types.

It is apparent from Figure 2 that a limiting distance of 40′, which was used above, will exclude the more distant companions. As pointed out in Part II, there are indications that in some cases the distance between physical companions may be very large. Table 5 gives examples of widely separated nebulae, most of them of type Sc, which probably form physical systems. It seems likely that many of the nebulae classified as single objects may have one, or more, distant companions. As regards the nebulae belonging to the Virgo cluster, as well as to other clusters, it may be remarked that all, or most, of them seem to be components of double or multiple systems. In summing up the above facts the problem of the distribution of nebular types may perhaps be simplified by presenting the observed facts as follows:

*a*) *Objects of late spiral type.*—This class consists principally of single nebulae and members of pairs of wide separation.

*b*) *Objects of elliptical or early spiral type.*—The main part of this class is formed by members of double and multiple systems of small separation (including cluster members).

**10.** This simplified scheme of distribution of nebular types suggests strongly that the type of an object is in some way dependent on the existence of physical companions. Furthermore, it suggests that the separation of the companions has some bearing on the problem of type. Part II presents a simplified picture of the formation and evolution of a double nebula according to the capture theory. It supposes that immediately after the capture the elliptical orbits of the two components are comparatively large. Each passage of the components through pericenter produces, however, certain tidal effects, and consequently the orbits gradually contract. If we combine this evolutional scheme with the observed distribution of types, it seems possible that the type of a member of a double (or multiple) system depends on the age of the system. The tidal effects corresponding to

successive pericenter passages may result in gradual changes in the form and the size of the nebula, just as the orbit is gradually contracted. Two criticisms might be urged against this suggestion. The first is the possibility that the difference in type between single and double nebulae may depend simply on a selective effect in the formation of double objects. This explanation does not seem very likely, however, because the smaller size of elliptical objects and early spirals, as compared with late spirals, should correspond to smaller tidal effects and, consequently, to a smaller probability of capture. The second objection is that it might be possible to explain the formation of double objects not only by captures but also by divisions of single nebulae. It seems improbable, however, that the latter process could account for the large number of multiple systems.

The following mechanism is suggested for the transformation of types of nebulae belonging to a double (or multiple) system, i.e., for the transformation of late spirals into early spirals or elliptical objects. Each passage of the components through the pericenter of the relative orbit will create a disturbance, by tidal forces, of mass elements belonging to the outer layers of the two nebulae. Some of these elements may acquire such large accelerations that the final velocities will be larger than the velocity of escape. Other elements may be forced over into elliptical orbits passing through the condensed nuclear region of the nebula. Still others may continue their motions in more or less circular orbits. It seems likely that the first two of these processes will correspond not only to a smoothing of structural details but also to a contraction of the object. Since these processes are repeated every time the components pass through pericenter, it seems likely that a final stationary state will be reached as soon as the nebulae have contracted to such an extent that the tidal forces can be neglected. It may be remarked in this connection that the dimensions of the orbits of double systems, corresponding to the data given in Part I, suggest an orbital period of the order of $10^9$ years. Thus a time scale of $10^{12}$ years would correspond to about $10^3$ orbital revolutions.

The transformation process outlined above should be considered as a possible solution of the problem of nebular types corresponding to, and consistent with, the capture theory. It supposes that a con-

traction, accompanied by a smoothing of structural details, will transform a spiral into an elliptical object. It should be remembered, however, that the stellar content of spirals differs from that of elliptical objects, at least as regards supergiant stars. Late spirals contain a comparatively large number of absolutely very bright stars, whereas stars of this type seem to be missing in elliptical objects. As a possible explanation of this difference, it may be suggested either that the above contraction process is accompanied by certain selection effects dependent on the masses of the stars or that the contraction of the object and the resulting change of gravitational field will affect the evolution of the stars.

The preceding discussion refers exclusively to a stationary universe. As regards the assumption of an expanding universe, it may be remarked that the time scale then available would seem to be too short to allow a transformation of the types of nebulae in accordance with the foregoing scheme. The orbital period of a double system would then be of the same order as the time scale. If no other way can be found for the explanation of the preponderance of early types in double and multiple systems, the conclusion seems unavoidable that the distribution of nebular types, as now observed, existed before the expansion began.

## V. CONCLUSIONS

**11.** In order to facilitate a comparison between the different assumptions that may be made regarding the extragalactic universe, the results of the present investigation are brought together in the following summary. The main conclusions relate to six points: (1) the formation of double and multiple nebulae, (2) the relative numbers of nebulae in systems of different orders, (3) the time scale of the nebular universe, (4) the high dispersion of radial velocities in clusters, (5) the formation of clusters, and (6) the preponderance of early types of nebulae in clusters.

As regards the structural evolution of the extragalactic universe, we may assume, a priori, that a random space distribution of nebulae is either an initial or a final stage—that the present groups and clusters are in a state of formation or in a state of disintegration. In a stationary universe, the former alternative seems to be consistent

with the present body of knowledge. Thus, if a random space distribution is used as a starting-point, the capture theory leads to results that are in good agreement with observed facts (points 2, 3, and 5). In an expanding universe, somewhat different results are obtained. A structural evolution according to the first alternative does not seem very likely, unless the expansion is assumed to be of a very irregular nature (points 1 and 5).

It does not seem possible at present to give any conclusive evidence for or against an expansion. However, several of the results of this investigation furnish strong support for the assumption of a stationary nebular universe. Points 3 and 4, dealing with the time scale and with the dispersion of radial velocities in clusters, seem to be of special significance in this connection. The summary follows.

*a*) *Stationary universe.*—(1) Assuming an originally random distribution in extragalactic space, we may explain the formation of double and multiple nebulae as the result of captures. The capture theory is founded on the assumption that the tidal effects accompanying a close encounter will considerably decrease the eccentricities of the hyperbolic orbits of the two objects. Although it does not seem possible at present to prove theoretically that a close encounter will result in a capture, there are several cases in which photographs of double objects suggest strong tidal disturbances.

(2) If the capturability of a system of nebulae is assumed to be proportional to the number of components, the capture theory leads to results in good agreement with observed facts regarding the relative frequencies of single, double, and multiple nebulae.

(3) On the assumption of an effective capture distance of 4000 parsecs, the present numbers of single, double, and multiple nebulae correspond to a time scale of about $2 \cdot 10^{12}$ years. A time scale of this order does not represent any inconsistency with the average orbital period of a double system of about $10^9$ years. The latter value corresponds to the observed average separation of physical companions and to the assumption of an average nebular mass of $10^{11}$ solar units.

(4) If the average mass of a nebula is assumed to be of the order of

$10^{11}$ solar units, it is possible to explain the high radial velocities observed in the large clusters of nebulae as belonging to temporary cluster members moving in hyperbolic orbits.

(5) By starting from a random space distribution and assuming an average nebular mass of the order of $10^{11}$ solar units, it seems possible to account for a cluster of nebulae by successive captures of outside objects during the same interval of time that is required for the formation of double and multiple systems.

(6) The preponderance of early nebular types, which has been observed in the large clusters, proves to be a general characteristic of double and multiple nebulae. If this difference in type is not due to selection effects in the formation of double and multiple systems, which seems unlikely, we must conclude that the mere presence of a physical companion results in a change in the state of equilibrium of a nebula. It seems possible that the tidal forces acting upon the components of a double, or multiple, system will effect a gradual smoothing of structural details and a contraction in size of the objects, i.e., an apparent transformation of late spirals into early spirals or elliptical objects.

*b*) *Expanding universe.*—(1) If the expansion is assumed to be uniform, the number of encounters between single nebulae will be too small to explain double and multiple systems as formed by captures. Since it does not seem possible to explain a multiple object as formed by divisions of a single object, the present clustering of nebulae in double and multiple systems must indicate either a corresponding nonuniformity of space distribution in the original universe (before the expansion) or the existence of certain irregularities in the expansion.

(2) The preceding conclusions regarding the origin of double and multiple systems do not offer any explanation of the observed relative numbers of nebulae in systems of different orders.

(3) The time scale must be smaller than $2 \cdot 10^9$ years—the time interval corresponding to an expansion from an infinitely large space density to the present density. A time scale of this order seems to be inconsistent with an average orbital period of a double system of about $10^9$ years.

(4) If the expansion is uniform, the number of temporary cluster members will be too small to explain the high radial velocities observed in the large clusters.

(5) On account of the small number of temporary cluster members, it does not seem possible to explain a cluster as having been formed by captures during the time interval available. The conclusions are the same as those regarding the formation of double and multiple nebulae.

(6) Since the time scale is of the same order as the average orbital period of a double system, it does not seem possible to explain the early types of nebulae found in double and multiple systems as a result of tidal disturbances.

MOUNT WILSON OBSERVATORY
CARNEGIE INSTITUTION OF WASHINGTON
March 1940

# A NOTE ON THE EVOLUTION OF EXTRAGALACTIC NEBULAE*

GUNNAR RANDERS[1]

ABSTRACT

The great variety of types of extragalactic nebulae which differ fundamentally from both spiral and elliptical nebulae indicates that the current theories of the formation of spiral arms by ejection of matter from rotating elliptical nebulae are not sufficient for an explanation of nebular evolution. Especially striking is the tendency, found rather frequently among all types of nebulae, to form a circular ring or a system of rings.

It is suggested that the ring formation may be an important step in the evolution and that the active agent in this process is viscosity in a differentially rotating system.

1. Discussions of the evolution of extragalactic nebulae have been concerned, for the most part, with the formation of spiral arms. It is generally assumed that the spiral pattern represents an advanced state which all nebulae will reach, sooner or later, in the course of their evolution. Elliptical nebulae, according to this view, represent early states from which the spiral arms develop by the ejection of matter from the rims. The ejection might be due to internal instability arising from high rotational velocities or to external influences or to both.[2]

This view of the evolutional process has the virtue of simplicity. Especially attractive is the idea of evolution from the simple, elliptical state toward the complicated spiral state. The idea was perhaps associated with the belief that elliptical nebulae were composed of gas from which stars would condense in the course of time. The accumulating spectra of elliptical nebulae indicate, however, that these nebulae, as well as the resolvable spirals, contain stars;

* *Contributions from Mount Wilson Observatory, Carnegie Institution of Washington*, No. 634.

[1] Research fellow from the Institute of Theoretical Astrophysics in Oslo.

[2] Two different views are distinguished by different assumptions about the points of ejection of the arms. If these points are fixed in space (as advocated by Lindblad), the arms represent stationary paths of the ejected particles and open up in the direction of rotation. If the points of ejection follow the rotation, the arms are formed by a succession of emitted particles but do not represent the track of a single particle. In this case the arms point in the opposite direction, that is, they lag behind in the rotation.

and, consequently, the earlier argument has lost much of its significance.

Apart from the existence of spiral patterns, there is no observational support for the current theories of the formation of spirals from elliptical nebulae. The abundance and the distribution of elliptical nebulae, relative to those of the spirals, suggest no difference in age. Furthermore, many physical groups (e.g., the Virgo cluster) are known in which all types are represented by members of the same order of luminosity. If the members are all of the same age, it is difficult to understand how those in the elliptical state could have been so greatly delayed in their development.[3] Finally, the energy required to eject the arms (according to the ejection theories) raises problems that may be quite serious. Many spirals suggest that the greater part of the material is located in the arms. If the arms were ejected from a system originally densely packed, the nearly complete dissolution of that system would have been accomplished against the pull of the gravitational forces. Such a process seems to raise difficult problems, even when large initial rotational momenta are assigned to the systems.

The mere existence of a spiral pattern indicates that the material must be in some kind of nonsteady motion. The spirals, however, do not directly support any special ejection hypothesis. Any radially proceeding structural change in a rotating, flattened system, such as a rapidly rotating elliptical nebula, will give rise to a spiral pattern. Because of gravity, a cut in the rim may grow inward and create a kind of empty lane, curving in toward the center (Pl. V*d*). In this way it is possible to think of the spiral pattern being formed by a differentiation of the matter already present.

The fact which shows most clearly that the ejection of arms from a rotating central body is not a sufficiently broad basis for a complete understanding of the forms of nebulae is the existence of a great variety of types which differ fundamentally from both spiral and elliptical nebulae.

The most frequent of these types are the barred spirals. Their characteristic feature is a straight bar which crosses the central re-

[3] This difficulty may not be serious if the capture theory of formation of clusters is accepted.

PLATE IV

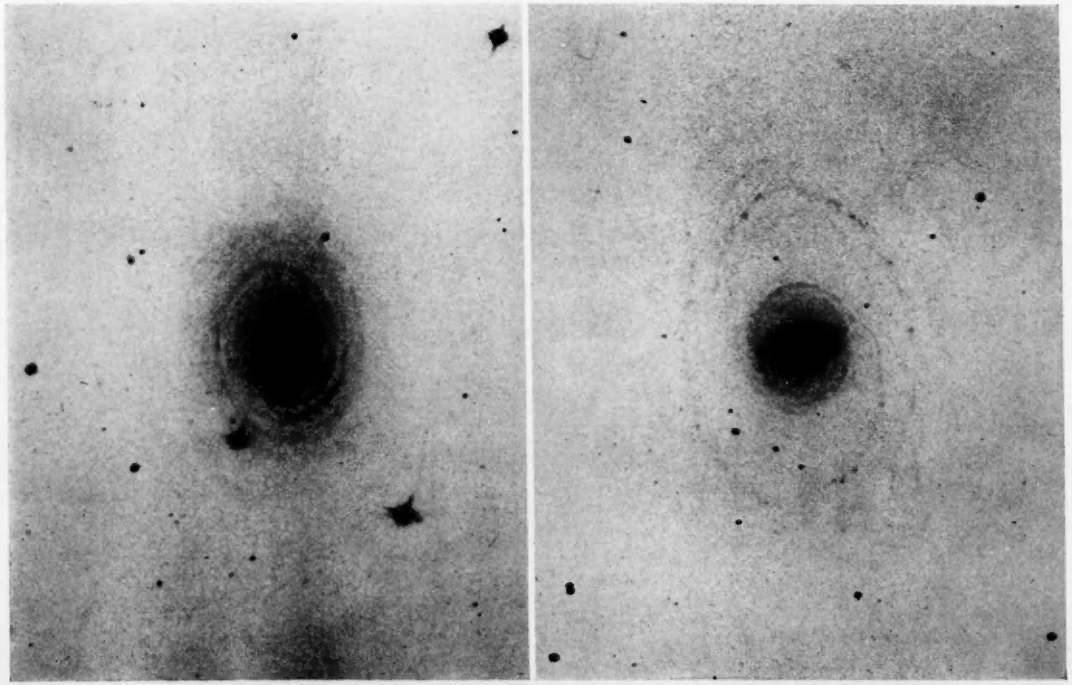

(*Left*) NGC 488, DEC. 11, 1923; (*right*) NGC 1398, NOV. 8, 1937

Both reproductions are made from plates with the 100-inch reflector. North is at the top; scale, 1 mm=6″.6

PLATE V

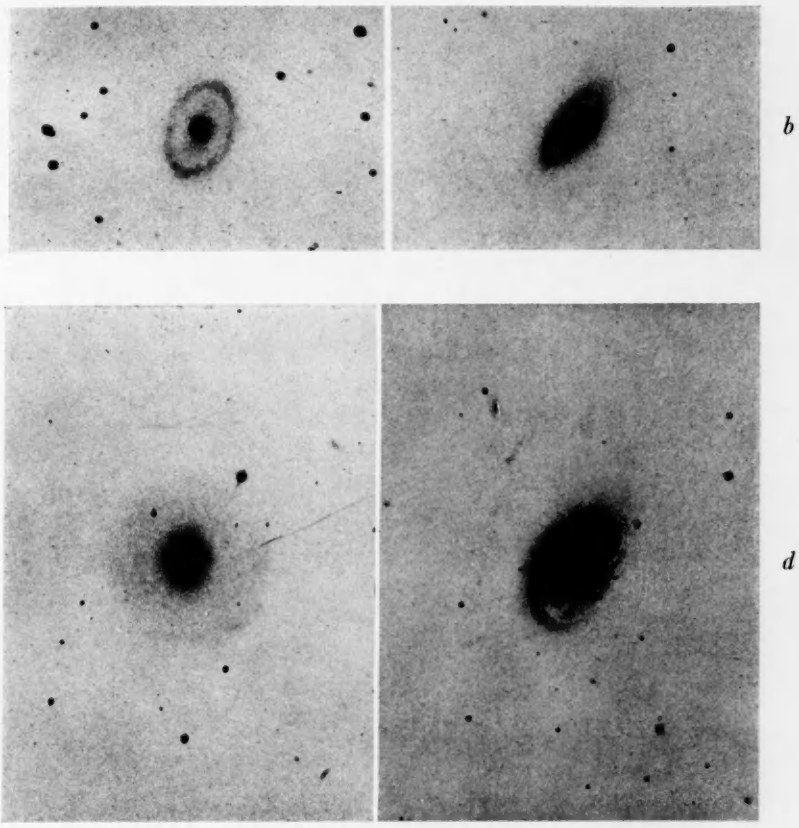


(*a*) NGC 3081, March 23, 1939; east at top; scale, 1 mm = 5″.3; (*b*) NGC 4324, May 24, 1936; west at top; scale, 1 mm = 4″.2; (*c*) NGC 1302, Oct. 11, 1937; north at top; scale, 1 mm = 9″.0; (*d*) NGC 3368, Nov. 26, 1924; north at top; scale, 1 mm = 9″.0. All plates with the 100-inch reflector.

gion. Shorter or longer spiral arms emerge perpendicularly from the ends of the bar. Sometimes the arms form a circular ring with the bar as a diameter. These configurations apparently cannot be explained by the ejection hypothesis. There must be conditions affecting the development which are not taken into account in the usual theories. A hypothesis which attempts to explain the general evolution of nebulae must be capable of accounting for all the different types if all are supposed to have developed from similar origins. An indication as to what the neglected effect on the evolution might be is given by some of the photographs of extraglactic nebulae in the Mount Wilson collection. A few typical examples are reproduced in the present article with the kind permission of Dr. Hubble.

A ring or a system of concentric rings seems to be a rather general feature among most types of nebulae. We find spiral types in which the structure is more like that of a set of concentric rings (Pl. IV) and barred spirals with accompanying rings, as already described.[4] Further, there are instances of a single ring centered on a more or less dense nucleus. Transition types, showing characteristics of both spirals and rings, of bars and symmetrical nuclei, are also found (Pls. IV and V).

The formation of a ring as a step in the evolution is not in any way explained by the current assumption of a transition from elliptical to spiral nebulae. Nevertheless, it is a relatively frequent phenomenon and may play an important role in the evolution. It is the purpose of the present discussion to show how the ring pattern may arise as a general feature in the development of the nebulae.

2. *Formation of a ring.*—We consider a rapidly rotating, flattened spheroid as the original structure from which the evolution starts. This original system need not be identified with an elliptical nebula. We make no assumption as to whether it consists of stars or of free atoms and molecules, or as to whether it rotates as a rigid body or has differential rotation.

A small volume of the constituent matter moves in a circular

[4] Examples of the simple bar and ring pattern are shown on Pls. II and III, *The Realm of the Nebulae*, by Hubble (1936). A good example of the "concentric rings" type of spiral, NGC 7217, is found on Pl. XIV, *Mt. W. Contr.*, No. 132; *Ap. J.*, **46**, 24, Pl. IX, 1917 (Pease).

orbit around the axis of rotation as a whole; but the individual stars or atoms have their individual motions, which are continually changed by collisions. Regarded from a hydrodynamical viewpoint, the internal motions, resulting in collisions, give rise to an effect of viscosity.

It is often supposed that the viscosity will merely make the system rotate ultimately as a rigid body. This, however, is not a correct statement. If the body is already rotating rigidly, no viscous force will arise at all. But if the angular velocity changes as we proceed along the radius from the axis of rotation, then the viscosity will affect not only the angular velocity but also the distribution of matter.

A volume element at a certain place will have its angular velocity either increased or decreased by the viscous force according to the behavior of the second spatial derivative of the velocity. If the velocity of the element is increased, the centrifugal force will drive it outward; if decreased, it will fall inward. Where the angular velocity is temporarily constant over a small region, no effect of viscosity appears, and matter will remain stationary, i.e., no radial motion will be started. The material will therefore tend to gather in these stationary zones, which will extend around the places of maximum and of minimum angular velocity as we pass along the radius. The motion will generally be away from a minimum toward a maximum, from both sides, as we shall see later.

Such a process must result in the formation of a ring pattern, each ring containing part of the total material of the system and rotating approximately as a rigid body. If there is a central body, it must rotate with constant angular velocity. Between the rings are regions of low density, where matter may be moving slowly toward the rings. This behavior is a necessary consequence of the assumption of differential rotation in a viscous medium. If our initial conditions are accepted, it must therefore be a general feature in the process of evolution.

The stage in the evolutional development at which stars are formed is not an essential feature of the problem, although the size of particles in the nebulae will evidently influence the magnitude of the viscosity and hence the rate of formation of the ring pattern. It

is further probable that the formation of a circular ring will often be disturbed by irregularities and unsymmetrical influences before being completed. Such influences may break down the ring pattern and lead to the formation of a spiral pattern.

We shall study the formation of a ring due to viscous forces a little more closely; but, before we do so, it may be of interest to point out that our discussion already provides an observational test.

We mentioned earlier that the ring pattern is found in most types of nebulae; and when no rings are found, there are often arms or arcs which may be parts of broken-down or uncompleted rings. In the elliptical nebulae, however, which are smooth and regular throughout, we may be sure that rings have never been formed. The reason for this smoothness, according to our theory, must be that there has been no viscous force to differentiate the matter, which again must be due to a lack of differential rotation. The reason why elliptical nebulae have not followed the development we observe in spiral nebulae is, then, that they rotated as rigid bodies from the start. They are not necessarily younger than the spirals or differently constituted but have another state of internal motion.

The conclusion that elliptical nebulae rotate as rigid bodies, or at least very nearly so, may be tested by observation. The few available measures of rotation in these nebulae seem to indicate that they do rotate as rigid bodies. The same condition probably occurs in the central nuclei of nebulae of other types, while the outer regions, where a pattern begins to develop, seem to have varying angular velocity. We shall now consider in greater detail the connection between angular velocity and the radial motion caused by viscous forces.[5]

**3.** *Viscosity in a rotating system.*—We consider a flat disk rotating about an axis. The angular velocity $W$ varies with the distance $R$ from the axis of rotation. The thickness of the disk is small, and we need not consider any variation in angular velocity perpendicular to the plane of the disk.

The disk is made of viscous material, with a constant coefficient of

[5] The idea of viscous forces playing a role in the evolution of extragalactic nebulae is not new. It has been discussed by G. Strömberg in *Mt. W. Contr.*, Nos. 492, 503; *Ap. J.*, **79**, 460; **80**, 327, 1934.

viscosity $\mu$. The viscous force in a velocity field $\mathsf{V}$, when $\mu$ is constant, is

$$\mathsf{F} = \mu\{\tfrac{1}{3}\,\text{grad div}\,\mathsf{V} + \nabla^2\mathsf{V}\}\,, \tag{1}$$

where $\mathsf{F}$ denotes the three rectangular components of the viscous force and $\nabla^2$ is the Laplacian operator in rectangular co-ordinates. In our case the motion occurs in the $xy$-plane and is axially symmetrical about the $z$-axis. When we assume the motion to be purely rotational, i.e., in circular orbits around the axis, the divergence of $\mathsf{V}$ vanishes, and at each point the force $\mathsf{F}$ is directed tangentially.

Introducing the distance from the axis $R$ and the angular velocity $W$, we may write for one of the rectangular velocity-components, say $V_y$,

$$V_y = WR\cos\varphi\,, \tag{2}$$

where $\varphi$ is the azimuth, or rotational angle from the $x$-axis. The Laplacian operator in the co-ordinates $R$, $\varphi$ is

$$\nabla^2 = \frac{\partial^2}{\partial R^2} + \frac{1}{R}\frac{\partial}{\partial R} + \frac{1}{R^2}\frac{\partial^2}{\partial\varphi^2}\,.$$

Hence the force in the $y$-direction is

$$F_y = \mu\left\{\frac{\partial^2 WR}{\partial R^2} + \frac{1}{R}\frac{\partial WR}{\partial R} - \frac{WR}{R^2}\right\}\cos\varphi\,.$$

The tangential component, which is actually the whole viscous force, becomes, by a simple reduction,

$$F = \frac{F_y}{\cos\varphi} = \frac{\mu}{R}\left\{\frac{\partial^2 WR^2}{\partial R^2} - \frac{1}{R}\frac{\partial WR^2}{\partial R}\right\}\,,$$

or

$$F = \mu\frac{d}{dR}\left(\frac{1}{R}\frac{dWR^2}{dR}\right)\,, \tag{3}$$

where we use total differentials, since $W$ is dependent on $R$ only.

When the force $F$ is positive, the angular velocity of the matter at the point in question will increase; when negative, the velocity will decrease. The result will be radial motion outward and inward, respectively.

In calculating the viscous force we have assumed purely circular motion. The radial motion arising as an effect of the viscosity is very slow, compared to the rotational velocity. The effect on the viscosity therefore amounts to second-order terms only. We can now assume an arbitrary distribution of angular velocity $W$ and, by means of formula (3), tell where the material will move slowly outward or inward, or remain at rest, according as $F$ is positive, negative, or zero.

To get a general idea of the circumstances, we consider $W$ as varying at each point according to a certain power of the radius $R$, i.e.,

$$W = kR^m ; \qquad k = \text{const} .$$

Then by equation (3),

$$F = \mu m(m + 2)kR^m . \tag{4}$$

As long as all parts of the system rotate in the same direction, $k$ is positive. We then immediately obtain the following results:

$F$ is positive (outward motion)

$$\text{when} \begin{cases} m > 0, \text{ i.e., when } W \text{ increases outward.} \\ m < -2, \text{ i.e., when } W \text{ decreases faster than } R^{-2}. \end{cases}$$

$F$ is negative (inward motion)

$$\text{when } -2 < m < 0, \text{ i.e., when } W \text{ decreases more slowly than } R^{-2}.$$

$F$ is zero (no radial motion)

$$\text{when} \begin{cases} m = 0, \text{ i.e., by rotation as rigid body.} \\ m = -2, \text{ i.e., when } WR^2 \text{ is spatially constant.} \end{cases}$$

Thus, if the angular velocity increases outward, the matter will tend to move outward until it arrives at a point where the increase stops and the angular velocity has reached its maximum.

In the region where the angular velocity begins to decrease slowly after passing the maximum, the matter will tend to move inward, i.e., again toward the maximum. At the point where the rate of decrease becomes as large as that of $R^{-2}$, the inward motion ceases, and, beyond this limit, the matter starts moving outward. It should be noticed, however, that the region where $W$ decreases more rapidly than $R^{-2}$ is no longer dynamically stable. A slight displacement of a

small volume of the material, either outward or inward, will automatically increase. This is easily demonstrated.

By the Helmholtz-Kelvin circulation theorem the quantity $WR^2$ remains constant when a certain ring of matter in our rotating system is displaced slightly outward. But if the distribution of $W$ in the system is such that $WR^2$ decreases outward, the ring, after the displacement, will have a higher angular velocity than the matter in equilibrium at the point, and, consequently, will continue to move outward. Similarly, a displacement inward will continue and will increase. In this region, therefore, the small viscous force will probably play a subordinate role.

The preceding consideration of the stability is strictly valid only for nonviscous media. The viscous force might be able to stop a very slight radial displacement, or at least to affect the critical limit. If the viscosity is low, however, we may expect the argument still to apply roughly. It is seen that the effect reverses in passing a minimum of the angular velocity, matter tending to move away from the minimum on both sides.

As already mentioned, we have deduced the viscous force on the assumption of a purely rotational, stationary motion in the whole system. It is obvious that in the long run the viscosity will also influence the angular velocity in the general field, which again will change the viscous forces. In a strict sense, the expression $F$ represents the force only at a certain instant, at which we have a given distribution of angular velocity. However, since the change in angular velocity will be exceedingly slow, we may safely consider the motion as a state of quasi-stationary rotation and may expect our formulae to apply through a rather extensive phase of the evolution without changing the field of angular velocity.

An exact treatment would demand a knowledge of the original distribution of density and angular velocity. Since we know nothing about these features, it would be of no value to work out a ring pattern from assumed initial conditions. We might as well make our assumptions directly about the resulting rings. The important point is that we find a general tendency toward the formation of a ring pattern and that a stationary state of motion cannot be reached before such a differentiation of the constituent matter has taken place.

**4.** *Distribution of mass.*—Since matter tends to avoid regions of

minimum angular velocity and to gather around those of maximum velocity, the general run of the mass-distribution-curve will roughly follow that of the angular velocity.

As an illustration we may consider the velocity-curve recently published by Dr. Horace W. Babcock[6] for the Andromeda nebula (Fig. 1).

On the basis of this velocity-curve, we may divide the radius in the diagram into four parts:

*a*) The central region of constant angular velocity and a narrow zone at the beginning of the downward slope, from which matter

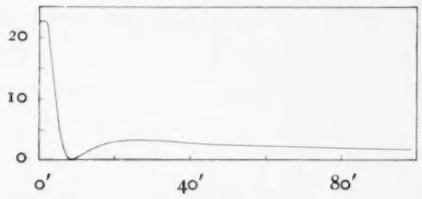


FIG. 1.—Angular velocity $W$ in units of $10^{-15}$ radians per second, plotted against radius (Horace W. Babcock).

will, according to our theory, move inwards toward the central region.

*b*) An unstable region (where the slope is steeper than $R^{-2}$) extending out to the point of minimum angular velocity, which is practically zero.

*c*) The region where $W$ rises from zero up to a maximum. In this region matter moves away from the minimum and out toward the maximum.

*d*) The outer region, showing a very slight, downward slope. In this region the gradually decreasing angular velocity leads to an exceedingly slow motion inward, tending to gather the matter toward the flat maximum extending from about 30′ outward.

The idealized result of such a velocity distribution would be a rigidly rotating central body, immediately surrounded by a narrow

[6] *Lick Obs. Bull.*, **19**, 41, 1939. This velocity-curve, as well as the curves obtained for elliptical nebulae, may be influenced more or less by the fact that the light measured does not arrive from a single point on the radius of the nebula but is the integrated light from a path along the line of sight. This circumstance, according to E. Holmberg, may tend to give an appearance of rotation as a rigid body (*M.N.*, **99**, 650, 1939).

unstable region. Outside a rather empty region in the interval between 10′ and 20′, a ring of matter, fading outward, would rotate approximately as a rigid body.

The Andromeda nebula is not a regular circular system; if it ever has been, the circular ring at present is broken down. It is interesting to notice, however, as Babcock mentions, that "the minimum of angular velocity occurs in a region of somewhat decreased density between the core of the nebula and the first encircling turn of the spiral arms," as would be predicted by the foregoing hypothesis if, as suggested, the evolution of the Andromeda nebula started with formation of a ring.

Thus it is not impossible that the present distribution of density is the remnant of an earlier ring pattern, disturbed during the evolution by unsymmetrical influences.

5. *Evolution of the nebulae.*—It is not the aim of the present discussion to attempt any detailed explanation of the evolution of all types of extragalactic nebulae. The main purpose is to suggest that the formation of a ring pattern may be an important step in the evolution, to explain how this phenomenon may arise, and finally to show that by accepting this hypothesis it seems possible to understand the development of different observed types of nebulae which are not explained by the ejection theory. Our hypothesis implies that the reason, or one of the reasons, for the different ways of evolution taken by different types of nebulae is the difference in the state of internal motion in the original system. For instance, the elliptical nebulae must be rotating approximately as rigid bodies, and for this reason such nebulae do not develop any structural pattern. If they were not rotating rigidly, they would have shown some structure.

It may be asked whether a system, in order to develop structure, must have been originally endowed with differential rotation. An affirmative answer would imply that the formation of rings is a necessary phase in the evolution through which all spirals and other nebulae showing any structural pattern must pass. Even if the ring formation were a necessary preliminary for the development of spiral arms, it would not necessarily follow that every spiral, once in its evolution, had appeared as a regular ring system. Of course there is the possibility that a ring may be completely developed and afterward broken down by some kind of disturbance; but it is also possible

that unsymmetrical disturbances may disarrange the circular pattern from the very moment it began to form and that the result is a more or less regular spiral pattern. Moreover, as a third possibility, the ejection of matter from unstable regions may play some role in the formation of normal spirals.

As already mentioned, the class of barred spirals includes a great variety of shapes. The most conspicuous feature is the straight bar through the center. In some nebulae the arms are short arcs from the ends of the bar; in others, the arms are longer and occasionally close to a circle inclosing the bar. In some cases, the bar appears as a dense nucleus at the center of the ring.

This last case is, of course, immediately explained as a result of viscous differentiation. But when the central body appears as a well-defined straight bar, the explanation is not so easily seen. A system consisting of a bar across a circular ring is a peculiar configuration, and indeed very difficult to explain, both as regards the formation and the dynamical state. However, there is one clue which indicates a possible solution of the problem, namely, the surprising dip to zero angular velocity seen in the velocity diagram of the Andromeda nebula. If this is a common phenomenon, it may have a bearing on the bar formation. In the Andromeda nebula the dip is rather short and steep and will cause an empty region separating the ring and the nucleus. If the dip were an extended, flat minimum, however, there would be a certain region at the bottom where matter would remain at rest and acquire no radial motion by viscous forces. After the ring and the nucleus were formed, this matter would remain as a resting cloud in the "empty" region. Such a resting cloud would be a very unstable configuration, easily influenced by perturbations. A weak perturbation might raise a tidal wave in the cloud, elongating it in the direction of the force. When once this motion was started, matter would probably continue to stream toward the ring in the direction of elongation, and inward to the nucleus in the perpendicular direction, thus tending to form a temporary bar across the ring. The reason why we obtain a bar and not a spiral pattern is, of course, that the matter in the cloud does not partake in the rotation. If the rotating ring itself were not broken up by the initial perturbation, it would probably be broken after a while because of the asymmetrical redistribution of the matter in the resting cloud (Pl. IV, right).

This explanation is naturally very uncertain and loose and does not claim to be more than a suggestion. However, it shows that, by considering the formation of a ring as a step in the evolution, we may explain types of nebulae which cannot possibly be accounted for by the ejection hypothesis alone.

It follows from our discussion that the elliptical nebulae are not to be considered as younger than the spirals. They have followed another route of development only because of a different initial state of motion. The argument furnishes no reason for believing that stars should not have developed in elliptical nebulae to the same extent as in spirals.[7]

The question of how the systems acquire their original rotation remains unanswered. However, the systematic increase in angular momentum when passing from earlier- to later-type nebulae (referring to Hubble's classification, not to evolutionary sequence) may be connected with the fact that later types, in general, will probably show a slight downward slope in the outer part of the curve of angular velocity, as in the Andromeda nebula, and hence have a slow radial stream of material inward increasing the angular momentum of the main body of the nebula. This will not be the case in the rigidly rotating elliptical nebulae.

In conclusion, one may say that the formation of a ring pattern during the early evolution of the nebulae seems to be possible as an effect of viscosity in the system. The ring formation provides possibilities for explaining types which cannot be accounted for by the ejection hypothesis.

I want to express my thanks to Dr. Hubble for helpful suggestions and for permission to publish some of his most interesting plates, taken with the 100-inch telescope at Mount Wilson.

CARNEGIE INSTITUTION OF WASHINGTON
MOUNT WILSON OBSERVATORY
April 1940

[7] This statement, of course, does not mean that there can be no systematic difference in the contents of elliptical nebulae and spirals. The different internal conditions arising during the development may be expected to influence the evolution of the stars. This remark is suggested by the fact that no supergiants are found in elliptical nebulae.

# ON THE POSSIBLE EXISTENCE OF FORMALDEHYDE IN THE ATMOSPHERE OF VENUS

RUPERT WILDT

ABSTRACT

Ultraviolet spectrograms of Venus, and of the moon for comparison, were obtained with the long-focus quartz spectrograph (dispersion 21.7 A/mm at λ 3300) attached to the 82-inch reflector of the McDonald Observatory, in order to search for the electronic absorption spectrum of formaldehyde gas, which might be formed in Venus' atmosphere by photochemical synthesis. The spectrograms revealed no sign of absorption by $CH_2O$, while a mass of this gas equivalent to 3 mm-atm, under standard conditions, should have been sufficient for spectroscopic identification. This negative result does not refute the assumption that the photochemical formation of $CH_2O$ has played an important role in Venus' atmosphere during the past. In the light of Tammann's theory of the origin of the terrestrial oxygen, the lack of oxygen on Venus indicates that the primordial atmosphere of this planet must have been extremely poor in water vapor. A tenuous atmosphere of water vapor and carbon dioxide affords the very conditions for the photochemical synthesis of formaldehyde, which appears to be capable of proceeding until the supply of either of these gases has been exhausted. In a moist atmosphere $CH_2O$ rapidly polymerizes into a mixture of polyoxymethylene hydrates, $(CH_2O)_x \cdot H_2O$, a white crystalline solid. From laboratory data it is concluded that the amount of gaseous $CH_2O$ existing in equilibrium with the solid polymers is exceedingly small, which would seem to account for the failure of the spectroscopic test. The vapor tension of the solid polymers in the presumable range of Venus' atmospheric temperature is high enough to permit the dissolution and formation of clouds by processes of sublimation and subsequent condensation. As Venus' atmosphere is now spectroscopically free from water vapor but is obviously filled with clouds, the nature of which has never been settled, it is tentatively suggested that solid polyoxymethylene hydrates constitute the clouds shrouding the planet's surface.

The great similarity of the two planets Venus and earth, with regard to their size and mass, has long been held indicative of a similar constitution of their surfaces and atmospheres, but modern spectroscopic observations have failed to support this view. According to St. John and Nicholson,[1] the amounts of oxygen and water vapor in Venus' atmosphere must be less than one-thousandth and one-tenth, respectively, of that in the earth's atmosphere. Because of the difficulties in disentangling the planetary absorption bands from the almost coincident telluric ones, this test for water vapor was by no means very delicate, and hence the idea has persisted that the visible surface of Venus, remarkable for its high albedo, is a layer of clouds. However, it does not seem to have been observed generally that the

[1] *Ap. J.*, **56**, 380, 1922.

subsequent discovery of carbon dioxide in Venus' atmosphere[2] makes it well-nigh impossible to reconcile the existence of a cloud layer with the failure to identify water vapor spectroscopically. Carbon dioxide is so highly opaque to its own heat radiation that it must produce a considerable greenhouse effect, which may raise the temperature at the bottom of Venus' atmosphere beyond the terrestrial boiling-point of water,[3] while the yet inconclusive temperature determination from the line intensities of the $CO_2$ bands situated in the near infrared points to a surface temperature of at least 50° C.[4] Notwithstanding the uncertainty as to the precise value of Venus' surface temperature, it can be confidently asserted that the existence of a layer of clouds condensed from water vapor would entail a vapor tension of the order of 100 mm. Such an enormous amount of water vapor could not have escaped the scrutiny of the spectroscopists, and so the conclusion is unavoidable that the partial pressure of $H_2O$ in Venus' atmosphere must be far below that required for saturation and condensation. Consequently, the concept that the visible surface of Venus consists of a layer of clouds of the same nature as the terrestrial ones has to be abandoned, and it appears necessary then to account for the high albedo of this planet in a different way. But Gerasimovič[5] demonstrated conclusively that the only model of Venus' surface which admits of an explanation both of the absolute brightness of the planet and of its phase-curve is a stratum of large scattering particles, which he believes to be products of condensation, without further specifying their character. A conjecture as to the nature of this scattering agent has emerged from speculations along chemical lines, which form the subject of this paper. Although they cannot lay any claim to absolute cogency, they are presented here as a working hypothesis because they afford a novel co-ordination of several data bearing upon the constitution of Venus' surface which hitherto do not seem to have been regarded as related.

In the light of certain geochemical ideas to be exposed presently, the extreme paucity, if not complete absence, of free oxygen is ob-

[2] W. S. Adams and T. Dunham, Jr., *Pub. A.S.P.*, **44**, 243, 1932.

[3] R. Wildt, *Ap. J.*, **91**, 266, 1940.

[4] A. Adel, *Ap. J.*, **86**, 337, 1937.

[5] *Poulkovo Bull.*, No. 127, 1937.

viously related to the lack of water on Venus. Tammann[6] has suggested that the free oxygen of the terrestrial atmosphere originated from thermal dissociation of water vapor before the earth had formed a solid crust. On evaporation of all the water of the oceans and of the polar caps, the partial pressure of $H_2O$ would be approximately 270 atm. At this pressure and at a temperature not far above the melting-point of the crustal magma the dissociation degree of steam is great enough to provide for all free oxygen now found in the atmosphere, while the velocity of escape of hydrogen is so high as to guarantee the rapid dissipation into space of the chemically equivalent amount of hydrogen. Part of the free oxygen was consumed by oxidation of the liquid magma, until solidification prevented further chemical loss. While Tammann seemed to think he could provide in this manner for the entire content of free oxygen of the present atmosphere, Goldschmidt[7] has criticized his quantitative analysis for the reason that through the geological ages a considerable amount of oxygen became "fossile," i.e., deposited in oxidized sediments. Still, there can be no doubt that the process conceived by Tammann has been instrumental in producing that initial ample supply of free oxygen upon which the first breathing organisms could draw. Later on, vast masses of additional oxygen were released by the assimilation in green plants, and so there exists no real difficulty in making up the geochemical balance of oxygen. Now the question arises as to the course of chemical events at the surface of a planet which originally had been less richly endowed with water than the earth. On lowering the partial pressure of steam in the primordial atmosphere, the dissociation degree will steadily increase, but there will be an equally steady diminishing return of free oxygen, since the mass per unit surface of the generating steam is being reduced. Finally, at a rather small partial pressure of steam—of the order of a few atmospheres, presumably—the oxygen freed by dissociation would be consumed, without residue, in oxidation of the liquid magmatic surface, and after solidification there would remain a tenuous atmosphere of water vapor, entirely devoid of oxygen. The writer is inclined to be-

[6] *Zs. f. phys. Chemie*, **110**, 17, 1924.

[7] *Fortschr. der Mineralogie, Kristallographie und Petrographie*, **17**, 140, 1933.

lieve that this limiting case represents the state of affairs on Venus in the remote past. Mars furnishes an example of an intermediate case. Though its atmosphere no longer contains a spectroscopically detectable amount of oxygen, in former ages there must have been enough oxygen on this planet to enable the formation of those reddish areas, which now are commonly interpreted as highly oxidized sediments. From the point of view of Tammann's theory it is significant that the great scarcity of oxygen on Mars is concomitant to a lack of water, manifesting itself most conspicuously by the absence of oceans.

Proceeding upon the hypothesis that Venus' primordial atmosphere was exceedingly poor in water vapor, it becomes evident that the acceptance of Tammann's theory implies a corresponding lack of oxygen. Despite the rich supply of oxygen in the earth's original atmosphere, the material of the crust is far from being fully oxidized. Hence, the same may be assumed as valid, a fortiori, for Venus, which must have shown a dark surface of solidified magma, having an albedo of the order of magnitude of that of Mercury and the moon, and must have been covered by a tenuous atmosphere consisting of water vapor and carbon dioxide, besides chemically inert elements like nitrogen and the noble gases. The absence of oxygen would deprive Venus of the protection this gas exerts against ultraviolet sunlight. Carbon dioxide and water vapor would be decomposed photochemically, and formation of formaldehyde would follow, according to the over-all equation

$$CO_2 + H_2O \rightarrow CH_2O + O_2 .$$

As oxygen is being formed continually while the reaction goes on, it would come to a halt automatically by the very screening-power of oxygen, unless subsequently oxygen is being consumed irreversibly by another reaction. Such reaction does indeed exist. In the moist atmosphere the surface of the planet is weathering and binding oxygen chemically. Hence, it would seem possible that the photochemical synthesis of formaldehyde can progress till the supply of either carbon dioxide or water vapor is exhausted. Incidentally, formaldehyde is highly resistent to chemical attack by oxygen, or even

ozone, i.e., no formation of formic acid is to be feared. The fact that the conditions prevalent in Venus' atmosphere favor the formation of formaldehyde had been pointed out in a review of the photochemistry of planetary atmospheres.[8] Since then several scientists[9] have brought forth the suggestion that the photochemical synthesis of formaldehyde was the first step toward the spontaneous generation of life on the earth. Without going any further into this highly controversial problem, we may note that the authorities quoted did not pay any regard to Tammann's theory, which by implication excludes the very photochemical formation of formaldehyde under the powerful oxygen screen of the earth's primordial atmosphere. Neither is the surface of Venus a substrate suitable for sustaining life, both because of its higher temperature and because of the lack of liquid water. The writer wishes to guard his views on the chemistry of Venus against the possible imputation that they lend support to any speculations concerning the existence of life on this planet.

The molecule $CH_2O$ has an electronic absorption spectrum covering the range from λ 3600 to λ 2500, which has been studied by Henri and Schou,[10] with absorbing layers varied between 3 and 45 mm-atm. As the total amount of ozone in the stratosphere is equivalent to a layer of about 3 mm-atm, the intrinsic strength of the formaldehyde absorption must be of the same order of magnitude as that of the ozone molecule, in the same range of wave lengths. By experiments on fluorescence and variation of the band intensities as functions of the gas temperature it has been established that this band system is produced by absorption from the ground state. During a recent stay at the McDonald Observatory, the writer obtained a series of ultraviolet spectra of Venus, and of the moon for comparison, in order to investigate whether there are any signs of absorption by formaldehyde in Venus' atmosphere. The spectra were taken at the Cassegrain focus of the 82-inch reflector with the 500-mm camera. The dispersion of the spectrograms is 21.7 A/mm at λ 3300. By variation of the exposure time, spectrograms of medium density were se-

[8] Wildt, *Ap. J.*, **86**, 321, 1937.

[9] W. Groth and H. Suess, *Naturwissenschaften*, **26**, 77, 1938; E. Desguin and A. Dauvillier, *C.R.*, **208**, 294, 1939.

[10] *Zs. f. Phys.*, **49**, 774, 1928.

cured between λ 3600 and λ 3200, the limit imposed by the transparency of the optics of the spectrograph. In this range of wave lengths there are located five strong bands of formaldehyde, distinguished by letters assigned to them by Henri and Schou as shown in Table 1. A careful examination of pairs of spectrograms of equal density revealed no recognizable difference between the spectra of Venus and of the moon in the suspected regions. Below λ 3400 the terrestrial ozone bands show up identically in both spectra. With respect to the observation made by Henri and Schou, that the five bands given in the preceding table can readily be produced with a

TABLE 1

| Designation | Extension | Strongest Line |
|---|---|---|
| A | 3567–3515 | 3530.7 |
| B′ | 3456–3418 | 3430.9 |
| B | 3416–3377 | 3389.3 |
| C′ | 3324–3288 | 3294.7 |
| C | 3288–3249 | 3260.4 |

layer equivalent to not more than 3 mm-atm of $CH_2O$, this value must be regarded as an upper limit to the hypothetical formaldehyde content of Venus' atmosphere. Without further qualification this result would seem to refute the alleged accumulation of formaldehyde at Venus' surface. However, gaseous formaldehyde is extremely susceptible to polymerization and precipitation in solid form. Therefore, the spectroscopic test refers only to the small amount of gaseous $CH_2O$ in equilibrium with the solid phase. An appraisal of the failure to identify $CH_2O$ spectroscopically must be deferred until the chemistry of the formaldehyde polymers has been discussed in outline.

Monomolecular gaseous formaldehyde, $CH_2O$, is difficult to purify from water vapor.[11] When absolutely dry, it seems to be stable at temperatures higher than about 80° C, while at lower temperatures, and even in the liquefied state, it polymerizes rapidly into a solid white mass of unknown, but certainly very high, molecular weight $(CH_2O)_x$. Two lower polymers, trioxymethylene $(CH_2O)_3$ and tetra-

[11] M. Trautz and E. Ufer, *J. f. prakt. Chemie*, **113**, 105, 1926.

oxymethylene $(CH_2O)_4$, have been isolated in pure form. They are cyclic compounds with a melting-point of 65° C and 112° C, respectively. The constitution of the higher solid polymers has not yet been ascertained, but they are believed to consist of long parallel chains of $(-CH_2-O-)$ groups which are joined at the ends. The hydrated polymers of formaldehyde, of the general formula $(CH_2O)_x \cdot H_2O$ have been extensively studied by Staudinger and his collaborators.[12] Formaldehyde gas dissolves freely in water and can be expelled from the solution by heating. The vapor existing in equilibrium with the aqueous solution appears to be monomolecular $CH_2O$.[13] According to Staudinger, the aqueous solution contains the hydrates of the lower polymers ($x = 1$–$8$, approximately). As they transform rapidly into each other, they cannot be isolated by fractionization. When the solution is being concentrated by evaporation, a mixture of hydrates of the higher polymers (up to $x = 50$) is precipitated as a white mass, known as paraformaldehyde, and a mixture of still higher polymers (up to $x = 100$) forms the so-called α-polyoxymethylene, which is precipitated from the aqueous solution by strong dehydrating agents, like sulphuric acid. Staudinger's comprehensive investigations culminated in the proof that all these hydrated polymers are chainlike molecules of the general formula $HO-(-CH_2-O-)_x-H$ and thus are properly designated as polyoxymethylene hydrates. The linear structure makes it plausible for the different polymers to be so easily transformed into each other on removal or addition of water. In fact, water vapor is a powerful catalyst for the polymerization of gaseous formaldehyde. Trautz and Ufer[11] describe a striking experiment, in which a minute amount of water vapor is injected into absolutely dry monomolecular formaldehyde gas, with the result that the reaction vessel instantaneously becomes filled with dense white clouds. The reaction product is obviously a polyoxymethylene hydrate of extremely high degree of polymerization.

Unfortunately, the chemical literature does not contain any precise statements with regard to the vapor tension of the solid for-

[12] Liebig's *Annalen der Chemie*, **474**, 245, 1929; *Die hochmolekularen organischen Verbindungen*, Berlin: Julius Springer, 1932.

[13] F. Walker, *J. Phys. Chem.*, **35**, 1104, 1931.

maldehyde polymers and their hydrates, for two different reasons. First, such mixtures of inseparable compounds have no well-defined physical characteristics, which rather deters investigators from measuring irreproducible data. Second, the vapor in contact with α-polyoxymethylene partially depolymerizes at an extremely slow rate, so that even during the course of several months no true equilibrium is reached, as Auerbach and his collaborators[14] have observed. It is important to note that the vapor emanating from solid α-polyoxymethylene does not contain monomolecular formaldehyde, according to Auerbach, and that it is necessary to raise the temperature to about 200° C in order to produce depolymerization into $CH_2O$. This seems to account for the negative result of the spectroscopic search for $CH_2O$ in Venus' atmosphere. The vapor tension of the solid high polymers is of the order of a few per cent of that of water at the same temperature. Consequently, in the temperature range of Venus' atmosphere, i.e., 350°–400° K, presumably, the polyoxymethylene hydrates should be capable of playing the same role as water in the earth's atmosphere. The melting-point of the polyoxymethylene hydrates is 140°–170° C, according to composition; hence the dissolution of the hypothetical clouds on Venus would be a process of sublimation proper, and their formation would be strictly analogous to the condensation of ice crystals as cirrus clouds in the terrestrial atmosphere. If the photochemical synthesis of formaldehyde has proceeded to the point where Venus' atmosphere has become entirely depleted of water vapor, it is likely that now most of the reaction product covers the surface of the planet as what might be called "formaldehyde-snow," viz., solid polyoxymethylene hydrates.

The starting-point of the argument presented was the assumption that the original atmosphere of Venus was exceedingly poor in water vapor, compared to that of the earth. No a priori reason for this presumed difference can be given, but it does imply a simple explanation of the lack of free oxygen on Venus, on the basis of Tammann's theory, and, moreover, affords the conditions necessary for the photochemical synthesis of formaldehyde, as realized by the writer

[14] *Arb. a. d. kaiserl. Gesundheitsamte*, **22**, 584, 1905; **27**, 183, 1908; **47**, 116, 1914.

several years ago. It may be mentioned that the writer was not aware of the spontaneous polymerization of $CH_2O$ when he eventually found an opportunity to investigate the ultraviolet spectrum of Venus. It was the failure to detect any absorption that prompted a more detailed study of the chemistry of formaldehyde and finally suggested the hypothesis that the polyoxymethylene hydrates might constitute the substance of Venus' cloud formations.

It is a pleasure to record here the writer's appreciation of the privilege of working at the McDonald Observatory, extended to him by Dr. O. Struve, and to thank Mr. W. Linke for his assistance during the observations.

PRINCETON UNIVERSITY OBSERVATORY
APRIL 1940

# ON THE CLASSIFICATION OF THE A STARS. I. THE SPECTRAL TYPES OF THE BRIGHTER MEMBERS OF THE HYADES CLUSTER

JOHN TITUS AND W. W. MORGAN

ABSTRACT

The problem of the classification of the A stars is discussed. Revised spectral types of seventy-two of the brighter Hyades are given on a system which is in close agreement with that of the *Henry Draper Catalogue*. The main sequence defined by the ordinary Hyades stars appears to coincide with the main sequence determined from stars in the sun's neighborhood over the spectral range A5–Go. Attention is called to a group of six A1–A5 stars which appear to be of lower luminosity than the ordinary main sequence. The most striking characteristic of these objects is the great strength of the metallic arc lines in their spectra. The latter can be described as composite. In each case, however, the spectrum probably originates in a single star.

## I. INTRODUCTION

To be of the greatest general usefulness, a spectral classification should fulfil the following conditions: (*a*) it should be directly interpretable in terms of color index or temperature; (*b*) it should permit the separation of the stars into luminosity groups directly interpretable in terms of absolute magnitude; (*c*) it should have high systematic accuracy over a large range in apparent stellar magnitude; and (*d*) it should have as low accidental errors as is feasible with regard to conditions (*a*)–(*c*).

In the case of certain specific problems which are concerned exclusively with the brightest stars, spectrograms of the highest dispersion are of great value in assigning spectral types. For investigations which depend on a translation of physical properties to faint stars, however, the most important requirement is that there be no serious systematic error in the spectral types as a function of apparent magnitude or of position in the sky.

The present series of investigations is concerned with the spectral classification of the A stars. It is planned to investigate each of the aforementioned points.

The first step is the critical examination of the spectral changes observed when the temperature and luminosity are varied. We shall

utilize three general groups of objects having known luminosities: (1) stars in clusters, (2) stars of large parallax, and (3) systems for which dynamical parallaxes are available. The present paper discusses the spectral features of seventy-two of the brighter members of the Hyades cluster.

## II. THE CLASSIFICATION OF THE HYADES STARS OF CLASSES A AND F

There are two widely used methods of classifying the spectra of the A stars: (1) from the ratio of the K line to $H\delta$ or $H\epsilon$ and (2) by the intensity of the metallic arc lines. Both methods allow the subdivision of the A stars into a number of groups, and it is a question of suitability to the dispersion used and personal preference as to which method is employed. In the present work we have preferred method (1) for the following reasons: (*a*) it can be used on plates of very low dispersion; (*b*) there are certain advantages in using a ratio rather than an intensity estimate; (*c*) it lessens the difficulty of comparing the spectra of stars having greatly different line widths; and (*d*) it is in good systematic agreement with the Draper system.

We have, therefore, preferred to use as our fundamental standard the ratio of K to the hydrogen lines and to note separately any abnormalities in the intensity of the metallic lines. The system has been adjusted so that it agrees closely with that of the *Henry Draper Catalogue*.

The spectrograms were obtained by Titus with the Bruce spectrograph attached to the 40-inch telescope. The plates have a dispersion of about 110 A/mm at $H\gamma$ and were obtained on Agfa Super Plenachrome Press films. Under these arrangements it is possible to get considerably widened spectra of stars to the ninth magnitude in relatively short exposures.

The spectral types are listed in Table 1. The types F5–K have been determined in a manner already outlined by one of us.[1] The columns give the number in Smart's list,[2] the HD number and spectral type, the Yerkes type as determined by Titus on the basis of the ratios K/$H\delta$ and K/$H\epsilon$, the apparent magnitude, and the absolute magnitude as determined by Smart.

[1] *Ap. J.*, **87**, 460, 1938. [2] *M.N.*, **99**, 168, 1938.

TABLE 1

| Smart No. | HD | | Yerkes Sp. | $m_v$ | $M$ | Remarks |
|---|---|---|---|---|---|---|
| | No. | Sp. | | | | |
| 1..... | 24357 | Fo | F4 | 6.0 | 3.3 | |
| 2..... | 25202 | Fo | F3 | 5.8 | 3.0 | |
| 3..... | 25570 | Fo | F4 | 5.5 | 3.3 | |
| 4..... | 26162 | G5 | K1 | 5.7 | 2.6 | 43 Tauri (1) |
| 5..... | 26462 | Fo | F4 | 5.7 | 3.4 | 45 Tauri |
| 6..... | 26911 | F5 | F5 | 6.4 | 3.6 | 48 Tauri |
| 7..... | 27176 | A5 | A8 | 5.6 | 2.4 | 51 Tauri |
| 8..... | 27371 | Ko | G9 | 3.9 | 1.2 | $\gamma$ Tauri |
| 9..... | 27383 | Go | F9 | 7.1 | 4.4* | 55 Tauri |
| 10..... | 27459 | Fo | Fo | 5.3 | 2.4 | 58 Tauri |
| 11..... | 27483 | F2 | F6 | 6.1 | 3.4 | |
| 12..... | 27628 | A3 | A3p | 5.8 | 3.0 | 60 Tauri (2) |
| 13..... | 27697 | Ko | Ko | 3.9 | 1.1 | $\delta$ Tauri |
| 14..... | 27749 | A2 | A1p | 5.7 | 2.8 | 63 Tauri (3) |
| 15..... | 27819 | A5 | A6 | 4.8 | 2.2 | 64 Tauri |
| 16..... | 27901 | Fo | F4 | 6.0 | 3.2 | |
| 17..... | 27934 | A3 | A5 | 4.4 | 1.4 | 65 Tauri |
| 18..... | 27946 | Fo | A7 | 5.4 | 2.7 | 67 Tauri |
| 19..... | 27962 | A2 | A1 | 4.2 | 1.5 | 68 Tauri |
| 20..... | 27991 | F8 | F8 | 6.4 | 3.6 | 70 Tauri |
| 21..... | 28024 | A5 | Fo | 4.4 | 1.6 | $\upsilon$ Tauri |
| 22..... | 28052 | A5 | Fo | 4.6 | 1.9 | 71 Tauri |
| 23..... | 28226 | A5 | A5p | 5.7 | 2.7 | |
| 24..... | 28294 | Fo | F2 | 6.0 | 3.3 | 76 Tauri |
| 25..... | 28305 | Ko | Ko | 3.6 | 1.0 | $\epsilon$ Tauri |
| 26..... | 28307 | Ko | G8 | 4.0 | 1.2 | $\theta^1$ Tauri |
| 27..... | 28319 | Fo | A7 | 3.6 | 0.8 | $\theta^2$ Tauri |
| 28..... | 28355 | A5 | A7 | 5.1 | 2.4 | 79 Tauri |
| 29..... | 28485 | Fo | Fo | 5.8 | 3.0* | 80 Tauri |
| 30..... | 28527 | A5 | A6 | 4.8 | 2.2 | |
| 31..... | 28546 | A5 | A5p | 5.5 | 2.7 | 81 Tauri (3) |
| 32..... | 28556 | Fo | F3: | 5.5 | 2.8 | 83 Tauri |
| 33..... | 28677 | Fo | F4 | 6.0 | 3.3 | 85 Tauri |
| 34..... | 28910 | A5 | Fo | 4.8 | 2.0 | $\rho$ Tauri |
| 35..... | 29375 | Fo | F2 | 5.8 | 3.0 | 89 Tauri |
| 36..... | 29388 | A3 | A6 | 4.3 | 1.6 | 90 Tauri |
| 37..... | 29499 | Fo | F4 | 5.6 | 2.6 | |
| 38..... | 29488 | A3 | A7 | 4.8 | 1.8 | 92 Tauri |
| 39..... | 30034 | A3 | Fo | 5.4 | 2.8 | |
| 40..... | 30780 | Fo | Fo | 5.1 | 2.2 | 97 Tauri |
| 41..... | 31845 | F5 | F5 | 6.7 | 4.3 | 101 Tauri |
| 42..... | 33254 | A2 | A2p | 5.4 | 2.6 | 16 Orionis (3) |
| 43..... | 25102 | F2 | F5 | 6.4 | 4.2 | |
| 44..... | +19°641 | Go | G4 | 8.8 | 6.3 | |
| 45..... | 26015 | Fo | F4 | 6.0 | 3.4* | |
| 46..... | 26345 | F8 | F6 | 6.6 | 3.7 | |
| 47..... | 26737 | F2 | F5 | 7.0 | 3.6 | |
| 48..... | 26874 | Go | G4 | 8.1 | 5.1 | |
| 49..... | 27397 | Fo | F3 | 5.6 | 2.8 | 57 Tauri |

* Magnitude corrected for effect of secondary component.

TABLE 1—*Continued*

| Smart No. | HD | | Yerkes Sp. | $m_v$ | $M$ | Remarks |
|---|---|---|---|---|---|---|
| | No. | Sp. | | | | |
| 50..... | 27429 | Fo | F3: | 6.0 | 3.2 | |
| 51..... | 27524 | F8 | F6 | 6.9 | 3.9 | |
| 52..... | 27534 | F5 | F6 | 6.7 | 3.7 | |
| 53..... | 27561 | Fo | F5 | 6.7 | 4.0 | |
| 54..... | 27685 | G5 | G4 | 7.8 | 5.6 | |
| 55..... | 27731 | F5 | F6 | 7.2 | 4.0 | |
| 56..... | 27808 | F5 | F8 | 8.0 | 5.3 | |
| 57..... | 27859 | Go | G2 | 8.0 | 5.3 | |
| 58..... | 28034 | Go | Go | 7.4 | 4.8 | |
| 59..... | 28033 | F8 | F9 | 7.5 | 4.5 | |
| 60..... | 28363 | F8 | F9 | 7.0 | 4.2* | |
| 61..... | 28406 | F8 | F5 | 7.1 | 4.5 | |
| 62..... | 28483 | F5 | F5 | 7.2 | 4.1 | |
| 63..... | 28568 | F2 | F5 | 6.7 | 3.9 | |
| 64..... | 28736 | F2 | F5 | 6.4 | 3.9 | |
| 65..... | 28911 | F2 | F6 | 6.7 | 4.2 | |
| 66..... | 29225 | F8 | F6 | 6.7 | 4.0 | |
| 67..... | 30210 | Ao | A3p | 5.4 | 2.2 | (3) |
| 68..... | 30676 | F8 | F9 | 7.2 | 4.7 | |
| 69..... | 30810 | F5 | F8 | 7.8 | 5.5* | |
| 70..... | 30869 | F5 | F5 | 6.8 | 4.7* | |
| 71..... | 31236 | Fo | F2 | 6.2 | 3.0 | |
| 72..... | 32301 | A5 | A7 | 4.7 | 1.7 | $\iota$ Tauri |

NOTES TO TABLE 1

1. The spectrum is similar to that of the subgiant $\delta$ Eridani; the luminosity is, however, somewhat brighter, as judged from the *Sr* II lines.

2. The metallic arc lines are as in class F; the hydrogen lines are weak.

3. The metallic arc lines are as strong as in class F.

The stars are plotted in a Hertzsprung-Russell diagram in Figure 1. The dotted lines define the approximate limits of a normal main sequence as determined from the stars in the sun's neighborhood. It is seen that the stars, in general, lie within these limits with the exception of the four G–K giants and the single subgiant. We can, therefore, draw the conclusion that for the stars of types A5–Go there is no marked systematic departure from the random main-sequence stars.

There is one group which is, however, of interest. The six stars in Table 1 whose spectra are classified as peculiar appear to be systematically fainter than the main sequence. The spectra of these

objects are all similar in the characteristic that the metallic arc lines are considerably stronger than normal; they are of the same strength as in a normal F star. From the intensity of the metallic lines in the green and ultraviolet it seems likely that all lines originate in the atmosphere of a single star. They are of the same general type as the fourth-magnitude star 15 Ursae Majoris, whose Draper type is A3p.

If the A stars had been classified by the intensity of the metallic arc lines, these objects would be classed as F stars with unusually

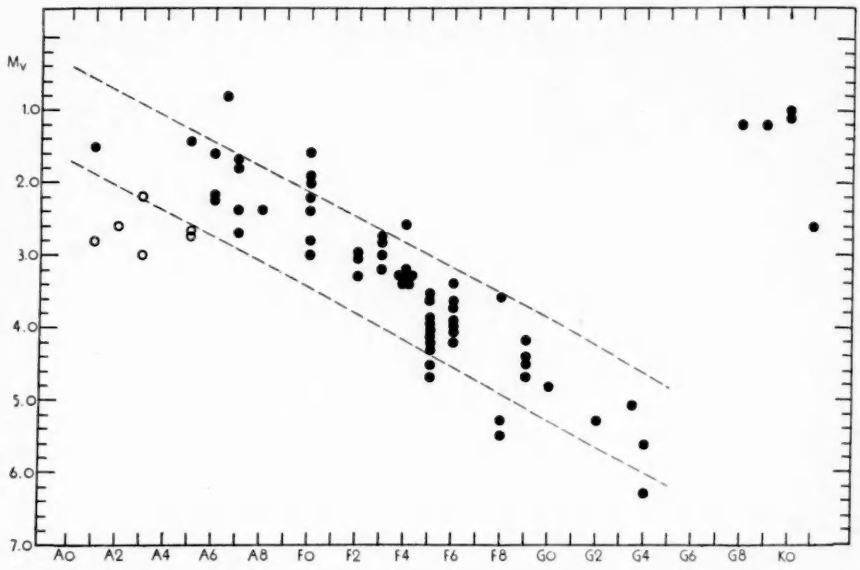


FIG. 1.—The spectrum-luminosity diagram for the members of the Hyades cluster

weak K lines; they would then not have been considered systematically different in luminosity from other F stars. We have preferred to consider them as A stars for the following reasons: (*a*) they are classified as A stars in the *Henry Draper Catalogue;* and (*b*) similar objects among the faint stars will be classified as A stars because of the necessity of observing them with such low dispersion that the faint metallic lines would not be visible. Thus, if the frequency of these objects in the Hyades is any criterion of their general frequency in space, they must have high weight in the determination of mean absolute magnitudes of the faint A stars. If, therefore, a luminosity function

of the A stars is determined from the near-by objects and transferred to more distant ones in various types of investigations, it is important to include these absolutely faint objects in the same spectral class for apparently bright and faint stars.

A superficial examination of other bright A stars with well-determined parallaxes indicates that such low-luminosity early A stars may be quite frequent. The two brightest members of this absolutely faint pseudo-composite class are $\alpha$ Geminorum B, which has a spectral type of about A1, as determined from the K line, and an absolute magnitude of about $+2.1$; and $\zeta$ Ursae Majoris B, which has a spectral type of about A2 and an absolute magnitude of about $+2.0$.

If the close correlation of intensity of metallic arc lines with luminosity is confirmed by further investigation, an accurate method of determining the absolute magnitudes and parallaxes of the A stars will be provided. The investigation is being extended to the other bright clusters and to the bright A stars in general.

*Note added in proof:* It appears that the star No. 4, HD 26162, is not a member of the Hyades. Moore's *Catalogue of Radial Velocities* gives $+24.0 \pm 0.5$ km/sec for the radial velocity, and a later plate taken at Victoria (*Pub. Dom. Ap. Obs.*, **6**, No. 10, 1934) gives $+22.0$. These differ by more than 10 km/sec from the computed value.

YERKES OBSERVATORY
March 31, 1940

# A SPECTROPHOTOMETRIC STUDY OF NOVA LACERTAE, 1936

DANIEL M. POPPER

ABSTRACT

Nova Lacertae, 1936, was observed with the quartz slitless spectrograph of the Lick Observatory between July 2 and November 21, 1936. Plates obtained on nine nights were chosen for reduction over the spectral region *Hα* to λ 3100. The intensities of various features were referred to the intensity in 1 A of the continuum of the star $\pi^1$ Cygni at the wave lengths of these features. The results were converted to relative intensities by applying an assumed intensity distribution in the spectrum of $\pi^1$ Cygni and by correcting for space absorption. The resulting intensities are shown for the background spectrum in Figure 2 and for the emission lines in Table 2. Figures 3 and 4 give the variations of emission-line intensities with time.

The results are discussed on the basis of the expanding envelope model of the nova. Brief comparisons are made with some results found in the literature for planetary nebulae and for other novae.

The spectrum of Nova Lacertae, 1936, and its changes have been described by Harper[1] and by Edwards and Barber.[2] The visual light-curve (Fig. 1) is from material supplied by Mr. L. Campbell, of the Harvard College Observatory. Changes in luminosity and in the spectrum were interrupted by very few of the irregularities observed in most novae.

The present investigation consists of a study of the intensities of emission lines and of the continuous spectrum during the period from July 3 to November 21, 1936. In this interval the nova decreased in brightness from fifth to ninth magnitude. In the first part of July the spectrum was undergoing a rapid transition from the "post-maximum" stage to the "nebular" stage. By the end of July the nebular-type spectrum was well developed.

Spectrograms of the nova were obtained on forty-four nights from July 1 to November 21. All exposures were made with the two-prism quartz slitless spectrograph[3] placed in the prime focus of the Crossley reflector of the Lick Observatory. This instrument gives spectrograms in excellent focus from *Hα* to λ 3600. The definition becomes poorer at shorter wave lengths, although the spectrograms are still

[1] *Pub. Dom. Ap. Obs., Victoria*, **6**, 317, 1937.

[2] *M.N.*, **98**, 42, 1937.

[3] W. H. Wright, *Lick Obs. Bull.*, **9**, 52, 1917.

usable at λ 3040. The emulsion used was Ilford Hypersensitive Panchromatic. The dispersion of the spectrograms is given.

| Wave Length | Dispersion | Wave Length | Dispersion |
|---|---|---|---|
| 6563 A..... | 401 A/mm | 4340 A..... | 119 A/mm |
| 5876..... | 298 | 3969..... | 89 |
| 5179..... | 204 | 3130..... | 38 |

On each night exposures were also taken of $\pi^1$ Cygni (magnitude 4.8, spectrum B3k). Beginning October 14, BD+51°3341 (magnitude 7.1, spectrum B2ek) was included on the observing program.

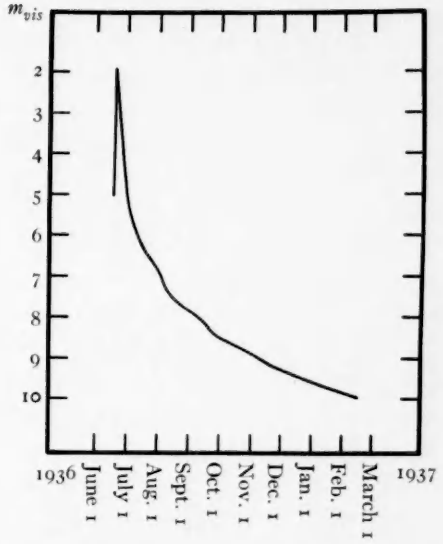


FIG. 1.—Visual light-curve of Nova Lacertae, 1936

These stars serve as spectrophotometric standards. All spectra were widened about 1/5 mm by trailing in right ascension. A coarse-wire grating, its dispersion crossed with that of the spectrograph, was placed over the telescope tube for most of the exposures. Two chief purposes are served by this arrangement: the usable range of intensity in a single exposure is increased, and images of sources of a known intensity ratio aid in the photometric calibration.

Spectrograms obtained on nine of the nights were chosen for reduction. The details of the observations are given in Table 1. The coarse-wire grating was used unless otherwise stated.

TABLE 1

| $m_{vis}$ | Date (U.T.) | Nova Lacertae | | Standard Star | | Remarks† |
|---|---|---|---|---|---|---|
| | | Exposure | sec $z$ | Exposure | sec $z$ | |
| | 1936 | | | | | |
| 5.4..... | July 3.5 | 4 runs* | 1.056 | 16 runs* | 1.032 | a |
| | | 16 | 1.055 | 32 | 1.032 | |
| | | 32 | 1.054 | 70 | 1.032 | |
| | | 80 | 1.053 | | | |
| 5.8..... | July 8.5 | 4 runs | 1.052 | 16 runs | 1.029 | a |
| | | 16 | 1.052 | 32 | 1.029 | |
| | | 32 | 1.052 | 60 | 1.030 | |
| | | 80 | 1.058 | | | |
| 6.3..... | July 16.5 | 8 runs | 1.076 | 16 runs | 1.032 | a |
| | | 32 | 1.064 | 32 | 1.031 | |
| | | 64 | 1.056 | 64 | 1.030 | |
| | | 128 | 1.053 | | | |
| 6.8..... | July 28.5 | 8 runs | 1.098 | 16 runs | 1.104 | a |
| | | 32 | 1.094 | 34 | 1.106 | |
| | | 64 | 1.085 | 64 | 1.124 | |
| | | 128 | 1.071 | | | |
| | | 40 min. | 1.125 | | | |
| 7.1..... | Aug. 5.4 | 16 runs | 1.057 | 16 runs | 1.055 | a |
| | | 64 | 1.071 | 32 | 1.057 | |
| | | 128 | 1.063 | | | |
| 7.7..... | Aug. 26.3 | 4 min. | 1.115 | 4 min. | 1.119 | a, e |
| | | 30 | 1.092 | 30 | 1.092 | d |
| | | 60 | 1.055 | | | c |
| 8.1..... | Sept. 11.2 | 8.9 min. | 1.029 | 3.4 min. | 1.054 | a |
| | | 50 | 1.052 | 45 | 1.036 | d |
| | | 59 | 1.170 | | | c |
| 8.7..... | Oct. 15.2 | 45 min. | 1.149 | 28 min. | 1.058 | b |
| | | 75 | 1.054 | | | c |
| 9.2..... | Nov. 21.2 | 120 min. | 1.460 | 35 min. | 1.190 | b |
| | | 129 | 1.066 | | | c, f |

*"Runs" indicates number of times trailed with slow-motion motor.

† (a) Standard star for night was $\pi^1$ Cygni.
(b) Standard star for night was BD+51°3341.
(c) Grating was not used for nova exposure.
(d) $\pi^1$ Cygni exposed for third-order image.
(e) This is the only one of the nights on which transparency was poor. Differences in sec $z$ are small.
(f) Nova exposure somewhat fogged by scattered moonlight.

## REDUCTIONS

The data obtained directly from the observations are total intensities in the emission lines and intensity per angstrom in the background spectrum of the nova, both relative to the intensity in 1 A of the continuum of the standard star at the same wave lengths. With an assumption as to the energy distribution in the spectrum of the standard star, we can determine relative intensities in the nova spectrum; with one as to the non-variability of intensities in the spectrum of the standard star, we can obtain variations of nova intensities with time.

The characteristic curves of the photographic emulsion, used in the reduction of the spectrograms, were obtained on five excellent nights by means of stellar spectra calibrated with a series of diaphragms placed over the aperture of the telescope. The relation between density and the logarithm of intensity for the emulsion, at least in the low-density region used, was found to vary considerably with exposure time as well as with wave length. Mean curves were drawn for five wave-length regions and for six ranges in exposure time. The applicability of these mean curves to the spectrograms obtained on a given night was checked by means of spectra obtained with the coarse-wire grating. The logarithm of the intensity ratio of zero to first-order grating images, used in this check, was found to be 0.379 from spectra which were calibrated by means of the diaphragms. There were no significant variations of this quantity with wave length.

When the exposure times of nova spectrum and standard star spectrum differ (see Table 1), reciprocity-law failure must be applied in order to obtain relative intensities. A mean value of the Schwarzschild exponent was obtained from exposures made at the telescope. The use of a Schwarzschild exponent is, at best, an approximate procedure, but the ratios of exposure times were not large. In the cases of the larger ratios, it was usually possible to avoid direct use of the exponent by comparing intensities of several features measurable on two nova spectrograms taken during the same night.

It frequently happens that the exposure best suited for determining the intensity of an emission line is not strong enough to show the underlying background spectrum. In such a case the total apparent

intensity of the line is, in reality, the sum of the line intensity and the intensity of the background, integrated over the width of the line. This second term, which must be subtracted from the sum, is determined from stronger exposures made during the same night.

Corrections for differential atmospheric extinction were made in the usual way. The extinction factors were determined and, after correction for the air mass above Mount Hamilton, were found to agree satisfactorily with Fowle's values,[4] in so far as variations with wave length are concerned. For wave lengths shorter than 3600 A the observed values agreed well with an extrapolation of Fowle's data on a $\lambda^{-4}$ relation, the corrections for ozone absorption having been included for the shortest wave lengths. The zenith extinction at $\lambda$ 4500 is 0.31 mag., which may be compared with the value 0.32 mag. found by Fath[5] with a photoelectric cell for a $B_3$ star on a "good" night.

In the preceding paragraphs we have discussed the procedure involved in obtaining the fundamental observational quantities, namely, the intensities in the spectrum of the nova at various wave lengths relative to those in the spectrum of the standard star at the same wave lengths. The uncertainty of these quantities for the emission lines should be of the order of 0.1 in the logarithm, or about 25 per cent, though in favorable cases and for the continuum the second decimal possibly has significance. The greatest single cause of inaccuracy in the case of the emission lines probably lies in the difficulty of separating the lines on the microphotometer tracings from the background spectrum and from neighboring emission lines. The lines in the spectrum of Nova Lacertae were very broad.

In order to obtain relative intensities of features in the nova spectrum on any date, the intensity distribution in the continuous spectrum of the standard star must be known. No reliable determinations of intensity distribution in the spectra of stars are available; hence assumptions must be made. As a guide for our assumptions, the standard star, $\pi^1$ Cygni, was compared spectrophotometrically with $\epsilon$ Persei. The star $\epsilon$ Persei has been included on the observing programs of nearly all investigators of spectral-energy distribution,

[4] *Smithsonian Physical Tables*, 1933.

[5] *Lick Obs. Bull.*, **17**, 121, 1934.

with varying results. The following parameters were adopted for the intensity distribution in the spectrum of $\epsilon$ Persei:

| | |
|---|---|
| $\lambda\lambda$ 6600–3700..... | Black body at 18,000° K |
| $\lambda\lambda$ 3700–3100..... | Black body at 25,000° K |

As a result of the comparisons, I have assumed for $\pi^1$ Cygni

| | |
|---|---|
| $\lambda\lambda$ 6600–3700..... | Black body at 16,500° K |
| $\lambda\lambda$ 3700–3100..... | Black body at 20,000° K |

$$D = 0.19$$

where $D$ is the logarithmic decrease in intensity at the limit of the Balmer series. This quantity is to be considered more an observed than an assumed quantity. Changes of two or three thousand degrees in the temperatures used would not lead to significant corrections of the results.

The star $\pi^1$ Cygni was tested for variability by means of observations with photoelectric photometers at Mount Hamilton by Fath and by Kron, whose co-operation is gratefully acknowledged. The results obtained justify the use of $\pi^1$ Cygni as a standard of constant energy.

On the last two nights for which spectrograms were reduced, the fainter star, $+51°3341$, was used as standard. Its spectral-energy distribution was found from numerous comparisons with $\pi^1$ Cygni. This choice of star was an unfortunate one, as it was found by Kron in the fall of 1937 to be variable over a range greater than 0.2 mag. The relative energies in the spectra of $+51°3341$ and $\pi^1$ Cygni at the wave length effective for the photoelectric cell is assumed to be the mean of the values found by Kron on five nights. The evidence for or against variation in the spectral-energy distribution of the fainter star is inconclusive.

It is desirable to free the results of the observations from the effects of interstellar absorption as far as is possible. According to Greenstein,[6] the $\lambda^{-1}$ law of absorption is indicated by recent work. The results of Baade and Minkowski[7] for regions in Orion and Perseus show serious departures from this law for longer wave lengths,

[6] Greenstein, *Ap. J.*, **87**, 151, 1938; Stebbins, Huffer, and Whitford, *Ap. J.*, **90**, 209, 1939.

[7] *Ap. J.*, **86**, 159, 1937.

but not for those in which we are interested, except possibly around *Hα*. The extension of this law to the short wave-length limit of our work, however, must be considered an extrapolation.

Greenstein reports that a small amount of dark nebulosity, extending from the north, covers the field of the nova, the logarithmic decrement, from star counts, being 0.15, with an uncertainty of less than 0.04. He also reports that star counts by J. W. Evans indicate a general photographic absorption in the southern Cepheus region, in which the nova is located, of 0.25 mag. per kiloparsec. Determinations at Mount Wilson[8] and at Victoria[9] from the intensities of interstellar lines set the distance of the nova at about 850 parsecs. Hence, we may take the general absorption as 0.08 in the logarithm, and the total photographic dimming as $0.08+0.15=0.23$, with an uncertainty of about 0.06. Then the correction to be applied to reduce the nova intensities, $I$, to transparent space is

$$\Delta \log I = +0.23 \frac{4400}{\lambda},$$

where 4400 A is the photographic effective wave length as used by Greenstein. The writer is indebted to Dr. Greenstein for this information.

With a visual magnitude at maximum light of 1.9 mag., as reported by several observers, a distance of 850 parsecs, and a visual obscuration by absorbing material of 0.5 mag., the absolute visual magnitude of the nova at maximum appears to have been about $-8.3$.

The results of the reductions are given for the background spectrum in Figure 2 and for some of the emission lines in Table 2. In both cases the more uncertain values are indicated by parentheses. The unit of intensity is that contained in 1 A of the continuum of $\pi^1$ Cygni at λ 5000. Uncertainties in the law of interstellar absorption, as well as in the assumed energy distribution of $\pi^1$ Cygni, affect directly the relative intensities for a given date but not their variations with time.

[8] Merrill and Wilson, *Pub. A.S.P.*, **48**, 230, 1936.

[9] Pearce, *Pub. A.S.P.*, **49**, 148, 1937.

Reductions were carried out for most of the emission lines which were comparatively unblended or for which the relative contributions of blending components could be obtained with fair accuracy. Exceptions are listed in the footnotes to Table 2. The points plotted for the background spectrum in Figure 2 are not necessarily in the continuous spectrum of the nova, though they were chosen as carefully as possible from that standpoint. Their choice for wave lengths greater than 3900 A was guided by an examination of the slit spectrograms available at the Lick Observatory.

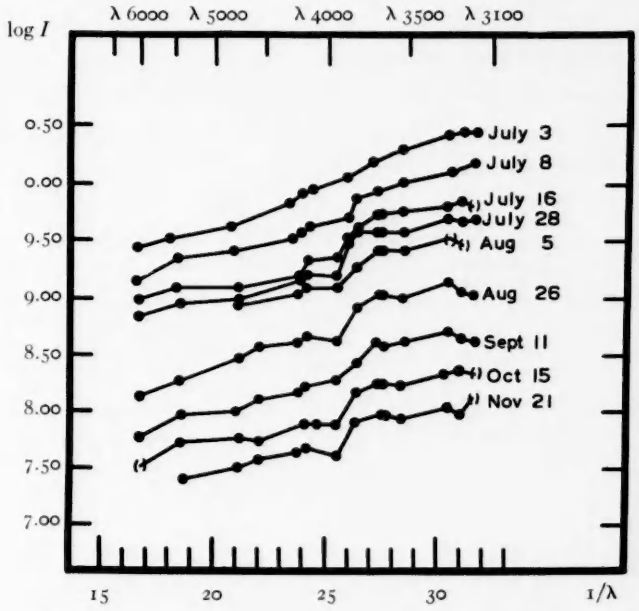


FIG. 2.—Logarithm of intensity per angstrom in the background spectrum of Nova Lacertae, corrected for interstellar absorption. Log intensity equals 0 for 1 A of the continuum of $\pi^1$ Cygni at λ 5000.

The results in Figure 2 and Table 2 may be reduced approximately to intensities received at the sun in ergs per square centimeter per second and less accurately to total energies emitted by the star in ergs per second, if we know the value of the unit of intensity. From the data given by Pettit and Nicholson[10] for the total energies re-

[10] *Ap. J.*, **58**, 279, 1928.

TABLE 2

LOGARITHMS OF TOTAL ENERGY IN EMISSION LINES CORRECTED FOR INTERSTELLAR ABSORPTION*

(Unit: The Energy in 1 A of the Continuum of $\pi^1$ Cygni at λ 5000)

| Line | July 3 | July 8 | July 16 | July 28 | Aug. 5 | Aug. 26 | Sept. 11 | Oct. 15 | Nov. 21 |
|---|---|---|---|---|---|---|---|---|---|
| λ 6563 *Hα* | 2.78 | 2.71 | 2.53 | 2.32 | 2.15 | 1.70 | 1.31 | 1.01 | 0.78 |
| 6300 [*O* I] | 0.87 | 0.92 | (0.50) | (0.41) | (0.36) | (0.21) | (9.84) | 9.36 | 9.34 |
| 5893 *Na* I | 0.97 | (0.64) | ..... | ..... | ..... | ..... | ..... | ..... | ..... |
| 5876 *He* I | ..... | ..... | 1.18 | 0.94 | 0.77 | 0.32 | 0.02 | 9.40 | 9.18 |
| 5755 [*N* II] | ..... | 1.28 | 1.24 | 0.97 | 0.89 | 0.86 | 0.70 | 0.56 | 0.30 |
| 5680 *N* II multiplet | ..... | 0.73 | 0.91 | 0.87 | 0.61 | 0.32 | (9.95) | (9.38) | (9.24) |
| 5577 [*O* I] | 0.87 | 0.36 | ..... | ..... | ..... | ..... | ..... | ..... | ..... |
| 5018 *Fe* II | 1.52 | 1.07 | ..... | ..... | ..... | ..... | ..... | ..... | ..... |
| 5007 4959 [*O* III] | ..... | ..... | 1.48 | 1.67 | 1.59 | 1.52 | 1.48 | 1.41 | 1.26 |
| 4861 *Hβ* | 1.97 | 2.02 | 1.70 | 1.59 | 1.39 | 1.02 | 0.73 | 0.36 | 0.01 |
| 4686 *He* II | ..... | ..... | (1.10) | (0.88) | (0.81) | (0.52) | (0.20) | (9.77) | (9.51) |
| 4640 *N* III *et al.* | 1.76 | 1.78 | 1.42 | 1.54 | 1.46 | 0.97 | 0.66 | 0.12 | 9.88 |
| 4363 [*O* III] | ..... | ..... | (1.01) | (1.14) | 1.14 | 1.13 | 1.09 | 0.68 | 0.30 |
| 4340 *Hγ* | 1.68 | 1.69 | 1.41 | 1.29 | 1.19 | (0.72) | (0.32) | (9.97) | (9.42) |
| 4101 *Hδ*, *N* III | 1.74 | 1.64 | 1.39 | 1.45 | 1.26 | 0.89 | 0.62 | 0.05 | 9.60 |
| 3970 *He*, [*Ne* III] | 1.40 | 1.29 | 1.01 | 0.88 | 0.80 | 0.43 | 0.09 | 9.72 | 9.45 |
| 3590 [*Fe* VII] | ..... | ..... | ..... | ..... | ..... | ..... | ..... | 9.02 | 8.88 |
| 3432 [*Ne* V], *O* III | ..... | ..... | ..... | 1.03 | 0.88 | 0.82 | 0.47 | 0.10 | 9.85 |
| 3335 [*Ne* III], [*Ne* V], *O* III | ..... | ..... | ..... | ..... | ..... | 0.08 | 9.83 | 9.42 | 9.17 |
| 3270 *O* III | ..... | ..... | ..... | ..... | ..... | 9.95 | 9.62 | 9.12 | ..... |
| 3203 *He* II | ..... | ..... | ..... | 0.78 | ..... | 0.21 | 9.90 | (9.17) | (8.84) |
| 3125 *O* III | ..... | ..... | ..... | 1.30 | ..... | 0.94 | 0.55 | 0.03 | 9.48 |

* Values in parentheses are considered somewhat less reliable than the remaining values.

Notes on blends:

λ 6563 Undoubtedly blended with λ 6548 and λ 6584 of [*N* II], particularly on the later dates. Effects of blending unimportant. See p. 280.

6300 Seriously blended with λ 6364. That the latter line is not due to [*O* I] exclusively is indicated by the great variations in the relative intensities of the two lines. The probable contributor to λ 6364 is *N* II.

5876+5893 Probably *Na* I exclusively on July 3 and 8. *He* I much stronger by July 16. *Na* I absent by July 28.

5018 Probably contributes slightly to λ 5007 on July 16.

4640 The contributions due to the various elements undoubtedly vary considerably. The whole blend from about λ 4610 to λ 4660 is included.

4363+4340 The intensity of the sum is measured. The relative contributions of the two components from July 16 onward were calculated from measures of those parts of the separate lines visible, λ 4340 being the sole contributor before that date. Slit spectrograms were used for this purpose on July 16 and 28.

4101 This line includes the important *N* III pair at λ 4097 and λ 4103. No means of separating the elements directly from the observations is envisaged. *N* III probably becomes important beginning July 16 or 28.

3970 The remarks on the preceding line hold with respect to the *H* and [*Ne* III] contributions.

ceived outside the atmosphere from six $B_3$ stars, the energy flux from a star of the visual magnitude of $\pi^1$ Cygni, 4.78 mag., and this spectral type should be $1.65 \times 10^{-12}$ cal $cm^{-2}$ $min^{-1}$. Then, from the laws of Stefan and Planck for perfect radiators and a temperature of 16,500° we find the intensity in 1 A at 5000 A to be $7.8 \times 10^{-11}$ erg $cm^{-2}$ $sec^{-1}$, which is the unit of intensity. Thus, 10.11 should presumably be subtracted from the values of Table 2 and of Figure 2 to reduce them to logarithms of intensities received at the sun if space were transparent. Using a distance of the nova of 850 parsecs, we find the quantity to be added to the values of Table 2 and of Figure 2 to obtain logarithms of energies emitted in ergs per second by the nova in the spectral features under consideration to be 30.9.

## DISCUSSION

In this discussion the point of view is taken that the emission lines are produced in a rarefied envelope surrounding a central star or nucleus. It is further assumed that radiation from this nucleus is the agent exciting the atoms of the envelope to emission and also that it is the source of the observed continuous spectrum for wave lengths greater than 3700 A.

### 1. THE CONTINUOUS SPECTRUM

The reduced intensities in the background spectrum are shown in Figure 2, plotted as logarithm of intensity $\equiv \log I$ against $1/\lambda$. It is not claimed that all of the plotted points lie on the true continuous spectrum of the star, and hence they are not suitable for a statistical treatment.

Beginning July 16, or possibly July 8, there is observed a pronounced strengthening of the spectrum on the violet side of $\lambda$ 3700,[11] which is near the Balmer series limit. July 16 is, however, the first of the dates on which we could expect to detect this emission with certainty, even if it were present earlier. In the first place, on the earlier dates the ultraviolet spectrum is so dominated by metallic emissions and absorptions that the intensities measured are considered unreliable indications of the continuum. But by July 16 the metallic lines are weak; and from this date on, the ultraviolet points

[11] The continuous absorption in this region of the spectrum of $\pi^1$ Cygni has, of course, been taken into account in the reductions.

measured are more likely to be in the true continuum than any other series of points. In the second place, and probably more important, the strengthening is best indicated with respect to the point at 3930 A. This point becomes available only after the disappearance, by July 16, of K emission and $H + H\epsilon$ absorption. If the continuum in this region could be observed on the earlier dates, it is possible that a strengthening at λ 3700 would be apparent.

The course of the continuous spectrum on the red side of λ 3700 is uncertain. In drawing its slope, the weights given the individual points shown in the plots depend on their behavior from night to night and on the appearance of the slit spectrograms. The point at λ 3930 was usually given high weight. No significant change in intensity distribution over the period of observation is indicated. This result is at a variance with that of Petrie.[12] The average slope, relative to that of $\pi^1$ Cygni, leads to a color temperature of $1.43 \times 10^4$ degrees K, with values falling between 1.37 and $1.54 \times 10^4$. Just what may be the physical significance of this quantity is not clear. Theories[13] relating to the production of a spectrum of the nebular type indicate that much more radiation is required from the exciting source in the far ultraviolet region, beyond the head of the Lyman series of hydrogen, than is emitted by a black body at 14,000°. If we grant that the observed continuum redward of 3700 A originates in the same exciting source, radical departures from black-body distribution are indicated. This has been pointed out by other observers of energy distribution in the spectra of novae.

If we could take the approximate constancy of the nova's color temperature as an indication of constancy of distribution of energy throughout the spectrum of the exciting star, changes in the radius of the star's photosphere could be computed directly from the fading of this spectrum. Such a computation, based on the decrease in intensity at λ 3930, yields a decrease in the radius by a factor of 7.5 between July 16 and November 21. Calculation of the actual values of the radius is dependent on the assumption of at least approximately black-body distribution of intensity, and hence it is felt that a statement of the results would be misleading.

[12] *Pub. Dom. Ap. Obs., Victoria*, **6**, 338, 1937.

[13] E.g., Zanstra, *Ap. J.*, **65**, 63, 1927; Bowen, *Ap. J.*, **81**, 1, 1935.

The intensity and course of the continuous spectrum in the ultraviolet region, which contains the continuous Balmer emission, is probably best shown by averaging the observed values of log $I$ in two groups of three points each, centered at wave lengths 3600 A and 3230 A. The relative intensities $I_{3930} : I_{3600} : I_{3230}$ undergo very little change, the average and nearly constant values being

$$\log \frac{I_{3600}}{I_{3930}} = 0.38 \text{ and } \log \frac{I_{3230}}{I_{3930}} = 0.46 .$$

It is a curious fact that the value of $\log I_{3230}/I_{3600} = 0.08$ corresponds to a black-body temperature of $1.38 \times 10^4$ degrees, very near the color temperature found for the longer wave-length region. In fact, extrapolation of the continuum through $\lambda$ 3930 to $\lambda$ 3600 and $\lambda$ 3230 shows $I_\lambda/C_\lambda = 2.0$ at both wave lengths, where $C_\lambda$ is the extrapolated intensity; i.e., the ultraviolet continuum is twice as strong as that obtained by an extrapolation of the intensity distribution at longer wave lengths.

There is little doubt that the ultraviolet continuum consists of the sum of the radiations from the stellar nucleus and from continuous emission at the head of the Balmer series in the envelope. Given the distribution of intensity in one source, the distribution in the other can be deduced from the observations. As pointed out by Page,[14] however, the stellar radiation may suffer considerable continuous absorption in the same region. The distribution of intensity in the continuous emission at the head of the Balmer series, if due to electron captures by hydrogen, as seems most likely, depends on the electron temperature. For any probable value of this parameter (see below), the intensity of the emission should decrease fairly rapidly with decreasing wave length. To account for the observed distribution, then, we must postulate that the stellar intensity rises considerably more rapidly through the ultraviolet region observed here than in the case of a black body at 14,000°.

### 2. THE EMISSION LINES

In order to show variations with time, the logarithms of the reduced intensities of the emission lines, $E$, are plotted in Figures 3

[14] *M.N.*, **96**, 604, 1937.

and 4, in which the abscissae are the logarithms of ($t^{days}$ − June 20). June 20 was the date of maximum light. The first, Figure 3, shows the values of log $E$; the second, Figure 4, the values of log $E/C$, where $C$ is a mean intensity of the continuous spectrum. All the prominent lines of the later stages of the nova's development in the wave-length region of observation are shown, with the exception of the very broad blends due to *He* I, *H*, and [*Ne* III] near λ 3880 and to [*O* II], *H*, and *O* III near λ 3750. Plots for several of the weaker lines also are given.

Study of the plotted results leads to the following conclusions and inferences.

*a*) Metallic lines and λ 5577 of [*O* I] disappear rapidly during the transition period of the first part of July, while the observable permitted lines of higher excitation strengthen. Evidently conditions become more favorable, during this transition period, for the production of lines of higher excitation and ionization energies. The fact that after July 16 or 28, however, differences in behavior due to differences in the stage of ionization are secondary, may be regarded as evidence that, after the transition period, departures from a steady state are not great. More specifically, the number of ionizations of an element in unit time does not differ greatly from the number of recombinations.

*b*) Permitted lines keep approximately constant intensities relative to the continuum from the latter part of July until September or later. Nova Lacertae is not typical among novae with respect to variations of $E/C$. Some novae show marked fluctuations of these ratios, which are closely correlated with fluctuations in light. The light-curve of Nova Lacertae shows almost no such irregularities.

The constancy of $E/C$ with time is puzzling. Consider the case of hydrogen, for example. Let it be assumed that the predominant agency for Balmer emission lines is the recombination of hydrogen ions with electrons, and that the observed continuous spectrum, $C$, has its source, at least for the most part, in the radiation of the central star. It can then be shown by relatively simple arguments that $E$ is not determined directly by $C$, and in particular that $E$ should be expected to decrease more rapidly than $C$; and that the observed constancy of their ratio implies either a fortuitous relation connecting the radiation of the star with conditions in the (expanding) nebu-

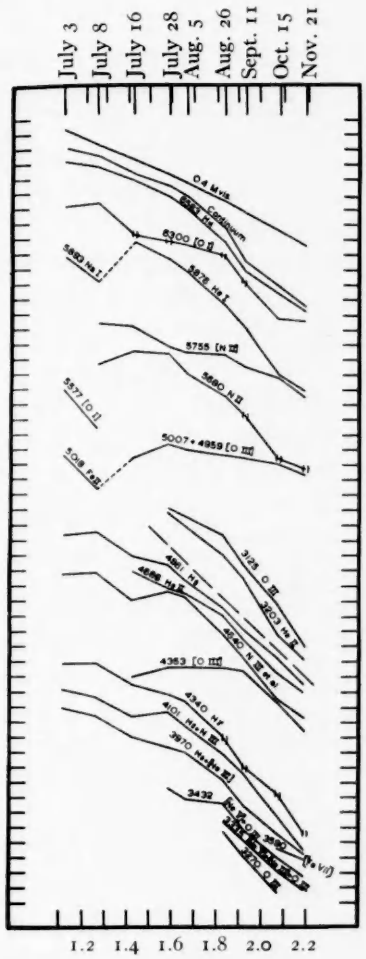


FIG. 3

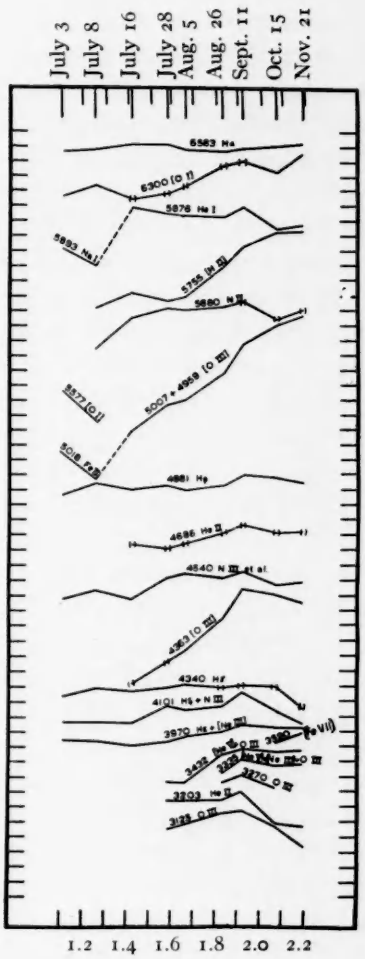


FIG. 4

FIG. 3.—Logarithm of total intensities of emission lines. Scale of ordinates: one division equals 0.2 in log intensity. Zero points of ordinates of different curves are arbitrarily adjusted.

FIG. 4.—Logarithm of total intensities of emission lines relative to the continuous spectrum. Ordinates as in Fig. 3.

la or some causal relationship of an obscure nature. Neither of these alternatives is very satisfactory. It is conceivable that a continuous ejection of matter from the nucleus at the proper rate could be instrumental in maintaining the observed relations.

*c*) Forbidden lines rise rapidly with respect to the background till the first of September or later. Increases in absolute intensity of the forbidden lines are either very slight or unobservable.

Many of the emission lines show a pronounced rise on September 11 relative to the continuum, and it is seen from the absolute plots that this is a case of an unusually rapid drop in the continuum rather than of a slower decrease of the lines. A careful examination of the reductions leads the writer to believe that the effect is real.

Due caution must be exercised in attempting to draw conclusions concerning physical conditions in the expanding envelope from the behavior and relative intensities of the emission lines. Three difficulties may be mentioned. First, it is evident that conditions vary greatly in different parts of the envelope. For example, the [*O* I] nebular lines are fairly strong at the same time that the [*O* III] lines are very prominent. Second, changes in intensity may be caused by gain or loss of matter in the envelope. Third, it is not always a straightforward matter to predict what effect changes in physical conditions may have on the intensity of a line. The discussion by Menzel[15] and by Bowen and Minkowski,[16] for example, points out that it is possible to draw various conclusions concerning the effect of electron pressure on the intensity of a forbidden line by oversimplifying the physical picture in various ways.

Whatever conclusions are drawn from the intensities of the lines must refer to a set of conditions averaged over the regions of the envelope in which the lines under consideration are produced.

*Hydrogen.*—In the accompanying table are given the intensities relative to those of $H\beta$ of the hydrogen lines believed to be unblended, or, in the case of $H\gamma$, freed of serious blends. The values for $H\alpha$ are included, since in the discussion of [*N* II] below it is concluded that the intensities of the nebular pair at λ 6548 and λ 6584 are very small with respect to the intensity of $H\alpha$. Also shown in the table are the relative intensities predicted[17] on the assumption

[15] *Nature*, **142**, 644, 1938.

[16] *Nature*, **142**, 1079, 1938.

[17] Baker and Menzel, *Ap. J.*, **88**, 52, 1938.

that the upper levels are populated as a result of electron captures and subsequent downward transitions. The effects of population by absorption of Lyman line emission are also taken into account. These values are for an electron temperature of 10,000° K. They are not very sensitive to changes in $T_e$. Values in the columns head-

LOGARITHMS OF RELATIVE INTENSITIES IN THE BALMER SERIES

| | *Hα* | | *Hβ* | *Hγ* | | *Hδ* | | *Hε* | |
|---|---|---|---|---|---|---|---|---|---|
| | Lick | V | | Lick | V | Lick | V | Lick | V |
| July 3 | 0.81 | 0.21 | 0.00 | 9.71 | 9.44 | 9.77 | 9.50 | blend | 9.41 |
| July 8 | .69 | ..... | .00 | 9.67 | 9.91 | 9.62 | 9.82 | 9.27 | 9.45 |
| July 16 | .83 | ..... | .00 | 9.71 | 9.83 | blend | 9.83 | 9.31 | 9.52 |
| July 28 | .73 | ..... | .00 | 9.70 | 9.86 | blend | 9.76 | 9.29 | 9.40 |
| Aug. 5 | .76 | ..... | .00 | 9.80 | 9.96 | blend | 9.70 | blend | 9.31 |
| Aug. 26 | .68 | ..... | .00 | (9.70) | ..... | blend | ..... | blend | ..... |
| Sept. 11 | .58 | ..... | .00 | (9.59) | ..... | blend | ..... | blend | ..... |
| Oct. 15 | .65 | ..... | .00 | (9.61) | ..... | blend | ..... | blend | ..... |
| Nov. 21 | .77 | ..... | .00 | (9.41) | ..... | blend | ..... | blend | ..... |
| Theoretical | 0.40 | ..... | 0.00 | 9.71 | ..... | 9.49 | ..... | 9.31 | ..... |

ed "V" are from McKellar's paper.[18] In each case the Victoria spectrograms were exposed within one or two days of those at Lick.

No definite trends with time are shown by the Lick observations. All fluctuations, with the possible exceptions of the value for *Hα* on September 11 and for *Hγ* on November 21, are within observational uncertainty. The observed relative intensities of *Hβ*, *Hγ*, and *Hε* are in good agreement with those predicted. Against this agreement of observation and theory may be set the results for *Hα* and *Hδ*. The large *Hα*/*Hβ* ratio is in the direction found in various objects. Self-reversal has been advanced[19] as an explanation of this phenomenon. The strength of *Hδ* on the earliest dates is puzzling. Its behavior later on is compatible with the assumption that blending with *N* III radiations is involved.

The electron-capture theory[20] predicts the way in which the number of electron captures per second by protons is distributed among the different energy levels of the hydrogen atom as a function of the velocity distribution (or temperature) of the electrons. The theory

[18] *Pub. Dom. Ap. Obs., Victoria*, **6**, 347, 1937.

[19] E.g., Woolley, *M.N.*, **96**, 514, 1936. [20] Cillié, *M.N.*, **92**, 820, 1932; **96**, 771, 1936.

yields, in addition to the method of the Balmer gradient, two methods of computing the electron temperature from observed intensities. The assumption is made that the velocity distribution is Maxwellian. In both of these methods the intensities involved are more sensitive to differences of electron temperature than is the Balmer gradient. The first of the methods uses the intensity of a Balmer line relative to the intensity per unit wave length of continuous emission at the head of the Balmer series. The second method is based upon the distribution of energy in the continuous emission.

For the first method, the intensity of $H\beta$ and of the continuous emission at λ 3600 is used; for the second, the slope of the emission in a region about 140 A in extent centered at λ 3600, which is free from emission and absorption features from about July 12 till the middle of September. In the application of both methods, correction is made for the underlying stellar continuum by extrapolating a black-body distribution for $1.43 \times 10^4$ degrees through the continuum at λ 3930. Although the justification of this procedure is admittedly dubious, it is to be noted that the results obtained by the two methods are affected by it in entirely different manners. The values cannot be obtained for July 3, while those for July 8 are of very low weight. It should be mentioned again that the relative intensities of emission at λ 3600 and λ 3200 lead to nearly infinite electron temperatures. The values of the electron temperature found by the two methods are herewith listed.

$T_e \times 10^{-3}$

| | Method 1* | Method 2† | | Method 1* | Method 2† |
|---|---|---|---|---|---|
| July 8..... | (10.3) | (14.2) | Aug. 26..... | 11.2 | 4.9 |
| July 16..... | 9.9 | 11.1 | Sept. 11..... | 19.0 | 4.7 |
| July 28..... | 11.2 | 10.6 | Oct. 15..... | 18.7 | 6.9 |
| Aug. 5..... | 9.8 | 8.6 | Nov. 21..... | 13.4 | 11.3 |

* Method 1: Ratio of $H\beta$ to Balmer continuum.
† Method 2: Slope of Balmer continuum at λ 3600.

The trend shown by the latter set of values is reversed in the former set. These reductions indicate that the electron temperature was around 11,000° during the period of observation. Values that

may be more reliable are found in the discussion of [*O* III]. It is of interest to compare the foregoing results with those found from measures of the Balmer continuum in other objects.[21] For the solar chromosphere at the 1932 eclipse Menzel and Cillié find $T_e \approx$ 10,000°, using Method 2. They find the same value from Method 1 if $H\gamma$, $H\delta$, etc., are used, but much higher values if $H\beta$ is used. Page's observations for two planetary nebulae give values near $T_e =$ 2000° from Method 2 but give extremely high values from Method 1.

*Forbidden lines.*—Under the conditions prevailing in the "nebular" stage of a nova's development, electron collisions are considered[13] to be the agency principally responsible for the excitation of the low-lying metastable levels from which the forbidden lines arise. If changes in electron temperature are not large, then changes in the relative intensities of two forbidden lines of the same atom must be due to changes in electron pressure. The way in which pressure affects the relative intensities is well known.[22] During the period over which the relative intensities of the nebular and auroral lines of an atom remain constant, it is tempting to conclude that the electron pressure is so high that electron collisions predominate over radiation in depopulating the metastable states, and their relative population depends only upon the electron temperature according to Boltzmann's formula.[23] As the pressure decreases, so that this is no longer the case, the intensity of the auroral line will decrease relative to that of the nebular lines of the same atom. For [*O* III] the relative intensities of nebular ($\lambda$ 4959 and $\lambda$ 5007) and auroral ($\lambda$ 4363) lines remained about constant till around September 11. Assuming that Boltzmann's formula is applicable in this case, we can calculate the electron temperature in the relevant parts of the envelope. The required data are the observed relative intensities and the relative transition probabilities[24] of the lines. The results are:

| | $T_e \times 10^{-3}$ | | |
|---|---|---|---|
| July 16..... | 8.3 | Aug. 26..... | 8.7 |
| July 28..... | 8.0 | Sept. 11 ..... | 8.6 |
| Aug. 5..... | 8.4 | | |

[21] Quoted by Cillié, *M.N.*, **96**, 771, 1936.

[22] E.g., Menzel and Payne, *Proc. Nat. Acad. Sci.*, **19**, 641, 1933.

[23] K. Wurm, *Zs. f. Ap.*, **14**, 321, 1937. [24] S. Pasternack, *Pub. A.S.P.*, **51**, 160, 1939.

If the procedure described is a valid one, the value of 8500° for the electron temperature is a more reliable one than the value of 11,000° derived from hydrogen.

It is desirable to compute the combined intensity of the nebular pair of [*N* II], λ 6548, and λ 6584, to determine its probable effect on the intensities of *Hα*. This can be readily accomplished by use of the intensity of λ 5755, the transition probabilities, and an electron temperature of 8500°, if a Boltzmann distribution of atoms is assumed for the metastable levels in this case also. The computed effect of the [*N* II] lines is never more than 0.02 in the logarithm, so that our neglect of it appears to be justified.

*Comparison with planetary nebulae.*—Aside from obvious differences due to the expansion velocity, conditions in the envelope surrounding a nova in the later stages of its development are usually considered to become similar to those in the planetary nebulae. Dr. Swings points out that the chief differences in the appearances of the spectra of the two kinds of objects are due to the presence of lines of atoms of higher atomic weight in the case of the novae. It is of interest to compare some of the results of this study with intensities obtained for the planetary nebulae. The latter are taken from the papers of Plaskett,[25] Berman,[26] and Page.[14] The accompanying table gives the largest and smallest values observed by them for the logarithms of various ratios. Intensities were chosen for a restricted wave-length region to minimize effects of reduction methods.

COMPARISON WITH PLANETARY-NEBULAE LOGARITHMS OF RELATIVE INTENSITIES

| | Planetary Nebulae | | Nova Lacertae |
|---|---|---|---|
| | Largest Measured | Smallest Measured | |
| 1. *He* II 4686/*Hβ* | 9.8 | 9.1 | 9.4; remains about constant |
| 2. [*O* III] 5007+4959/*Hβ* | 1.3 | 0.7 | 0.1 to 1.2, increasing steadily |
| 3. [*O* III] 5007+4959/[*O* III] 4363 | 2.3 | 1.7 | 0.4 till Sept. 11; increases to 1.0 |

[25] *Pub. Dom. Ap. Obs., Victoria*, **4**, 187, 1928.

[26] *Lick Obs. Bull.*, **15**, 86, 1930.

If we assume absorption of ultraviolet stellar radiation followed by recombinations to be responsible for the permitted lines, we may conclude from item 1 of the table that the distribution of energy emitted by the nuclear star of the nova in the far ultraviolet is not greatly different from that emitted by the nuclear star of an average planetary, provided the relative abundances of *H* and *He* are the same. The effect of the special resonance mechanism mentioned by Bowen[13] for the excitation of λ 4686 should not alter the conclusion greatly. The strength of λ 3203 of *He* II relative to that of λ 4686 indicates that this mechanism is by no means the predominant one for the excitation of λ 4686 in the nova.

If the electron temperature of the nova were comparable with that in the planetary nebulae, we could readily conclude from item 3 of the table that, although the electron density in the nova was decreasing, by November 21 it had not yet become so low as in the planetary nebulae. If the low electron temperatures obtained for planetary nebulae by Page[14] are correct, however, we cannot draw this conclusion. The same difficulty is encountered in a consideration of item 2 of the table above.

*Comparison with other novae.*—As indicated by its spectrum, Nova Herculis, 1934, has been in the nebular stage since June, 1935. Intensities for the period July–September, 1935, have been published by Oehler.[27] Some comparisons with Nova Lacertae follow:

COMPARISON WITH NOVA HERCULIS: LOGARITHMS OF RELATIVE INTENSITIES

| | Nova Herculis | | Nova Lacertae |
|---|---|---|---|
| | June–July | Aug.–Sept. | |
| $4686/H\beta$ | 9.2 | 9.3 | 9.4 |
| $5007+4959/H\beta$ | 1.0 | 1.5 | 0.1–1.2, increasing |
| $5007+4959/4363$ | 0.7 | 1.1 | 0.4 till Sept. 11, increasing to 1.0 |

The comparisons require little comment. The results for the two novae are of the same order, and the trends are in the same direction. The value of $E_{5007+4959}/E_{4363}$ remained approximately constant in

[27] *Zs. f. Ap.*, **12**, 281, 1936.

Nova Herculis from June 20, 1935, the first date listed by Oehler, to July 25, 1935. From his value, using the method discussed above, we derive an electron temperature for Nova Herculis of $7.5 \times 10^3$ degrees, slightly lower than the value found in the same manner for Nova Lacertae.

Sayer has published measures of the spectrum of RS Ophiuchi after its maximum in 1933.[28] Reductions were made for dates quite closely spaced, and the results show large fluctuations. The values listed below are means. The $H\alpha/H\beta$ ratio found by Sayer is markedly greater than the value for Nova Lacertae.

COMPARISON WITH RS OPHIUCHI: LOGARITHMS OF RELATIVE INTENSITIES

| | RS Ophiuchi (1933) | | | Nova Lacertae |
|---|---|---|---|---|
| | Aug. | Sept. | Oct. | |
| $H\alpha/H\beta$ | 1.0 | 1.2 | ..... | 0.7 |
| $4686/H\beta$ | 9.3 | 9.6 | 9.6 | 9.4 |
| $4363/H\beta$ | ..... | 8.8 | 9.2 | Increasing from 9.3 to 0.3; constant after Sept. 11 |

I wish to express my gratitude to Director Wright of the Lick Observatory for the facilities granted me for carrying out this work. To Dr. A. B. Wyse and Dr. J. H. Moore I am indebted for their continued encouragement and advice. The investigation was made possible by the awards of fellowships at the Lick Observatory for the years 1936–37 and 1937–38.

McDonald Observatory
Fort Davis, Texas
March 1940

[28] *Harvard Ann.*, **105**, 21, 1937.

# DO AQUILAE 1925—AN UNUSUAL NOVA OF THE NOVA PICTORIS 1925 TYPE

B. VORONTSOV-VELYAMINOV

ABSTRACT

The star in its decline showed strong lines of [*Fe* II], and its light-curve appears to be a duplicate of that of Nova Pictoris. The comparison leads to the reconstruction of unobserved parts of both curves.

Very few slow novae are known, and still fewer have been studied in detail. Among them, Nova Pictoris 1925 is quite unique, especially in its slow rise to maximum. It is known that 109 days before maximum it was fainter than magnitude 12. The date of its outburst is unknown, but on a plate taken 55 days before maximum the star was of magnitude 3. No further information is available until 13 days before maximum, when the star was discovered and when continuous observations were started. The spectrum of the star from its discovery until 3 days after maximum was of the absorption type. No other nova has been studied spectroscopically so long before maximum. The unusual character of this nova raised the question whether the observed maximum was the principal one, or whether it had occurred before the date when the star was of the third magnitude or between this date and the date of its discovery by Watson.

It was also supposed, in order to explain the late discovery of the nova, that before its discovery it had faded from the third magnitude to below the sixth. Finally, Nova Pictoris was the first nova in which the forbidden lines of ionized iron were clearly observed and recognized after they were first identified by Merrill[1] in $\eta$ Carinae. Since then these lines, so rarely encountered in spectra of novae, were observed only in the novalike star RS Ophiuchi 1933 and for a few days in Nova Herculis (during its sudden decline in April of 1935).

In the course of an extensive investigation of the luminosity and spectral changes of novae, the writer received, a few years ago, the majority of the results recently published by Dean B. McLaughlin,[2]

[1] *Ap. J.*, **67**, 391, 1928.

[2] *Pop. Astr.*, **47**, 410, 481, 538, 1939.

as well as many others, establishing definite and striking relationships between the characteristic stages of the development in spectrum and luminosity and the drop in magnitude after maximum brightness. However, the publication of these results was postponed until the photometric and spectroscopic data on all novae could be reviewed. This was found necessary because many of the statements relating to individual faint novae in the literature were found to be seriously in error. The case described here is one of the striking examples of this kind.

In the course of the final revision (soon to be completed) of all the photometric and spectroscopic data on all novae thus far observed, Nova DO Aquilae 1925 proved to be of special interest. Its light-curve was known only approximately, and no study of its spectrum was undertaken, though some spectrograms were obtained. Generally, no attention was paid to the star, which was occasionally designated as "Wolf's variable" and not as a nova.

The light-curve of the star, based on all photometric data available and compiled in collaboration with Mr. Kalashnikov, shows an unusually flat maximum, which lasted 250 days. There is a gap in the data for 53 days, approximately in the middle of this prolonged maximum. The objective-prism plates of the star taken at the Harvard Observatory[3] in the period of constant maximum brightness show a continuous spectrum. No bright or dark lines could be recognized with certainty, but a resemblance to the early spectrum of Nova Pictoris was suspected. However, near maximum brightness all novae possess absorption spectra with broad and shallow lines. Such lines sometimes are barely visible on objective-prism spectrograms of small dispersion, and this explains the continuous character of the spectrum. A spectrogram taken by Merrill[4] on August 11, 1926, was reproduced by him "without discussion for the benefit of other observers." A careful examination of this spectrogram revealed 30 bright bands, of which 10 (and 2 in blends) are due to *Fe* II, 12 (and 3 in blends) to forbidden [*Fe* II], and 2 (and 2 in blends) to [*Fe* III]. Of 30 lines, 83 per cent are due to iron, and 60 per cent are forbidden lines. These are of unusual strength for a nova, as may be seen from Table 1 and from the plate of spectra. The forbidden

[3] *Harvard Bull.*, **826**, 1925.

[4] *Pub. A.S.P.*, **38**, 387, 1926.

TABLE 1

SPECTRUM OF DO AQUILAE 1925*

| λ Obs. | P.E. | Identification | Multiplet | DO Aql | Intensity | | |
|---|---|---|---|---|---|---|---|
| | | | | | Nova Pic | η Car | Nova Her |
| 5021 | ±2 A | 5018 *Fe* II | $a^6S_{5/2}-z^6P^\circ_{5/2}$ | 10 | 4 | 5 | 4 |
| 5003 | 2 | 5007 [*O* III] | $a^3P^\circ_2-a^1D_2$ | 7 | (2) | ..... | ..... |
| 4996 | 1 | 4924 *Fe* II | $a^6S_{5/2}-z^6P^\circ_{3/2}$ | 10 | 6 | 7 | 7 |
| 4889 | 3 | 4890 [*Fe* II] | $a^6D_{7/2}-b^4P_{5/2}$ | 3 | [2] | 2 | 1 |
| 4861 | 2 | 4861 *Hβ* | $2^2P^o-4^2D$ | 25 | (40) | 30 | 5 |
| 4814 | 2 | 4815 [*Fe* II] | $a^4F_{9/2}-b^4F_{9/2}$ | 7 | 4 | 5 | 1 |
| 4774 | 2 | 4775 [*Fe* II] | $a^4F_{9/2}-b^4F_{7/2}$; 4770 *Fe* III $^5D_2-{}^3F_3$ (?) | 2 | 1 | 0 | ..... |
| 4729 | 2 | 4728 [*Fe* II] | $a^6D_{5/2}-b^4P_{3/2}$; 4734 *Fe* III $^5D_2-{}^3F_2$ (?) | 6 | 4 | 5 | 1 |
| 4700 | 4 | 4702 [*Fe* III] | $^5D_3-{}^3F_3$ | 10 | ..... | ..... | ..... |
| 4656 | 8 | 4658 [*Fe* III] | $^5D_4-{}^3F_4$ | 20 | 2 | ..... | ..... |
| 4628 | 5 | 4629 *Fe* II | $b^4F_{9/2}-z^4F^\circ_{9/2}$ | 17 | 7 | 8 | 2 |
| 4585 | 4 | 4584 *Fe* II | $b^4F_{9/2}-z^4D^\circ_{7/2}$ | 15 | 6 | 9 | 10 |
| 4554 | 4 | 4556 *Fe* II | $b^4F_{7/2}-z^4F^\circ_{7/2}$ | 15 | 5 | 5 | 4 |
| 4520 | 4 | 4520 *Fe* II | $b^4F_{9/2}-z^4F^\circ_{7/2}$; 4523 *Fe* II $b^4F_{5/2}-z^4D^\circ_{3/2}$ | 15 | 4 | 4 | 2 |
| 4490 | 2 | 4491 *Fe* II | $b^4F_{3/2}-z^4F^\circ_{3/2}$; 4489 *Fe* II $b^4F_{7/2}-z^4F^\circ_{5/2}$ | 8 | 2 | 4 | 3 |
| 4474 | 2 | 4475 [*Fe* II] | $a^6D_{1/2}-a^6S_{5/2}$ | 8 | 3 | 3 | 2 |
| 4455 | 2 | 4458 [*Fe* II] | $a^6D_{7/2}-b^4F_{7/2}$; 4452 *Fe* II $a^6D_{3/2}-a^6S_{5/2}$ | 10 | 3 | 4 | 2 |
| 4432 | 2 | ? | ..... | 5 | ..... | ..... | ..... |
| 4416 | 1 | 4416 [*Fe* II] | $a^6D_{9/2}-b^4F_{9/2}$; 4414 *Fe* II $a^6D_{5/2}-a^6S_{5/2}$ | 18 | 5 | 9 | 15? |
| 4386 | 2 | 4385 *Fe* II | $b^4P_{1/2}-z^4D_{1/2}$ | 5 | 2 | 2 | 3 |
| 4362 | 4 | 4363 [*O* III] | $a^1D_2-a^1S_0$; 4359 *Fe* II $a^6D_{7/2}-a^6S_{5/2}$ | 15 | (7) | ..... | 20 |
| 4341 | 2 | 4341 *Hγ* | $2^2P^o-5^2D$ | 15 | (22) | 5 | 7 |
| 4320 | 1 | 4320 [*Fe* II] | $a^4F_{5/2}-a^4G_{7/2}$ | 6 | 0 | 0 | 2 |
| 4306 | 1 | 4306 [*Fe* II] | $a^4F_{5/2}-a^4G_{5/2}$ | 4 | 1 | 1 | 2 |
| 4287 | 2 | 4287 [*Fe* II] | $a^6D_{9/2}-a^6S_{5/2}$ | 12 | 5 | 10 | 15 |
| 4275 | 1 | 4277 [*Fe* II] | $a^4F_{7/2}-a^4G_{9/2}$ | 2 | 2 | 5 | 5 |
| 4246 | 1 | 4244 [*Fe* II] | $a^4F_{9/2}-a^4G_{11/2}$ | 10 | 4 | 8 | 12 |
| 4233 | 1 | 4233 *Fe* II | $b^4P_{5/2}-z^4D^\circ_{7/2}$ | 10 | 4 | 5 | 10 |
| 4206 | 2 | 4207 ? | Observed in N Pic | 1 | ((0)) | ..... | ..... |
| 4181 | 1 | 4179 *Fe* II | $b^4P_{5/2}-z^4F^\circ_{7/2}$ | 2 | 2 | 1 | 5 |
| 4117 | 2 | 4115 ? | Observed in N Pic in 1926 | 1 | ((1)) | ..... | ..... |
| 4102 | ±2 | 4102 *Hδ* | $2^2P^o-6^2D$ | 18 | (16) | 0 | 7 |

* The intensities for Nova Pictoris refer to January 5, 1926, except in the following cases: the values underlined singly are for January 7; those underlined doubly are for January 8; the value in square brackets is for December 8, 1925; the values in single parenthesis are means for the period December 25—March 26; those in double parenthesis are means for the period March–October, 1926.

lines of [*Fe* III], recently computed by Edlén and Swings,[5] and identified by them in RY Scuti and other stars, are the dominant feature in the spectrum of DO Aquilae.

None other of the few novae having forbidden lines of [*Fe* II] shows similar intensity, and the strength of the [*Fe* III] lines is still more exceptional. In RY Scuti, RT Serpentis, and some other stars possessing λ 4658, this line accompanies a rather different set of emission lines. It may be noticed that in DO Aquilae the relative intensities within the separate multiplets of [*Fe* II] and [*Fe* III] are fairly consistent with their intensities in other stars. On the original negative obtained by Merrill some additional faint emissions can probably be measured and identified.

A month later, on September 10, 1926, G. Tikhov[6] obtained an objective-prism spectrogram with low dispersion. He mentions the bright hydrogen lines and the typical nova band 464 $\mu\mu$. No doubt the spectrum of the star at this date was practically the same as in August, and the band at 464 $\mu\mu$ is actually a wide blend, including λ 4658 of [*Fe* III], which is seen in Plate VI. On the whole, the spectrum is nearly identical with the spectrum of Nova Pictoris on January 5, 1926.

Table 1 gives the identification of the bands in the spectrum of DO Aquilae in comparison with the identifications for $\eta$ Carinae,[7] Nova Pictoris,[8] and Nova Herculis[9] at the similar spectral stage. The comparative plate of these spectra reduced to a common scale makes evident this similarity and the exceptional strength of the forbidden [*Fe* II] lines in Nova DO Aquilae 1925. The latter are marked at the bottom; the [*Fe* III] lines are marked by arrows. The velocity of expansion of the hydrogen shell surrounding the star, estimated from the width of the bands, is 1000 km/sec, and that of the iron shell is 700 km/sec. Probably there is a set of absorption lines of hydrogen shifted by 1050 km/sec toward the violet.

After the spectrum of the star in its decline had been interpreted,

[5] *Observatory*, **62**, 234, 1939.

[6] *A.N.*, **228**, 295, 1926.

[7] Moore and Sanford, *Lick Obs. Bull.*, **8**, 55, 1914.

[8] Spencer Jones, *Cape Obs. Ann.*, X, Part 9, 1931.

[9] Adams and Joy, *Ap. J.*, **84**, 14, 1936.

# PLATE VI

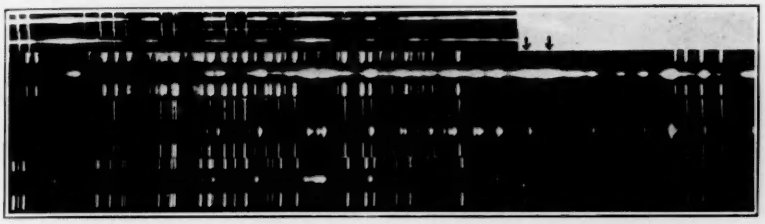


SPECTRA OF: (1) NOVA PIC, 1925 DEC. 29; (2) NOVA PIC, 1926 JAN. 5; (3) DO Aql, 1926 AUG. 11; (4) $\eta$ CAR, 1913 MARCH; (5) NOVA HER, 1935 APR. 4.

its light-curve was superposed over the light-curve of Nova Pictoris so as to bring to coincidence the dates when the spectra of these stars were identical. The scale of magnitudes was shifted in an appropriate manner (Fig. 1). The dotted curve for DO Aquilae represents oscillations based upon scanty observations of low accuracy. There is a striking similarity in both curves (DO Aql being $4\frac{1}{2}$ mag. fainter). There are two features: (1) the maximum of Nova Pictoris coincides with the gap in the light-curve of DO Aquilae men-

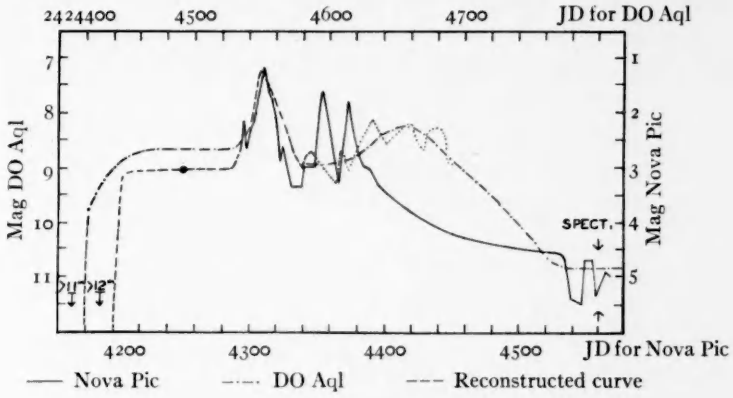


FIG. 1

tioned previously; (2) the observations of DO Aquilae definitely suggest that the outburst was sudden, when the star reached the ninth magnitude, and that this luminosity was maintained for 70 days—until the beginning of the gap.

The later history of both novae is identical. The decline was very slow. In 1927 the magnitude of DO Aquilae was about 10.6 to 10.7; of Nova Pictoris, 6.3 to 6.5 (the difference $10^m6 - 6^m4 = 4^m2$). At the end of 1928 the magnitude of DO Aquilae was 11.7 and of Nova Pictoris 7.5 (the difference $11^m7 - 7^m5 = 4^m2$). In 1934 DO Aquilae was still of magnitude 14.8 to 14.9. Nova Pictoris at this time was of magnitude 9.5, or 8.3 mag. fainter than at maximum (the difference $14^m8 - 9^m5 = 5^m3$). The magnitudes of the comparison stars for DO Aquilae are less certain than for Nova Pictoris, especially at the fainter magnitudes, and this may explain that the latter difference is larger. Since the observed range of

DO Aquilae from below $16^m$ to $8^m.3$ (or brighter) is too large for irregular novae or for novalike stars, such as RT Serpentis, it must be classed among the true novae. This is supported by the luminosity and spectral changes, which are identical to those of Nova Pictoris.

In conclusion, we suggest that (1) a sharp maximum of DO Aquilae occurred at the period when the star was not being observed and when it must have reached magnitude 7 or somewhat fainter; (2) Nova Pictoris has risen not slowly but suddenly, and was of nearly the third magnitude, at least during 45 days (probably 70 days) before maximum; (3) the forbidden lines of [*Fe* II] are excited in a narrow range of physical conditions, which are present for a sufficiently long time only in slow novae.

Moscow, U.S.S.R.
November 27, 1939

# THE SPECTRUM OF NGC 6543 AND ITS NUCLEUS

P. SWINGS*

ABSTRACT

In the nebula NGC 6543 Bowen's fluorescence mechanism is absent, and the recombination process is especially efficient, giving relatively strong lines of *C* II, *C* III, and *N* III. The nucleus is a Wolf-Rayet star showing lines of *N* IV and *C* IV of similar intensities; it is thus an object intermediate between the WN and WC sequences.

1. W. H. Wright[1] has shown that the nuclei of planetaries are frequently Wolf-Rayet stars, and he has recorded the wave lengths and intensities of the bright and dark bands in a number of these objects. But heretofore the classification of these Wolf-Rayet spectra in the nitrogen and carbon sequences (or in others) has not been determined with certainty.

On the basis of the data published by Wright, C. S. Beals[2] has tried to classify the planetary nuclei having spectra of the Wolf-Rayet type, either in the carbon or in the nitrogen sequence. But "since many of these objects are extremely faint and the data consequently meager, too much confidence should not be placed in this list."[3] Beals considers the nucleus of NGC 6543 as a nitrogen star, WN 6. On the other hand, starting from the same data by Wright, C. H. Payne[4] has classified the nucleus of NGC 6543 among the carbon stars. The laboratory investigations by Edlén have led to a better understanding of the Wolf-Rayet spectra, and his discussion[5] shows clearly that the spectra of typical Wolf-Rayet stars contain either carbon or nitrogen lines but not both of them with comparable intensities. R. H. Stoy[6] has obtained spectra of nebulae in the visible region and has expressed the view that the *C* IV lines λλ 5800–5812, which he observed in the spectrum of NGC 6543, may belong to the nucleus; but no certain decision was reached by him.

2. It is important to reinvestigate the spectra of planetary nuclei

* *Contributions from the McDonald Observatory, University of Texas*, No. 24.

[1] *Lick Obs. Pub.*, **13**, 211, 1918.

[2] *Victoria Pub.*, **4**, 286, 1930.

[3] *Ibid.*

[4] *Zs. f. Ap.*, **7**, 1, 1933.

[5] *Zs. f. Ap.*, **7**, 378, 1933.

[6] *Lick Obs. Bull.*, **17**, 179, 1935.

of the Wolf-Rayet type. The present paper is concerned with NGC 6543, which has a sharp nucleus.[7] Three spectrograms of good definition were obtained with the 82-inch reflector of the McDonald Observatory, two with glass prisms (exposures, 1 and $2\frac{1}{2}$ hours; dispersion, 53 A/mm at λ 4000) and one with quartz prisms (exposure, 2 hours; dispersion, 125 A/mm at λ 4000). In all three cases the emulsion was Agfa Superpan Press. We guided as accurately as possible in order to separate the spectrum of the nucleus from that of the nebula. The spectrograms extend from λ 3400 to λ 6600.

3. *Lines present in the nebular part of the spectrum.*—Table 1 contains all the sharp lines which extend beyond the nucleus. As has already been pointed out by Wright, NGC 6543 shows remarkably clearly the distribution of the physical conditions within the nebula. This appears in a very striking manner on our spectrograms when we compare the shapes of lines belonging to the same atom in different states of ionization, namely, [*O* I, II, and III]; [*S* II and III]; *C* II and *C* III; and [*N* II] and *N* III.

The permitted lines of *N* III and *C* III do not extend far from the nucleus, although their attribution to the nebula is certain because of their sharpness and length. The *C* II line λ 4267 is longer.[8]

4. *Excitation processes in the nebula.*—For a discussion of the physical conditions prevailing in NGC 6543 it is useful to tabulate the successive ionization potentials of the observed atoms (Table 2).

The absence of *He* II 4686 and *O* III 3760 in the nebula shows that the *N* III lines are not excited by Bowen's fluorescence mechanism. The observed spectra of *C* II, *C* III, and *N* III are, therefore, all due to recombinations, this process being unusually efficient in this nebula. The third ionization potentials of *C* and *N* are almost identical (47.64 v. and 47.20 v.), while the corresponding value for *O* is appreciably higher (54.62 v.). On the other hand, the ionizing potentials of *O* III and *He* II are practically equal (54.62 v. and 54.14 v.). The ionization of the nebula by the ultraviolet radiation of the nucleus is such that $C^{+++}$ and $N^{+++}$ are present in the same regions of the nebula which give rise to recombination spectra (*C* III and

[7] This is the bright planetary in Draco, in which bright lines were discovered by Sir William Huggins.

[8] Wright has attributed the lines of *C* II, *C* III, and *N* III to the nucleus.

TABLE 1

LIST OF NEBULAR LINES OF NGC 6543

| Nebular λ and Int.* | Identification | | Nebular λ and Int. | Identification | | Nebular λ and Int. | Identification | |
|---|---|---|---|---|---|---|---|---|
| | Elem. | λ and Int. | | Elem. | λ and Int. | | Elem. | λ and Int. |
| 3614 (0) | *He* I | 3613.64 (3) | 3889.0 (5)W | $H_8$ | 3889.05 | 4649 (2) | *C* III | 4647.40 (10) |
| 3634 (0) | *He* I | 3634.24 (2) | | *He* I | 3888.65 (10) | | | 4650.16 (9) |
| 3683 (0) | $H_{20}$ | 3682.81 | 3964.9 (1)W | *He* I | 3964.73 (4) | | | 4651.35 (8) |
| 3687 (0) | $H_{19}$ | 3686.83 | 3967.4 (5)W | [*Ne* III] | 3967.5 | 4711 (2)W | [*A* IV] | 4711.4 |
| 3691.5 (1) | $H_{18}$ | 3691.56 | 3970.1 (6)W | $H\epsilon$ | 3970.08 | 4713 (2)W | *He* I | 4713.14 (3) |
| 3697.3 (1) | $H_{17}$ | 3697.15 | 4026.2 (3)W | *He* I | 4026.19 (5) | 4740.2 (3) | [*A* IV] | 4740.3 |
| 3704.3 (2) | $H_{16}$ | 3703.85 | 4068.7 (3) | [*S* II] | 4068.5 | 4861.6 (12)W | $H\beta$ | 4861.34 |
| | *He* I | 3705.00 (3) | 4076.3 (1) | [*S* II] | 4076.5 | 4921.8 (2) | *He* I | 4921.93 (4) |
| 3712.0 (1) | $H_{15}$ | 3711.97 | 4097.4 (2)W | *N* III | 4097.31 (10) | 4959.2 (15)W | [*O* III] | 4959.5 |
| 3722.0 (2) | $H_{14}$ | 3721.94 | 4101.8 (8)W | $H\delta$ | 4101.75 | 5007.7 (40)W | [*O* III] | 5007.6 |
| 3726.1 (6)W | [*O* II] | 3726.2 | 4120.6 (1) | *He* I | 4120.81 (3) | 5875.6 (7)W | *He* I | 5875.62 (10) |
| 3729.0 (4)W | [*O* II] | 3729.1 | 4143.6 (1) | *He* I | 4143.77 (2) | 6300.3 (3)S | [*O* I] | 6300.2 |
| 3734.2 (2) | $H_{13}$ | 3734.37 | 4267.3 (2) | *C* II | 4267.02 (8) | 6311 (2)S | [*S* III] | 6310.2 |
| 3750.3 (2) | $H_{12}$ | 3750.15 | | | 4267.27 (10) | 6364 (1)S | [*O* I] | 6363.9 |
| 3770.7 (2)W | $H_{11}$ | 3770.63 | 4340.5 (10)W | $H\gamma$ | 4340.48 | 6548 (6)S | [*N* II] | 6548.4 |
| 3797.8 (2)W | $H_{10}$ | 3797.90 | 4363.0 (3)W | [*O* III] | 4363.2 | 6563 (15)W | $H\alpha$ | 6562.82 |
| 3819.7 (1) | *He* I | 3819.61 (4) | 4388.0 (2)W | *He* I | 4387.93 (3) | 6584 (8)W | [*N* II] | 6583.9 |
| 3835.3 (3)W | $H_9$ | 3835.39 | 4471.6 (6)W | *He* I | 4471.48 (6) | | | |
| 3868.8 (8)W | [*Ne* III] | 3868.7 | 4634.3 (2) | *N* III | 4634.16 (8) | | | |
| | *He* I | 3867.46 (2) | 4640.6 (3)W | *N* III | 4640.64 (10) | | | |

* W, observed by Wright; S, observed by Stoy.

*N* III), whereas $O^{+++}$ and $He^{++}$ are practically absent. The wave lengths corresponding to 47.5 v. and 54.5 v. are λ 260 and λ 228, respectively. The observations suggest that the nuclear radiation is much stronger near λ 260 than near λ 228 when it reaches the nebular regions. Besides the general decrease of the continuous spectrum toward short wave lengths, this may be due to a crowding of strong, bright, nuclear lines of *He* II (λλ 256 A, 243 A, etc.), *O* IV, *C* IV, *N* IV, and *N* V appearing between λ 260 and λ 230. The region below λ 228 is much poorer in such lines.

TABLE 2

SUCCESSIVE IONIZATION POTENTIALS OF THE ATOMS OBSERVED IN THE NGC 6543 NEBULA

| | *H* | *He* | *C* | *N* | *O* | *Ne* | *S* | *A* |
|---|---|---|---|---|---|---|---|---|
| I | 13.53 | 24.46 | 11.20 | 14.46 | 13.55 | 21.47 | 10.31 | 15.69 |
| II | ..... | 54.14 | 24.26 | 29.44 | 34.94 | 40.9 | 23.3 | 27.74 |
| III | ..... | ..... | 47.64 | 47.20 | 54.62 | 63.2 | 34.9 | 40.7 |
| IV | ..... | ..... | 64.17 | 77.04 | 77.03 | ..... | ..... | ..... |

The simultaneous appearance of [*Ne* III] and [*A* IV] in roughly the same regions is also quite understandable, the ionization potentials of $Ne^{+}$ and $A^{++}$ being 40.9 v. and 40.7 v., respectively.

5. *Radiations appearing in the nucleus only.*—The continuous spectrum of the nucleus is rather strong, and there are not many outstanding bright lines in the astronomical region. Their nuclear character is detected by their width, which is appreciably greater than for the nebular lines, and by their length, which does not extend beyond the continuous spectrum.

Four elements—*He* II, *N* IV, *C* IV, and *O* IV—appear conspicuously in the Wolf-Rayet spectrum; the presence of weak *N* V and *Si* IV seems also certain. The comparison is very striking between the *N* III, *C* II, or *C* III nebular lines (long and sharp) and the neighboring *N* IV, *C* IV, or *He* II nuclear lines (short and broad).

*Helium:* λ 4685.81 of *He* II is a strong nuclear emission (int. 6) with a weak violet absorption; it does not extend beyond the continuous spectrum of the nucleus.

*Nitrogen:* The *N* IV triplet $3s^3S - 3p^3P^o$ at λ 3478.69 (lab. int. 7), λ 3482.98 (5), and λ 3484.90 (3) is present in emission as a blend of intensity 3. There is a weak absorption component on the violet side. The $3p^1P^o - 3d^1D$ transition at λ 4057.8 is also present in emission (int. 2) and absorption (int. 1).

A faint nuclear line has been measured at λ 4604 and is probably $3s^2S - 3p^2P^o$ of *N* V (λ 4603.2).

*Carbon:* *C* IV is identified with certainty by the emission lines listed in Table 3.

TABLE 3

*C* IV LINES IN THE NUCLEUS OF NGC 6543

| λ Lab. | Lab. Int. | Designation | Int. in Nucleus |
|---|---|---|---|
| 4658.54..... | 5d | $5gf^2G$, $^2F-6hg^2H^o$, $^2G^o$ | 3 |
| 5801.51..... | 4 | $3s^2S-3p^2P^o$ | 4 |
| 5812.14..... | 3 | | 2 |

The $^2S - ^2P^o$ doublet was not separated on Wright's plates, but it was on Stoy's spectrograms. The *C* IV doublet is the most conspicuous feature on our spectrograms of this Wolf-Rayet object, and its attribution to the nucleus is certain by comparison with the nebular lines and also with the nuclear features. The identification of λ 5812 attributed to *C* IV has been discussed in the ordinary WC stars.[9] But there is no doubt about the identification in the present case, as we have observed the two components of the doublet with the correct intensity ratio. There is a *N* IV multiplet $3p' {}^3P^o - 3d' {}^3P$ predicted at λλ 5812–5828–5846,[10] but its influence on the observed *C* IV doublet is certainly unimportant.

*Oxygen:* *O* III is absent in the nebula, but some weak trace of λ 3759.87 (strongest laboratory line) may possibly be present in the nucleus.

*O* IV is characterized by the lines of Table 4.

*Silicon:* A trace of λ 4088.86 *Si* IV is present.

6. *Conclusions concerning the nucleus.*—The characteristic lines of the three ions *N* IV, *C* IV, and *O* IV appear with similar intensities. It

[9] C. S. Beals, *Victoria Pub.*, **6**, 129, 1934.

[10] Edlén, *loc. cit.*

seems that the abundance of carbon is comparable with the abundance of nitrogen or oxygen, although it may be somewhat lower, since the fourth ionization potential is smaller for carbon (64.17 v.)

TABLE 4

*O* IV LINES IN THE NUCLEUS OF NGC 6543

| λ Lab. | Lab. Int. | Designation | Int. in Nucleus |
|---|---|---|---|
| 3403.58 | 3 | $3p\,^2P^o - 3d\,^2D$ | 2 |
| 3411.76 | 4 | | 3 |
| 3560.42 | 1 | $3p'\,^2D - 3d'\,^2F^o$ | 1 |
| 3563.36 | 2 | | |

than for nitrogen (77.04 v.) or oxygen (77.03 v.). In any case, as the same effect of the ionization potentials would apply to the usual WN stars, it is safe to assume that the nucleus of NGC 6543 is much richer in carbon than the WN stars and that it is thus an intermediate object between the WN and WC sequences.

McDONALD OBSERVATORY
March 21, 1940

# THE NEBULAR SPECTRA OF TWO SLOW NOVAE DQ HERCULIS AND RT SERPENTIS*

P. SWINGS† AND O. STRUVE

ABSTRACT

The spectrum of Nova Herculis has been measured in the region λλ 3200–6700, and many new lines have been identified. The character of the spectrum has not changed greatly since the observations by Adams and Joy in 1935–1936, but the increased separation between the two visual components of the Nova has now made it possible to observe separately the two spectra. The ionization seems to be identically the same in the two objects, but some differences in the structure of the lines was noticed. Spectra taken with the slit along the major axis of the elongated image show a marked depression between the two outside components of the emission lines, while at least the preceding component of the binary shows a fairly strong central component between the two outside components. The observations are sensitive to conditions of seeing, and it is not possible at this stage to unravel the true nature of the spectroscopic structure of the lines.

The spectrum of Nova Serpentis, which had an outburst in 1909 and which is known to have developed abnormally slowly, was last described by Joy in 1931. Since that time the spectrum has undergone marked changes: the lines of [*Fe* III], which were strong in 1931, are very weak on our spectrogram. Instead, [*Ne* III], [*Ne* V], and [*Fe* VI] are strong, in addition to *H*, *He* I, *He* II, and [*O* III].

Nova DQ Herculis, 1934,[1] is a typical representative of the slowly developing type of novae, while the evolution of Nova RT Serpentis, 1909,[2] is usually regarded as having been quite abnormally slow. Former observations of Nova Herculis have shown that the bright lines have a complex structure, and the suggestion has been made by Whipple and Payne-Gaposchkin[3] that this structure may be related to the duplicity of the object discovered by Kuiper. It is important to examine the present structure of the lines after several years have elapsed since the outburst. In addition, we have investigated the

* *Contributions from the McDonald Observatory, University of Texas*, No. 25.

† Visiting scientist of the Belgian-American Foundation and visiting astronomer at the Yerkes Observatory.

[1] Adams and Joy, *Ap. J.*, **84**, 14, 1936; McLaughlin, *Pub. Obs. U. Michigan*, **6**, 107, 1937; Dufay, *Zs. f. Ap.*, **13**, 36, 1936; Vorontsov-Velyaminov, *Zs. f. Ap.*, **11**, 145, 1935; Beer, *M.N.*, **96**, 236, 1936; Popper, *Pub. A.S.P.*, **51**, 168, 1939.

[2] Joy, *Pub. A.S.P.*, **43**, 353, 1931.

[3] *Proc. Nat. Acad. Sci.*, **22**, 195, 1936. Attention is also called to a suggestion by Morgan (*Ap. J.*, **83**, 252, 1936) that two sets of absorption lines observed in January, 1935, may have been produced by the two components.

ultraviolet region of the spectrum which has not previously been described in detail.

The spectrum of Nova Serpentis, when last observed by Joy in 1931, was characterized by a strong group of bright lines at λλ 4658, 4701, and 4733, which has recently been attributed to forbidden [*Fe* III] by Edlén and Swings.[4] Since the evolution of this nova has been very slow, it would be reasonable to expect that after an interval of some nine years the spectrum would show some higher stage of ionization of iron, such as was found after a relatively short course of development in Nova Pictoris, Nova Herculis, and Nova Lacertae, 1936.

Fifteen spectrograms of Nova Herculis were secured at the McDonald Observatory between April 19 and May 13, 1940, with dispersions of 100 A/mm (quartz prisms and f/2 camera), 50 A/mm (glass prisms and f/2 camera), and 40 A/mm (quartz prisms and f/5 camera) at λ 3933. One spectrogram of Nova Serpentis[5] was obtained on May 3, 1940, with a dispersion of 200 A/mm at λ 3933 (quartz prisms and f/1 camera). The star was then approximately of magnitude 14.0.

The results of the measurements of all the spectrograms of N Her are collected in Table 1. The wave lengths have been corrected for the motion of the earth but not for the stellar velocity. Almost all lines are satisfactorily identified. The Balmer series is observed to $H_{17}$ and is followed by a strong continuum. Many *He* I lines are present, the strongest unblended series being $2p^3P^o - 3, 4, 5, 6d^3D$. The series $4f^2F^o - ng^2G$ of *He* II has been observed to $n = 17$. Weak lines of *C* II, *C* III, and *C* IV are present; the excitation of these lines is certainly not due to some fluorescence mechanism of the type found by Bowen for *O* III and *N* III. Several lines of *N* II are observed (lab. int. from 5 to 10; stellar int. from 0 to 3), for which no fluorescence mechanism is responsible. The *N* III spectrum is strong, and Bowen's mechanism, if present, is not the only one which operates, since λ 4379, which cannot be excited by fluorescence, is present. *O* II is weak; possibly also *O* IV. *O* III is strong, and its excita-

[4] *Observatory*, **62**, 234, 1939.

[5] A map of the region of RT Ser was published by Barnard, *Pop. Astr.*, **27**, 374, 1919.

## TABLE 1

### THE SPECTRUM OF N HER

| Nova | | | Identification | | |
|---|---|---|---|---|---|
| Feature | λ | Int. | Element | λ | Int. |
| M* | 3311.6 | 1 | *O* III | 3312.30 | 5 |
| v† | 3335.8 | | *O* III | 3340.74 | 6 |
| M | 3341.0 | 2 | [*Ne* V] | 3345.8 | ..... |
| r‡ | 3345.8 | | [*Ne* III] | 3342.8 | ..... |
| v | 3378.6 | | *O* III | 3384.95 | 4 |
| M | 3384.5 | 1 | *O* IV | 3385.55 | 6 |
| r | 3390.8 | | *O* II | 3390.25 | 8 |
| v | 3404.2 | | *O* IV | 3411.76 | 4 |
| M | 3409.7 | 2 | *O* II | 3407.38 | 7 |
| r | 3414.5 | | | | |
| v | 3425.3 | | | | |
| M | 3426.7 | 3 | [*Ne* V] | 3425.8 | ..... |
| r | 3428.0 | | | | |
| C§ | 3441.0 | 3 | | | |
| C | 3443.8 | 2 | *O* III | 3444.10 | 5 |
| C | 3447.2 | 3 | | | |
| C | 3583.7 | 1s | [*Fe* VII] | 3586.6 | ..... |
| C | 3588.0 | 0 | | | |
| M | 3696.2 | 1 | $H_{17}$ | 3697.15 | ..... |
| C | 3700.5 | 2 | $H_{16}$ | 3703.85 | ..... |
| C | 3706.3 | 2 | | | |
| M | 3710.2 | 2 | $H_{15}$ | 3711.97 | ..... |
| C | 3722.7 | 6 | [*O* II] | 3726.1 | ..... |
| C | 3725.8 | 1 | [*O* II] | 3728.6 | ..... |
| C | 3729.7 | 5 | $H_{14}$ | 3721.94 | ..... |
| M | 3734.0 | 2 | $H_{13}$ | 3734.37 | ..... |
| M | 3751.1 | 2 | $H_{12}$ | 3750.15 | ..... |
| C | 3756.4 | 6 | *O* III | 3759.87 | 9 |
| C | 3761.2 | 5 | [*Fe* VII] | 3759.9 | ..... |
| C | 3768.0 | 2 | | | |
| C | 3770.5 | 1 | $H_{11}$ | 3770.63 | ..... |
| C | 3774.2 | 1–2 | | | |
| C | 3787.1 | 1 | *O* III | 3791.26 | 6 |
| C | 3792.8 | 1 | | | |
| C | 3795.1 | 2 | $H_{10}$ | 3797.90 | ..... |
| C | 3800.5 | 2 | | | |
| C | 3814.8 | 1 | *He* I | 3819.61 | 4 |
| C | 3822.2 | 1 | | | |
| C | 3832.6 | 3 | $H_9$ | 3835.39 | ..... |
| C | 3837.8 | 2 | | | |
| M | 3854.6 | 1 | *He* II | 3858.10 | ..... |
| v | 3864.2 | ..... | | | |
| C | 3866.8 | 6 | [*Ne* III] | 3868.7 | ..... |
| C | 3871.1 | 5–6 | | | |
| r | 3872.9 | ..... | | | |
| M | 3879.1 | 0 | *O* II | 3882.19 | 7 |
| v | 3884.8 | ..... | | | |
| C | 3886.0 | 6 | $H_8$ | 3889.05 | ..... |
| C | 3888.4 | 1 | *He* I | 3888.65 | 10 |
| C | 3891.9 | 6 | | | |
| r | 3893.6 | ..... | | | |
| C | 3922.0 | 0 | *He* II | 3923.51 | ..... |
| C | 3926.5 | 0 | | | |
| C | 3965.0 | 7s | [*Ne* III] | 3967.5 | ..... |
| C | 3967.4 | 5 | *He* I | 3964.73 | 4 |
| C | 3969.6 | 7s | | | |
| C | 3971.6 | 4 | *He* | 3970.08 | ..... |
| C | 3973.9 | 5s | | | |
| M | 4009. | 0 | *He* I | 4009.27 | 1 |
| C | 4021.8 | 1 | *He* I | 4026.19 | 5 |
| C | 4027.8 | 1 | *He* II | 4025.64 | ..... |
| C | 4039.5 | 1 | *N* II | 4041.32 | 5 |
| C | 4044.3 | 1 | | | |
| C | 4066.4 | 3 | [*S* II] | 4068.5 | ..... |
| C | 4070.6 | 4 | *C* III | 4069.1 | 6+7+8 |
| C | 4075.2 | 3 | [*S* II] | 4076.5 | ..... |
| C | 4079.0 | 2 | | | |
| v | 4091. | 1 | ..... | ..... | ..... |
| C | 4093.1 | 5 | | | |
| C | 4097.6 | 7 | *N* III | 4097.31 | 10 |
| C | 4099.4 | 5 | | | |
| C | 4101.4 | 7 | *Hδ* | 4101.75 | ..... |
| C | 4104.2 | 5 | *N* III | 4103.37 | 9 |
| C | 4106.4 | 5 | | | |
| v | 4186.2 | 1 | *C* III | 4187.05 | 10 |
| C | 4196.2 | 2 | | | |
| C | 4201.7 | 1 | *He* II | 4199.87 | ..... |
| r | 4203.5 | 0 | | | |
| C | 4234.4 | 1 | *N* II | 4236.98 | 6 |
| C | 4240.2 | 1 | *N* II | 4241.80 | 8 |
| C | 4263.3 | 3 | C II | 4267.02 | 8 |
| C | 4266.0 | 2 | *C* II | 4267.27 | 10 |
| C | 4271.1 | 2 | | | |
| M | 4312.1 | 1 | *O* II | 4317.16 | 8 |
| | | | *O* II | 4319.65 | 8 |
| C | 4336.4 | 6 | | | |
| C | 4339.9 | 4 | *Hγ* | 4340.48 | ..... |
| C | 4344.3 | 5 | | | |
| C | 4359.5 | 4 | | | |
| C | 4363.2 | 3 | [*O* III] | 4363.2 | ..... |
| C | 4367.0 | 3–4 | | | |
| C | 4375.1 | 3 | | | |
| C | 4378.6 | 2 | *N* III | 4379.09 | 10 |
| C | 4383.3 | 2 | | | |
| C | 4411.3 | 2 | *O* II | 4414.89 | 10 |
| C | 4418.4 | 1 | *O* II | 4416.97 | 8 |
| M | 4433. | 1 | *He* I | 4437.55 | 1 |
| | | | *N* II | 4432.71 | 6 |
| M | 4449.7 | 1 | *N* II | 4447.03 | 10 |
| | | | *O* II | 4448.21 | 6 |
| | | | *O* II | 4452.38 | 6 |
| C | 4467.7 | 2 | *He* I | 4471.48 | 6 |
| C | 4475.1 | 1 | | | |
| C | 4508.1 | 2 | *N* III | 4510.92 | 6 |
| M | 4512.4 | 2 | *N* III | 4514.89 | 7 |
| C | 4515.8 | 1 | | | |
| C | 4538.2 | 2 | *He* II | 4541.63 | ..... |
| C | 4548.2 | 1 | | | |
| M | 4598.6 | 1 | *N* II | 4601.49 | 8 |
| M | 4606.9 | 2 | *N* II | 4607.17 | 7 |
| C | 4630.4 | 3 | *N* III | 4634.16 | 9 |
| C | 4636.8 | 6 | *N* III | 4640.64 | 10 |
| C | 4641.1 | 4 | *N* III | 4641.90 | 3 |
| C | 4645.1 | 5 | | | |
| C | 4649.7 | 2 | *O* II | 4649.15 | 10 |
| | | | *C* III | 4650. | 10+9+ |
| C | 4655.1 | 2 | [*Fe* III] | 4658.18 | ..... |
| C | 4659. | 1 | *C* IV | 4658.64 | 5 |
| v | 4662. | 1 | | | |
| C | 4682.3 | 5 | | | |
| C | 4686.2 | 3 | *He* II | 4685.81 | ..... |
| C | 4690.1 | 4–5 | | | |
| M | 4801.8 | 1 | *N* II | 4803.27 | 6 |

* M = maximum intensity of the band.

† v = violet edge.

‡ r = red edge.

§ C = component.

TABLE 1—*Continued*

| Nova | | | Identification | | | Nova | | | Identification | | |
|---|---|---|---|---|---|---|---|---|---|---|---|
| Feature | λ | Int. | Element | λ | Int. | Feature | λ | Int. | Element | λ | Int. |
| C..... | 4856.9 | 8 | *Hβ* | 4861.34 | ..... | M.... | 5599.4 | 2 | *O* III? | 5592.37 | 6 |
| C..... | 4861.3 | 6 | | | | M.... | 5678.6 | 3 | *N* II | 5679.56 | 10 |
| C..... | 4865.9 | 7 | | | | | | | *N* II | 5666.64 | 8 |
| M.... | 4920.3 | 1 | *He* I | 4921.93 | 4 | M.... | 5755.5 | 6 | [*N* II] | 5755.0 | ..... |
| C..... | 4954.0 | 15 | [*O* III] | 4958.91 | ..... | M.... | 5796.3 | 1 | *C* IV | 5801.5 | 4 |
| C..... | 4958.3 | 10 | | | | M.... | 5876. | 4 | *He* I | 5875.62 | 10 |
| C..... | 4962.6 | 15 | | | | M.... | 5913. | 1 | ..... | ..... | ..... |
| C..... | 5004.1 | 25 | [*O* III] | 5006.84 | ..... | M.... | 5941. | 2 | *N* II | 5941.67 | 8 |
| C..... | 5006.5 | 20 | | | | M.... | 6088. | 1 | [*Fe* VII] | 6089. | ..... |
| C..... | 5010.0 | 25 | | | | M.... | 6300. | 5 | [*O* I] | 6300.2 | ..... |
| M.... | 5175.3 | 1 | [*Fe* VI] | 5177.0 | ..... | M.... | 6364. | 3 | [*O* I] | 6363.9 | ..... |
| M.... | 5197.6 | 2 | [*N* I] | 5198.5 | ..... | M.... | 6549. | 9 | [*N* II] | 6548.4 | ..... |
| | | | [*N* I] | 5200.7 | ..... | M.... | 6564. | 10 | *Hα* | 6562.82 | ..... |
| M.... | 5275.0 | 1 | [*Fe* VII] | 5276.1 | ..... | M.... | 6584. | 12 | [*N* II] | 6583.9 | ..... |
| M.... | 5412. | 2 | *He* II | 5411.57 | ..... | | | | *C* II | 6582.85 | 8 |
| M.... | 5532. | 1 | *N* II | 5535.39 | 5 | | | | *C* II | 6578.03 | 10 |

tion may be due mainly to Bowen's process. The forbidden lines in order of decreasing intensity are [*O* III] (giving something like 95 per cent of the total light of the object), [*Ne* III], [*N* II], [*O* I], [*S* II], [*Ne* V], and [*O* I]. There are indications of [*Fe* III], [*Fe* VI], [*Fe* VII], and [*N* I].

There has been no great change in the spectrum since the observations by Adams and Joy. But the structure of the lines is different.

Besides the bright lines, the spectrograms show a faint continuous spectrum with maximum near λ 4150; the intensity of this spectrum corresponds to a star of magnitude between 13 and 14. There is some suspicion of broad absorption features, the strongest of which is to the red of the emission band at λ 4200. However, it is difficult to distinguish between true absorption features and spaces between emission bands.

The unblended emission lines consist of two symmetrical components. On some of the best plates there is a third, central, component between them. The spaces between the components are filled in with weaker emission.

With the large scale of the Cassegrain combination (7″.4 per mm) the nova, though not completely resolved on the slit, shows a markedly elongated image, and in good seeing the two visual components may be observed separately by placing the slit at right angles to the major axis of the ellipse and by guiding accurately on the preceding

or on the following tip of the elongated image. Several spectrograms were obtained in this manner, while for others the slit was placed along the major axis of the ellipse.

The two visual components have very similar spectra. The lines and their relative intensities are identical. However, the structure of the lines shows some slight differences. On the night of April 25, in excellent seeing, the preceding tip of the elongated image showed strong central lines with weak outside components. On the same night the following tip showed little, if any, structure within the broad emission bands. Several plates taken with the slit along the major axis of the ellipse show a marked depression between the two outside lines.

The observations are sensitive to conditions of seeing, and the dispersion is barely sufficient to show the triple structure. We are not quite certain whether the difference between the preceding and the following tip is real, but there can be no doubt about the difference between the preceding tip and the integrated spectrum taken along the major axis. Nor can there be much doubt that the following tip gives nearly equally strong outside components.

This latter result contradicts the conclusion of Whipple and Payne-Gaposchkin: "There can be little doubt that the red and violet components of the doubled emission lines correspond respectively to the fainter and brighter components of the nova observed visually."[6] Incidentally this view has been criticized by McLaughlin,[7] who states:

> Such an apparent duplicity of the emission bands has characterized every well observed nova of the twentieth century, regardless of the uniformity or the knottiness of the nebulosity ejected by it. In the case of Nova Persei, the southern bright fan-shaped knot now gives both approaching and receding velocities.

The continuous spectrum probably corresponds to a star of very early type, and it seems safe to attribute it to the hot nucleus which excites the nebular radiation.

Only the unblended lines showing the triple structure may be used for radial-velocity determinations. The central component is quite indistinct for many lines. The results are collected in Table 2.

[6] *Loc. cit.* [7] *Op. cit.*, p. 209.

The last published determination is by Stratton;[8] it was based on $N_1$ observed on August 17, 1939; his values are −280, −50, and +240 km/sec.

The continuous spectrum of RT Serpentis is extremely weak and does not contribute appreciably to the brightness of the object. The measured bright lines are collected in Table 3. They have been corrected for the earth's motion but not for the stellar velocity.

Besides *Hα*, the strongest line is [*Ne* III] 3869; the [*Ne* III] lines were also exceptionally strong in several other novae, viz., N Persei,

TABLE 2

RADIAL VELOCITIES OF N HER IN KM/SEC

| Element | λ Lab. | Violet Component | Central Component | Red Component |
|---|---|---|---|---|
| *O* III | 3444.10 | −269.7 | −26.1 | +269.7 |
| $H_{11}$ | 3770.63 | −209.1 | −10.3 | +283.8 |
| *C* II | 4267.2 | −274.2 | −84.4 | +274.2 |
| *Hγ* | 4340.48 | −281.9 | −40.1 | +264.0 |
| [*O* III] | 4363.2 | −254.2 | 0 | +261.1 |
| *N* III | 4379.09 | −273.3 | −33.6 | +288.4 |
| *Hβ* | 4861.34 | −273.9 | − 2.5 | +281.3 |
| [*O* III] | 4958.91 | −297.0 | −36.9 | +223.2 |
| Mean (assuming weight 3 for *Hγ*) | ..... | −269.7 | −31.4 | +267.4 |

1901, and N Sagittarii, 1936. The absence of *O* III lines shows that the observed *N* III lines are not excited by fluorescence. There is no trace of lines due to carbon ions, and the permitted oxygen lines, if present, are extremely weak; there is no trace of [*O* II]. The [*Fe* III] lines which were outstanding in 1931 are now very weak, the strongest transition, λ 4658.18, $^5D_4 - {}^3F_4$, having only intensity 1 on our spectrogram. The evidence for the presence of [*Fe* V] is based mainly on a weak extension of $H_9$ (λ 3835.39) toward the red; one of the strongest [*Fe* V] lines, $^5D_3 - {}^3F_3$, has the wave length 3838.9. The strongest [*Fe* V] line to be expected, $^5D_4 - {}^3F_4$, at λ 3891.8 is blended with $H_8$ and *He* I λ 3888.65. The evidence in favor of the $^4F - {}^2G$ forbidden transition of [*Fe* VI] is conclusive. On our spectrogram

[8] *Observatory*, **62**, 236, 1939.

TABLE 3

THE SPECTRUM OF N SER

| Nova | | Identification | | | Notes | Nova | | Identification | | | Notes |
|---|---|---|---|---|---|---|---|---|---|---|---|
| λ | Int. | Element | λ | Int. | | λ | Int. | Element | λ | Int. | |
| 3427.2 | 2 | [*Ne* V] | 3425.8 | | | 4657.7 | 1 | [*Fe* III] | 4658.18 | | |
| 3839.5 | 2 | $H_9$ | 3835.39 | | 1 | 4685.8 | 7 | *He* II | 4685.81 | | |
| | | [*Fe* V] | 3838.9 | | | 4717.0 | 2 | *He* I | 4713.14 | 3 | |
| 3870.1 | 10 | [*Ne* III] | 3868.7 | | | | | [*A* IV] | 4711.4 | | |
| 3892.0 | 4 | $H_8$ | 3889.05 | | | | | [*Ne* IV] | 4714.1 | | |
| | | *He* I | 3888.65 | 10 | | | | [*Ne* IV] | 4719.7 | | |
| | | [*Fe* V] | 3891.8 | | | 4728.1 | 2 | | | | |
| 3968.6 | 7 | [*Ne* III] | 3967.5 | | | 4750.2 | 2 | [*A* IV]? | 4740.3 | | |
| | | *He* | 3970.08 | | | 4865.7 | 8 | *Hβ* | 4861.34 | | |
| 4011.4 | 0 | *He* I | 4009.27 | 1 | | 4961.1 | 3 | [*O* III] | 4959.5 | | |
| 4026.2 | 1 | *He* I | 4026.19 | 5 | | 4969.4 | 2 | [*Fe* VI] | 4968.8 | | |
| | | *He* II | 4025.64 | | | | | [*Fe* VI] | 4974.0 | | |
| 4072.1 | 2 | [*S* II] | 4068.5 | | | 5011.2 | 7 | [*O* III] | 5007.6 | | |
| 4080.0 | 0 | [*S* II] | 4076.5 | | | 5131.4 | 1 | | | | |
| 4102.0 | 2 | *N* III | 4097.3 | 10 | | 5148.7 | 2 | [*Fe* VI] | 5146.8 | | |
| 4103.9 | 5 | *Hδ* | 4101.75 | | | 5178.4 | 2 | [*Fe* VI] | 5177.0 | | |
| | | *N* III | 4103.37 | 9 | | 5275.7 | 0 | [*Fe* III] | 5270.3 | | |
| 4142.9 | 1 | *He* I | 4143.77 | 2 | | | | [*Fe* VI] | 5279.2 | | |
| 4172.9 | 1 | *He* I | 4168.97 | 3 | | 5410.0 | 2 | *He* II | 5411.57 | | |
| 4199.2 | 1 | *He* II | 4199.87 | | | 5675 | 0 | [*Fe* VI] | 5678.0 | | |
| 4342.0 | 6 | *Hγ* | 4340.48 | | | 5752 | 2 | [*N* II] | 5755.0 | | |
| 4354.3 | 2 | | | | 2 | 5877 | 3 | *He* I | 5875.62 | 10 | 3 |
| 4366.0 | 6 | [*O* III] | 4363.2 | | | 6310 | 2 | [*O* I] | 6300.2 | | |
| 4473.0 | 2 | *He* I | 4471.48 | 6 | | | | [*S* III] | 6310.2 | | |
| 4540.8 | 2 | *He* II | 4541.63 | | | 6574 | 25n | *Hα* | 6562.82 | | 4 |
| 4587.1 | 1 | *O* II? | 4590.98 | 9 | | | | [*N* II] | 6548.4 | | |
| 4638.2 | 3 | *N* III | 4634.16 | 9 | | | | [*N* II] | 6583.9 | | |
| | | *N* III | 4640.64 | 10 | | | | | | | |

NOTES TO TABLE 3

1. The line has an extension to the red.
2. This line is probably not due to [*Fe* II], as the other [*Fe* II] lines are absent.
3. There is a broad feature from λ 6025 to λ 6176.
4. The line is broad and is certainly due to both H*α* and [*N* II].

TABLE 4

RADIAL VELOCITIES OF N SER IN KM/SEC

| Element | λ Lab. | Radial Velocity |
|---|---|---|
| | | km/sec |
| [Ne V] | 3425.8 | +124 |
| [Ne III] | 3868.7 | +110 |
| Hγ | 4340.48 | +114 |
| He I | 4471.48 | +100 |
| Mean | | +112 |

there is a fairly broad feature extending from λ 6025 to λ 6176; this may contain the strongest [*Fe* VII] line λ 6089.

Because of the low dispersion, no accurate determination of the radial velocity of RT Serpentis is possible. The most reliable measures are collected in Table 4.

In 1931 the radial velocity determined by Joy from the known bright lines was +92.3 km/sec.

In both objects the forbidden lines of [*Ne* III], [*Ne* V], [*Fe* III], and [*Fe* VI] are present. If we assume that the relative abundance of neon and oxygen is the same in the two objects, the greater intensity of [*Ne* III] in N Ser, compared to [*O* III], indicates that the excitation conditions observed at present are slightly higher in N Ser; the ionization potentials of $O^+$ and $Ne^+$ are 34.9 and 40.9 volts, respectively. This agrees also with the observed intensities of [*O* II] (absent in N Ser and strong in N Her) and of [*S* II] (weak in N Ser and strong in N Her).

MACDONALD OBSERVATORY
May 18, 1940

# THE GALACTIC CLUSTERS NGC 6649 AND NGC 6694

JAMES CUFFEY

ABSTRACT

Red color indices have been obtained for 528 stars in and near the heavily obscured galactic clusters NGC 6649 and NGC 6694 in Scutum. The relations between color and apparent magnitude show that NGC 6694 contains a well-defined main sequence and a slight indication of a giant branch. For NGC 6649 the color-magnitude diagram resembles that of h and $\chi$ Persei or of Messier 7, shifted to the red by $1^m.65$. A zone of low star density 3′ from the center of NGC 6694 is noted.

The color excesses ($\lambda\lambda$ 4300–6200) and distance moduli derived are: NGC 6649, $1^m.65$ and $12^m.1$; NGC 6694, $0^m.55$ and $11^m.1$.

The ratio between general and selective absorption is estimated from the available data on red color indices in obscured clusters. Although uncertain in many cases, the results tend to confirm the ratio $A_r/(A_b - A_r) = 2$, predicted by the $1/\lambda$ law of scattering. The moduli for NGC 6649 and NGC 6694 have accordingly been corrected for the general red absorption, and the distances are 570 and 1000 parsecs, respectively.

The Milky Way between Sagittarius and Scutum is a beautifully complex structure, characterized by rich star clouds and sharply accentuated by dense lanes of obscuration. The obviousness of the absorption makes this area of the Milky Way simpler for analysis than many other galactic fields, in which gradual changes of star density across the regions are almost inextricably intermingled with the slowly thinning-out borders of large obscuring clouds. It is for this reason that the galactic clusters NGC 6649 and NGC 6694 are of great interest; for they, more certainly than any other clusters in the northern Milky Way, are seen through heavy obscuration whose borders are well defined and easily recognizable. Reference to the *Ross-Calvert Milky Way Atlas*, Plate 7, will show the situation of the clusters with respect to the absorption; NGC 6649 is seen through the central and densest part of the cloud which separates the Scutum star cloud from the rich star fields in Sagittarius, and NGC 6694 through a less dense part of the absorption near Scutum.

The co-ordinates and other data for the clusters are as tabulated (p. 304).

## OBSERVATIONAL DETAILS

A photometric study, based upon polar comparisons made with the 36-inch reflector of the Goethe Link Observatory, has resulted in photographic and red magnitudes for 528 stars. Cramer Hi-Speed

Special plates and Agfa Super Pan Press films with a Ciné Red filter (Eastman No. 28) were used. In addition, several plates of longer exposure, taken with the 36-inch reflector at the Steward Observatory in Tucson, have been used for measuring the faint stars. A summary of the observational material is given in Table 1. The probable errors of the color indices are $\pm 0^m.066$ for most of the cluster stars in NGC 6649 and $\pm 0^m.065$ for those in NGC 6694.

The red exposures made in Tucson are on Eastman I-C Special plates. However, no measurable color equation between the red

| 1900 | Diam. | Class* | Spectra* | Distance (Parsecs) | |
|---|---|---|---|---|---|
| | | | | Trumpler* | Shapley† |
| NGC 6649 $\left\{\begin{matrix}18^h28^m-10^\circ.5\\349^\circ\ -2^\circ.3\end{matrix}\right\}$ ..... | 8′ | I2m | ..... | 1830 | 2090–3310 |
| NGC 6694 $\left\{\begin{matrix}18^h40^m-9^\circ.5\\352^\circ\ -4^\circ.4\end{matrix}\right\}$ ..... | 9′ | II2m | 16B8–A2 | 1610 | 1910–3020 |

* *Lick Obs. Bull.*, **14**, 154, 1930. † *Star Clusters*, Appen. B, 1930.

magnitudes given by the plates and those given by the Afga films could be found. Apparently, the effective wave lengths of the two emulsions, when used with the No. 28 filter, are nearly the same, namely, 6200 A.

While the polar comparisons were being made, the mirror, being mounted in an unsatisfactory cell which was later discarded, gave astigmatic images. Since the polar plates were, in general, more astigmatic than the plates of the clusters, it was necessary to estimate the seriousness of scale errors introduced into the magnitudes by the astigmatism. Plates taken at one astigmatic focus were compared with those taken midway between the two astigmatic foci in order to obtain as symmetrical an image as possible. The measurements indicate that the scale errors caused by the astigmatism are less than $0^m.2$ from the eleventh to the sixteenth magnitudes. However, the astigmatism, combined with the coma, led to an asymmetrical distance correction which varied with the orientation of the mirror in hour-angle as well as with the direction and distance of the image

from the plate center. It is, therefore, possible that further work on the magnitude sequences with a large photographic refractor situated in a lower latitude would be profitable.

The Tucson plates were taken with a Ross coma corrector and have a field 30′ in diameter, free from distance correction. There should be, therefore, no photometric errors in the colors depending upon distance from the center of the cluster.

All measurements were made with scales having intervals between images of approximately $0^m.5$.

TABLE 1

| | Number of Comparison Exposures of Cluster 5–20 Min. Exp. | | Number of Long Exposures 30–40 Min. Exp. | | Mean Numerical Extinction Correction | |
|---|---|---|---|---|---|---|
| | Red | Blue | Red | Blue | Red | Blue |
| NGC 6649 | 6 | 8 | 3 | 3 | $0^m.04$ | $0^m.05$ |
| NGC 6694 | 8 | 6 | 3 | 3 | 0.03 | 0.11 |

PROBABLE ERRORS

| | Red | | Blue | |
|---|---|---|---|---|
| NGC 6649 | $8^m.0$–$10^m.5$ | $\pm 0^m.068$ | $10^m.0$–$13^m.5$ | $\pm 0^m.085$ |
| | 10.5–13.2 | .045 | 13.5–16.0 | .049 |
| | 13.2–15.0 | .091 | 16.0–16.7 | .053 |
| NGC 6694 | 9.0–11.0 | .072 | 9.0–13.0 | .162 |
| | 11.0–13.5 | .040 | 13.0–15.0 | .088 |
| | 13.5–14.5 | 0.054 | 15.0–16.5 | 0.037 |

## RESULTS AND CONCLUSIONS

*NGC 6694.*—The relations between color and apparent red magnitude (Figs. 1*a*, 1*b*, 1*c*) show that NGC 6694 has a well-defined main sequence and a slight indication of a giant branch. An unusual number of stars with high color indices ($m_r$, 12–14; $C_r$, 2.3–3.5) have been measured; but they are field stars, since they are contributed mainly by the outer zones of the cluster. The color-magnitude array for the field stars in an area of the sky equal to that included by ring 5 and situated 10′ from the center of the cluster (Fig. 1*c*) con-

firms this conclusion. Inasmuch as the galactic center lies only 25° from the cluster, these stars may be distant red giants, seen through

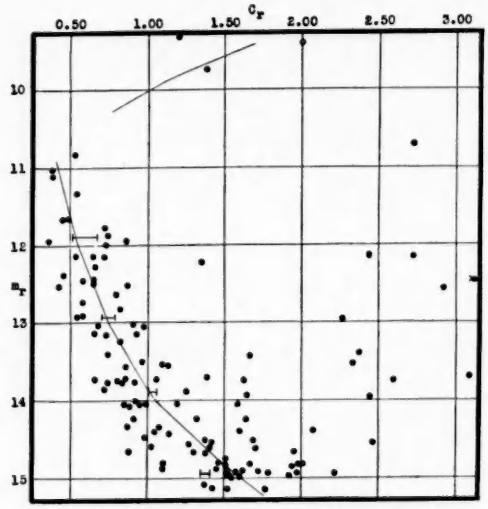


FIG. 1*a*.—NGC 6694; rings 1, 2, 3

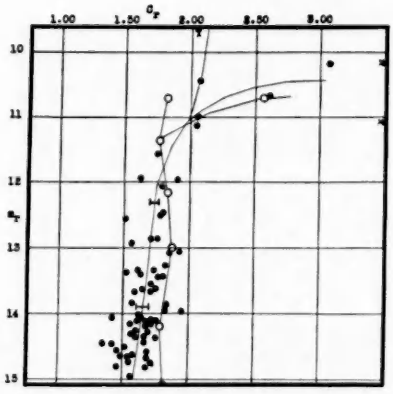


FIG. 2*a*.—NGC 6649; rings 1, 2, 3

selective obscuration. Thus, G or K giants with intrinsic colors of $1^{m}.5$, and distant between 2000 and 3000 parsecs, would give apparent magnitudes similar to those observed.

A striking feature of NGC 6694 is the well-defined zone of low

star density immediately surrounding the nucleus.[1] The boundaries of the zone appear somewhat more sharply defined on the blue-sensitive than on the red-sensitive plates. Figure 3 shows the areal density in stars per 0.494 square minutes as a function of the distance from the center of the cluster; in a zone 3′.1 from the center of the cluster the areal density is 13 per cent less than that in adjacent regions. The position and width of the zone, as estimated by inspection before the star counts were made, are also indicated.

The explanation of the ring has two possibilities: it may represent a spherical shell in which the star density is low, or it may result from a shell of obscuration. The latter alternative, however, is unlikely in the case of NGC 6694, since an obscuring shell would cause the distance modulus obtained from the center of the cluster, where most of the stars are obscured by the shell, to be greater by the amount of the absorption than the modulus given by the stars in the outer zones of the cluster, in which the stars lie predominantly outside the obscuration. Comparison of Figures 1*a* and 1*b*, however, shows a slight effect in the opposite direction. It seems probable, therefore, that the zone represents a spherical shell of low stellar space density in the cluster.

The star counts indicate a diameter of 11′.0 for the cluster, and a total of 150 cluster stars brighter than $m_r = 15.3$.

A comparison of the color-magnitude diagram for NGC 6694 with that of Messier 38 leads to the estimates of color excess, $0^m.55$, and of distance modulus, $11^m.1$. The modulus, corrected for general absorption equal to twice the color excess, is $10^m.0$. The corresponding distances are 1660 parsecs, uncorrected, and 1000 parsecs, corrected for absorption.

*NGC 6649.*—NGC 6649 is a remarkable cluster, for the color indices are all very nearly the same ($1^m.7$) from the eleventh to the fifteenth red magnitude. The color-magnitude diagram (Fig. 2) resembles that of h and $\chi$ Persei, the Pleiades, and, perhaps most

[1] A feature found by Klauder and Siedentopf (*A.N.*, **268**, 13–14, 1939) in several clusters appears to be of a somewhat different nature. In the case of NGC 6694 the zone of low star density is only 3′ from the center of the cluster, while the regions of low density found by Klauder and Siedentopf are, for clusters whose apparent diameters are similar to that of NGC 6694, distant from the centers by five or more times this distance.

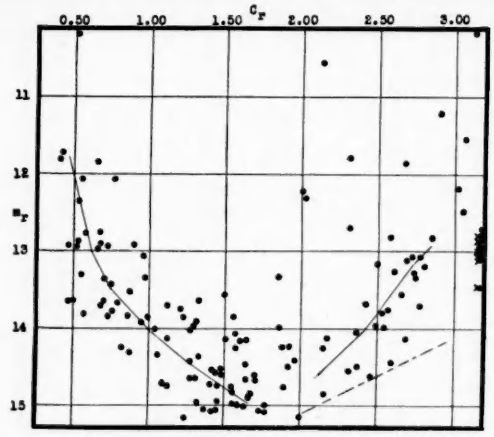


FIG. 1*b*.—NGC 6694; rings 4, 5, 6

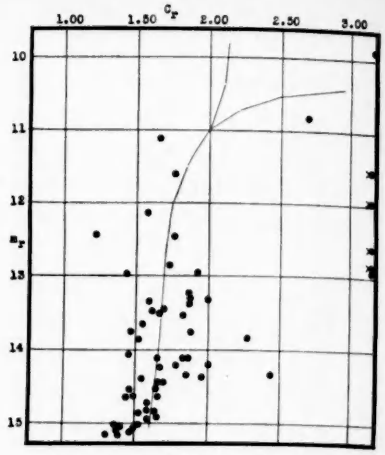


FIG. 2*b*.—NGC 6649; rings 4, 5, 6

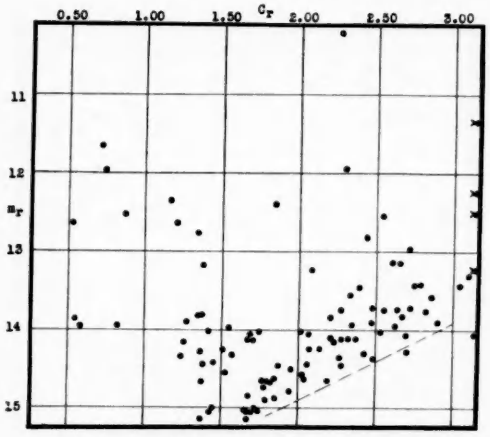


FIG. 1*c*.—NGC 6694; exterior regions (dashed line shows observational limit).

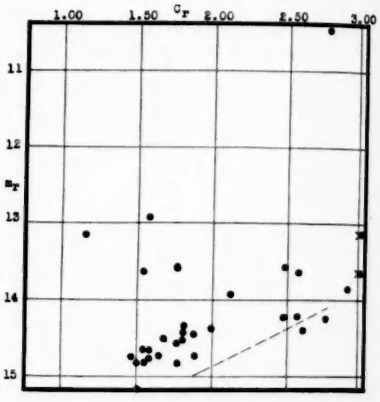


FIG. 2*c*.—NGC 6649; exterior regions

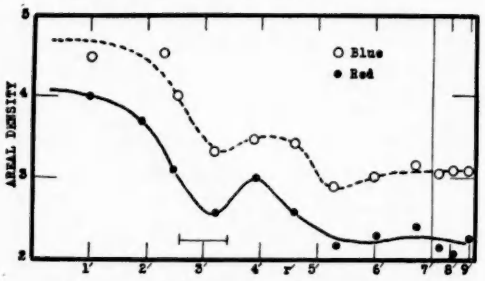


FIG. 3.—NGC 6694, areal density (stars per 0.494 sq. min.) against distance from center of cluster. Limiting magnitudes; red, 15.3, blue, 17.4.

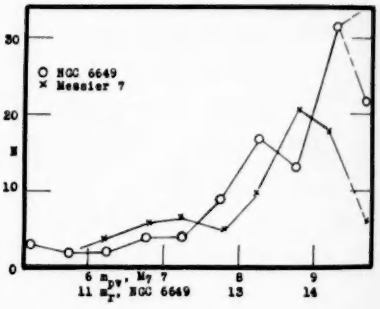


FIG. 4.—Luminosity-curves for NGC 6649 and Messier 7.

closely, Messier 7[2]. In all these clusters the stars have approximately zero color indices for the four brightest magnitudes. The color excess indicated by the redward shift of the color-magnitude diagram for NGC 6649 is thus $1^m.65$. Again, as in NGC 6694, an unusual number of very red stars are noted, three of them having color indices over $4^m.0$.

The lack of dependence of color upon apparent magnitude makes an accurate determination of the distance of NGC 6649 difficult. The close resemblance of the color-magnitude array for NGC 6649 to that of Messier 7, however, suggests that a reliable value for the distance may be obtained by comparing the luminosity-curves of the two clusters. Although this method of estimating distances is unreliable when applied indiscriminately to clusters in general, it should be satisfactory in the present case. For the distance of Messier 7, a mean of Wallenquist's and Trumpler's values, 230 parsecs was used. Allowance was made for the difference between the photovisual and the red-magnitude scales. Thus, the stars in NGC 6649, had they been measured on photovisual plates like those used on Messier 7, would have appeared approximately $0^m.3$ fainter, because of the smaller yellow indices ($C_r = 1.2C_v$).

The luminosity-curves for NGC 6649 and Messier 7 are compared in Figure 4. The resulting modulus for NGC 6649 is $12^m.1$; and, corrected for general absorption by means of the observed selective absorption and the $1/\lambda$ law of scattering, this becomes $8^m.8$. The corresponding distances are 2650 parsecs, uncorrected, and 570 parsecs, corrected for absorption.

The slight but unusual slope in the color-magnitude diagram for NGC 6649 may be the result of small scale errors in the magnitude systems. The Tucson plates afforded a means of rederiving the magnitudes in NGC 6649 by comparison with those in NGC 6694. Because of the normal appearance of the color-magnitude array for NGC 6694, it was assumed that the magnitude sequences in NGC 6694 are free from errors. This comparison suggests corrections to the magnitudes and colors in NGC 6649 which will give the relation indicated by the circles in Figure 2. Thus, the color-magnitude array for NGC 6649 resembles still more closely that of Messier 7. The

[2] Wallenquist, *Bosscha Ann.*, **3**, Part 4, 1931.

corrections have not been applied to the catalogued magnitudes of cluster stars, however, for the available plates furnish not an independent determination of the magnitudes in NGC 6649 but merely a comparison between the sequences in the two clusters.

## THE RATIO OF GENERAL TO SELECTIVE ABSORPTION

The color excesses observed in obscured clusters furnish a relatively direct means for evaluating the ratio of general to selective absorption. The general absorption may be estimated in a manner similar to that used by Trumpler in deriving the photographic absorption. The linear diameters of the obscured clusters are assumed to be equal to those of clusters of similar type in unobscured regions, and the angular diameters of the clusters are assumed to be unaffected by the absorption. Both assumptions may lead to uncertain results when applied to individual clusters, the first because of the dispersion in size of clusters even of the same type and the second, in most instances, because of the greater concentration of the bright stars to the centers of the clusters. The moduli obtained from the diameter-distances may be compared with the photometric moduli, and the general red absorption obtained directly.

In Table 2 the photometric moduli, uncorrected for absorption, are taken from the present paper and from *Harvard Annals*, **106,** No. 2. The moduli based on diameter-distances are from Trumpler's data.[3]

The mean, if we omit the discordant values, which may be due to irregular structure in the clusters as well as to a real variation in $K_r$ $[K_r = A_r/(A_b - A_r)]$ in different obscuring clouds, is 1.6. A smaller value for $K_r$ than the factor 3 adopted in *Harvard Annals*, **106,** No. 2, is indicated.

Schalén has estimated the general photographic absorption in the direction of NGC 6649 to be at least 3 mag., beginning in the immediate vicinity of the sun.[4] His data, however, are not sufficiently detailed to give a good estimate of the absorption in the direction of

[3] *Lick Obs. Bull.*, **14,** 154, 1930.

[4] *Medd. Upsala Obs.*, No. 58, 1934.

## PLATE VII

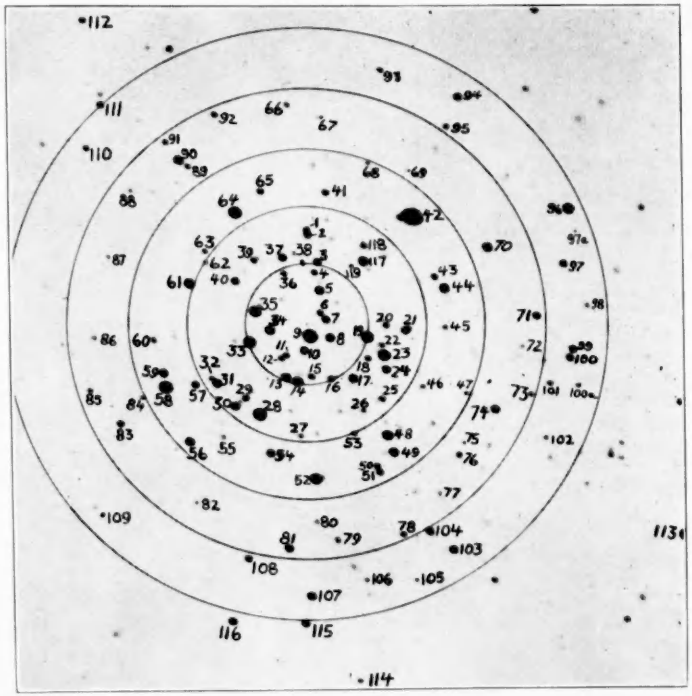

NGC 6649

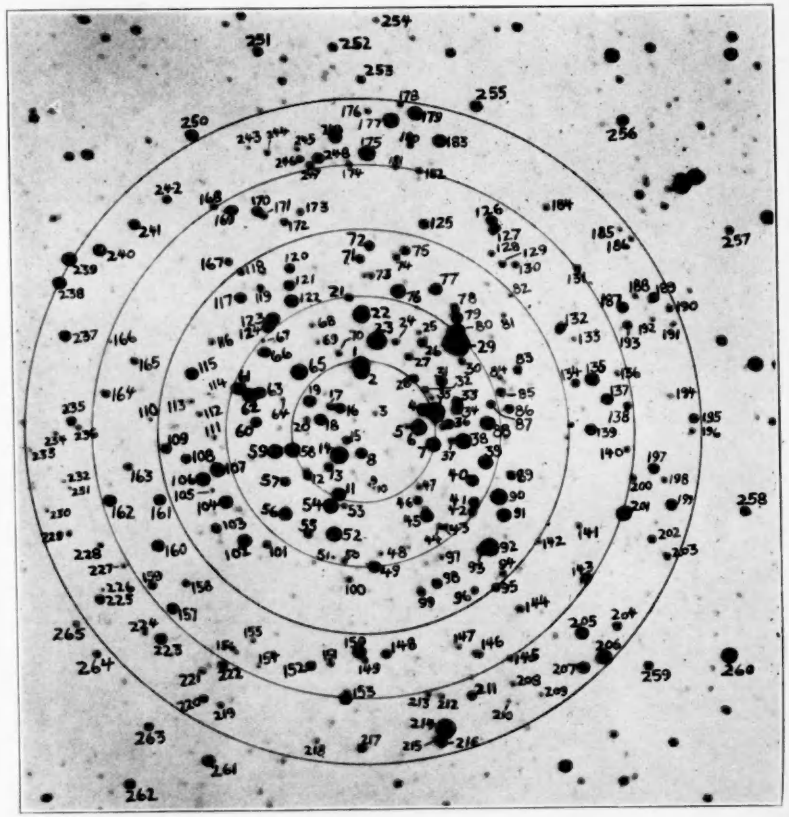

NGC 6694

NGC 6694. A value of $3^{m}.0$, or greater, for $A_b$, combined with the selective absorption measured in NGC 6649, leads to a ratio of $K_b$ [$K_b = A_b/(A_b - A_r)$] at least greater than 1.9, which agrees qualitatively with the value $K_b = 3.1$ predicted by the $1/\lambda$ law of scattering.

The moduli for the clusters are, of course, based upon the red-magnitude system, and it is the value of $K_r$ with which we are concerned. In *Harvard Annals*, **106**, No. 2, it was assumed that $K_r$ and $K_b$ were, to a first approximation, equal. In view of the present

TABLE 2

| | Photometric Modulus | Diameter-Distance Modulus | Color Excess | $A_r$ | $(A_r/A_b-A_r)$ |
|---|---|---|---|---|---|
| NGC 6649 | $12^{m}.1$ | $10^{m}.8$* | $1^{m}.65$ | $+1^{m}.3$ | 0.8 |
| 6694 | 11.1 | 11.1 | 0.55 | +0.0 | ..... |
| 1746 | 9.4 | 9.75 | 0.30 | −0.3 | ..... |
| 1647 | 9.2 | 8.8 | 0.30 | +0.4 | 1.3 |
| 1817 | 11.25 | 10.7 | 0.70 | +0.55 | 0.8 |
| Messier 38 | 9.7 | 9.8 | 0.15 | −0.1 | ..... |
| NGC 1893 | 10.4 | 9.8 | 0.10:: | +0.6 | 6.0:: |
| Messier 35 | 9.8 | 9.4 | 0.15 | +0.4 | 2.7 |
| NGC 2158 | 14.6 | 12.6 | 0.80 | +2.0 | 2.5 |
| 2266 | 12.45 | 12.0 | 0.30: | +0.4 | 1.3 |
| 2281 | 9.45 | 9.2 | 0.00 | +0.2 | ..... |

* From Messier 7 comparison.

data, however, and also in view of the general acceptance of the $1/\lambda$ law of scattering, it seems best to adopt the predicted value, $K_r = 2$. Most of the distances given in *Harvard Annals*, **106**, No. 2, are not seriously affected by the change, except those for NGC 1817 and NGC 2158, which become 930 and 4000 parsecs, instead of 690 and 2700 parsecs.

It is a pleasure to thank Dr. Goethe Link for the use of the 36-inch reflector of his observatory; Dr. Edwin F. Carpenter for the use of plates taken with the reflector at Tucson; and Indiana University for the postdoctoral fellowship in astronomy, which enabled me to complete the measurement and observation of the clusters.

## TABLE 3

### CATALOGUE OF STARS IN NGC 6649 AND NGC 6694*

| NGC 6649 | | | | | NGC 6649 | | | | | NGC 6694 | | | | |
|---|---|---|---|---|---|---|---|---|---|---|---|---|---|---|
| No. | $R$ | $m_{pg}$ | $m_r$ | $C_r$ | No. | $R$ | $m_{pg}$ | $m_r$ | $C_r$ | No. | $R$ | $m_{pg}$ | $m_r$ | $C_r$ |
| 1 | 2 | 15.69 | 13.86 | 1.83\| | 66 | 4 | 16.20 | 14.21: | 1.99:s | 1 | 1 | 11.39 | 11.02 | 0.37\| |
| 2 | 2 | 15.40 | 13.83 | 1.57\| | 67 | 4 | 16.51 | 14.88 | 1.63 | 2 | 1 | 12.83 | 11.97 | 0.86\| |
| 3 | 2 | 15.40 | 13.68 | 1.72 | 68 | 4 | 16.35 | 15.01 | 1.34 | 3 | 1 | 16.54 | 14.97 | 1.57 |
| 4 | 1 | 15.89 | 14.20 | 1.69 | 69 | 4 | 16.54 | 14.95 | 1.59 | 4 | 1 | 13.43 | 10.71 | 2.72 |
| 5 | 1 | 14.92 | 13.07 | 1.85 | 70 | 4 | 14.39 | 12.97 | 1.42s | 5 | 1 | 16.49 | 14.96 | 1.53c |
| 6 | 1 | 15.73 | 14.12 | 1.61 | 71 | 4 | 15.22 | 13.76 | 1.46s | 6 | 1 | 12.63 | 11.89 | 0.74 |
| 7 | 1 | 15.37 | 13.63 | 1.74 | 72 | 4 | 16.54 | 14.90 | 1.64 | 7 | 1 | 12.95 | 12.52 | 0.43 |
| 8 | 1 | 14.94 | 13.33 | 1.61 | 73 | 4 | 16.15 | 14.51 | 1.64 | 8 | 1 | 14.52 | 13.78 | 0.74 |
| 9 | 1 | 12.51 | 10.44 | 2.07 | 74 | 4 | 14.91 | 13.32 | 1.59 | 9 | 1 | 16.83 | 14.88 | 1.95\| |
| 10 | 1 | 15.24 | 13.46 | 1.78 | 75 | 4 | 16.57 | 15.11 | 1.46 | 10 | 1 | 17.00 | 14.53 | 2.47\| |
| 11 | 1 | 15.98 | 14.29 | 1.69\| | 76 | 4 | 15.98 | 14.21 | 1.77 | 11 | 1 | 13.69 | 13.02 | 0.67 |
| 12 | 1 | 16.01 | 14.34 | 1.67\| | 77 | 4 | 16.57 | 15.08 | 1.49 | 12 | 1 | 15.45 | 14.37 | 1.08 |
| 13 | 1 | 14.98 | 13.06 | 1.92 | 78 | 4 | 15.94 | 14.40 | 1.54 | 13 | 1 | 15.23 | 12.97 | 2.26c |
| 14 | 1 | 14.25 | 12.45 | 1.80 | 79 | 4 | 16.13 | 14.46 | 1.67 | 14 | 1 | 11.42 | 9.42 | 2.00 |
| 15 | 1 | 15.86 | 14.12 | 1.74 | 80 | 4 | 16.41 | 14.83 | 1.58 | 15 | 1 | 15.86 | 13.53 | 2.33 |
| 16 | 1 | 15.86 | 14.30 | 1.56 | 81 | 4 | 14.90 | 12.98 | 1.92 | 16 | 1 | 14.93 | 14.01 | 0.92 |
| 17 | 2 | 14.94 | 13.09 | 1.85 | 82 | 4 | 16.46 | 15.17 | 1.29 | 17 | 1 | 16.33 | 14.82 | 1.51 |
| 18 | 2 | 15.88 | 14.28 | 1.60 | 83 | 4 | 15.52 | 14.08 | 1.44 | 18 | 1 | 14.16 | 13.42 | 0.74 |
| 19 | 2 | 13.27 | 10.66 | 2.61 | 84 | 4 | 16.26 | 14.62 | 1.64 | 19 | 1 | 13.79 | 13.14 | 0.65 |
| 20 | 2 | 15.74 | 14.09 | 1.65 | 85 | 4 | 16.08 | 14.65 | 1.43 | 20 | 1 | 16.42 | 14.90 | 1.52 |
| 21 | 2 | 15.25 | 13.54 | 1.71 | 86 | 4 | 16.53 | 15.03 | 1.50 | 21 | 2 | 15.52 | 14.64 | 0.88 |
| 22 | 2 | 16.11 | 14.44 | 1.67 | 87 | 4 | 16.39 | 14.87 | 1.52 | 22 | 2 | 11.87 | 11.34 | 0.53 |
| 23 | 2 | 13.81 | 12.02 | 1.79 | 88 | 4 | 16.45 | 15.08 | 1.37 | 23 | 2 | 11.10 | 9.72 | 1.38 |
| 24 | 2 | 15.26 | 13.61 | 1.65 | 89 | 4 | 15.99 | 14.53 | 1.46 | 24 | 2 | 16.18 | 14.51 | 1.67c |
| 25 | 2 | 15.87 | 14.44 | 1.43 | 90 | 4 | 14.57 | 12.84 | 1.73 | 25 | 2 | 16.64 | 14.92 | 1.72 |
| 26 | 2 | 16.28 | 14.59 | 1.69 | 91 | 4 | 16.07 | 12.91 | 3.16s | 26 | 2 | 15.54 | 14.23 | 1.31 |
| 27 | 2 | 16.48 | 14.76 | 1.72 | 92 | 4 | 15.97 | 14.12 | 1.85s | 27 | 2 | 15.92 | 14.82 | 1.10 |
| 28 | 2 | 13.16 | 11.11 | 2.05 | 93 | 5 | 16.19 | 14.34 | 1.85s | 28 | 2 | 15.45 | 14.48 | 0.97 |
| 29 | 2 | 15.64 | 14.01 | 1.63 | 94 | 5 | 15.19 | 13.65 | 1.54s | 29 | 2 | 10.50: | 9.30: | 1.20: |
| 30 | 2 | 15.05 | 13.31 | 1.74 | 95 | 5 | 15.93 | 14.11: | 1.82:s | 30 | 2 | 16.31 | 14.61 | 1.70c |
| 31 | 2 | 14.90 | 13.38 | 1.52\| | 96 | 5 | 13.63 | 12.42 | 1.21s | 31 | 2 | 14.38 | 13.72 | 0.66 |
| 32 | 2 | 16.12 | 14.37 | 1.75\| | 97 | 5 | 15.39 | 13.86 | 1.53s | 32 | 2 | 16.06 | 14.69 | 1.37 |
| 33 | 2 | 13.33 | 11.58 | 1.75 | 97a | 5 | 16.74 | 14.32 | 2.42 | 33 | 2 | 14.78 | 13.73 | 1.05\| |
| 34 | 1 | 14.62 | 12.86 | 1.76 | 98 | 5 | 16.46 | 15.08 | 1.38 | 34 | 2 | 14.58 | 13.73 | 0.85\| |
| 35 | 1 | 13.57 | 11.95 | 1.62 | 99 | 5 | 15.30 | 13.31 | 1.99 | 35 | 2 | 11.48 | 11.11 | 0.37c |
| 36 | 1 | 15.92 | 14.32 | 1.60 | 100 | 5 | 15.35 | 13.54 | 1.81 | 36 | 2 | 15.11 | 13.45 | 1.66 |
| 37 | 2 | 15.24 | 13.44 | 1.80 | 100a | 5 | 16.10 | 14.61 | 1.49 | 37 | 2 | 16.33 | 14.88 | 1.45c |
| 38 | 2 | 16.49 | 14.80 | 1.69 | 101 | 5 | 16.11 | 14.45 | 1.66 | 38 | 2 | 12.31 | 11.96 | 0.35 |
| 39 | 2 | 15.86 | 14.12 | 1.74 | 102 | 5 | 16.35 | 14.39 | 1.96b | 39 | 2 | 13.07 | 12.43 | 0.64 |
| 40 | 2 | 15.27 | 13.67 | 1.60 | 103 | 5 | 15.23 | 13.37 | 1.86 | 40 | 2 | 14.05 | 13.07 | 0.98 |
| 41 | 3 | 15.72 | 14.16 | 1.56 | 104 | 5 | 15.13 | 13.45 | 1.68 | 41 | 2 | 14.91 | 14.04 | 0.87 |
| 42 | 3 | 10.40 | 8.36: | 2.04:s | 105 | 5 | 16.51 | 15.14 | 1.37 | 42 | 2 | 15.94 | 14.64 | 1.30 |
| 43 | 3 | 15.69 | 14.34 | 1.35 | 106 | 5 | 16.32 | 14.74 | 1.58 | 43 | 2 | 16.27 | 13.47 | ..... |
| 44 | 3 | 14.48 | 12.92 | 1.56 | 107 | 5 | 15.09 | 13.23 | 1.86s | 44 | 2 | 16.34 | | ..... |
| 45 | 3 | 16.26 | 14.71 | 1.55 | 108 | 5 | 15.66 | 13.79 | 1.87s | 45 | 2 | 13.89 | 13.16 | 0.73 |
| 46 | 3 | 16.26 | 14.80 | 1.46 | 109 | 5 | 16.53 | 12.92 | 3.61 | 46 | 2 | 15.61 | 14.59 | 1.02 |
| 47 | 3 | 16.20 | 14.63 | 1.57 | 110 | 5 | 15.96 | 12.60 | 3.36 | 47 | 2 | 16.46 | 15.08 | 1.38 |
| 48 | 3 | 14.27 | 12.49 | 1.78 | 111 | 6 | 15.72 | 11.55 | 4.17s | 48 | 2 | 16.91 | 14.98 | 1.93 |
| 49 | 3 | 14.78 | 11.05 | 3.73 | 112 | 6 | 16.10 | 11.98 | 4.12s | 49 | 2 | 14.09 | 13.16 | 0.93 |
| 50 | 3 | 15.86 | 14.11 | 1.75\| | 113 | 6 | 12.77 | 11.12 | 1.65s | 50 | 2 | 16.39 | 13.94 | 2.45 |
| 51 | 3 | 15.80 | 14.12 | 1.68\| | 114 | 6 | 16.12 | 13.86 | 2.26s | 51 | 2 | 16.83 | ..... | ..... |
| 52 | 3 | 13.83 | 11.93 | 1.90 | 115 | 6 | 15.23 | 13.35 | 1.88s | 52 | 2 | 12.66 | 12.13 | 0.53 |
| 53 | 3 | 16.02 | 14.50 | 1.52 | 116 | 6 | 15.11 | 13.45 | 1.66s | 53 | 2 | 16.49 | 14.83 | 1.66 |
| 54 | 3 | 15.07 | 13.25 | 1.82 | 117 | 2 | 14.56 | 10.14 | 4.42s | 54 | 2 | 12.83 | 12.38 | 0.45 |
| 55 | 3 | 16.53 | 14.97 | 1.56 | 118 | 2 | 15.93 | 13.98 | 1.95s | 55 | 2 | 15.80 | 12.45 | 3.35 |
| 56 | 3 | 14.57 | 12.85 | 1.72 | 119 | 2 | 16.36 | 14.67: | 1.69s: | 56 | 2 | 13.47 | 12.90 | 0.57 |
| 57 | 3 | 15.50 | 14.08 | 1.42 | 120† | 6 | 15.11 | 13.49 | 1.62s | 57 | 2 | 15.14 | 13.89 | 1.25 |
| 58 | 3 | 13.05 | 10.99 | 2.06 | 121† | 6 | 15.92 | 14.26 | 1.66s | 58 | 2 | 12.49 | 11.78 | 0.71 |
| 59 | 3 | 15.01 | 13.39 | 1.62 | 122† | 6 | 13.53 | 10.84 | 2.69s | 59 | 2 | 12.85 | 12.13 | 0.72 |
| 60 | 3 | 16.04 | 14.58 | 1.46 | 123† | 6 | 15.76 | 14.11 | 1.65s | 60 | 2 | 14.57 | 13.86 | 0.71 |
| 61 | 3 | 14.04 | 12.53 | 1.51 | 124† | 6 | 13.35 | 11.60 | 1.75s | 61 | 2 | 13.92 | 13.02 | 0.90 |
| 62 | 3 | 16.25 | 14.69 | 1.56 | 125† | 6 | 13.69 | 12.12 | 1.57s | 62 | 2 | 12.72 | 12.00 | 0.72 |
| 63 | 3 | 16.11 | 14.63 | 1.48 | 126† | 6 | 13.09 | 9.91 | 3.18s | 63 | 2 | 14.42 | 13.56 | 0.86 |
| 64 | 3 | 13.24 | 10.17 | 3.07s | 127† | 6 | 14.21 | 12.45 | 1.76s | 64 | 2 | 16.84 | 14.83 | 2.01 |
| 65 | 3 | 15.78 | 13.95 | 1.83s | | | | | | 65 | 2 | 12.14 | 11.66 | 0.48 |

* Symbols: † = off chart; d = double; b = blend; c = close to bright star; s = sequence star; | = stars close together.

TABLE 3—*Continued*

| NGC 6694 | | | | | NGC 6694 | | | | | NGC 6694 | | | | |
|---|---|---|---|---|---|---|---|---|---|---|---|---|---|---|
| No. | $R$ | $m_{pg}$ | $m_r$ | $C_r$ | No. | $R$ | $m_{pg}$ | $m_r$ | $C_r$ | No. | $R$ | $m_{pg}$ | $m_r$ | $C_r$ |
| 66 | 2 | 14.58 | 12.15 | 2.43 | 133 | 4 | 16.63 | 15.00: | 1.63: | 200 | 5 | 16.11 | 14.47 | 1.64 |
| 67 | 2 | 16.82 | 14.83 | 1.99 | 134 | 4 | 15.81 | 13.09 | 2.72 | 201 | 5 | 12.69 | 10.56 | 2.13s |
| 68 | 2 | 16.79 | 13.70 | 3.09 | 135 | 4 | 13.44 | 12.77 | 0.67 | 202 | 5 | 15.55 | 12.50 | 3.05s |
| 69 | 2 | 16.93 | 15.17 | 1.76 | 136 | 4 | 16.53 | 14.86 | 1.67 | 203 | 5 | 15.83 | 13.85 | 1.98ds |
| 70 | 2 | 16.36 | 13.76 | 2.60 | 137 | 4 | 14.29 | 13.32 | 0.97 | 204 | 5 | 15.17 | 13.32 | 1.85s |
| 71 | 3 | 15.18 | 14.32 | 0.86 | 138 | 4 | 15.89 | 14.62 | 1.27 | 205 | 5 | 13.41 | 12.93 | 0.48 |
| 72 | 3 | 14.87 | 12.14 | 2.73 | 139 | 4 | 14.30 | 12.29 | 2.01 | 206 | 5 | 12.62 | 12.07 | 0.55 |
| 73 | 3 | 16.47 | 14.40 | 2.07d | 140 | 4 | 16.40 | 14.49 | 1.91 | 207 | 5 | 14.13 | 11.20 | 2.93 |
| 74 | 3 | 16.02 | 14.61 | 1.41 | 141 | 4 | 16.19 | 14.74 | 1.45 | 208 | 5 | 16.53 | 14.87 | 1.66 |
| 75 | 3 | 15.26 | 14.06 | 1.20 | 142 | 4 | 16.66 | 14.77 | 1.89 | 209 | 5 | 16.78 | 15.00: | 1.78: |
| 76 | 3 | 12.95 | 12.29 | 0.66 | 143 | 4 | 14.38 | 13.82 | 0.56 | 210 | 5 | 16.88 | 15.10 | 1.78 |
| 77 | 3 | 14.09 | 13.26 | 0.83 | 144 | 4 | 15.86 | 13.26 | 2.60 | 211 | 5 | 15.21 | 12.20 | 3.01 |
| 78 | 3 | 15.61 | 13.96 | 1.65 | 145 | 4 | 16.23 | 13.58 | 2.65 | 212 | 5 | 16.34 | 14.64: | 1.70: |
| 79 | 3 | 14.47 | 13.50 | 0.97 | 146 | 4 | 15.65 | 14.08 | 1.57d | 213 | 5 | 16.31 | 14.67: | 1.64:d |
| 80 | 3 | 14.63 | 13.53 | 1.10c | 147 | 4 | 16.50 | 15.06 | 1.44 | 214 | 5 | 10.70 | 10.18 | 0.52 |
| 81 | 3 | 16.52 | 14.99 | 1.53 | 148 | 4 | 15.00 | 12.69 | 2.31 | 215 | 5 | 16.86:: | 14.55 | 2.31::c |
| 82 | 3 | 16.55 | 15.12 | 1.43 | 149 | 4 | 16.06 | 14.59 | 1.47 | 216 | 5 | 15.26 | 13.97 | 1.29c |
| 83 | 3 | 15.60 | 14.46 | 1.14 | 150 | 4 | 13.41 | 12.89 | 0.52 | 217 | 5 | 15.07 | 13.57 | 1.50 |
| 84 | 3 | 16.63 | 14.68 | 1.95d | 151 | 4 | 15.87 | 14.75 | 1.12 | 218 | 5 | 16.40 | 15.16 | 1.24 |
| 85 | 3 | 15.36 | 13.74 | 1.62 | 152 | 4 | 14.50 | 11.83 | 2.67 | 219 | 5 | 16.21 | 12.91 | 3.30 |
| 86 | 3 | 15.45 | 14.40 | 1.05 | 153 | 4 | 14.04 | 13.07 | 0.97d | 220 | 5 | 15.67 | 14.16 | 1.51 |
| 87 | 2 | 15.64 | 14.07 | 1.57 | 154 | 4 | 16.82 | 15.08: | 1.74: | 221 | 5 | 16.11 | 12.95 | 3.16 |
| 88 | 2 | 13.11 | 12.47 | 0.64 | 155 | 4 | 16.27 | 14.10: | 2.17: | 222 | 5 | 14.97 | 13.64 | 1.33 |
| 89 | 3 | 15.17 | 14.26 | 0.91 | 156 | 4 | 16.51 | 13.97: | 2.54: | 223 | 5 | 14.09 | 13.39 | 0.70s |
| 90 | 3 | 12.15 | 11.69 | 0.46 | 157 | 4 | 14.21 | 12.21 | 2.00 | 224 | 5 | 16.14 | 14.27 | 1.87 |
| 91 | 3 | 13.43 | 12.64 | 0.79 | 158 | 4 | 15.79 | 14.70 | 1.09 | 225 | 5 | 15.08 | 14.26 | 0.82 |
| 92 | 3 | 11.36 | 10.83 | 0.53 | 159 | 4 | 15.39 | 13.83 | 1.56 | 226 | 5 | 16.85 | 14.16 | 2.69 |
| 93 | 3 | 16.00 | 14.40 | 1.60d | 160 | 4 | 13.64 | 12.98 | 0.66 | 227 | 5 | 16.51 | 15.09: | 1.42: |
| 94 | 3 | 15.99 | 14.89 | 1.10 | 161 | 4 | 14.09 | 11.78 | 2.31 | 228 | 5 | 16.40 | 12.89 | 3.51 |
| 95 | 3 | 15.52 | 12.59 | 2.93 | 162 | 4 | 13.59 | 12.92 | 0.67 | 229 | 5 | 16.37 | 14.81 | 1.56 |
| 96 | 3 | 15.86 | 14.59 | 1.27 | 163 | 4 | 15.78 | 14.13 | 1.65 | 230 | 5 | 17.14 | 15.15: | 1.99: |
| 97 | 3 | 16.67 | 15.15 | 1.52d | 164 | 4 | 15.70 | 14.37 | 1.33 | 231 | 5 | 16.87 | 14.50: | 2.37: |
| 98 | 3 | 15.01 | 14.06 | 0.95 | 165 | 4 | 15.79 | 14.18 | 1.61 | 232 | 5 | 17.05 | 14.46: | 2.59: |
| 99 | 3 | 15.89 | 14.25 | 1.64 | 166 | 4 | 17.14 | 13.42 | 3.72 | 233 | 5 | 16.94 | ..... | ..... |
| 100 | 3 | 16.27 | 14.81: | 1.46: | 167 | 4 | 15.84 | 14.26 | 1.58 | 234 | 5 | 6.47 | 13.98 | 2.49 |
| 101 | 3 | 15.77 | 13.40 | 2.37 | 168 | 5 | 15.94 | 14.52 | 1.42 | 235 | 5 | 15.12 | 13.89 | 1.23 |
| 102 | 3 | 13.32 | 12.74 | 0.58 | 169 | 4 | 14.58 | 11.52 | 3.06 | 236 | 5 | 16.37 | 14.41 | 1.96 |
| 103 | 3 | 15.10 | 13.71 | 1.39d | 170 | 4 | 14.82 | 13.70 | 1.12 | 237 | 5 | 14.19 | 13.45 | 0.74 |
| 104 | 3 | 13.46 | 12.92 | 0.54 | 171 | 4 | 16.10 | 13.68 | 2.42 | 238 | 5 | 13.36 | 12.78 | 0.58 |
| 105 | 3 | 16.90 | 14.93 | 1.97 | 172 | 4 | 15.92 | 14.62 | 1.30 | 239 | 5 | 12.85 | 12.09 | 0.76s |
| 106 | 3 | 13.05 | 12.47 | 0.58 | 173 | 4 | 15.99 | 14.55 | 1.44 | 240 | 5 | 13.47 | 12.95 | 0.52s |
| 107 | 3 | 12.82 | 12.17 | 0.65 | 174 | 5 | 16.48 | 13.71 | 2.77d | 241 | 5 | 14.38 | 13.52 | 0.86s |
| 108 | 3 | 15.06 | 14.06 | 1.00 | 175 | 5 | 12.13 | 11.71 | 0.42 | 242 | 5 | 15.28 | 14.01 | 1.27s |
| 109 | 3 | 14.58 | 13.77 | 0.81 | 176 | 5 | 16.07 | 13.33 | 2.74 | 243 | 5 | 17.08 | 14.63 | 2.45 |
| 110 | 4 | 16.98 | 14.83 | 2.15 | 177 | 5 | 12.51 | 11.85 | 0.66 | 244 | 5 | 16.33 | 13.77 | 2.56 |
| 111 | 3 | 16.75 | 14.97 | 1.78 | 178 | 5 | 16.43 | 14.29 | 2.14d | 245 | 5 | 16.43 | 15.06 | 1.37 |
| 112 | 3 | 16.53 | 14.92 | 1.61 | 179 | 5 | 12.88 | 12.35 | 0.53 | 246 | 5 | 16.05 | 13.31 | 2.74 |
| 113 | 3 | 16.57 | 14.97 | 1.60d | 180 | 5 | 16.15 | 14.74 | 1.41 | 247 | 5 | 15.81 | 13.12 | 2.69 |
| 114 | 3 | 17.18 | 14.96: | 2.22:d | 181 | 5 | 16.39 | 14.69 | 1.70 | 248 | 5 | 14.38 | 13.68 | 0.70 |
| 115 | 3 | 13.56 | 12.21 | 1.35 | 182 | 5 | 16.30 | 12.91 | 3.39 | 249 | 5 | 13.87 | 13.32 | 0.55 |
| 116 | 3 | 16.30 | 14.79 | 1.51 | 183 | 5 | 13.33 | 10.19 | 3.14 | 250 | 6 | 13.67 | 12.95 | 0.72s |
| 117 | 3 | 14.58 | 13.76 | 0.82 | 184 | 5 | 16.30 | 12.92 | 3.38 | 251 | 6 | 14.83 | 13.85 | 0.98s |
| 118 | 3 | 15.88 | 14.51 | 1.37 | 185 | 5 | 16.58 | 14.99 | 1.59 | 252 | 6 | 15.26 | 14.14 | 1.12s |
| 119 | 3 | 15.98 | 14.56 | 1.42 | 186 | 5 | 16.42 | 14.06 | 2.36 | 253 | 6 | 15.67 | 12.81 | 2.86s |
| 120 | 3 | 14.92 | 14.07 | 0.85 | 187 | 5 | 14.37 | 13.70 | 0.67 | 254 | 6 | 16.29 | ..... | .....s |
| 121 | 3 | 14.68 | 13.55 | 1.13 | 188 | 5 | 16.40 | 14.94 | 1.46 | 255 | 6 | 14.11 | 13.62 | 0.49s |
| 122 | 3 | 13.41 | 12.54 | 0.87 | 189 | 5 | 14.88 | 13.93 | 0.95 | 256 | 6 | 14.48 | 13.69 | 0.79s |
| 123 | 3 | 13.63 | 12.81 | 0.82 | 190 | 5 | 15.99 | 14.51 | 1.48 | 257 | 6 | 15.69 | 14.41 | 1.28s |
| 124 | 3 | 14.69 | 13.78 | 0.91 | 191 | 5 | 16.43 | 12.99 | 3.44 | 258 | 6 | 14.71 | 13.86 | 0.85s |
| 125 | 4 | 15.03 | 13.99 | 1.04 | 192 | 5 | 16.54 | 14.99 | 1.55 | 259 | 6 | 15.23 | 13.93 | 1.30s |
| 126 | 4 | 15.00 | 13.79 | 1.21 | 193 | 5 | 15.42 | 14.36 | 1.06 | 260 | 6 | 12.20 | 11.80 | 0.40s |
| 127 | 4 | 15.82 | 13.86 | 1.96d | 194 | 5 | 16.33 | 14.78 | 1.55d | 261 | 6 | 13.81 | 12.92 | 0.89s |
| 128 | 4 | 16.33 | 13.80 | 2.53 | 195 | 5 | 15.19 | 14.31 | 0.88 | 262 | 6 | 14.56 | 13.83 | 0.73s |
| 129 | 4 | 15.84 | 13.99 | 1.85 | 196 | 5 | 16.18 | 14.25 | 1.93d | 263 | 6 | 15.39 | 12.81 | 2.58s |
| 130 | 4 | 15.85 | 13.07 | 2.78 | 197 | 5 | 14.55 | 13.79 | 0.76 | 264 | 6 | 15.66 | 13.16 | 2.50s |
| 131 | 5 | 15.90 | 12.72 | 3.18 | 198 | 5 | 16.30 | 14.97 | 1.33 | 265 | 6 | 16.01 | 13.21 | 2.80s |
| 132 | 4 | 15.09 | 13.06 | 2.03d | 199 | 5 | 14.12 | 13.65 | 0.47s | | | | | |

## NOTE ADDED IN PROOF

Spectral types for several stars in NGC 6649 have been obtained at the writer's request by Dr. Struve and Dr. Elvey with the slitless spectrograph of the McDonald Observatory. The brightest star in the cluster, No. 42 ($m_{pg}$ = 10.40, $C_r$ = 2.04:), shows the hydrogen lines clearly, but they are considerably weaker than in A0–A2 stars. Dr. Struve is inclined to estimate the spectrum as about B8, possibly of supergiant characteristics. Star No. 117 ($m_{pg}$ = 14.56, $C_r$ = 4.42) is definitely of late type; it may be K or M. Star 9 ($m_{pg}$ = 12.51, $C_r$ = 2.07) has emission at $H\alpha$ and is probably of class Be. Star 58 ($m_{pg}$ = 13.05, $C_r$ = 2.06) may be an F or a very early B. Two spectrograms taken with the slit Cassegrain arrangement tend to confirm the estimate of spectral type for No. 42; the spectrum shows practically no features in the red region, and the hydrogen lines in the violet are definitely weak. The spectrum for No. 9 definitely shows a bright line at $H\alpha$ and is therefore of spectral class Be. Unfortunately, the stars are so exceptionally red that they require long exposures even with small dispersion. The spectra confirm the conclusion that NGC 6649 is intrinsically similar to h and $\chi$ Persei, which contain B and A stars in long extensions of their main sequences to bright absolute magnitudes. They indicate also, that the color excess for NGC 6649 ($1^m65$) may have been somewhat underestimated and that it may lie closer to $1^m9$. For a more precise determination of the color excess from spectra, however, spectral types for somewhat fainter stars, whose intrinsic colors are probably more normal than those of the very brightest stars in clusters of this type, would be desirable. It is a pleasure to thank Dr. Struve and Dr. Elvey for the above data.

KIRKWOOD AND GOETHE LINK OBSERVATORIES
May 1, 1940

# NOTES

## SIX NEW Be STARS

In the course of a survey of all B-type stars brighter than sixth magnitude, with the two-prism spectrograph and the 28½-inch reflector of the Cook Observatory, the *Hα* line was found to be bright in the following stars not mentioned in the catalogue by Merrill and Burwell[1] or in Merrill's list of c stars.[2]

| Henry Draper No. | Spectral Class | Magnitude | Estimated Emission Intensity | JD of First Cook Observation |
|---|---|---|---|---|
| 18552* | B9 | 5.92 | 3 | 2429 655 |
| 22780 | B5 | 5.57 | 1 | 711 |
| 23552 | B8 | 5.92 | 2 | 722 |
| 60855 | B5 | 5.57 | 2 | 746 |
| 142926† | B8 | 5.61 | 1 | 439 |
| 171780‡ | B5 | 5.93 | 1 | 532 |
| 174237 | B5 | 5.76 | 1 | 547 |
| 183914 | B9 | 5.36 | 2 | 554 |
| 185037 | B9 | 5.86 | 2 | 570 |

* Announced as a bright-line star in *Pub. Dom. Ap. Obs., Victoria*, **1**, 178, 1920.
† Announced as a bright-line star in *J.R.A.S. Can.*, **33**, 384, 1939.
‡ Announced as a bright-line star in *Harvard Ann. Card.*, No. 507, 1939.

Twenty-four other stars apparently have abnormally weak *Hα* absorption. The Henry Draper numbers of these stars follow:

| | | | | |
|---|---|---|---|---|
| 6676 | 24504 | 55879 | 169033 | 197511 |
| 6811 | 33328 | 87504 | 175869 | 204172 |
| 21291 | 34078 | 91316 | 188209 | 205551 |
| 21856 | 42087 | 164353 | 189687 | 210191 |
| 24131 | 53974 | 167264 | 195554 | |

The abnormality may be a photographic defect in some cases, but slit spectrograms with dispersion greater than 300 A/mm should reveal some emission components of the *Hα* lines of these stars.

ORREN MOHLER

COOK OBSERVATORY
WYNNEWOOD, PENNSYLVANIA
June 1, 1940

[1] *Ap. J.*, **78**, 87, 1933. [2] *Ap. J.*, **81**, 351, 1935.

## THE SPECTRUM OF THE COMPANION OF α SCORPII*

Seven spectrograms of the companion of α Scorpii were obtained with the Cassegrain spectrograph of the McDonald Observatory on three nights of good seeing: April 20, July 1, and July 6, 1940. The dispersion of the instrument was 40 A/mm at λ 3933, and the spectra extend to λ 3200. The Balmer lines are broad and can be seen to about *H* 16 or *H* 17. This would place the B4n star among the normal B stars of low luminosity in the diagram of Unsöld and Struve[1] and does not reflect in the spectrum the well-established underluminous character of this object.[2] The drop in intensity near the Balmer limit is conspicuous. There are no emission lines in the ultraviolet region, and the few absorption lines of *He* I are weak and diffuse.

The existence of moderately strong emission lines of [*Fe* II], discovered by Wilson and Sanford[3] in the ordinary photographic region, has been confirmed. The radial velocity, as determined from the two plates of best quality, is −18.4 km/sec for the absorption lines of *H* and *He* I and +12.5 km/sec for the [*Fe* II] emission lines. The difference between the absorption lines and the emission lines is doubtless real, but the large difference between our measures for the emission lines and those published by Wilson and Sanford, −0.1 km/sec, may be due to a tendency in our observations to guide on one edge of the image of the companion. The slit of our spectrograph was set in position angle at right angles to the line joining the two stars, and it is possible that, in order to avoid the light of the bright star, we have illuminated the slit more on one side than on the other. The light of the red star is completely negligible to the violet side of *Hβ*. But in the visual region the overlapping is serious.

The principal purpose of these observations was an attempt to find whether the [*Fe* II] emission lines are present only in the light of the B-type companion, or whether they can be photographed in a region surrounding that star. On the first two exposures the star

* *Contributions from the McDonald Observatory, University of Texas*, No. 26.

[1] *Ap. J.*, **91**, 365, 1940.

[2] Adams and Joy, *Pub. A.S.P.*, **33**, 206, 1921.

[3] *Pub. A.S.P.*, **49**, 221, 1937.

was permitted to drift along the slit (by means of the drive in declination, because the slit was oriented almost exactly north-south). An exposure of 45 minutes on Agfa Super-Pan-Press film produced a very strong spectrum, 1.4 mm in width. If the emission lines originate in a nebulosity surrounding the star, this exposure-time should, therefore, be sufficient to bring out the lines when the star is held without motion on the slit. A spectrogram obtained in this manner gave a greatly overexposed continuous spectrum, which, because of photographic spreading, has a width of about 3″.9. The emission lines extend beyond the edges of the continuous spectrum and are sharp and strong. The extensions are about 1″.0 in length, on each side of the continuous spectrum.

The evidence is, thus, strongly in favor of a small nebulosity surrounding the B-type companion. The extensions of the emission lines are so strong that they could hardly have been produced by an underexposed spectrum of scattered light from the B star or of light spilled over the normal tremor disk in moments of less satisfactory seeing. In order to test this, we obtained several short exposures, ranging from 1 minute to 10 minutes, of the B-type companion, held stationary on the slit. On the shortest exposure the width of the continuous spectrum is 1″.6, and the density corresponds to the steepest part of the characteristic curve. Yet, in spite of a width greater than that of the extensions, the contrast between continuous spectrum and emission lines is so small that the latter are not visible with certainty. In fact, the contrast is so small that widened spectra are required to show them clearly.

There remains, of course, the possibility that the lines are variable in intensity. Not all of our observations were obtained on the same night, and a marked strengthening of the lines on July 1 with a decline in intensity on July 5 would also explain our results. Hence, it would be important to repeat the observations on several occasions.

If the nebulosity is confirmed, it would help in the interpretation of several other stars which, together with α Scorpii, consist of a late-type star with a B-type companion and which show [*Fe* II] emission lines. The normal appearance of the B spectrum of α Scorpii and of other representatives of this group[4] suggests that the emis-

[4] *Ap. J.*, **91**, 619, 1940.

sion lines originate not in the reversing layers of these stars but in nebulosities whose presence is somehow connected with the existence of a cool supergiant in the system. The diameter of the nebulosity, $5''.9$, appears reasonable in comparison to the separation of $3''$ between the two components. In exceptionally good seeing it should be possible to set the slit between the two stars. But during the past season we have not been able to make such an observation.

O. STRUVE
P. SWINGS

YERKES OBSERVATORY
AND
MCDONALD OBSERVATORY
July 26, 1940

---

## ERRATUM

In Volume **88** of this *Journal:*

On page 91, middle of page: *read* "$\epsilon$ Capricorni (Pl. V)" *instead of* "$\epsilon$ Capricorni (Pl. IV)."

On page 105, eighth line from bottom: *read* "A close inspection of Plate II" *instead of* "A close inspection of Plate V."

# REVIEWS

*The Birth and Death of the Sun: Stellar Evolution and Subatomic Energy.* By GEORGE GAMOW. New York: Viking Press, 1940. Pp. xiv+238. $3.00.

The problem of energy generation in the stars has come into prominence partly through Professor Gamow's theory of the "leaking-out" of radioactive $\alpha$-decay, which he proposed in 1928. Since that time he and his associates at George Washington University have taken an active part in discussions of stellar evolution. The author has attempted "to give, in the simplest terms of which he is capable, an outline of the fundamental discoveries and theories that now permit us a general view of the evolution of our world." In this attempt he has been eminently successful. With a noteworthy regard for accuracy in presenting astronomical facts and physical theory Professor Gamow has combined the sparkling humor which distinguished his other recent popular book, *Mr. Tompkins in Wonderland*. Although the book is not intended for professional astronomers, the form of presentation, the choice of suitable analogies, and the novelty of the entire subject suggest it as a valuable aid in teaching and as stimulating reading in research. To an astronomically trained reader the author's frequent reference to Capella and $\delta$ Cephei as "red giants" will appear strange, until on page 141 he will find a footnote justifying the designation but not removing the confusion. He will disagree when the author identifies the interstellar clouds of obscuring matter with gaseous nebulae (p. 187) and when he attributes to a gaseous nebula the obscuration of the central regions of the galaxy (p. 209). Since the book is frankly popular in character it is not surprising that some rather important steps in the development of the theory of stellar structure have been omitted. But the "chronology" on page 233 is hardly fair to the theoretical astrophysicists. The last "important step" of an astrophysical character which the author has listed is R. H. Fowler's work, in 1926, on "white dwarfs as collapsed stars." These minor differences in opinion are, of course, not important. The important thing is that within the past few years a number of distinguished physicists have taken interest in the fundamental problems of astrophysics and have made available to astronomers the fruits of their research in nuclear physics.

O. S.

*Copernicus: The Founder of Modern Astronomy.* By ANGUS ARMITAGE. London: George Allen & Unwin, Ltd. (W. W. Norton & Co., Inc., 70 Fifth Avenue, New York, distributors), 1938. Pp. 183. $3.00.

This book consists of six chapters: i, planetary theories before Copernicus; ii, the life-story of Copernicus; iii, the mobility of the earth; iv, the Copernican system: theory of the earth's motion; v, the Copernican system: theory of the moon's motion; vi, the Copernican system: theory of planetary motions. There are a short epilogue and three notes explaining, respectively, the equivalence of eccentric and epicyclic systems, the table of chords used by Copernicus, and the origin of the *Commentariolus* of Copernicus and the *Narratio prima* of Rheticus. The book is an important commentary on the work of Copernicus and should be read by anyone who wishes to study the original volume *De revolutionibus orbium coelestium* or the earlier and abbreviated form of the Copernican theory presented in the *Commentariolus* or the *Narratio prima*. It is difficult for a modern reader to understand the original writings of Copernicus. For example, we follow him readily when he attributes to the earth a motion of rotation around its axis and one of revolution around the sun. But we are likely to be perplexed when Copernicus introduces a third motion, in declination, the purpose of which is to account for the seasons. Mr. Armitage supplies the necessary notes and explanations and reminds us that it was Kepler who, about fifty years after Copernicus, wrote: "The said motion is, in truth, not motion at all, but rather rest." Mr. Armitage's book can be very highly recommended not only to students of the history of astronomy but to all those who are interested in the development of human thought.

O. S.

---

*Les hautes températures.* By G. RIBAUD. Paris: Librairie Félix Alcan, 1940. Pp. 173. Fr. 18.

This book is devoted to the methods of obtaining and measuring high temperatures in the laboratory. The first chapter discusses optical and thermoelectric methods of measurement; the second chapter is devoted to the physical properties of various substances at high temperatures; the third chapter treats various chemical reactions at high temperatures; the fourth discusses the chemical reaction as a source of high temperature; the fifth discusses the technique of producing high temperatures; the sixth deals with thermal radiation; and the seventh describes various industrial applications.